

**The Pennsylvania State University**

**The Graduate School**

**College of Agricultural Sciences**

**STRUCTURE AND FUNCTION OF ENDOSPERM STARCH FROM MAIZE  
MUTANTS DEFICIENT IN ONE OR MORE STARCH-BRANCHING ENZYME  
ISOFORM ACTIVITIES**

A Dissertation in

Food Science

by

Huan Xia

© 2009 Huan Xia

Submitted in Partial Fulfillment  
of the Requirements  
for the Degree of

Doctor of Philosophy

December 2009

The dissertation of Huan Xia was reviewed and approved\* by the following:

Donald B. Thompson  
Professor of Food Science  
Dissertation Co-Adviser  
Co-Chair of Committee

Mark J. Gultinan  
Professor of Plant Molecular Biology  
Dissertation Co-Adviser  
Co-Chair of Committee

John N. Coupland  
Associate Professor of Food Science

Devin G. Peterson  
Associate Professor of Food Science

Ming Tien  
Professor of Biochemistry

John D. Floros  
Professor of Food Science  
Head of the Department of Food Science

\*Signatures are on file in the Graduate School

## ABSTRACT

Maize starch-branching enzyme (SBE) isoforms are important in endosperm starch biosynthesis and consequently are expected to influence starch structure and function. The *ae* mutant, which is deficient in SBEIIb, has a profound effect on endosperm starch structure, leading to an increased amylose content and a reduced amylopectin branching. The study of the *ae* mutant suggests an important function of SBEIIb on starch structure. Although no effect of the *sbe1a* mutant, which is deficient in SBEI, on starch structure has been noted previously, for starch deficient in SBEIIb, a further deficiency of SBEI increased branching (Yao et al. 2004). A related study showed that for starch deficient in SBEIIb, a further deficiency of SBEIIa also increased branching (Yao et al. 2003). Taken together, these studies suggest a reciprocal inhibition between SBEI and SBEIIa. It can be reasoned from these studies that the effect of individual SBE isoform on starch structure may not be independent. The overall goal of this continuing line of SBE research is to understand the role of each of the SBE isoform in starch biosynthesis. The goal of this thesis is to understand the effects of deficiency of maize SBE isoform activities on endosperm starch molecular and granular structure and starch digestion, with emphasis on the effect of SBEI deficiency.

A preliminary test of endosperm starch digestibility for the *sbe1a* mutant showed that deficiency of SBEI caused a decreased susceptibility of starch granules to pancreatic  $\alpha$ -amylase. This was the first indication of an effect of deficiency of SBEI alone in synthesis of endosperm starch and justified further investigation of the function of SBEI isoform. Consequently, this thesis describes the study of the

structure and function of *sbe1a* mutant endosperm starch compared to non-mutant (wild-type, Wt) starch.

Starch from Wt and *sbe1a* mutant endosperm was subjected to *in vitro* pancreatic  $\alpha$ -amylase digestion for 16 hr by the AOAC procedure for resistant starch (RS), to determine the proportion of RS. The digestion kinetics were analyzed using a double-exponential decay fit. *sbe1a* starch had a higher RS value (13.2%) compared to Wt (1.6%). Kinetic analysis showed that *sbe1a* starch had a lower proportion of a rapidly-digested component than Wt.

Chain length profile was examined for the non-granular starch and starch fractions from Wt and *sbe1a*, as well as for the RS from Wt and *sbe1a*. Although chain length profiles of native starch molecules appeared very similar for Wt and *sbe1a*, some small differences between the two genotypes were observed in the chain length profile of their RS, as well as in the comparison of the chain length profile of their RS to native starch. Compared to Wt, fewer amylose-like chains were digested in RS from *sbe1a*. Iodine binding analysis of starch fractions showed that *sbe1a* samples had higher  $\lambda_{\max}$  than Wt samples.

Amylopectin fractionated from Wt and *sbe1a* starch was subjected to *in vitro*  $\beta$ -amylase hydrolysis over 24 hr. Hydrolysis of *sbe1a* chains was less complete as compared to Wt. The less complete hydrolysis is consistent with a higher proportion of closely associated branch points in amylopectin from *sbe1a*. The amylose fraction from Wt and *sbe1a* starch was subjected to exhaustive  $\beta$ -amylolysis. *sbe1a* starch had more long residual chains, suggesting that the distribution of branch points on these long amylose chains may be closer to the non-reducing ends. Debranching of  $\beta$ -limit dextrin from amylose by isoamylase was less complete in *sbe1a*, suggesting that closely associated branch points may be more prevalent in amylose from *sbe1a*.

Granule structure for native starches and residual granule structure for the respective RS were examined by microscopy. Scanning and transmission electron micrographs show that the RS from *sbe1a* mutant retained more of the granule integrity. A resistant peripheral layer by microscopy observed for the *sbe1a* RS may help understand the decreased digestibility of *sbe1a* starch. *Sbe1a* is more strongly expressed in the later stage of endosperm development (Gao et al. 1996). Thus, if most of the later-synthesized starch is deposited in the peripheral region of the growing granule, starch synthesized in the *sbe1a* mutant would be expected to be affected predominantly in the peripheral region. A reasonable speculation is that the branching pattern might differ between the RS and the digested portion of *sbe1a* starch, and this difference might also account for the decreased digestibility of the peripheral region in *sbe1a* granule.

Starch utilization and coleoptile growth of Wt and *sbe1a* mutant kernels were measured during kernel germination. After Day 6 germinating *sbe1a* kernels exhibited a slower rate of coleoptile growth and an accordingly decreased rate of starch hydrolysis as compared to Wt kernels, suggesting compromised starch utilization in germinating *sbe1a* kernels.

Comparisons of RS values among two sets of mutant combinations both show a main effect of *sbe1a* and a significant difference between *sbe1a* and Wt. This consistent result substantially confirms our preliminary indication of an effect of *sbe1a* alone. For the first set of mutant combinations, *sbe1a* and *sbe2a*, the effects of *sbe1a* and *sbe2a* on both RS values and amylopectin branching are not independent, as a significant interaction is observed. In contrast, for the second set of mutant combinations, *sbe1a* and *ae*, the effects of *sbe1a* and *ae* on RS values are independent, but the effects of *sbe1a* and *ae* on amylose content are not independent. The

significant statistical interaction terms suggest possible physical interactions among SBEs. These interactions might be mediated by other starch synthetic enzymes.

The evidence obtained in this thesis, coupled with previous research, leads to several hypotheses about the specific functions of the three maize SBE isoforms in endosperm starch biosynthesis: 1) The SBEIIb protein is the dominant form of SBE, and is responsible for synthesizing branch points that are clustered. 2) When SBEIIb is present, SBEI is responsible for modulating the branching pattern by synthesizing branch points that are less locally clustered, and SBEIIa is responsible for modulating the branching pattern by synthesizing branch points that are more locally clustered. 3) When SBEIIb is absent, SBEI and SBEIIa may have a reciprocal inhibitory function on synthesis of branch points.

This thesis also for the first time reports that a lack of SBEI activity resulted in an observable effect, which was seen on both starch molecular structure and starch function. Structural and functional analysis of endosperm starch deficient in SBEI activity strongly supports the hypothesis that SBEI is required to synthesize starch granules for normal kernel development, allowing efficient hydrolysis and utilization. Evidence from this thesis reveals a unique and essential function of SBEI in normal plant development, consistent with the evolutionary conservation of SBEI in all higher plants.

The new knowledge generated in this thesis will contribute to our understanding of the function and evolution of the maize SBEs, and of their roles in the biosynthesis, hydrolysis and utilization of starch granules. Moreover, the novel *sbe1a* starch might have application as a food ingredient with nutritional benefit.

## TABLE OF CONTENTS

LIST OF FIGURES .....	xii
LIST OF TABLES .....	xvii
ACKNOWLEDGEMENTS .....	xx
 Chapter 1. LITERATURE REVIEW .....	 1
1.1 Introduction: The Structure and Function of Maize Starch.....	1
1.2 Starch Biosynthesis .....	2
1.2.1 Starch Biosynthetic Pathway in Maize Endosperm.....	2
1.2.2 Roles of Maize Starch Branching Enzymes in Endosperm Starch Biosynthesis.....	3
1.2.3 Roles of Maize Starch Branching Enzymes in Endosperm Starch Structure ...	7
1.2.3.1 Identification of Maize <i>sbe</i> Mutants.....	7
1.2.3.2 Effects of Deficiency of Maize Starch Branching Enzymes on Endosperm Starch Structure .....	8
1.3 Starch Structure .....	18
1.3.1 Levels of Starch Structure .....	18
1.3.1.1 Molecular Structure.....	18
1.3.1.2 Granular Structure .....	21
1.3.2 Methods for Structural Analysis.....	24
1.3.2.1 Molecular Structure Analysis .....	24
1.3.2.2 Granular Structure Analysis .....	31
1.4 Starch Digestion by $\alpha$ -Amylase.....	32
1.4.1 Digestion Rate and Extent.....	32
1.4.2 Nutritional Value .....	34
1.4.3 Factors Influencing Digestibility of Starch Granules.....	35
1.5 Starch Utilization during Germination .....	38
1.6 Statement of the Problem .....	40
1.7 Goal .....	41
1.8 Objectives.....	41
1.9 References-Chapter 1 .....	42
 Chapter 2. MATERIALS AND METHODS.....	 54
2.1 Maize Genotypes .....	54

2.2 Identification of Maize <i>sbe</i> Mutants.....	54
2.3 Generation of Segregating Populations for Endosperm Analysis .....	58
2.4 Endosperm Starch Extraction.....	63
2.5 Starch Digestibility Analysis.....	64
2.5.1 Resistant Starch Determination .....	64
2.5.2 Digestion Time-Course Analysis .....	65
2.6 Starch Molecular Structure Analysis.....	66
2.6.1 Preparation of Non-Granular Starch and Starch Fractions.....	66
2.6.2 Iodine Binding Analysis of Starch Molecules.....	68
2.6.3 Sepharose CL-2B Chromatography of Intact Molecules .....	69
2.6.4 Preparation of Resistant Starch .....	70
2.6.5 $\beta$ -Amylolysis of Amylopectin and Debranching of $\beta$ -Dextrins .....	70
2.6.6 Preparation of Isoamylase Debranched and Isoamylase plus Pullulanase Debranched $\beta$ -Limit Dextrins from Amylopectin and Amylose Fractions....	71
2.6.7 High-Performance Chromatography of Debranched Molecules.....	71
2.7 Starch Granular Structure Analysis.....	72
2.7.1 Light Microscopy .....	72
2.7.2 Scanning Electron Microscopy.....	73
2.7.3 Transmission Electron Microscopy.....	73
2.8 Kernel Germination Assay .....	74
2.9 References-Chapter 2 .....	75
Chapter 3. EFFECTS OF MAIZE SBEI DEFICIENCY ON ENDOSPERM STARCH STRUCTURE AND FUNCTION.....	77
3.1 Introduction and Objectives .....	77
3.2 Results .....	78
3.2.1 Starch Digestibility .....	78
3.2.1.1 Resistant Starch Value.....	78
3.2.1.2 Digestion Time-Course Kinetics .....	80
3.2.2 Starch Molecular Structure.....	86
3.2.2.1 Starch Fractionation.....	86
3.2.2.2 Iodine Binding Properties of Non-Granular Starch and Starch Fractions.	88
3.2.2.3 Size Distribution of Intact Amylopectin and Amylose Fractions .....	88
3.2.2.4 Chain Length Distribution of Debranched Non-Granular Starch and Starch Fractions.....	94

3.2.2.5 Chain Length Distribution of Debranched Resistant Starch .....	98
3.2.2.6 Starch Branching Pattern Exploration .....	98
3.2.2.6.1 Time-Course of $\beta$ -Amylolysis of the Amylopectin Fraction Followed by Complete Debranching .....	98
3.2.2.6.2 Isoamylase-Debranched and Isoamylase-plus-Pullulanase- Debranched $\beta$ -Limit Dextrins from the Amylopectin Fraction .....	102
3.2.2.6.3 Isoamylase-Debranched and Isoamylase-plus-Pullulanase- Debranched $\beta$ -Limit Dextrins from the Amylose Fraction .....	106
3.2.3 Starch Granular Structure .....	109
3.2.3.1 Light Microscopy .....	109
3.2.3.2 Scanning Electron Microscopy .....	112
3.2.3.3 Transmission Electron Microscopy .....	121
3.2.4 Kernel Germination Analysis .....	126
3.3 Discussion .....	129
3.3.1 Starch Digestibility .....	129
3.3.2 Starch Molecular Structure .....	131
3.3.3 Starch Granular Structure .....	143
3.3.4 Structural Basis for Decreased Digestibility of <i>sbe1a</i> Starch .....	147
3.3.5 Starch Utilization during Kernel Germination .....	149
3.4 References-Chapter 3 .....	150
Chapter 4. EFFECTS OF DEFICIENCY OF MAIZE SBEs ALONE AND IN COMBINATION ON ENDOSPERM STARCH DIGESTIBILITY AND MOLECULAR STRUCTURE .....	153
4.1 Introduction and Objectives .....	153
4.2 Results .....	156
4.2.1 Resistant Starch Value .....	156
4.2.2 Starch Molecular Structure .....	159
4.2.2.1 Starch Fractionation .....	159
4.2.2.2 Iodine Binding Properties of Non-Granular Starch and Starch Fractions. ....	159
4.2.2.3 Size Distribution of Intact Amylopectin and Amylose Fractions .....	164
4.2.2.4 Chain Length Distribution of Debranched Non-Granular Starch and Starch Fractions .....	170
4.2.2.5 Chain Length Distribution of Debranched Resistant Starch .....	170
4.2.2.6 Isoamylase-Debranched and Isoamylase-plus-Pullulanase-Debranched $\beta$ -Limit Dextrins from the Amylopectin Fraction of <i>sbe1a</i> and <i>sbe2a</i> Mutant Combinations .....	181
4.3 Discussion .....	185
4.3.1 Resistant Starch Value for Maize Endosperm Starch of <i>sbe1a</i> and <i>sbe2a</i>	

Mutant Combinations and of <i>sbe1a</i> and <i>ae</i> Mutant Combinations .....	185
4.3.2 Molecular Structure for Maize Endosperm Starch of <i>sbe1a</i> and <i>sbe2a</i> Mutant Combinations .....	186
4.3.3 Molecular Structure for Maize Endosperm Starch of <i>sbe1a</i> and <i>ae</i> Mutant Combinations.....	188
4.3.4 Effects of Deficiency of Maize SBEs Alone and In Combination on Endosperm Starch Digestibility and Molecular Structure.....	190
4.4 References-Chapter 4 .....	191
Chapter 5. CONCLUSIONS AND FUTURE WORK.....	193
5.1 Conclusions .....	193
5.1.1 Effects of Maize SBE Isoforms on Endosperm Starch Structure.....	193
5.1.2 Effects of Maize SBE Isoforms on Endosperm Starch Digestion.....	199
5.1.3 Function of Maize SBE Isoforms in Starch Biosynthesis .....	203
5.1.4 An Evolutionary Perspective on the Function of Maize SBE Isoforms.....	206
5.2 Suggestions for Future Work.....	208
5.2.1 Understanding of Structural Basis for Starch Digestibility.....	208
5.2.1.1 Extended Digestion of Starch.....	208
5.2.1.2 Characterization of Starch Structure During Digestion.....	208
5.2.1.3 Characterization of Branching Pattern for Resistant Starch.....	209
5.2.1.4 Characterization of Starch Structure and Digestion from Differentially Iodine-Stained Granules .....	209
5.2.2 Structural Analysis of Starch from Different Biological Replications.....	209
5.2.3 Breeding Strategies for Generating All the Combinations of <i>sbe</i> Mutants In Isogenic Lines.....	210
5.2.4 Functions of Maize SBE Isoforms in Other Tissues .....	211
5.2.5 Interactions of Maize SBEs with Other Starch Synthetic Enzymes in Starch Biosynthesis.....	213
5.3 References-Chapter 5 .....	214
Appendix A. ADDITIONAL FIGURES AND TABLES FOR CH3 & CH4 .....	218
Appendix B. EFFECT OF DEFICIENCY OF MAIZE SBES ON LEAF STARCH DIGESTIBILITY AND GRANULAR STRUCTURE .....	225
B.1 Introduction and Objectives.....	226
B.2 Materials and Methods.....	227
B.2.1 Plant germplasms and growth conditions .....	227
B.2.2 Leaf Starch Extraction .....	227
B.2.3 Starch Digestibility Analysis .....	228
B.2.4 Scanning Electron Microscopy.....	228

B.3 Results.....	228
B.3.1 Leaf Starch Digestibility.....	228
B.3.2 Leaf Starch Granular Structure.....	234
B.4 Discussion.....	234
B.5 References-Appendix B.....	239

## LIST OF FIGURES

Figure 1.1	HPSEC of debranched endosperm starches from wild-type (left) and <i>sbe2a</i> mutant (right) in the W64A background (figure from Blauth et al. 2001 with permission).....	10
Figure 1.2	Size-exclusion chromatography of whole endosperm starches (upper graph) and HPSEC of debranched endosperm starches (bottom graph) from wild-type (left) and <i>sbe1a</i> mutant (right) in the W64A background (figures from Blauth et al. 2002 with permission).....	11
Figure 1.3	HPSEC of debranched starch (left) and debranched $\beta$ -limit dextrin (right) from maize genotypes of <i>wx</i> , <i>sbe1a wx</i> , <i>ae wx</i> , and <i>sbe1a ae wx</i> in the W64A background (figures from Yao et al. 2004 with permission).....	13
Figure 1.4	HPSEC of debranched amylopectin (left) and debranched $\beta$ -limit dextrin (right) of amylopectin fractioned from maize genotypes of wild-type (normal), <i>sbe2a</i> , <i>ae</i> , and <i>sbe2a ae</i> in the W64A background (figures from Yao et al. 2003 with permission).....	15
Figure 1.5	HPSEC of debranched $\beta$ -dextrins resulting from 2 hr of $\beta$ -amylolysis (250 U /mL), from maize genotypes of <i>wx</i> , <i>sbe1a wx</i> , <i>sbe1a wx</i> , <i>ae wx</i> , and <i>sbe1a ae wx</i> in the W64A background (figure from Xia 2005 with permission).....	17
Figure 1.6	Amylopectin cluster model proposed by Robin et al. (1974).....	20
Figure 1.7	Schematic view of the hierarchical order within starch granule.....	23
Figure 1.8	Amylopectin branching pattern model in the form of $\beta$ -limit dextrin that would not be readily attacked by isoamylase but that would be easily attacked by pullulanase to release a short residual B chain.....	30
Figure 2.1	Gel electrophoresis of PCR amplification products.....	56
Figure 2.2	Pedigree of <i>sbe</i> mutants: A description of the breeding work by Blauth et al. (2002; 2001).....	59
Figure 2.3a	Pedigree of <i>sbe</i> mutants: Attempt to produce a population segregating for all three <i>sbe</i> genes, using seed population bred by Blauth et al. (2002; 2001).....	60
Figure 2.3b	Pedigree of <i>sbe</i> mutants: Attempt to produce a population	

	segregating for <i>sbe1a</i> and <i>sbe2a</i> genes, using seed population bred by Blauth et al. (2002; 2001).....	61
Figure 3.1	Hierarchical order of experimental design for resistant starch value determination.....	79
Figure 3.2	Time course of digestion of the resistant starch assay for Wt and <i>sbe1a</i> mutant starch from one biological replication. ....	84
Figure 3.3	Best fit curves for digestion of the resistant starch assay for Wt (above) and <i>sbe1a</i> mutant (below) starch, using combined data from 2 independent digestions for each biological replication (B1, B2, B3).....	85
Figure 3.4	Iodine binding by non-granular starch and starch fractions obtained by differential alcohol precipitation from Wt and <i>sbe1a</i> mutant starch.....	89
Figure 3.5a	Size-exclusion chromatograms of amylopectin fraction from Wt and <i>sbe1a</i> mutant starch.....	91
Figure 3.5b	Size-exclusion chromatograms of amylose fraction from Wt and <i>sbe1a</i> mutant starch.....	92
Figure 3.6a	Chromatograms of isoamylase-debranched non-granular starch and amylopectin fractions from Wt and <i>sbe1a</i> mutant starch.....	95
Figure 3.6b	Chromatograms of isoamylase-debranched amylose and intermediate material fractions from Wt and <i>sbe1a</i> mutant starch.....	96
Figure 3.7	Chromatograms of isoamylase-debranched resistant starch from Wt and <i>sbe1a</i> mutant starch.....	99
Figure 3.8	Chromatograms of debranched $\beta$ -dextrins from amylopectin from Wt and <i>sbe1a</i> mutant starch using $\beta$ -amylase (250 U/mL).....	101
Figure 3.9	Proportions of chains from debranched $\beta$ -dextrins during time course of $\beta$ -amylolysis of amylopectin from Wt and <i>sbe1a</i> mutant starch using $\beta$ -amylase (250 U/mL).....	103
Figure 3.10	Chromatograms of isoamylase-debranched and isoamylase-plus-pullulanase-debranched $\beta$ -limit dextrins from amylopectin fraction from Wt and <i>sbe1a</i> mutant starch.....	104
Figure 3.11	Chromatograms of isoamylase-debranched and isoamylase-plus-	

	pullulanase-debranched $\beta$ -limit dextrans from amylose fraction from Wt and <i>sbe1a</i> mutant starch.....	107
Figure 3.12a	Bright field (left) and polarized light (right) micrographs of native starch from Wt and <i>sbe1a</i> mutant.....	110
Figure 3.12b	Bright field (left) and polarized light (right) micrographs of resistant starch from Wt and <i>sbe1a</i> mutant.....	111
Figure 3.13a	Bright field (left) and polarized light (right) micrographs of native starch from Wt and <i>sbe1a</i> mutant stained with 0.04% iodine and viewed within 5 min.....	113
Figure 3.13b	Bright field (left) and polarized light (right) micrographs of resistant starch from Wt and <i>sbe1a</i> mutant stained with 0.04% Iodine and viewed within 5 min.....	114
Figure 3.14a	Scanning electron micrographs of Wt native starch. ....	115
Figure 3.14b	Scanning electron micrographs of <i>sbe1a</i> native starch.....	116
Figure 3.15	Scanning electron micrographs of Wt resistant starch.....	117- 118
Figure 3.16	Scanning electron micrographs of <i>sbe1a</i> resistant starch.....	119- 120
Figure 3.17a	Transmission electron micrographs of Wt native starch.....	122
Figure 3.17b	Transmission electron micrographs of <i>sbe1a</i> native starch.....	123
Figure 3.18a	Transmission electron micrographs of Wt resistant starch.....	124
Figure 3.18b	Transmission electron micrographs of <i>sbe1a</i> resistant starch.....	125
Figure 3.19	Germination of Wt and <i>sbe1a</i> mutant kernels: The lengths of the emerged coleoptiles were measured on successive days during the incubation period.....	127
Figure 3.20	Germination of Wt and <i>sbe1a</i> mutant kernels: Starch content in the germinating endosperm was quantified at Day 1, 6, 8, 11, and percentage of starch content at each day against the dry weight of Day 1 kernels was plotted.....	128
Figure 3.21	Branching pattern models for amylopectin from <i>sbe1a</i> and Wt	

	starches.....	135
Figure 3.22	Branching pattern models for amylose from <i>sbe1a</i> and Wt starches...	141
Figure 3.23	Proposed overall amylose branching pattern models for <i>sbe1a</i> and Wt starches, consistent with the differences in actions of $\beta$ -amylase and isoamylase.....	142
Figure 4.1a	Iodine binding by non-granular starch and amylopectin fraction obtained by differential alcohol precipitation from Wt, <i>sbe1a</i> , <i>sbe2a</i> , and <i>sbe1a sbe2a</i> starch.....	161
Figure 4.1b	Iodine binding by amylose and intermediate material fractions obtained by differential alcohol precipitation from Wt, <i>sbe1a</i> , <i>sbe2a</i> , and <i>sbe1a sbe2a</i> starch.....	162
Figure 4.2	Iodine binding by non-granular starch from Wt, <i>sbe1a</i> , <i>ae</i> , and <i>sbe1a ae</i> starch.....	165
Figure 4.3a	Size-exclusion chromatograms of amylopectin fraction from <i>sbe2a</i> and <i>sbe1a sbe2a</i> starch .....	167
Figure 4.3b	Size-exclusion chromatograms of amylose fraction from <i>sbe2a</i> and <i>sbe1a sbe2a</i> starch.....	168
Figure 4.4a	Chromatograms of isoamylase-debranched non-granular starch and amylopectin fractions from Wt, <i>sbe1a</i> , <i>sbe2a</i> , and <i>sbe1a sbe2a</i> starch.....	171
Figure 4.4b	Chromatograms of isoamylase-debranched amylose and intermediate material fractions from Wt, <i>sbe1a</i> , <i>sbe2a</i> , and <i>sbe1a sbe2a</i> starch .....	172
Figure 4.5	Chromatograms of isoamylase-debranched non-granular starch from Wt, <i>sbe1a</i> , <i>ae</i> , and <i>sbe1a ae</i> starch .....	175
Figure 4.6	Chromatograms of isoamylase-debranched resistant starch from Wt, <i>sbe1a</i> , <i>sbe2a</i> , and <i>sbe1a sbe2a</i> starch.....	176
Figure 4.7	Chromatograms of isoamylase-debranched resistant starch from Wt, <i>sbe1a</i> , <i>ae</i> , and <i>sbe1a ae</i> starch .....	177
Figure 4.8	Chromatograms of isoamylase-debranched and isoamylase-plus-pullulanase-debranched $\beta$ -limit dextrins from amylopectin fraction from <i>sbe2a</i> and <i>sbe1a sbe2a</i> starch .....	182

Figure A.1a	Additional scanning electron micrographs of Wt native starch.....	220
Figure A.1b	Additional scanning electron micrographs of <i>sbe1a</i> native starch.....	221
Figure A.2a	Additional scanning electron micrographs of Wt resistant starch .....	222
Figure A.2b	Additional scanning electron micrographs of <i>sbe1a</i> resistant starch...	223
Figure B.1	Digestion time-course for maize leaf starch deficient in different starch-branching enzyme activities.....	231-232
Figure B.2	Digestion rate constants ( $k_1$ ) of component 1 for several maize leaf starch and <i>aeVII</i> starch .....	233
Figure B.3	Scanning electron micrographs of native 2-month leaf starch from <i>sbe2a wx</i> and <i>sbe1a ae wx</i> mutant .....	235
Figure B.4	Scanning electron micrographs of residual 2-month leaf starch from <i>sbe2a wx</i> and <i>sbe1a ae wx</i> mutant, digested by $\alpha$ -amylase for 0.5 min.....	236
Figure B.5	Scanning electron micrographs of residual 2-month leaf starch from <i>sbe2a wx</i> and <i>sbe1a ae wx</i> mutant, digested by $\alpha$ -amylase for 2 hr.....	237
Figure B.6	Scanning electron micrographs of residual 2-month leaf starch from <i>sbe2a wx</i> and <i>sbe1a ae wx</i> mutant, digested by $\alpha$ -amylase for 16 hr...	238

## LIST OF TABLES

Table 2.1	PCR Primers for genotyping the maize <i>sbe</i> mutants used in this study.....	57
Table 2.2	Kinetics of digestion of the resistant starch assay: Process for obtaining two technical replications for each biological replication for analysis of Wt and <i>sbe1a</i> starch.....	67
Table 3.1	Nested ANOVA results of resistant starch value versus the three sequentially nested factors of genotype, biological replication, and technical replication, for endosperm starch from Wt and <i>sbe1a</i> mutant.....	81
Table 3.2	Resistant starch values for Wt and <i>sbe1a</i> mutant starch.....	82
Table 3.3	Kinetics of digestion of the resistant starch assay for Wt and <i>sbe1a</i> mutant starch.....	83
Table 3.4	Recovery of starch fractions (% w/w) by differential alcohol precipitation from Wt and <i>sbe1a</i> mutant starch.....	87
Table 3.5	Iodine binding properties of non-granular starch and starch fractions recovered by differential alcohol precipitation from Wt and <i>sbe1a</i> mutant starch.....	90
Table 3.6	Partial chromatogram areas of amylopectin and amylose fractions from size-exclusion chromatography for Wt and <i>sbe1a</i> mutant starch.....	93
Table 3.7	Chain length distribution of isoamylase-debranched non-granular starch and starch fractions from Wt and <i>sbe1a</i> mutant starch.....	97
Table 3.8	Chain length distribution of isoamylase-debranched native starch and resistant starch from Wt and <i>sbe1a</i> mutant starch.....	100
Table 3.9	Chain length distribution of isoamylase-debranched and isoamylase-plus-pullulanase-debranched $\beta$ -limit dextrins from the amylopectin fraction from Wt and <i>sbe1a</i> mutant starch.....	105
Table 3.10	Chain length distribution of isoamylase-debranched and isoamylase-plus-pullulanase-debranched $\beta$ -limit dextrins from the amylose fraction from Wt and <i>sbe1a</i> mutant starch.....	108

Table 4.1	Various <i>sbe</i> mutants differing in SBE isoform activities.....	154
Table 4.2	Resistant starch values for starch from mutant combinations of <i>sbe1a</i> and <i>sbe2a</i> (Wt, <i>sbe1a</i> , <i>sbe2a</i> , and <i>sbe1a sbe2a</i> ).....	157
Table 4.3	Resistant starch values for starch from mutant combinations of <i>sbe1a</i> and <i>ae</i> (Wt, <i>sbe1a</i> , <i>ae</i> , and <i>sbe1a ae</i> ).....	158
Table 4.4	Recovery of starch fractions (% w/w) by differential alcohol precipitation from Wt, <i>sbe1a</i> , <i>sbe2a</i> , and <i>sbe1a sbe2a</i> starch.....	160
Table 4.5	Iodine binding properties of non-granular starch and starch fractions recovered by differential alcohol precipitation from Wt, <i>sbe1a</i> , <i>sbe2a</i> , and <i>sbe1a sbe2a</i> starch.....	163
Table 4.6	Iodine binding properties of non-granular starch from Wt, <i>sbe1a</i> , <i>ae</i> , and <i>sbe1a ae</i> starch.....	166
Table 4.7	Partial chromatogram areas of amylopectin and amylose fractions from size-exclusion chromatography for Wt, <i>sbe1a</i> , <i>sbe2a</i> , and <i>sbe1a sbe2a</i> starch.....	169
Table 4.8a	Chain length distribution of isoamylase-debranched non-granular starch and amylopectin fraction from Wt, <i>sbe1a</i> , <i>sbe2a</i> , and <i>sbe1a sbe2a</i> starch.....	173
Table 4.8b	Chain length distribution of isoamylase-debranched amylose and intermediate material fractions from Wt, <i>sbe1a</i> , <i>sbe2a</i> , and <i>sbe1a sbe2a</i> starch.....	174
Table 4.9	Chain length distribution of isoamylase-debranched native starch and resistant starch from Wt, <i>sbe1a</i> , <i>sbe2a</i> , and <i>sbe1a sbe2a</i> starch...	178
Table 4.10	Chain length distribution of isoamylase-debranched native starch and resistant starch from Wt, <i>sbe1a</i> , <i>ae</i> , and <i>sbe1a ae</i> starch.....	179
Table 4.11	Chain length distribution of isoamylase-debranched and isoamylase-plus-pullulanase-debranched $\beta$ -limit dextrins from the amylopectin fraction from Wt, <i>sbe1a</i> , <i>sbe2a</i> , and <i>sbe1a sbe2a</i> starch.....	183-184
Table 5.1	Evidence of effects of maize SBE isoforms on endosperm starch structure.....	194-196
Table 5.2	Evidence of effects of maize SBE isoforms on endosperm starch digestion.....	200-202

Table A.1	Resistant starch values for Wt, <i>sbe1a</i> , <i>sbe2a</i> , and <i>sbe1a sbe2a</i> starch from the 2-gene segregating population.....	219
Table A.2	Resistant starch values for Wt, <i>sbe1a</i> , <i>ae</i> , and <i>sbe1a ae</i> starch from the 3-gene segregating population. ....	224
Table B.1	Resistant starch values for maize leaf starch deficient in different SBE activities.....	230

## ACKNOWLEDGEMENTS

I would like to convey my sincere thanks to my dissertation advisor, Dr. Donald Thompson, for guiding me with his strong logical thinking and detail-oriented problem solving skills, and to my co-advisor, Dr. Mark Gultinan, for his creative thinking and generous support. I would also like to thank my committee member, Dr. John Coupland, Dr. Devin Peterson, and Dr. Ming Tien for offering me valuable suggestions and providing me with their expertise without reservation. The thesis could not have been completed without their help.

Mostly importantly, I would like to thank my parents, husband, and daughter for their continuous support and care.

## Chapter 1

### LITERATURE REVIEW

#### 1.1 Introduction: The Structure and Function of Maize Starch

The starch granule is a highly-ordered structure with alternating crystalline and amorphous growth rings (for reviews of starch structure and function see Buleon et al. 1998; Gidley 2001). Starch molecules are biopolymers of anhydrodextrose units linked by  $\alpha$ -1,4 and  $\alpha$ -1,6 glycosidic bonds. They are composed of two glucan polymers, the generally linear fraction, amylose, and the branched fraction, amylopectin. As demanded by plant physiological needs, reserve starch in cereal grains is programmed to have dual functions, to preserve energy efficiently and stably, and to release energy by hydrolytic enzymes upon kernel germination. Although the capacity to produce this structure evolved millions of year ago during the evolution of plants, and although starch has been consumed by humans for thousands of years, research into the molecular structure and function of starch began only several decades ago.

Today, maize provides starch used widely in food and nonfood applications. Worldwide, in 2005 to 2006, over 701.6 million metric tons of maize starch was used in food and other non food applications (Corn Refiners Association, 2007). Starch from normal maize contains about 27% amylose and 73% amylopectin (Swinkels 1985). Depending upon the genotype, the amylose fraction in maize starch can vary from almost zero (*waxy* maize) to higher than 80% (high-amylose maize). The diverse varieties of maize starch provide opportunities for specialty applications in food processing and for improved nutrition, such as to provide starch with altered

digestibility (Annison and Topping 1994). In addition, the use of starch as a renewable source for production of other chemicals is a rapidly expanding field (White 1994; Bastioli 2001). Recently, its use in fuel ethanol production has increased due to rising oil costs. Maize starch represents an important biodegradable and renewable energy source.

## **1.2 Starch Biosynthesis**

The mechanisms controlling starch biosynthesis are still only partially understood. Even though the general pathway for starch biosynthesis has been described, the function of individual biosynthetic enzymes, their regulation, and the interactions between them and other cellular components are not yet fully understood.

### **1.2.1 The Starch Biosynthetic Pathway in Maize Endosperm**

The coordinated functions of four major enzymes in starch biosynthesis, ADP-glucose pyrophosphorylase (ADPGPPase; EC 2.7.7.23), starch synthase (SS; EC 2.4.1.21), starch-branching enzyme (SBE; EC 2.4.1.18), and starch-debranching enzyme (DBE; EC 2.4.1.41) (Myers et al. 2000) result in the two forms of starch molecules, amylose and amylopectin.

The primary substrate for starch synthesis is generally considered to be sucrose (Martin and Smith 1995). Most sucrose is hydrolyzed into glucose and fructose before it enters the endosperm amyloplast, where starch synthesis takes place. ADP-glucose, synthesized from glucose-1-phosphate and ATP in an ADPGPPase-catalyzed reaction, initiates glucose synthesis of the starch molecule (Press 1991).

SS isoforms are responsible for the polymerization of starch. SS catalyzes the synthesis of an  $\alpha$ -1,4 bond between the non-reducing end of a preexisting glucan

chain and the glucosyl moiety of ADP-glucose. SS can use both amylose and amylopectin as substrates *in vitro* (Martin and Smith 1995). Based on sequence relationships, at least four distinct SS isoforms can be defined, including granule-bond starch synthase (GBSS), SSI, SSII, and SSIII (Cao et al. 1999; Li et al. 1999). The deficiency of GBSS produces *waxy* (*wx*) mutants with essentially amylopectin only.

SBEs, which hydrolyze an  $\alpha$ -1,4 bond within a chain and then transfer the reducing end of the resulting  $\alpha$ -1,4 glucan to the C-6 position of the same or another  $\alpha$ -1,4 glucan, create the  $\alpha$ -1,6 branches in starch (Drummond et al. 1972).

Introduction of branches by a SBE facilitates starch synthesis by increasing the number of non-reducing ends, the reaction sites of glucose addition by SSs. DBEs also play a role in determining starch branching by hydrolyzing  $\alpha$ -1,6 bonds (Pan and Nelson 1984). The balanced action of SBE and DBE may be critical for determining the ultimate branching pattern in starch (Myers et al. 2000).

## **1.2.2 Roles of Maize Starch Branching Enzymes in Endosperm Starch**

### **Biosynthesis**

SBE plays an important role in starch biosynthesis by introducing the branch points in starch. Branch points are not distributed randomly in starch (Burchard and Thurn 1985; Thompson 2000). *In vitro* studies showed different SBE isoforms had different specificities for the length of the  $\alpha$ -1,4 glucan chain that they use as a substrate (Guan and Preiss 1993; Takeda et al. 1993), which may partly explain the non-random nature of the branching patterns created by SBEs.

Boyer and Preiss (1978) identified three major SBE isoforms in developing maize kernels: SBEI, SBEIIa, and SBEIIb. The SBE isoforms have been shown to be encoded by different genes. The *Sbe1a* gene encodes SBEI (Kim et al. 1998), the

*Sbe2a* gene encodes SBEIIa (Gao et al. 1997), and the *Sbe2b* (also called *Ae*, from the term *amylose-extender*) gene encodes SBEIIb (Boyer and Preiss 1981; Kim et al. 1999). Maize *Sbe1a*, *Sbe2a*, and *Ae* genes show different expression patterns in both tissue-specific and temporal dimensions (Fisher et al. 1993; Gao et al. 1996; 1997). In maize, *Sbe1a* and *Sbe2a* genes are expressed in both vegetative (leaf and root) and reproductive (endosperm and embryo) tissue, while *Ae* is highly expressed in endosperm and embryo development but is undetectable in leaf and root tissue (Gao et al. 1996; 1997).

The multiple isoforms of SBE have been found in many plants, and been categorized into Class A and B, based on differences in primary amino acid sequences and catalytic properties (Martin and Smith 1995). Maize SBEI belongs to Class B, and maize SBE IIa and IIb belong to Class A. The proteins of SBEII contain an additional N-terminal domain that is lacking in those of SBEI (Baba et al. 1991; Fisher et al. 1993). *In vitro* studies showed that both maize SBEII isoforms had a lower affinity for amylose than SBEI isoform and preferentially transferred shorter glucan chains during branch formation (Guan and Preiss 1993; Takeda et al. 1993). A conserved structural distinction between the two isoform types may be the most likely cause for this catalytic difference (Jespersen et al. 1993). As members of the  $\alpha$ -amylase super family, SBEs consist of a central  $(\beta\alpha)_8$  barrel structure involved in hydrolysis, and show conservation of amino acid residues in the loops connecting each central  $\beta$ -strand with a following  $\alpha$ -helix (Jespersen et al. 1993). The loop between  $\beta$ -strand 8 and  $\alpha$ -helix 8 is very similar among the Class A isoforms and distinct from that in Class B isoforms, in length and sequence composition, supporting the idea that this loop is involved in substrate specificity and in creating branches with different length (Burton et al. 1995).

The significance of the contribution of the SBEII isoforms to starch biosynthesis is evident from analysis of the maize *ae* mutant which is deficient in SBEIIb. The *ae* mutant has a profound effect on starch granule morphology, as well as on starch structure (Garwood et al. 1976; Boyer et al. 1977; Boyer and Preiss 1981). Studies of the maize *sbe2a* mutant found that deficiency of SBEIIa isoform decreased plant fitness and resulted in lower kernel yield, but did not affect kernel starch properties as SBEIIb does (Blauth et al. 2001; personal communication, Drs. Marna Yandea-Nelson and Mark Guiltinan). The maize *sbe1a* mutant, deficient in SBEI, has not been well studied. Unlike the SBEIIb deficiency, which reduces starch synthesis during seed formation and causes a wrinkling or puckering of the dry seed, inactivation of maize SBEI or SBEIIa isoforms does not limit starch biosynthesis sufficiently to give rise to a visible phenotype (Blauth et al. 2002; 2001). Consequently the effect of the single deficiency of SBEI or SBEIIa isoforms in starch biosynthesis remains unclear.

*In vitro* biochemical analysis has been used to understand functions of maize SBEs in starch synthesis. Guan and Preiss (1993) used an iodine staining assay to test both amylose and amylopectin as substrates for different SBE isoforms with an *in vitro* system. Among the three isoforms, SBEI had the highest activity in branching amylose, but its rate of branching amylopectin was about 3% of that of amylose. In contrast, SBEIIa and SBEIIb branched amylopectin at twice the rate as they branched amylose. A related study from same group (Takeda et al. 1993) showed that the *in vitro* action of SBEIIa and SBEIIb on amylose preferentially resulted in shorter chains than the action of SBEI. These studies suggested a different *in vitro* action pattern by SBEII isoforms as compared to SBEI. A caution underlying these studies is that the *in vitro* property of SBEs tested with a controlled amount of amylose or amylopectin

may not replicate the actual function *in vivo*, as biosynthesis occurs in the presence of SSs and DBEs. In addition, the complex molecular components in a starch granule expose SBEs to different substrates than fractionated amylose or amylopectin. In the process of synthesizing a starch granule, it is tempting to speculate that the steric interaction between the starch molecular chains and the protein conformation of the enzyme may influence the efficacy of a SBE. The question whether there are functional differences among SBE isoforms in *in vivo* starch synthesis remains to be answered.

However, the evolutionary conservation of gene sequences encoding maize SBE isoforms across wide evolutionary distances, strongly suggests that these enzymes play unique and important roles in plant development (Gao et al. 1996; 1997; Blauth et al. 2001; 2002). Gene sequencing studies have shown that the SBEI and SBEII isoforms are conserved between all plants, and that SBEIIa and SBEIIb isoforms are conserved between most monocots (Burton et al. 1995; Gao et al. 1996; Morell et al. 1997; Blauth et al. 2001; Rahman et al. 2001; Xu and Messing 2008). The evolutionary conservation of maize SBEs indicates an essential role in starch synthesis during plant development.

Pleiotropic reduction in SBE activity has been observed in several maize mutants of other enzymes involved in starch biosynthesis, which suggests possible protein-protein or regulatory interactions (Gao et al. 1998; Beatty et al. 1999; Nishi et al. 2001; Seo et al. 2002; Colleoni et al. 2003; Dinges et al. 2001; 2003). Indeed, in wheat endosperm, SBEI and SBEIIb were shown to together interact with starch phosphorylase in a phosphorylation-dependent manner (Tetlow et al. 2004). The interaction of SBEs with SSs on starch biosynthesis has also been studied (Tetlow et al. 2004; 2008). These studies have begun to reveal the interaction between SBEs and

other starch synthetic enzymes, and have suggested that a multi-protein starch synthesizing complex(s) exist and that interactions within these complexes comprise the mechanisms for modulating the intricate structure of a developing starch granule.

### **1.2.3 Roles of Maize Starch Branching Enzymes in Endosperm Starch Structure**

#### **1.2.3.1 Identification of Maize *sbe* Mutants**

Important roles of SBEs have been indicated in directly determining the fine structure of starch (Blauth et al. 2001; 2002; Yao et al. 2003; 2004; Xia 2005) and in indirectly influencing starch granule structure (Li et al. 2007). A way to understand the *in vivo* function of SBE is by employing analytical approaches to examine starch structure of *sbe* mutants that are deficient in one or more SBE isoform activities. The study of maize genetics especially maize SBEs had a long-standing tradition at The Pennsylvania State University (PSU), starting with the research of Drs. Creech and Garwood, and continuing with Drs. Shannon and Boyer. The initial research focused on understanding the genetic control of the quantity and quality of storage carbohydrate in kernel development (Shannon and Garwood 1984). Through the identification of an *ae* mutation, Moore and Creech (1971) genetically defined a single locus that encodes the starch-branching enzyme (SBE) IIb isoform. Boyer et al. (1976) showed that the *ae* mutant produces endosperm starch with a higher proportion of amylose, consistent with previous findings (Vineyard and Bear 1952), and fewer branch points than normal in its amylopectin fraction. Boyer and Preiss (1978) then confirmed the absence of SBEIIb activity in *ae* endosperm. The *ae* research provided the first evidence for independent genetic control of a maize SBE isoform. By cloning and sequencing the cDNA, Fisher et al. (1993) showed that the *Ae* locus encodes SBEIIb and thus is synonymous with the *Sbe2b* gene.

Subsequently, Gao et al. (1997) cloned and sequenced the cDNA that encodes SBEIIa, and Kim et al. (1998; 1999) cloned and sequenced the genomic DNA that encodes SBEI.

Owing to its pronounced wrinkled kernel phenotype, the identification of the *ae* mutation resulting in the loss of SBEIIb is straightforward, and accounts for observation of this mutant in the 1950's (Vineyard and Bear 1952). However, mutations for the *Sbe2a* and *Sbe1a* gene were not identified based on visual phenotypic screening of kernels. Subsequent to the cloning of their genes, identification of the *sbe2a* and *sbe1a* mutants was accomplished via reverse-genetics strategies using *Mutator* (*Mu*) transposons (Blauth et al. 2001; 2002). To look for a *Mu* insertion within *Sbe2a* or *Sbe1a* gene, the Trait Utility System for Corn (TUSC) system at Pioneer Hi-bred International was utilized to screen a *Mu*-containing population of approximately 40,000 plants. From this screen, several unrelated F1 mutant plants, designated as *sbe2a::Mu* or *sbe1a::Mu* were identified. In the remainder of this work, *sbe2a* and *sbe1a* mean *sbe2a::Mu* and *sbe1a::Mu*, respectively. Blauth et al. (2001; 2002) then selfed the F1 plants to obtain the F2 progeny for screening homozygous *sbe2a* or *sbe1a* mutants (see details in Fig.2.2). While the *sbe1a* mutation did not exhibit any visible phenotype distinct from wild-type (Wt), the *sbe2a* mutation caused a severe leaf phenotype characterized by premature leaf senescence (Blauth et al. 2001).

### **1.2.3.2 Effects of Deficiency of Maize Starch Branching Enzymes on Endosperm Starch Structure**

A dominant role of SBEIIb on kernel starch structure has been well documented through the study of the maize *ae* mutant, which is deficient in SBEIIb.

Maize *ae* mutant produces starch with fewer branch points, longer average chain length (CL), as well as a much higher amylose percentage (Garwood et al. 1976; Boyer et al. 1977; Boyer and Preiss 1981). However, the role of the two other SBEs (SBEI and SBEIIa) and the coordinated role of multiple SBEs on starch structure are not well understood. Prior work in our group has explored the effect of SBEI or SBEIIa deficiency on starch structure (Blauth et al. 2001; 2002). However, those investigations failed to observe a difference in endosperm starch structure of *sbe1a* or *sbe2a* as compared to a Wt control. Blauth et al. (2001) studied the effect of *sbe2a* on endosperm starches by characterizing the size distribution of the debranched whole starches using high-performance size exclusion chromatography (HPSEC), and did not observe a difference in either CL profile or amylose percentage when comparing *sbe2a* to Wt (Fig.1.1). Blauth et al. (2002) then studied the effect of *sbe1a* by characterizing the size distribution of both whole starch and the debranched whole starch. No obvious difference was observed between *sbe1a* and Wt either (Fig.1.2). Although these two reports did not directly compare endosperm starches from *sbe1a* and *sbe2a*, there was no discernable difference from Wt for either mutation.

A subsequent study by Yao et al. (2004) examined the effect of *sbe1a* on the structure of amylopectin by backcrossing the *sbe1a* gene to the *wx* W64A background and selecting homozygous *sbe1a wx* mutants. Use of starch from the *wx* background allowed evaluation of an effect of *sbe1a* on amylopectin. There are two limitations for this study: (1) The amylopectin in *wx* may not be representative of the amylopectin in Wt; (2) the effect of *ae* in the *wx* background may not parallel the effect of *ae* on the amylopectin in the Wt background. The work of Klucinec and Thompson (2002) for commercial starches addressed the first limitation, as the CL profiles of *ae wx* and AP of *ae* were not identical.

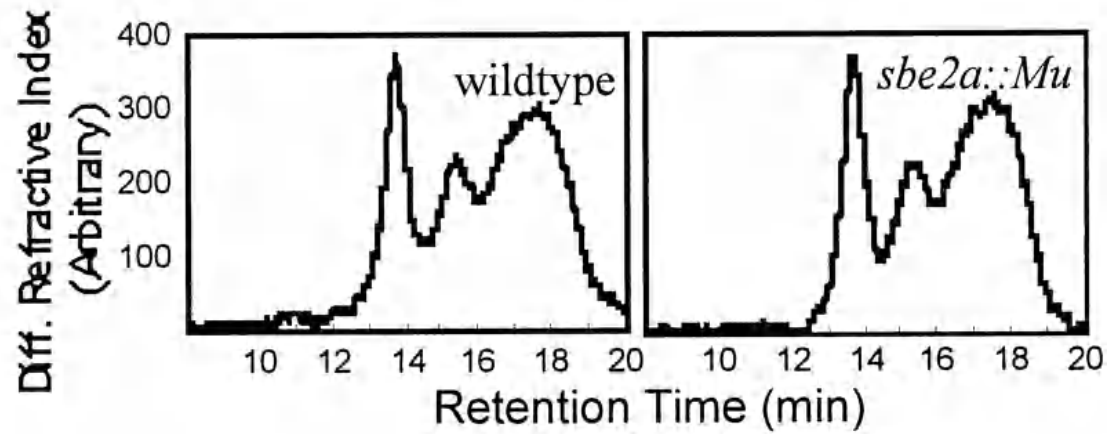


Figure 1.1 HPSEC of debranched endosperm starches from wild-type (left) and *sbe2a* mutant (right) in the W64A background (figure from Blauth et al. 2001 with permission).

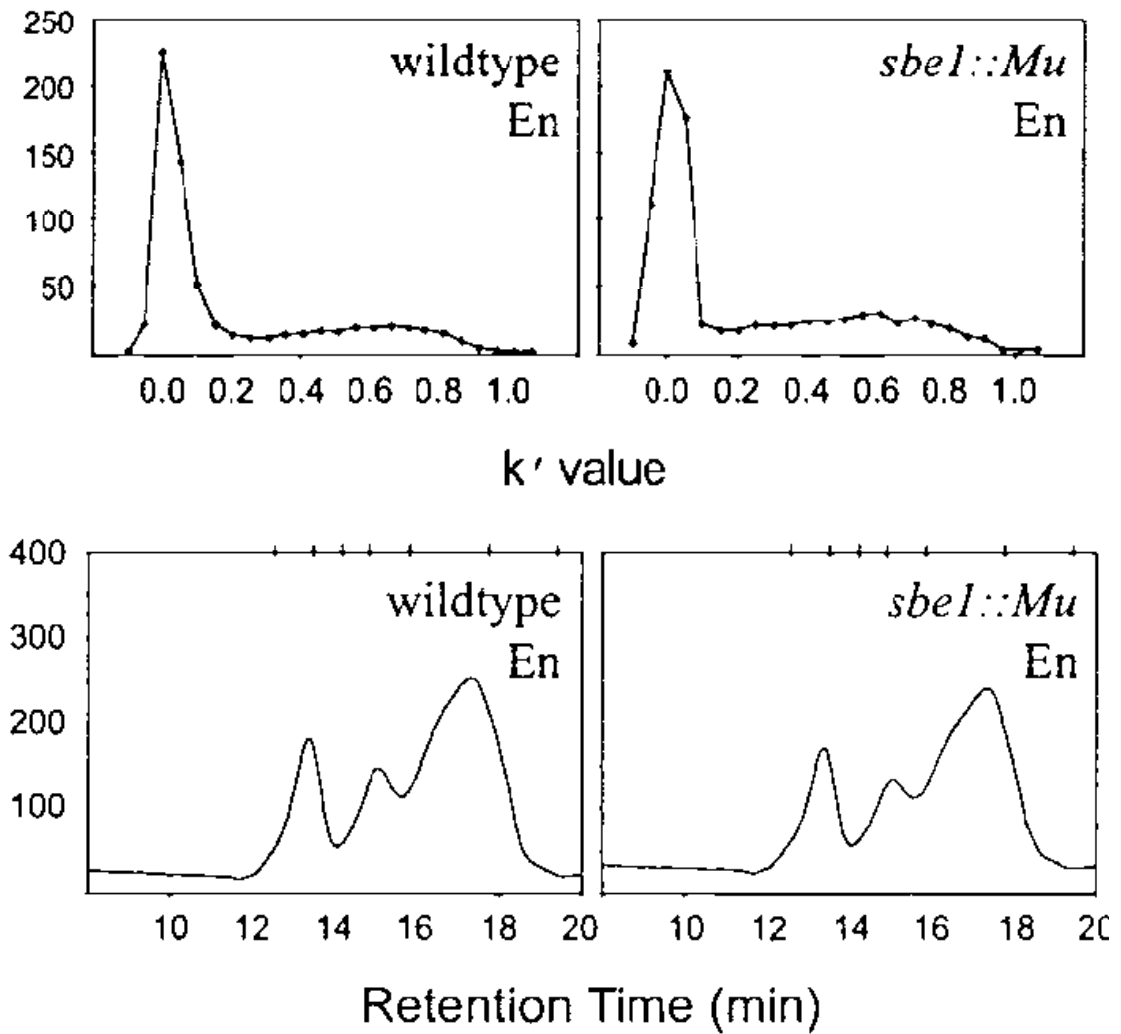


Figure 1.2 Size-exclusion chromatography of whole endosperm starches (upper graph) and HPSEC of debranched endosperm starches (bottom graph) from wild-type (left) and *sbel1a* mutant (right) in the W64A background (figures from Blauth et al. 2002 with permission). “En” indicates endosperm starch. “*sbel1::Mu*” indicates *sbel1a* mutant.

The work of Yao et al. (2004) determined CL profiles of both whole amylopectin and its  $\beta$ -limit dextrin ( $\beta$ -LD), which was obtained after exhaustive  $\beta$ -amylolysis on amylopectin. Their work (Fig.1.3) showed that compared to amylopectin of *wx*, *sbe1a wx* displayed essentially the same proportions of chain populations; *ae wx* had a lower proportion of B1 (B1a + B1b) chains, and a higher proportion of B2 and B3 chains; and the proportion of B1 chains and B2 + B3 chains for *sbe1a ae wx* was intermediate of *ae wx* and *sbe1a wx*. If B2 and B3 chains link amylopectin clusters, and B1 chains sit within clusters (Klucinec and Thompson 2002), a higher proportion of B1 chains over B2 and B3 chains may indicate a higher number of chains per cluster, which is another way of saying there is more branching in this starch. Based on this reasoning, Yao et al. (2004) showed that for *sbe1a* alone, no effect was observed, but for the double mutant *sbe1a ae*, for which only SBEIIa activity remained, more branching was observed as compared to *ae* alone. This result seemed to be a paradox as fewer SBE isoform introduced more branching in amylopectin. This work provided the first evidence of any kind of effect of the *sbe1a* mutation on endosperm starch structure. A later study by Li et al. (2007) found that the *sbe1a ae* and the *ae* genotypes differed at several different levels of structure, including granule morphology, birefringence, growth rings, and crystallinity. However, Li et al. did not observe an effect of *sbe1a* alone by any of these techniques; thus, the possible function of SBEI alone was not elucidated.

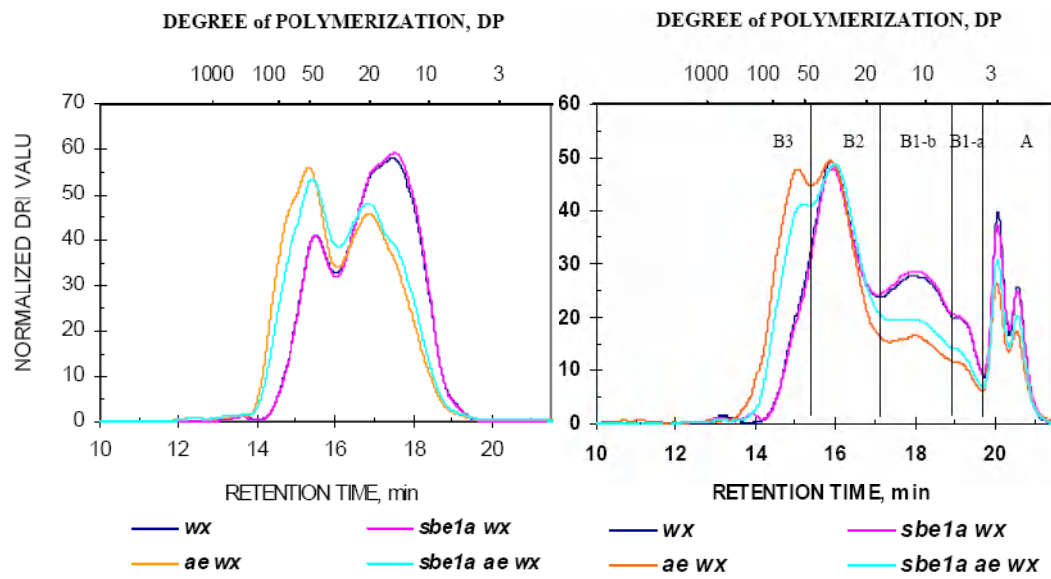


Figure 1.3 HPSEC of debranched starch (left) and debranched  $\beta$ -limit dextrin (right) from maize genotypes of *wx*, *sbe1a wx*, *ae wx*, and *sbe1a ae wx* in the W64A background (figures from Yao et al. 2004 with permission).

Yao et al. (2003) examined the effect of *sbe2a* and *ae* in the W64A background due to unavailability of seeds in *wx* background. Although occasional individual homozygous *sbe2a ae* seeds could be produced from segregating ears, it turned out to be very difficult to then grow them to produce homozygous ears to generate sufficient starch. Due to the deleterious leaf phenotype produced by the *sbe2a* mutation, the plants had severely compromised plant fitness and failed to produce ears. Thus, Yao et al. failed to generate comparable *wx*, *sbe2a wx*, *ae wx*, and *sbe2a ae wx* starch samples. Given the failure to produce *sbe2a ae* seeds from homozygous ears, a single-kernel-sampling (SKS) procedure was developed and used (Yao et al. 2002). Yao et al. (2003) first self pollinated plants heterozygous for *sbe2a* and homozygous for *ae*. They then removed a portion of endosperm and planted the seeds. They identified the homozygous *sbe2a ae* plants by genotyping the leaf tissues by PCR. For the homozygous plants they returned to analyze the previously sampled endosperm. A small-scale endosperm fractionation protocol for purification of amylopectin based on the fractionation procedure of Klucinec and Thompson (1998) was used to study amylopectin structure from the single kernels (Yao et al. 2003). Compared to amylopectin of Wt, no effect of *sbe2a* was observed (Fig. 1.4). However, similar to the comparison between *sbe1a ae wx* and *ae wx* (Fig. 1.3), for *sbe2a ae*, more branching was observed as compared to *ae* alone.

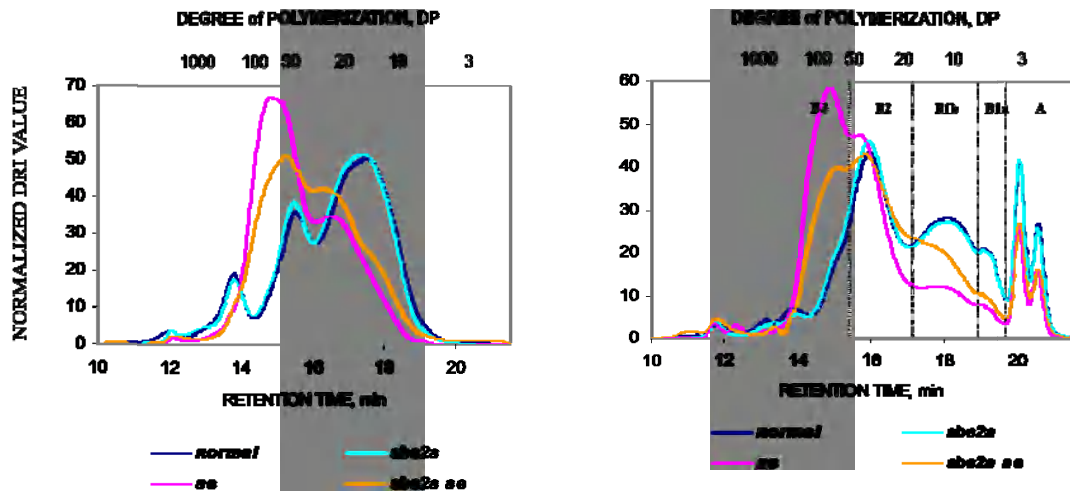


Figure 1.4 HPSEC of debranched amylopectin (left) and debranched  $\beta$ -limit dextrin (right) of amylopectin fractionated from maize genotypes of wild-type (*normal*), *sbe2a*, *ae*, and *sbe2a ae* in the W64A background (figures from Yao et al. 2003 with permission).

Methods used by Yao et al. (2003; 2004) employed analyses of  $\beta$ -LD to study the characteristic chains in amylopectin, and they succeeded in distinguishing the chain length profiles of amylopectin of *sbe1a* or *sbe2a* against that of *sbe1a ae* or *sbe2a ae*, respectively. Because  $\beta$ -LD is the product of exhaustive  $\beta$ -amylolysis of amylopectin, an altered branching pattern could be overlooked by examining only the  $\beta$ -LD structure. It is possible that an altered amylopectin branching pattern might cause differences during the  $\beta$ -amylolysis. A recent study using starch in the *wx* W64A background followed the progress of  $\beta$ -amylolysis of several *sbe* mutants (Xia 2005). The study showed that during the later stages of  $\beta$ -amylolysis, the residual degree of polymerization (DP) 4 chains had different susceptibility to further hydrolysis (Fig. 1.5). Xia (2005) reasoned that a slower rate of DP 4 reduction may be caused by steric hindrance from a higher proportion of closely associated branch points in the amylopectin in question. Based on the reasoning, the  $\beta$ -amylolysis result indicated that both of the single *sbe1a* and the single *sbe2a* mutant may have higher proportions of closely associated branch points than Wt. Thus, for the first time, evidence suggested a structural effect for the *sbe1a* or *sbe2a* mutation alone on endosperm starch. However the analysis was only conducted once due to limited starch samples at that time. Nevertheless, this study showed that  $\beta$ -amylolysis was a promising approach for exploring differences in starch branching structure.

In a different line of research, preliminary work on a limited number of samples suggested that *sbe1a* may have effect on endosperm starch digestibility (Xia et al. 2007). Using an analytical technique designed to evaluate the rate and extent of starch digestion in the human digestive tract (Evans and Thompson 2008; Rees 2008), it appeared that over 10% of the endosperm starch from *sbe1a* is resistant to digestion, whereas, almost none of the endosperm starch from Wt is resistant to digestion.

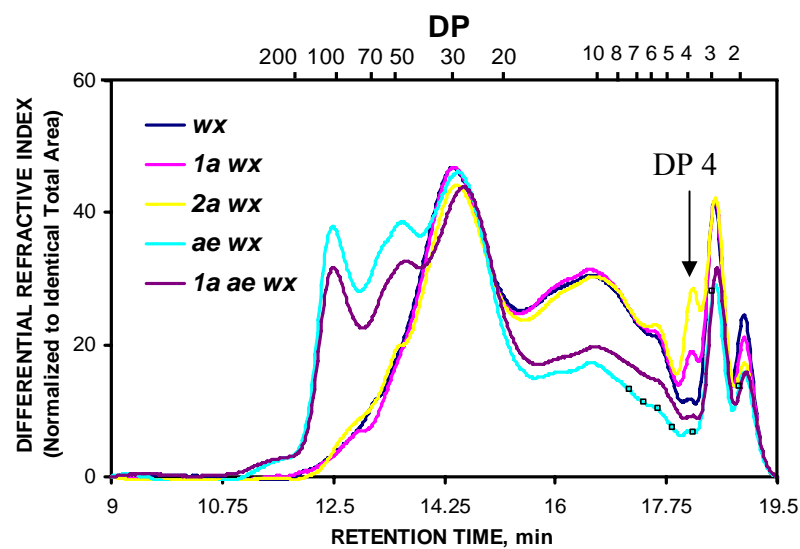


Fig. 1.5. HPSEC of debranched  $\beta$ -dextrins resulting from 2 hr of  $\beta$ -amylolysis (250 U/mL), from maize genotypes of *wx*, *sbela wx*, *sbela wx*, *ae wx*, and *sbela ae wx* in the W64A background (figure from Xia 2005 with permission).

This effect on starch digestion, coupled with the effect on fine structure seen in the previously mentioned study of  $\beta$ -amylolysis, led to further study starch structure from endosperm varying in SBE activities.

### **1.3 Starch Structure**

Although starch is often depicted as a “simple” polymer of glucose, it is a complex material. There are two fundamental factors behind this complexity. One is the existence of several characteristic levels of structure from macro to nano scales, and the second is the heterogeneity of structures at all of these different scales both within a single granule and across granules of different species. Methods probing the starch structure at each scale have been advanced, and structures at molecular and granular levels have been extensively studied and discussed below.

#### **1.3.1 Levels of Starch Structure**

##### **1.3.1.1 Molecular Structure**

From a molecular perspective, starch mainly consists of two types of  $\alpha$ -D-glucose homopolymers, amylose and amylopectin. Amylose consists of essentially linear  $\alpha$ -1,4-linked glucan chains with very few  $\alpha$ -1,6 branches (*ca.* 0.1%) (Hizukuri and Takagi 1984; Takeda et al. 1984; 1986). In contrast, although amylopectin also mainly consists of  $\alpha$ -1,4-linked glucan chains, it has a far higher proportion of  $\alpha$ -1,6 branch points (*ca.* 4%). Amylopectin is a much larger molecule than amylose, as the former has a molecular weight between  $10^7$  to  $10^8$ , while amylose reaches a molecular weight of  $5 \times 10^5$  to  $10^6$  (Hizukuri 1996). In some cases, a third molecular fraction of starch, called intermediate material (Adkins and Greenwood 1969), behaves as neither normal amylose (it does not precipitate with 1-butanol) nor normal amylopectin, and

pathway of starch degradation in germinating cereal endosperm (Smith et al. 2005). During germination, the  $\alpha$ -amylase hydrolyzes  $\alpha$ -1,4 linkages at the surface of the semi-crystalline granule, rendering it deeply pitted, with loss of internal material before much of the surface has been attacked (Smith et al. 2005). The degradation of the soluble glucans released from starch granules by  $\alpha$ -amylase probably proceeds via limit dextrinase (debranching enzyme),  $\alpha$ -amylase,  $\beta$ -amylase, and  $\alpha$ -glucosidase to produce maltose and glucose (Smith et al. 2005). The end products of the starch degradation are then taken up by the living scutellum in the embryo, which thereupon synthesizes sucrose for the growing seedling (Bewley and Black 1985). Thus, the susceptibility of endosperm starch granules to hydrolytic enzymes, including  $\alpha$ -amylase, would influence the efficiency of starch utilization by plant.

The efficiency of starch utilization during germination in turn would affect the young plantlets' ability to compete for resources such as light and soil nutrients and in turn, reproductive fitness. The efficiency of starch utilization during germination would be a powerful evolutionary force to select for genotypes of plants with starch molecules optimized for molecular structure as well as optimized for efficient storage and utilization. It is reasonable to hypothesize that since energy metabolism is so important to growth, development and reproduction, that complex mechanisms would evolve in higher plants. Gene duplication and neo-functionalization are well known mechanisms by which specific genes can evolve to express different isoforms of enzymes with slightly specialized expression patterns or different enzymatic activities (Gingerich et al. 2007; Prokhnevsky et al. 2008; Saleh et al. 2008). The evidence accumulated on the evolution and biochemistry of the SBEs support this hypothesis, and the research described in this thesis was designed to add a new dimension to this growing body of knowledge, at the level of starch structure and function.

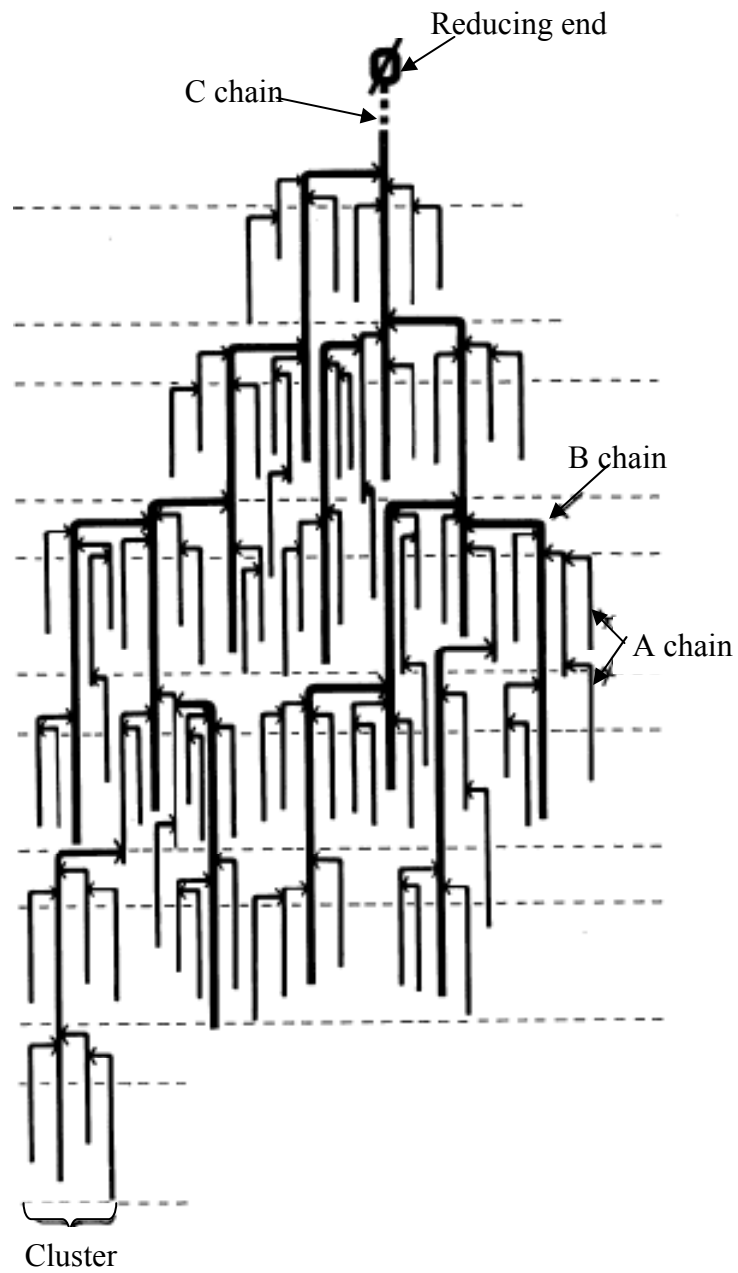


Figure 1.6 Amylopectin cluster model proposed by Robin *et al.* (1974). The figure is adapted from Robin *et al.* (1974) with permission. All the lines indicate constituent chains of amylopectin.

The constituent amylopectin chains may be further categorized according to characteristic segments using branch points as dividing lines to gain some insight about the relationship between branch points. An “external chain” represents the part of a chain that extends from the outmost branch point to the non-reducing end (Manners 1989). Thus, all A chains are external; whereas, only a part of every B chain is external. An “internal chain” represents the segment(s) of the B chain between two adjacent branch points. Since the word “chain” commonly refers to a continuous linear region, the term *internal segment length* (ISL) has been suggested to be preferable for describing the average distance between branch points (Thompson, 2000). Thus, an A chain has only one segment, an external segment, and a B chain has at least 2 segments, and more if it bears multiple branches. If a B chain bears one branch, then the B chain will have two segments: one exterior segment and one interior segment. A description of the ISL distribution would help clarify the relationship among branch points (Thompson, 2000), but no method is available to produce this information. Nevertheless, the work of Xia and Thompson (2006) has provided insight into the nature of the amylopectin branching pattern, by predicting structures for a portion of closely associated branch points.

### **1.3.1.2 Granular Structure**

Native starch granules are semi-crystalline, with the degree of crystallinity varying between 15 and 45% (Zobel 1988). The crystallinity is predominantly associated with the amylopectin, based on packing of double helices from pairs of adjacent branches within clusters. The external chain lengths in the amylopectin in part determine the degree of crystallinity (Hizukuri 1985). Amylopectin crystallites are radially symmetrical in the granules, resulting in a perpendicular arrangement of

the crystals to the radius. The chains are oriented with their non-reducing ends pointing toward the surface of the granule and are arranged into alternating crystalline and amorphous lamellae with a periodicity of 9 to 10 nm (Waigh et al. 1997; Ball and Morell 2003) (Fig. 1.7). In the crystalline lamellae, the external chains are associated in double helices and are packed together in an array to form clusters, while it is generally accepted that the branch points reside within the amorphous lamellae (Fig. 1.7). The starch granule is also known to contain relatively amorphous regions alternating with relatively crystalline regions (Gallant et al. 1997). The term “growth ring” has been suggested to describe the repeat of the alternating regions, which can be observed using electron microscopy after partial hydrolysis of starch granule (Fig. 1.7). Amylose molecules form single helical structures, and are thought to be packed into the amorphous regions, which are present throughout the granule (Jane and Shen 1993). Research also suggested that amylose molecules can participate in the helical structure with amylopectin external chains (Jenkins and Donald 1995).

As a result of different packing of helical structures in starch granules, different X-ray diffraction patterns (A, B, C, or V) can be obtained from starches of different plants. The A-type starches have more densely packed double helices (monoclinic lattice); whereas, the B-type starches have double helices arranged to form a void in which water molecules can be accommodated (hexagonal lattice) (Imberty et al. 1991; Gallant et al. 1997). The C-type is thought to be a combination of the A- and B-type patterns (Gallant et al. 1997). The V-type, formed by packed helices of an amylose and lipid complex, is not observed by itself in native granules.

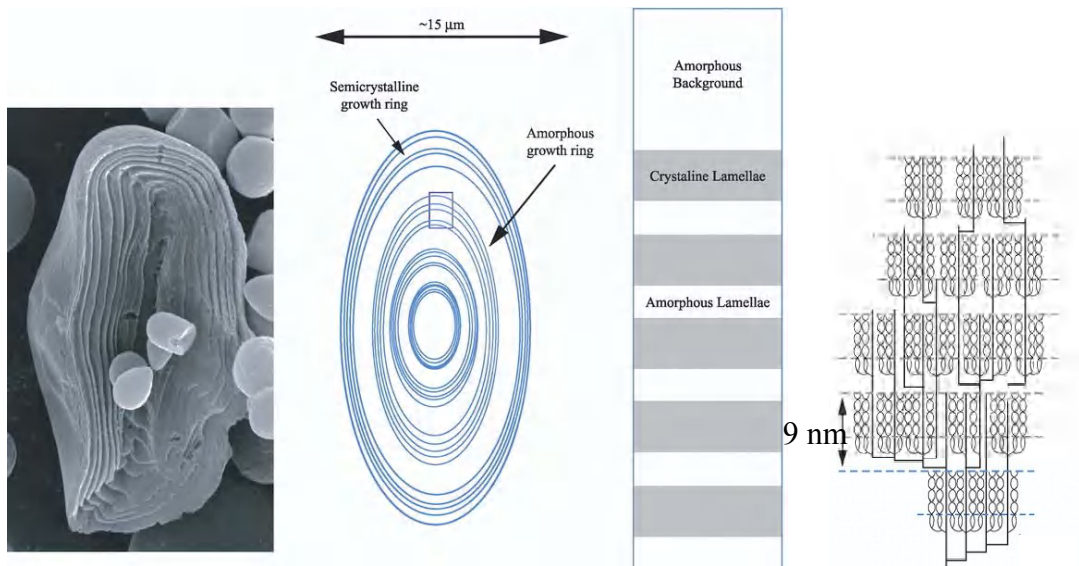


Figure 1.7 Schematic view of the hierarchical order within starch granule. The figure is adapted from Ball and Morell (2003) with permission.

Evidence from various microscopic techniques as well as from enzymatic degradation studies suggests that the crystalline and amorphous lamellae of the amylopectin molecules may be associated into larger spherical structures termed “blocklets” (Gallant et al. 1997). Gallant et al. (1997) proposed that the crystalline regions consist of larger blocklets (50 to 500 nm) than the amorphous regions, where the blocklet size ranges between 20 and 50 nm. However, blocklets have not been routinely observed by others.

### **1.3.2 Methods for Structural Analysis**

#### **1.3.2.1 Molecular Structure Analysis**

In order to perform starch molecular structure analysis, fractionation of starch into its components is often necessary. Fractionation is based on differences either in their binding behavior or in their molecular size. Amylose binds to small hydrophobic molecules such as 1-butanol to form an insoluble complex that precipitates from aqueous solution; intermediate material precipitates with a combination of isoamyl alcohol and 1-butanol, but not with 1-butanol alone (Takeda et al. 1986); whereas, amylopectin is the fraction remaining in the supernatant during isoamyl alcohol and 1-butanol precipitation (Klucinec and Thompson 1998).

In most of the starch molecular structure analysis done to date, the emphasis has been on amylopectin, the major fraction of starch. Probing the amylopectin molecular structure has been made possible by the use of different starch hydrolytic enzymes coupled with various chromatographic separation techniques. Three major classes of enzymes are useful for generating structural information by specific starch hydrolysis. The first group, debranching enzymes, includes isoamylase (EC 3.2.1.68) and pullulanase (EC 3.2.1.41), specifically hydrolyze  $\alpha$ -1,6-glycosidic linkages, and

thereby, release the unit chains from the macromolecule for determining the CL distribution. Isoamylase, generally considered as able to completely debranch intact amylopectin, is routinely used to obtain the CL distribution and the average CL, a number-average value that can be obtained by averaging the length of constituent linear chains in a completely-debranched amylopectin molecule. Isoamylase is less useful for hydrolyzing  $\beta$ -LDs, especially with respect to the DP 2 stubs, which result from residual A chains. The intact amylopectin does not have DP 2 stubs, allowing a complete debranching by isoamylase. For normal starches, isoamylase hydrolyzes the DP 2 chains from  $\beta$ -LDs only very slowly in comparison with DP 3 or longer chains (Yokobayashi et al. 1970; Kainuma et al. 1978; Hizukuri and Maehara 1990); whereas, pullulanase can readily and completely release the DP 2 chains at the activities commonly employed (Marshall and Whelan 1974). Some longer branches in starch have reduced susceptibility to pullulanase as compared to isoamylase (Harada et al. 1972; Xia and Thompson 2006). Thus, pullulanase is routinely used jointly with isoamylase to completely debranch  $\beta$ -LDs.

The second group includes the exo-acting enzymes. The most commonly used one is  $\beta$ -amylase (EC 3.2.1.2), which hydrolyzes amylopectin molecules at the second  $\alpha$ -1,4 linkage from the non-reducing ends until it nears a branch point. When  $\beta$ -amylolysis of branched molecules is complete, the products are  $\beta$ -maltose and  $\beta$ -LDs. The  $\beta$ -LD is useful for analysis of the branched nature of starch because it contains all the original branch points. The constituent chains in the  $\beta$ -LD include the residual A chains and the residual B chains. Thus, the A/B chain ratio of the original amylopectin molecule is identical to the A/B ratio determined for the  $\beta$ -LD, and can be estimated using the CL profile of the  $\beta$ -LD, where the DP 2 and DP 3 chains are assumed to be only from residual A chains. The CL profile of residual B chains obtained from

complete  $\beta$ -amylolysis is useful for differentiating amylopectin molecular architectures. Observations of the CL distribution of residual B chains appeared bimodal or even trimodal (Hizkuri 1986), and the ratio of short residual B chains to long residual B chains appeared different among amylopectins from different genotypes, suggesting a difference in the number of B chains per cluster (Klucinec and Thompson, 2002). The residual B1a chain, defined as short residual B1 chains, exhibited a shoulder around DP 4-7 (Yao et al. 2004). Structures resulting in the residual B1a chains of DP 4-7 were proposed to contain closely associated branch points (Xia and Thompson 2006).

The third group includes the endo-acting enzymes, often represented by  $\alpha$ -amylase (EC 3.2.1.1).  $\alpha$ -Amylase catalyzes the hydrolysis of most  $\alpha$ -1,4 linkages in starch. The nature and the distribution of hydrolysis products depend on the action pattern of the different  $\alpha$ -amylases, chiefly determined by their source. A frequently-used  $\alpha$ -amylase for determining human starch digestibility, porcine pancreatic  $\alpha$ -amylase (PPA), has been postulated to contain five subsites, with the catalytic site located between the second and third subsite from the reducing-end subsite (Robyt and French 1970; Robyt 1984). PPA hydrolysis on starch appeared to be an endwise, multiple-attack action pattern (Banks and Greenwood 1977; Mazur and Nakatani 1993). Using an  $\alpha$ -amylase from a bacterial source, Bertoft's group (Bertoft 1989; 2004; Gerard et al. 2000; Manelius et al. 2000; 2002; 2005) has employed limited  $\alpha$ -amylolysis to isolate fractions of amylopectin clusters for describing the branching characteristics of individual clusters.

Separation of debranched starch molecules provides easy access to the CL profile, and the reciprocal of average CL can be used to calculate "branching density". However, defining the branching pattern is more difficult. That branch points have a

general tendency to cluster is well established (Nikuni 1969; Robin et al. 1974; Hizukuri 1986), but to determine the specific molecular architecture in the regions of high branching density is difficult. One of the recent efforts to describe the starch branching pattern includes three parameters Yao et al. (2004) developed by analyzing the CL profiles of  $\beta$ -LDs. The assumption of their work was that amylopectin chains were connected in the cluster model of Hizukuri (1986), which assumed one B2 chain to initiate one cluster and one B3 chain to initiate two clusters. However, the assumption made may be questioned, as Thompson (2000) interpreted three possible ways a long B chain could be connected according to the models drawn in Robin et al. (1974), which would result in different cluster numbers and structures. The first parameter Yao et al. developed, termed the average number of branches per cluster (ANBPC), was calculated as the total number of chains divided by the total number of clusters. It is important to remember that their estimation about the total number of clusters as the number of B2 chains plus twice the number of B3 chains is made based on the assumption.

The second parameter, cluster repeat distance, was defined as the distance between two initiation points of two consecutive clusters. Based on the model Yao et al. (2004) chose, the average cluster repeat distance was equal the average internal length of a B2 chain or half of the average internal length of a B3 chain. However, the internal length of a long B chain could vary if the clusters are connected differently on them. Thus, the cluster repeat distance they obtained in the study is also based on an assumption. Therefore, their conclusion that cluster repeat distance was unaffected by the studied genotypes may be questioned.

The third parameter Yao et al. (2004) developed was the distance between adjacent branch points in the cluster. They subdivided the B1 chains to estimate this

parameter using the distance between branch points on residual B1a chain, defined as residual B1 chain of DP of 4-7, after debranching with both isoamylase and pullulanase. They assumed that only one chain is attached to each B1a chain. The modal peak DP value was used to estimate the average ISL of the B1a chains. Xia and Thompson (2006) debranched the  $\beta$ -LD first by isoamylase then further by pullulanase. They found that after debranching with isoamylase only, the proportion of residual B1a chains was fewer than that after debranching with both enzymes. They proposed that the portion of residual B1a chains that could be further debranched by pullulanase is likely to have two branches on the chain. This portion is about 15% of the weight percent of the total short B1 chains. Thus, if Yao et al. took into account the B1a chains with two branches, a more precise estimate for the third parameter would have been possible. In addition, for estimating the average ISL of B1a chains, the number-average DP of B1a chains may be better than the modal peak DP Yao et al. used. Given this more careful consideration, the third parameter, the distance between adjacent branch points in the cluster, may be more useful for differentiating among similar branching patterns than the first and second parameters, as these require an assumption about a precise definition of a cluster, a definition which is not yet available.

Lee (1971) concluded that the action of  $\beta$ -amylases on AP probably takes place in two stages. In the first stage, the most external portions of external chains are rapidly degraded. In the second stage, Lee suggested that partly degraded A chains of DP 4 are slowly degraded to DP 2. Xia and Thompson (2006) suggested that a differential extent of degradation of DP 4 stubs by  $\beta$ -amylase may be due to differences in steric hindrance due to differences in the proportion of closely associated branch points. Based on this reasoning, Xia and Thompson (2006)

suggested that the proportion of closely associated branch points varies among amylopectins from different maize genotypes.

By using  $\beta$ -LDs from amylopectin, Xia and Thompson (2006) developed another technique to explore amylopectin branching pattern, through stepwise debranching of  $\beta$ -LDs by isoamylase and pullulanase. Their work suggested that subsequent pullulanase debranching can release some DP 5-7 chains which are originally closely associated branch points with DP 2 stubs. Branching patterns including these DP 5-7 chains are illustrated in models B, C, D of Fig. 1.8.

Although amylose is a minor component in most granules, its influence on starch behavior can be substantial. The molecular structure of amylose may be an important factor influencing starch enzyme resistance. Peat et al. (1952) first suggested the presence of branches in amylose based on incomplete  $\beta$ -amylase degradation. The branches were later confirmed to be  $\alpha$ -1,6-glucosidic linkages as they were completely removed by concurrent action of  $\beta$ -amylase with isoamylase or pullulanase (Kjolberg and Manners 1963; Banks and Greenwood 1966). Without  $\beta$ -amylase, isoamylase alone was not capable of hydrolyzing all the branch linkages in intact amylose from both potato and maize (Hizukuri et al. 1981; Takeda et al. 1990). We have suggested that this specificity of isoamylase is also true for the most closely associated branch points in  $\beta$ -LDs from amylopectin (Xia and Thompson, 2006). Thus, a conceivable hypothesis to explore why isoamylase does not hydrolyze all the branch points in amylose is that some closely associated branch points may exist in the branched structure of amylose. The fact that the isoamylolysis products from amylose can be further debranched with pullulanase (Hizukuri et al. 1981) is consistent with the hypothesis of the presence of closely associated branch points,

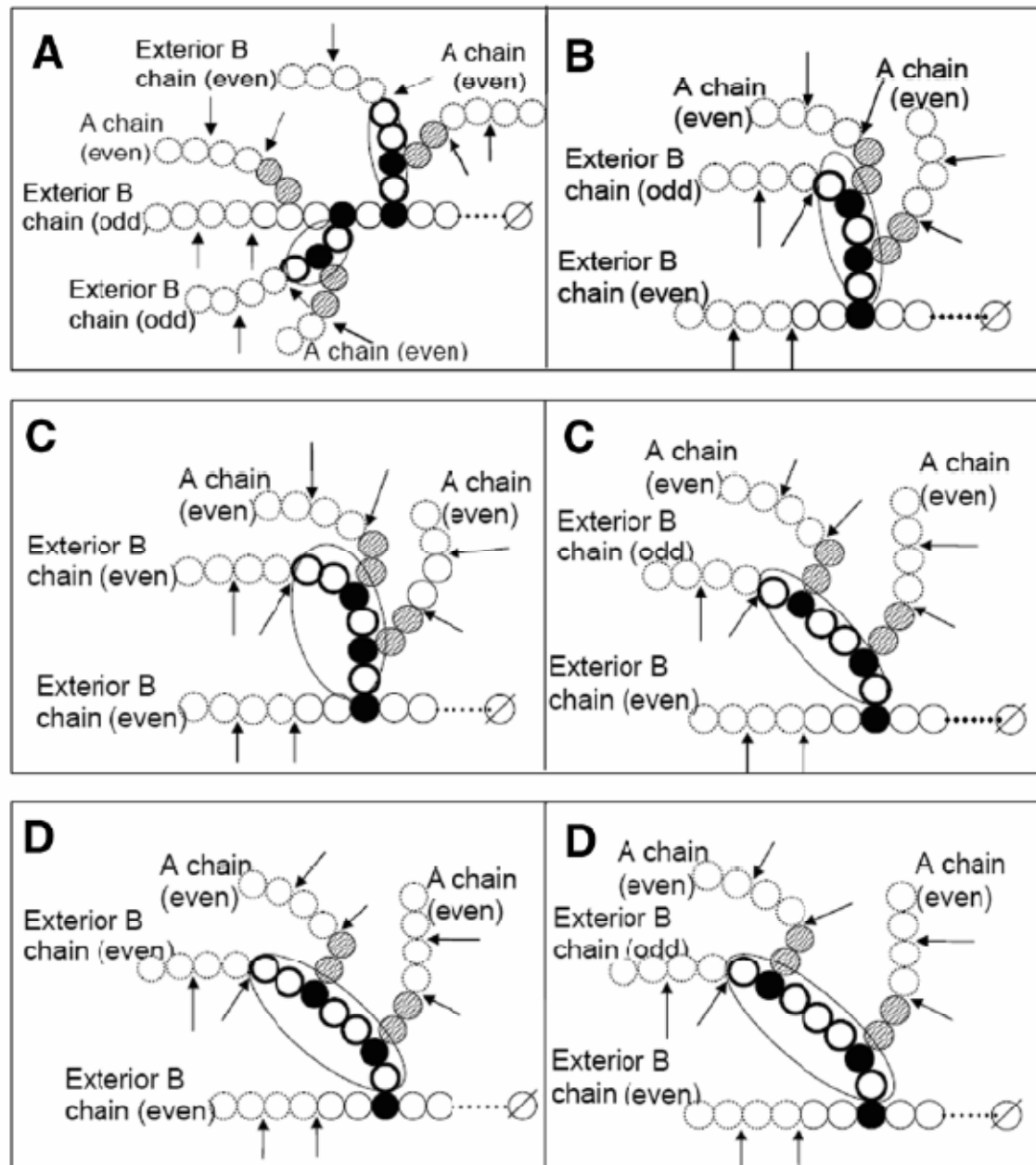


Figure 1.8. Amylopectin branching pattern model in the form of  $\beta$ -limit dextrin that would not be readily attacked by isoamylase but that would be easily attacked by pullulanase to release a short residual B chain. Circles with thicker edges and encircled in an ellipse indicate the glucose units of preserved short residual B chains. All circles indicate glucose units. Dotted circles represent the last part of the material cleaved in the formation of  $\beta$ -limit dextrin. Arrows indicate action sites of  $\beta$ -amylase. Solid black circles indicate closely associated branch points in  $\beta$ -limit dextrin that might be difficult for isoamylase to hydrolyze. Shaded circles indicate DP 2 stubs that are not hydrolyzed efficiently by isoamylase and that may protect other branch points from the action of isoamylase. Circles with a slash indicate reducing ends.

**A**, structure that preserves residual B chains of 3 or 4 units, with all the ISL = 1.  
**B**, 5-unit residual B chain with two branch points; ISL = 1.  
**C**, 6-unit residual B chains with two branch points; ISL = 1 or 2.  
**D**, 7-unit residual B chains with two branch points; ISL = 1, 2 or 3.

The figure and legend are adapted from Xia and Thompson (2006) with permission.

since pullulanase was shown to further debranch the most resistant structures in  $\beta$ -LDs, which had escaped isoamylase hydrolysis (Xia and Thompson 2006).

### **1.3.2.2 Granular Structure Analysis**

Substantial progress in investigating the supra-molecular architecture of starch granules has become possible by the use of various microscopic techniques. Bright field microscopy is commonly used to study granule shape and size, and to follow morphological changes during granule gelatinization or hydrolysis (Fitt and Snyder 1984; Eliasson and Gudmundsson 1996). Polarized light microscopy (PLM) can be used to examine the birefringence of starch granules due to the radial orientation of starch molecules (Evans and Thompson 2004). Scanning electron microscopy (SEM) has been used to detailed granule surface imaging as well as granule ultrastructure after fracture or partial hydrolysis (Gallant et al. 1997). Transmission electron microscopy (TEM) has been used to reveal the enzyme hydrolysis pattern inside granules (Evans and Thompson 2004). Additional microscopy techniques such as atomic force microscopy and confocal laser scanning microscopy have also been used for imaging starch granule (Baldwin 1998; Ridout et al. 2003; Juszczak et al. 2003; Blennow et al. 2003). Differential interference contrast (DIC) microscopy has been used to visualize starch granule growth rings after limited hydrolysis (Li et al. 2007).

Bright field microscopy and PLM are easy and cheap ways to visualize many starch granules at a relatively low magnification. A combination of SEM and TEM has been used successfully in our laboratory to examine the details of enzyme-digested starch granules (Evans and Thompson 2004; Rees 2008), drawing on the work of Faissant et al. (1995).

## 1.4 Starch Digestion by $\alpha$ -Amylase

### 1.4.1 Digestion Rate and Extent

Starch hydrolysis is an important feature of starch functionality both in the plant and when the plant is used for human food. Starch molecules in native granules are simply not as readily accessible to human digestive enzymes ( $\alpha$ -amylases) as when the molecules are dispersed by cooking, and consequently, hydrolysis is slower or incomplete (Neil et al. 2005). The rate and extent of starch digestion has been seen to vary according to starch source, as determined in *in vivo* human studies and *in vitro* measurements using pancreatic  $\alpha$ -amylase (Englyst et al. 1992). In the human digestive tract, the extent of starch digestion has become a subject of considerable interest; the undigested starch is termed resistant starch (RS). The most proper definition of RS is in physiological terms: starch and starch degradation products not absorbed in the small intestine of healthy individuals (EURESTA, 1991). According to several distinct mechanisms accounting for poor starch digestibility, RS was originally classified into three types (Englyst et al. 1992). Type 1 RS is due to physical inaccessibility of the starch granule, such as in whole grains or large particulates. Type 2 RS is due to the poor digestibility of native starch granules from certain sources, such as raw potato, banana, and high-amylose maize starches. Type 3 RS is due to the physical re-association or retrogradation of starch molecules after processing, often leading to formation of some crystallinity. Subsequently, type 4 RS was defined to account for resistance due to chemical modification (Eerlingen and Delcour 1995; Brown 1996).

Formally, the physiological definition of RS requires an *in vivo* method with human subjects, which is difficult, costly and time-consuming. Many attempts have been put forward to develop an effective *in vitro* method to simulate the *in vivo*

results. Various *in vitro* methods applying PPA hydrolysis at 37°C have been developed to determine a RS value (Englyst et al. 1992; Goni et al. 1996; McCleary and Monaghan 2002). The method developed by McCleary and Monaghan (2002) has been approved by both Association of Analytical Communities (AOAC) and American Association of Cereal Chemists (AACC) as an official *in vitro* RS determination method (AOAC 2002.02, AACC 32-40). This official method has provided results consistent with the *in vivo* data for several starch samples (Goni et al. 1996; McCleary and Rossiter 2004). To allow analysis of small samples (~20 mg wet basis) instead of 100 mg, the official method has been modified (Evans and Thompson 2008); the method has been further modified to follow starch digestion over time to calculate digestion rates (Rees 2008).

The rate of starch digestion from food determines the rate of glucose absorption, and is important for human health by helping to maintain proper blood glucose levels and to provide extended energy absorption. O'Dea et al. (1981) suggested that differences in glycemic and insulinemic responses to dietary starch are directly related to the rate of starch digestion. In an attempt to study the rate of starch digestion from a nutritional point of view, Englyst et al. (1992) developed an *in vitro* method to classify starch into three categories: rapidly digested starch (RDS), slowly digested starch (SDS), and RS. As described by Englyst et al. (1992), RDS is the portion of the starch that is completely digested to glucose within 20 min of enzyme addition; SDS is the portion that is digested after a further 100 min.

The rate of starch digestion was studied in a quantitative way by Rees (2008). She analyzed the kinetics of starch digestion over 16 h by use of a double exponential model to fit five parameters to the data, thus eliminating the use of an arbitrary 20-min time point as in the procedure of Englyst et al. (1992) to distinguish RDS and

SDS. Two components of starch substrate with two digestion rate constants were obtained from the model, one component digested more readily than the other. The amount of the two components and the two rate constants differed among different starches. The fifth parameter is the asymptotic limit of digestion. If the limit of digestion asymptotically reaches a plateau after 16 hr (the time that corresponds to the RS value), it can be used to estimate RS value.

#### **1.4.2 Nutritional Value**

Digestion of starch and absorption of glucose from starch occur in the small intestine. The rate and the extent of starch digestion in the small intestine are both nutritionally important.

RS has been considered to have similar beneficial effects as some types of dietary fiber (Englyst et al. 1987; Muir et al. 1995). Fermentation of RS in the large bowel has been assessed indirectly through the measurement of an increase in breath hydrogen and in fecal short-chain fatty acids, and of a decrease in fecal pH. Butyrate yield from RS has been shown to be comparatively high (Englyst and Cummings 1987; Weaver et al. 1992). Butyrate is a main energy substrate for large intestinal epithelial cells, and inhibits the malignant transformation of such cells *in vitro* (Asp and Bjorck 1992). These findings make the fermentable RS fractions especially interesting concerning the prevention of colonic cancer. In addition to affecting the extent of digestion and serving as a fermentation substrate, RS may also act as a prebiotic, favorably influencing the ecology of the microbial flora in the large intestine (Brown et al. 1997; Gibson and Roberfroid 1995; Wang et al. 2002). There is also evidence that RS is beneficial with respect to survival of beneficial microorganisms added to food (probiotics) (Topping et al. 2003). Topping et al.

(2003) argued that when RS and certain probiotics are both consumed, the RS acts as a substrate for the probiotic organisms.

### **1.4.3 Factors Influencing Digestibility of Starch Granules**

The refractory nature of type 2 RS is due to poor digestibility of the native starch granule by pancreatic  $\alpha$ -amylase (Englyst et al. 1992). Both granular and molecular structures could have effects on starch hydrolysis by  $\alpha$ -amylase. Granular structure includes granule surface features such as shape, size, and pores, as well as granule interior architecture. Interior structure has been examined using partially enzyme-hydrolyzed starch granules. Molecular structure mainly refers to the fine structure of amylose, amylopectin, and intermediate material, and may serve as the basis for granular structure. Thus, the molecular structure may be fundamental in understanding granule-scale enzymatic resistance.

The crystalline fraction of starch granules has received intense attention in the studies of granule enzymatic resistance. It is widely accepted that amylopectin molecule is predominantly responsible for granule crystallinity (Gallant et al. 1997). As introduced earlier (see 1.3.2), different packing arrangements of the amylopectin side-chain double helices results in different types of granule crystallinity (Zobel 1988). B-type crystallites are less densely packed than A-type and may be formed preferentially by longer chain than A-type (Whittam et al. 1990). Many B-type starch granules (potato, banana, and high-amylose starch) have high resistance to enzymatic attack (Planchot et al. 1995; Buleon et al. 1998).

Amylose content appears to be another important factor contributing to granule resistance to hydrolysis. Many of the granules in high amylose maize starch have non-symmetrical granule shapes (Buleon et al. 1998). This altered granule

phenotype implies the importance of a normal amount of amylose for granule structural order during starch biosynthesis. Starches containing high levels of amylose such as wrinkled pea, high-amylose maize, and the small wheat granules are more resistant to enzymatic attack than the corresponding starches with lower amylose content, such as smooth pea, normal and *wx* maize, and large wheat granules, respectively (Gallant et al. 1992). The fact that potato and banana starch with normal amylose content has high resistant starch suggests that granule amylose content cannot fully account for granule enzymatic resistance.

Other amylose-related factors may also have influences on granule enzymatic resistance. The location of amylose within the granules, as well as the complex formed by amylose and lipid may influence local crystallinity and granule enzymatic resistance (Morrison and Gadan 1987; Morrison 1995). Significant enrichment of amylose was found to exist toward the granule surface in starches such as wheat, potato and high-amylose maize (Morrison and Gadan 1987; Atkin et al. 1999), which was suggested to be responsible for the increased resistance of the granule surface (Gallant et al. 1992). The putative closely associated branch points in amylose (as elaborated earlier in 1.3.3.1), indicated by the incomplete isoamylase hydrolysis, may increase the enzyme resistance of granule surface enriched of amylose. Evidence also suggested that the interaction of amylose with amylopectin may influence local crystalline structure order and alter enzyme resistance (Gidley et al. 1995).

As the amylopectin molecule is mainly responsible for granule crystallinity, amylopectin molecular structure would have a significant influence on granule enzymatic resistance. A key concept of amylopectin molecular structure is the non-random nature of the branching. The distribution of the branch points (i.e. branching pattern) in amylopectin is important to the formation of granule crystallinity. The

elements of the crystallinity are pairs of linear AP external chains in the form of double helices. How the branch points are located on chains would determine the external chain length, influence the stability and packing of the double helices, and thus alter accessibility of starch to hydrolytic enzymes.

The specific action pattern of PPA on a dispersed amylopectin molecule has been studied to understand the influence of amylopectin molecular structure on starch digestion. An established concept was that the direction of multiple attack of PPA on starch is toward the non-reducing end of the substrate (Robyt and French 1970). Mazur and Nakatani (1993) further studied the action pattern of PPA on dispersed amylopectin and suggested the detailed pattern by proposing a model: at the initial stage of amylopectin digestion by PPA, most multiple attack is initiated near the end of the branches on an external chain (A or B1 chain), and is terminated when it reaches the non-reducing chain end. This model is consistent with the observation that the short double helices derived from the short A chains or short external B chains provided relatively more susceptible spots for enzymatic hydrolysis of amylopectin in native granules (Jane et al. 1997). Thus, the external CL distribution of amylopectin would influence the initial susceptibility of starch to PPA. In other studies of PPA action pattern on amylopectin, singly, doubly or triply branched PPA-limit dextrans were obtained after hydrolysis of dispersed amylopectin, indicating the action of PPA was resistant to compact branching arrangement (Kainuma and French 1969; Abdullah et al. 1966). It can be concluded from their work that amylopectin molecular structures with closely associated branch points are not able to be hydrolyzed by PPA. Normally, the initial attack on native granules is thought to be on the amorphous lamellae, where the branch points are located. If the branch points are too closely associated, the rate of PPA attack on granule would slow down.

Therefore, the precise nature of the amylopectin branching pattern could have a significant effect on starch digestion.

## **1.5 Starch Utilization during Germination**

Being the energy source for plant, maize starch is present in many maize tissues, such as endosperm, leaf, pollen, stem, and root. The transitory starch in leaf is synthesized during day and degraded in the night to maintain energy homeostasis and to provide substrate for storage starch synthesis. It is possible that the starch structure and function in various tissues differs, as demanded by the different physiological utility. Among starch in various maize tissues, endosperm starch, which functions as a long-term storage sink for starch, is the focus of study in this thesis.

Major seed starch reserves of cereals are located in endosperm (Bewley and Black 1985). Starch in endosperm is the most abundant seed carbohydrate and represents a major proportion of the total seed reserves of many species. For plant reproduction, an important function of cereal endosperm starch is to be easily broken down upon germination to provide energy and synthetic substrates for the early growth and development of the seedling (Ziegler 1995). In the cereal endosperm tissue of the seed, starch granules are embedded in a matrix of storage protein and surrounded by the walls of dead cells (Fincher 1989). Shortly after the onset of germination, the seed aleurone or scutellar cells respond to gibberellic acid produced by the embryo by synthesizing and secreting a battery of enzymes, including  $\alpha$ -amylase, that hydrolyze the stored starch and other seed components (Lopes and Larkins 1993).

It is generally considered that an  $\alpha$ -amylase initiates the first step in the

pathway of starch degradation in germinating cereal endosperm (Smith et al. 2005). During germination, the  $\alpha$ -amylase hydrolyzes  $\alpha$ -1,4 linkages at the surface of the semi-crystalline granule, rendering it deeply pitted, with loss of internal material before much of the surface has been attacked (Smith et al. 2005). The degradation of the soluble glucans released from starch granules by  $\alpha$ -amylase probably proceeds via limit dextrinase (debranching enzyme),  $\alpha$ -amylase,  $\beta$ -amylase, and  $\alpha$ -glucosidase to produce maltose and glucose (Smith et al. 2005). The end products of the starch degradation are then taken up by the living scutellum in the embryo, which thereupon synthesizes sucrose for the growing seedling (Bewley and Black 1985). Thus, the susceptibility of endosperm starch granules to hydrolytic enzymes, including  $\alpha$ -amylase, would influence the efficiency of starch utilization by plant.

The efficiency of starch utilization during germination in turn would affect the young plantlets ability to compete for resources such as light and soil nutrients and in turn, reproductive fitness. The efficiency of starch utilization during germination would be a powerful evolutionary force to select for genotypes of plants with starch molecules optimized for molecular structure as well as optimized for efficient storage and utilization. It is reasonable to hypothesize that since energy metabolism is so important to growth, development and reproduction, that complex mechanisms would evolve in higher plants. Gene duplication and neo-functionalization are well known mechanisms by which specific genes can evolve to express different isoforms of enzymes with slightly specialized expression patterns or different enzymatic activities (Gingerich et al. 2007; Prokhnovsky et al. 2008; Saleh et al. 2008). The evidence accumulated on the evolution and biochemistry of the SBEs support this hypothesis, and the research described in this thesis was designed to add a new dimension to this growing body of knowledge, at the level of starch structure and function.

## 1.6 Statement of the Problem

Starch biosynthesis has been an intriguing puzzle. Even though the general pathway of starch biosynthesis has been described, the function and regulation of individual biosynthetic enzymes have not been fully understood.

SBE plays an important role in starch biosynthesis by introducing the branches in starch. The distance between branch points could potentially alter starch accessibility to hydrolytic enzymes. Therefore, changes in the precise nature of the branching pattern during starch biosynthesis might have a fundamental effect on the enzyme hydrolysis of starch granule. One would expect that the three isoforms of maize SBE would differ in the specific ways of introducing branches in starch (Guan and Preiss 1993; Takeda et al. 1993; Blauth et al. 2001; 2002; Yao et al. 2004). Although the role of SBEIIb has been extensively studied (Garwood et al. 1976; Boyer et al. 1977; Boyer and Preiss 1981), the role of the two other SBEs (SBEI and SBEIIa), as well as the coordinated role of multiple SBEs on endosperm starch biosynthesis, are poorly understood. The reasons include insufficient homozygous mutant stock from a similar genetic background and the formidable analytical challenges for examining the resultant starch structures.

Starch digestibility is an important feature of starch functionality with respect to human consumption. A preliminary test using *sbe1a* endosperm starch has shown that deficiency of SBEI increased  $\alpha$ -amylase resistance as compared to Wt; however, the details remain to be elucidated. Starch digestibility of the single mutants *sbe2a* and *ae*, as well as of the double *sbe* mutants from a similar genetic background had not been previously studied. I reasoned that a thorough study of *sbe1a* starch digestion kinetics in combination with analytical characterization of both starch molecular and granular structures was necessary to understand the function of SBEI

deficiency on the synthesis of the resistant structures.

An important function of reserve starch is its efficient conversion to energy upon kernel germination, which requires rapid degradation by hydrolytic enzymes. I reasoned that if SBEI activity is important in determining the high accessibility of starch to degradation, that *sbe1a* mutant seeds might be slower to germinate and/or to grow upon germination.

## 1.7 Goal

The overall goal of this continuing line of SBE research is to understand the role of each of the SBE isoform in starch biosynthesis.

The goal of this thesis is to understand the effects of deficiency of maize SBE isoform activities on endosperm starch molecular and granular structure and starch digestion, with emphasis on the effect of SBEI deficiency.

## 1.8 Objectives

**Objective 1** (To be investigated in Chapter 3)

**1a.** To determine digestion rate and extent for a Wt and *sbe1a* starch using an *in vitro* resistant starch assay.

**1b.** To characterize molecular structure of the amylopectin and amylose fractions from a Wt and *sbe1a* starch.

**1c.** To characterize granule structure for a Wt and *sbe1a* native starch, and residual granule structure for resistant starch after pancreatic  $\alpha$ -amylase digestion.

**1d.** To develop a hypothesis about how starch structure differences in the *sbe1a* mutant might cause decreased susceptibility to starch digestion.

**Objective 2** (To be investigated in Chapter 3)

To compare starch utilization and cotyledon growth for Wt and *sbe1a* seeds during germination.

**Objective 3** (To be investigated in Chapter 4)

**3a.** To characterize resistant starch values of *sbe* mutant starches differing in SBE isoform activities.

**3b.** To characterize molecular structure of *sbe* mutant starches differing in SBE isoform activities.

**1.9 References-Chapter 1**

- Abdullah, M., French, D., and Robyt, J.F. (1966). Multiple attack by  $\alpha$ -amylases. *Arch. Biochem. Biophys.* 114, 595–598.
- Adkins, G.K., and Greenwood, C.T. (1969). Studies on starches of high amylose-content. X. An improved method for the fractionation of maize and amylo maize starches by complex formation from aqueous dispersion after pretreatment with methyl sulphoxide. *Carbohydr. Res.* 11, 217-224.
- Annison, G., and Topping, D.L. (1994). Nutritional role of resistant starch: chemical structure vs physiological function. *Annu. Rev. Nutr.* 14, 297-320.
- Asp, N.G., and Bjorck, I. (1992). Resistant starch. *Trends Food Sci. Technol.* 3, 111-114.
- Atkin, N.J., Cheng, S.L., Abeysekera, R.M. and Robards, A.W. (1999). Localisation of amylose and amylopectin in starch granules using enzyme-gold labelling. *Starch/Stärke*, 51, 163-172.
- Baba, T., Arai, Y., Yamamoto, T., and Itoh, T. 1982. Some structural features of amylo maize starch. *Phytochemistry* 21, 2291-2296.
- Baba, T., Kimura, K., Mizuno, K., Etoh, H., Ishida, Y., Shida, O., and Arai, Y. (1991). Sequence conservation of the catalytic regions of amylolytic enzymes in maize branching enzyme-I. *Biochem. Biophys. Res. Commun.* 181, 87-94.
- Baldwin, P.M., Adler, J., and Davies, M.C. (1998). Melia: High resolution imaging of starch granule surfaces by atomic force microscopy. *J. Cereal Sci.* 27, 255–

265.

- Ball, S.G., and Morell, M.K. (2003). From bacterial glycogen to starch: understanding the biogenesis of the plant starch granule. *Annu. Rev. Plant Biol.* 54, 207-233.
- Banks, W. and Greenwood, C. T. (1966). The fine structure of amylose: The action of pullulanase as evidence of branching. *Arch. Biochem. Biophys.* 117, 674.
- Banks, W. and Greenwood, C. T. (1977). Mathematical models for the action of alpha amylase on amylose. *Carbohydr Res*, 57, 301-315.
- Bastioli, C. (2001): Global status of the production of biobased packaging materials. *Starch/Staerke* 53, 351-355.
- Beatty, M.K., Rahman, A., Cao, H., Woodman, W., Lee, M., Myers, A.M., and James, M.G. (1999). Purification and molecular genetic characterization of ZPU1, a pullulanase-type starch-debranching enzyme from maize. *Plant Physiol.* 119, 255–266.
- Bertoft, E. (1989). Investigation of the fine structure of amylopectin using alpha- and beta-amylase. *Carbohydr. Res.*, 189, 195-207.
- Bertoft, E. (2004). On the nature of categories of chains in amylopectin and their connection to the super helix model. *Carbohydr. Poly.* 57, 211-224.
- Bewley, J.D., and Black, M. Seeds: Physiology of Development and germination. New York, Plenum Press, 1985. 367p.
- Blauth, S.L., Kim, K., Klucinec, J.D., Shannon, J.C., Thompson, D.B., and Gultinan, M.J. (2002). Identification of Mutator insertional mutants of starch branching enzyme 1 (sbe1) in *Zea mays* L. *Plant. Mol. Biol.* 48, 287-297.
- Blauth, S.L., Yao, Y., Klucinec, J.D., Shannon, J.C., Thompson, D.B., and Gultinan, M.J. (2001). Identification of Mutator insertional mutants of starch-branching enzyme 2a in corn. *Plant Physiol.* 125, 1396-1405.
- Blennow, A, Hansen, M., Schulz, A., Jorgensen, K., Donald, A.M., and Sanderson, J. (2003). The molecular deposition of transgenically modified starch in the starch granule as imaged by functional microscopy. *J. Struct. Biol.* 143, 229–241.
- Boyer, C.D., Daniels, R.R., and Shannon, J.C. (1976). Abnormal starch granule formation in *Zea mays* L. endosperms possessing the *amylose-extender* mutant. *Crop Sci.* 16, 298-301.
- Boyer, C.D., Daniels, R.R., and Shannon, J.C. (1977). Starch granule (amyloplast) development in endosperm of several *Zea mays* L. genotypes affecting kernel polysaccharides. *Amer. J. Bot.* 64, 50-56.

- Boyer, C. D. and Priess, J. (1978). Multiple forms of (1-4)- $\alpha$ -D-glucan, (1-4)- $\alpha$ -D-glycosyl transferase from developing *Zea mays* L. kernels. *Carbohydr. Res.* 61, 321-334.
- Boyer, C. D., and Priess, J. (1981). Evidence for independent genetic control of the multiple forms of maize endosperm branching enzymes and starch synthases. *Plant Physiol.* 67, 1141-1145.
- Brown, I. (1996). Complex carbohydrates and resistant starch. *Nutr. Rev.* 54, S115-S119.
- Brown, I., Warhurst, M., Arcot, J., Playne, M., Illman, R. J. and Topping, D. J. (1997). Fecal numbers of Bifidobacteria are higher in pigs fed Bifidobacterium longum with a high amylose cornstarch than with a low amylose cornstarch. *J. Nutr.* 127, 1822-1827.
- Burchard, W., and Thurn, A. (1985). Heterogeneity in branching: mathematical treatment of the amylopectin structure. *Macromolecules* 18, 2072-2082.
- Buléon, A., Ball, S., Planchot, V., and Colonna, P. (1998). Starch granules: structure and biosynthesis. *Int. J. Biol. Macromol.* 23, 85-112.
- Burton, R.A., Bewley, J.D., Smith, A.M., Bhattacharyya, M.K., Tatge, H., Ring, S., Bull, V., Hamilton, W.D.O., and Martin, C. (1995). Starch branching enzymes belonging to distinct enzyme families are differentially expressed during pea embryo development. *Plant J.* 7, 3-15.
- Cao, H., Imparl-Radosevich, J., Guan, H., Keeling, P.L., James, M.G., and Myers, A.M. (1999). Identification of the soluble starch synthase activities of maize endosperm. *Plant Physiol.* 120, 205-216.
- Colleoni, C., Myers, A.M., James, M.G. (2003). One- and two-dimensional native PAGE activity gel analyses of maize endosperm proteins reveal functional interactions between specific starch metabolizing enzymes. *J. Appl. Glycosci.* 50, 207-212.
- Corn Refiners Association (2007) <http://www.corn.org/wcornprod.htm>
- Dinges, J.R., Colleoni, C., James, M.G., and Myers, A.M. (2003). Mutational analysis of the pullulanase-type debranching enzyme of maize indicates multiple functions in starch metabolism. *Plant Cell* 15, 666-680.
- Dinges, J.R., Colleoni, C., Myers, A.M., and James, M.G. (2001). Molecular structure of three mutations at the maize *sugary1* locus and their allele-specific phenotypic effects. *Plant Physiol.* 125, 1406-1418.
- Drummond, G.S., Smith, E.E. and Whelan, W.J. (1972). Purification and properties of potato  $\alpha$ -1,4-glucan,  $\alpha$ -1,4-glucan-6-glycosyltransferase (Q enzyme). *Eur. J. Biochem.* 26, 168-176.

- Eerlingen, R.C. and Delcour, J.A. (1995). Formation, analysis, structure and properties of type III enzyme resistant starch. *J. Cereal Sci.* 22: 129-138.
- Eliasson, A.C., and Gudmundsson, M. (1996). Starch: Physicochemical and functional aspects, in *Carbohydrates in Food* (Ed. A. C. Eliasson) Marcel Dekker, New York.
- Englyst, H.N. and Cummings, J.H. (1987). Digestion of polysaccharides of potato in the small intestine of man. *Am. J. Clin. Nutr.* 45, 423-431.
- Englyst, H. N., Kingman, S. M. and Cummings, J. H. (1992). Classification and measurement of nutritionally important starch fractions. *Eur. J. Clin. Nutr.* 46, S33-S50.
- Englyst, H. N., Trowell, H, Southgate, D. A. and Cummings, J. H. (1987). Dietary fiber and resistant starch. *Am. J. Clin. Nutr.* 46, 873-874.
- EURESTA. (1991) Euresta Newsletter 11:1.
- Evans, A. and Thompson, D.B. (2004). Resistance to  $\alpha$ -amylase digestion in four aative high-amylose maize atarches *Cereal Chem.* 81, 31–37.
- Evans, A. and Thompson, B.D. (2008). Enzyme susceptibility of high-amylose starch precipitated from sodium hydroxide dispersions. *Cereal Chem.* 85, 480–487.
- Faisant, N., Buléon, A., Colonna, P., Molis, C., Lartigue, S., Galmiche, J.P., and Champ. M. (1995). Digestion of raw banana starch in the small intestine of healthy humans: structural features of resistant starch. *Br. J. Nutr.* 73,111-123.
- Fisher, D.K., Boyer, C.D., and Hannah, L.C. (1993). Starch branching enzyme II from maize endosperm. *Plant Physiol.* 102, 1045-1046.
- Fincher, G.B. (1989). Molecular and cellular biology associated with endosperm mobilization in germinating cereal grains. *Annu. Rev. Plant Physiol. Plant Mole. Biol.* 40, 305-346.
- Fitt, L.E. , Snyder, E.M. (1994). Photomicrographs of starches, in *Starch Chemistry and Technology*, 2nd ed. (Eds. R. L. Whistler, J. N. BeMiller, E. F. Paschall), Academic Press, Orlando, p. 675.
- Gallant, D.J., Bouchet, B., and Baldwin, P.M. (1997). Microscopy of starch: evidence of a new level of granule organization. *Carbohydr. Poly.* 32, 177-191.
- Gallant, D.J., Bouchet, B., Buleon, A., and Perez, S. (1992). Physical characteristics of starch granules and susceptibility to enzymatic degradation. *Eur. J. Clin. Nutr.* 46, S3-S16.
- Gao, M., Fisher, D.K., Kim, K.N., Shannon, J.C., and Guiltinan, M.J. (1996). Evolutionary conservation and expression patterns of maize starch branching enzyme I and IIb genes suggests isoform specialization. *Plant Mol. Biol.*, 30,

1223-1232.

- Gao, M., Fisher, D.K., Kim, K.N., Shannon, J.C. and Guiltinan, M.J. (1997). Independent genetic control of maize starch-branching enzymes IIa and IIb- Isolation and characterization of a *Sbe2a* cDNA. *Plant Physiol.* 114, 69-78.
- Gao, M., Wanat, J., Stinard, P.S., James, M.G., and Myers, A.M. (1998). Characterization of *dull1*, a maize gene coding for a novel starch synthase. *Plant Cell* 10, 339-412.
- Garwood, D.L., Shannon, J.C., and Creech, R.G. (1976). Starches of endosperms possessing different alleles at the *amylose-extender* locus in *Zea mays* L. *Cereal Chem.* 53, 355-364.
- Gerard, C., Planchot, V., Colonna, P., and Bertoft, E. (2000). Relationship between branching density and crystalline structure of A- and B-type maize mutant starches. *Carbohydr. Res.*, 326, 130-144.
- Gibson, G.R. and Roberfroid, M.B. (1995). Dietary modulation of the human colonic microbiota: introducing the concept of prebiotics. *J. Nutr.* 125, 1401-1412.
- Gidley, M.J. (2001). Starch structure/function relationships: achievements and challenges. In Tina et al., *Starch: advances in structure and function*. Royal Society of Chemistry (Great Britain). Food Chemistry Group, pp1-7.
- Gidley, M.J., Cooke, D., Drake, A.H., Hoffmann, R.A., Russell, A.L., and ad Greenwell, P. (1995). Molecular order and structure in enzyme-resistant retrograded starch *Carbohydr. Polym.* 28, 23-31.
- Gingerich, D.J., Hanada, K., Shiu, S.H., Vierstra, R.D. (2007). Large-scale, lineage-specific expansion of a bric-a-brac/tramtrack/broad complex ubiquitin-ligase gene family in rice. *Plant Cell.* 19, 2329-2348.
- Goni, I., Garcia-Diz, L., Manas, E. and Saura-Calixto, F. (1996). Analysis of resistant starch: a method for food and food products. *Food Chem.* 56, 445-449.
- Guan, H.P. and Preiss, J. (1993). Differentiation of the properties of the branching isozymes from maize (*Zea mays*). *Plant Physiol.* 102, 1269-1273.
- Harada, T., Misaki A., Akai, H., Yokobayashi, K., and Sugimoto, K. (1972). Characterization of *Pseudomonas* isoamylase by its actions on amylopectin and glycogen: comparison with *Aerobacter* pullulanase. *Biochem. Biophys. Acta.*, 268, 497-505.
- Hizukuri, S. (1985). Relationship between the distribution of the chain length of amylopectin and the crystalline structure of starch granules. *Carbohydr. Res.*, 141, 295-306.
- Hizukuri, S. (1986). Polymodal distribution of the chain lengths of amylopectins, and its significance. *Carbohydr. Res.*, 147, 342-347.

- Hizukuri, S. (1996). Starch: analytical aspects. *Carbohydrates in food*, (Eliasson, A.-C., ed.), Marcel Dekker, New York, 347-429.
- Hizukuri, S., and Maehara, Y. (1990). Fine structure of wheat amylopectin: the mode of A to B chain binding. *Carbohydr. Res.*, 206, 145-159.
- Hizukuri, S. and Takagi, T. (1984). Estimation of the distribution of molecular weight for amylose by the low-angle laser-light-scattering technique combined with high-performance gel chromatography. *Carbohydr. Res.* 134, 1-10.
- Hizukuri, S., Takeda, Y., Yasuda, M., and Suzuki, A. (1981). Multi-branched nature of amylose and the action of debranching enzymes. *Carbohydr. Res.* 94, 205-213.
- Imberty, A., Buléon, A., Tran, V., & Pérez, S. (1991). Recent advances in knowledge of starch structure. *Starch/Stärke* 43, 375-384.
- Jane, J.L. and Shen, J.J. (1993). Internal structure of the potato starch granule revealed by chemical gelatinization, *Carbohydr. Res.* 247, 279-290.
- Jane, J.L., Wong, K.S., and McPherson, A.E. (1997). Branch structure differences in starches of A and B types X-ray patterns revealed by their Naegli dextrans, *Carbohydr. Res.* 300, 219-227.
- Jenkins, P.J. and Donald, A.M. (1995). The influence of amylose on starch granule structure. *Int. J. Biol. Macromol.* 17, 315-321.
- Jesperon, H.M., MacGregor, E.A., Henrissat, B., Sierks, M.R., and Svensson, B. (1993). Starch- and glycogen-debranching and branching enzymes: prediction of structural features of the catalytic (b/a)8-barrel domain and evolutionary relationship to other amylolytic enzymes. *J. Protein Chem.* 12, 791-805.
- Juszczak, L., Fortuna, T., Krok, F. (2003). Non-contact atomic force microscopy of starch granules surface. Part I. Potato and tapioca starches. *Starch/Stärke* 55, 1-7.
- Kainuma, K. and French, D. (1969). Action of pancreatic amylase on starch oligosaccharides containing single glucose side chains. *FEBS Letters* 5, 257-261.
- Kainuma, K., Kobayashi, S., and Harada, T. (1978). Action of *Pseudomonas* isoamylase on various branched oligo- and poly-saccharides. *Carbohydr. Res.* 61, 345-357.
- Kim, K.N., Fisher, D.K., Gao, M., and Guiltinan, M.J. (1998). Genomic organization and promoter activity of the maize *Starch branching enzyme I* gene. *Gene* 216, 233-243.
- Kim, K.N., Gao, M., Fisher, D.K., and Guiltinan, M.J. (1999). Molecular cloning and

characterization of the *Amylose-Extender* gene encoding starch branching enzyme IIB in maize. *Plant Mol. Biol.* 38, 945–956.

- Kjolberg, O. and Manners, D. J. (1963). The action of isoamylase on amylose. *Biochem. J.* 86, 258–262.
- Klucinec, J.D., and Thompson, D.B. (1998). Fractionation of high amylose maize starches by differential alcohol precipitation and chromatograph of the fractions. *Cereal Chem.* 75, 887-896.
- Klucinec, J.D., and Thompson, D.B. (2002). Note: Structure of amylopectins from *ae*-containing maize starches. *Cereal Chem.*, 79, 19-23.
- Lee, E. Y. C. (1971). The action of sweet potato  $\beta$ -amylase on glycogen and amylopectin: formation of a novel limit dextrin. *Arch. Biochem. Biophys.*, 146, 488-492.
- Li, J.H., Thompson, D.B., and Gultinan, M. (2007). Mutation of the maize *sbe1a* and *ae* genes alters morphology and physical behavior of *wx*-type endosperm starch granules. *Carbohydr. Res.* 342, 2619–2627.
- Li, Z., Chu, X., Mouille, G., Yan, L., Kosar-Hashemi, B., Hey, S., Napier, J., Shewry, P., Clarke, B., Appels, R., Morell, M.K., and Rahman, S. (1999). The localization and expression of the class II starch synthases of wheat. *Plant Physiol.* 120, 1147–1156.
- Lopes, M.A. and Larkins, B.A. (1993). Endosperm Origin, Development, and Function. *Plant Cell* 5, 1383-1399.
- Manelius, R., Buleon, A., Nurmi, K, and Bertoft, E. (2000). The substitution pattern in cationised and oxidised potato starch granules. *Carbohydr. Res.* 329, 621-633.
- Manelius, R., Maaheimo, H, Nurmi, K. and Bertoft, E. (2002). Characterisation of fractions obtained by isoamylolysis and ion-exchange chromatography of cationic waxy maize starch. *Starch/Stärke* 54, 58-65.
- Manelius, R., Nurmi, K., and Bertoft, E. (2005). Characterization of dextrans obtained by enzymatic treatment of cationic potato starch. *Starch/Stärke* 57, 291-300.
- Manners, D. J. (1989). Recent developments in our understanding of amylopectin structure. *Carbohydr. Polym.* 11, 87-112.
- Marshall, J. J. and Whelan, W. J. (1974). Multiple branching in glycogen and amylopectin. *Arch. Biochem. Biophys.*, 161, 234-238.
- Martin, C., and Smith, A.M. (1995). Starch biosynthesis. *Plant Cell* 7, 971–985.
- Mazur, A.K. and Nakatani, H. (1993). Multiple attack mechanism in the porcine pancreatic alpha-amylase hydrolysis of amylose and amylopectin. *Arch*

*Biochem Biophys.* 306, 29-38.

- McCleary, B.V. and Monaghan, D.A. (2002). Measurement of resistant starch. *J. AOAC Intl.* 85, 665-675.
- McCleary, B.V. and Rossiter, P. (2004). Measurement of novel dietary fiber. *J. AOAC Intl.* 87, 707-717.
- Moore, C.W., and Creech, R.G. (1971). Genetic fine structure analysis of the amylose-extender locus in *Zea mays* L. *Genetics* 70, 611-619.
- Morell, M.K., Blennow, A., Kosar-Hashemi, B., Samuel, M.S. (1997). Differential expression and properties of starch branching enzyme isoforms in developing wheat endosperm. *Plant Physiol.*, 113, 201-208.
- Morrison, W.R. (1995) Starch lipids and how they relate to starch granule structure and functionality. *Cereal Foods World.* 40, 437-446.
- Morrison, W.R. and Gadan, H.J. (1987) The amylose content of starch granules in developing wheat endosperm. *J. Cereal Sci.* 5, 263-275.
- Muir, J.G., Lu, Z.X., Young, G.P. Cameron-Smith, D., Collier, G.R., and O'Dea, K. (1995). Resistant starch in the diet increases breath hydrogen and serum acetate in human subjects. *Am. J. Clin. Nutr.* 61, 792-799.
- Myers, A.M., Morell, M.K., James, M.G., and Ball, S.G. (2000). Recent progress toward understanding biosynthesis of the amylopectin crystal. *Plant Physiol.* 122, 989-997.
- Nikuni, Z. (1969). Science of Cookery 2:6 (cited in Nikuni, 1978).
- Nikuni, Z. (1978). Studies on starch granules. *Starch/Stärke*, 30, 105-111.
- Nishi, A., Nakamura, Y., Tanaka, N., and Satoh, H. (2001). Biochemical and genetic effects of amylose-extender mutation in rice endosperm. *Plant Physiol.* 127, 459-472.
- O'Dea, K., Snow, P., and Nestel, P. (1981). Rate of starch hydrolysis in vitro as a predictor of metabolic responses to complex carbohydrate in vivo. *Am. J. Clin. Nutr.* 34, 1991-1993.
- Pan, D., and Nelson, O.E. (1984). A debranching enzyme deficiency in endosperms of the *sugary-1* mutants of maize. *Plant Physiol.* 74, 324-328.
- Planchot, V., Colonna, P., Gallant, D.J., and Bouchet, B. (1995). Extensive degradation of native starch granules by alpha-amylase from *Apergillus fumigatus*. *J Cereal Sci.* 21, 163-171.
- Peat, S., Whelan, W.J., and Thomas, G.J. (1952). Evidence of multiple branching in waxy maize starch. *J. Chem. Soc.* 4546-4548.

- Preiss, J. (1991). Biology and molecular biology of starch synthesis and its regulation. *Oxf. Surv. Plant Mol. Cell Biol.* 7, 59–114.
- Prokhnevsky, A.I., Peremyslov, V.V., Dolja, V.V. (2008). Overlapping functions of the four class XI myosins in *Arabidopsis* growth, root hair elongation, and organelle motility. *Proc. Natl. Acad. Sci.* 105, 19744–19749.
- Rahman, S., Regina, A., Li, Z., Mukai, Y., Yamamoto, M., Kosar-Hashemi, B., Abrahams, S., Morell, M.K. (2001). Comparison of starch-branching enzyme genes reveals evolutionary relationships among isoforms. Characterization of a gene for starch-branching enzyme IIa from wheat D genome donor *Aegilops tauschii*. *Plant Physiol.* 125, 1314–1324.
- Rees, E. (2008). Effect of a heat-moisture treatment on alpha-amylase susceptibility of high amylose maize starches. MS thesis. The Pennsylvania State University, University Park, PA.
- Ridout, M.J., Parker, M.L., Hedley, C.L., Bogracheva, T.Y., and Morris, V.J. (2003). Atomic force microscopy of pea starch granules: granule architecture of wild-type parent, *r* and *rb* single mutants, and the *rrb* double mutant. *Carbohydr. Res.* 338, 2135–2147.
- Roby, J.F. (1984). Enzymes in the hydrolysis and synthesis of starch. Starch: Chemistry and Technology. R. L. Whistler, J. N. BeMiller and E. F. Paschall. New York, Academic Press.
- Roby, J.F. and French, D. (1970). The action pattern of porcine pancreatic  $\alpha$ -amylase in relationship to the subsite binding site of the enzyme. *J. Biol. Chem.*, 245, 3917-3927.
- Robin, J.P., Mercier, C., Charbonniere, R., and Guilbot, A. (1974). Lintnerized starches. Gel filtration and enzymatic studies of insoluble residues from prolonged acid treatment of potato starch. *Cereal Chem.* 51, 389-406.
- Roder, N., Ellis, P.R., and Butterworth, P.J. (2005). Starch molecular and nutritional properties: a review. *Adv. Mol. Med.* 1, 5-14.
- Saleh, A., Alvarez-Venegas, R., Yilmaz, M., Le, O., Hou, G., Sadler, M., Al-Abdallat, A., Xia, Y., Lu, G., Ladunga, I., Avramova, Z. (2008). The Highly Similar *Arabidopsis* homologs of trithorax ATX1 and ATX2 encode proteins with divergent biochemical functions. *Plant Cell.* 20, 568–579.
- Seo, B.S., Kim, S., Scott, M.P., Singletary, G.W., Wong, K.S., James, M.G., and Myers, A.M. (2002). Functional interactions between heterologously expressed starch-branching enzymes of maize and the glycogen synthases of Brewer's yeast. *Plant Physiol.* 128, 1189-1199.
- Shannon, J.C. and Garwood, D.L. (1984). Genetics and Physiology of Starch Development. In Whistler et al. (ed.) Starch Chemistry and Technology

Academic Press. San Diego, California U.S. pp. 25-89.

- Smith, A.M, Zeeman, S.C., and Smith, S.M. (2005). Starch Degradation. *Annu. Rev. Plant Biol.* 56, 73-98.
- Swinkels, J.J.M. (1985). Composition and properties of commercial native starches. *Starch/Stärke* 37, 1-5.
- Takeda, Y., Hizukuri, S., and Juliano, B. O. 1986. Purification and structure of amylose from starch. *Carbohydr. Res.* 148, 299-308.
- Takeda, Y., Guan, H.P., and Preiss, J. (1993). Branching of amylose by the branching isoenzymes of maize endosperm. *Carbohydr. Res.* 240, 253-263.
- Takeda, Y., Shirasaka, K., and Hizukuri, S. (1984). Examination of the purity and structure of amylose by gel-permeation chromatography. *Carbohydr. Res.* 132, 83-92.
- Takeda, Y., Shitaozono, T. and Hizukuri, S. (1990). Structures of sub-fractions of corn amylose. *Carbohydr. Res.* 199, 207-214.
- Tetlow, I.J., Beisel, K.G., Cameron, S., Makhmoudova, A., Liu, F., Bresolin, N.S., Wait, R., Morell, M.K., and Emes, M.J. (2008). Analysis of Protein Complexes in Wheat Amyloplasts Reveals Functional Interactions among Starch Biosynthetic Enzymes. *Plant Physiol.* 146, 1878 - 1891.
- Tetlow, I.J., Wait, R., Lu, Z., Akkasaeng, R., Bowsher, C.G., Esposito, S., Kosar-Hashemi, B., Morell, M.K., and Emes, M.J. (2004). Protein phosphorylation in amyloplasts regulates starch branching enzyme activity and protein-protein interactions. *Plant Cell* 16, 694-708.
- Thompson, D.B. (2000). On the non-random nature of amylopectin branching. *Carbohydr. Polym.*, 40, 223-239.
- Vineyard, M.L. and Bear, R.P. (1952). Amylose content. *Maize Genetics Coop. Newslett.* 26, 5.
- Waigh, T.A., Hopkinson, I., and Donald, A.M. (1997). Analysis of the Native Structure of Starch Granules with X-ray Microfocus Diffraction *Macromolecules* 30, 3813-3820
- Topping, D. L., Fukushima, M. and Bird, A. R. (2003). Resistant starch as a prebiotic and synbiotic: state of the art. *Proc. Nutr. Soc.* 62, 171-176.
- Wang, X., Brown, I. L., Khaled, D., Mahoney, M. C., Evans, A. J. and Conway, P. L. (2002). Manipulation of colonic bacteria and volatile fatty acid production by dietary high amylose maize (amylomaize) starch granules. *J. Appl. Microbiol.* 93, 390-397.
- Wang, Y.-J., White, P., Pollak, L., and Jane, J.L. (1993). Amylopectin and

intermediate materials in starches from mutant genotypes of the Oh43 inbred line. *Cereal Chem.* 70, 521-525.

- Weaver, G.A., Krause, J.A., Miller, T.L., and Wolin, M.J. (1992). Cornstarch fermentation by the colonic microbial community yields more butyrate than does cabbage fiber fermentation; cornstarch fermentation rates correlate negatively with methanogenesis. *Am. J. Clin. Nutr.* 55, 70-77.
- White, P.J. (1994). Properties of corn starch. In Specialty Corns, A.R. Hallauer, ed (Ann Arbor: CRC Press), pp. 29-54.
- Whittam, M.A., Noel, T.R., and Ring, S.G. (1990). Melting behaviour of A- and B-type crystalline starch. *Intl. J. Biol. Macromol.* 12, 359-362.
- Xia, H. (2005). Branching pattern differences among amylopectins of several maize genotypes. MS thesis. The Pennsylvania State University, University Park, PA.
- Xia, H. Yandeau-Nelson, M., Guiltinan, M.J., Thompson, D.B. (2007). SBE maize endosperm mutations are associated with different levels of resistant starch. Presentation at 2007 AACCC conference, Starch Round Table, San Antonio, Texas.
- Xia, H., and Thompson, D.B. (2006). Debranching of  $\beta$ -limit dextrans with isoamylase or pullulanase to explore the branching pattern of amylopectins from three maize Genotypes. *Cereal Chem.* 83, 668-676.
- Xu, J.H. and Messing, J. (2008). Organization of the prolamin gene family provides insight into the evolution of the maize genome and gene duplication in grass species. *Proc. Natl. Acad. Sci.* 105, 14330–14335.
- Yao, Y., Guiltinan, M., Shannon, J. C., and Thompson, D.B., (2002). Single kernel sampling method for maize starch analysis while maintaining kernel vitality. *Cereal Chem.*, 79, 757–762.
- Yao, Y., Thompson, D.B., and Guiltinan, M.J. (2003). Starch biosynthesis in Maize endosperm: in the absence of SBEIIb, the deficiency of SBEIIa leads to increased Amylopectin Branching. Presentation at 2003 AACCC conference, Portland, OR.
- Yao, Y., Thompson, D.B., and Guiltinan, M.J. (2004). Maize starch branching enzyme (SBE) isoforms and amylopectin structure: in the absence of SBEIIb, the future absence of SBEIa leads to increased branching. *Plant Physiol.*, 106, 293-316.
- Yokobayashi, K., Misaki, A., and Harada, T. (1970). Purification and properties of *Pseudomonas* isoamylase. *Biochem. Biophys. Acta.*, 212, 458-469.
- Ziegler, P. (1995). Carbohydrate degradation during germination. In Seed development and germination, Marcel Dekker Inc., New York. pp447-474.

Zobel, H. F. (1988) Molecules to granules: A comprehensive review. *Starch/Stärke*, 40, 1-7.

## Chapter 2

### MATERIALS AND METHODS

#### 2.1 Maize Genotypes

The maize starch branching enzyme isoforms (SBEI, SBEIIa and SBEIIb) are encoded by the genes *Sbe1a*, *Sbe2a*, and *Amylose extender (Ae)*. Null mutants for each of these genes were previously isolated and are referred to as *sbe1a*, *sbe2a* and *ae* following recommendations of the commission on plant gene nomenclature (1993). The inbred W64A is referred to as wild-type (Wt) in this thesis.

#### 2.2 Identification of Maize *sbe* Mutants

Genotyping of *sbe2a* or *sbe1a* mutants in this work followed the procedures of Blauth et al. (2001; 2002). Genomic DNA was extracted from leaf tissue of 10-day-after-emergence seedlings using the procedure as described by Dellaporta (1994), and detected using PCR protocols as described by Blauth et al. (2001; 2002). For genotyping of *ae* mutant, which was obtained as a natural mutation in a screen for shrunken seeds, rather than *Mu* transposon insertion, one pair of primers was designed by Dr. Marna Yandea-Nelson (personal communication) to detect both *Ae* and *ae* alleles (*ae6279F*: 5'-TACACCCCCTTTGGATCCTT-3' paired with *ae7675R*: 5'-AGTGCTCTTGATTGCCATT-3'). The *ae* allele has a 882 bp deletion (positions 6613-7494 relative to the *Ae*-B73 sequence published as GenBank Accession No AF072725), which includes all of exon 9 and portions of introns 8 and 9. Primers *ae6279F* in intron 8 and *ae7675R* in exon 10 flank the deletion and amplify a ~530 bp product in the *ae* allele and a ~1.4 kb product in the *Ae* allele (personal

communication, Dr. Marna Yandeu-Nelson).

Gel electrophoresis of amplification products indicated that detection of *Sbe1a* alleles using primers 1A4/1A5 (Blauth et al. 2002) resulted in a 0.4 kb fragment, and detection of *sbe1a* alleles using primers 1A4/*Mu*TIR9242 (Blauth et al. 2002) resulted in a 0.4 kb fragment (Fig. 2.1, Table 2.1). The presence of *Sbe1a* band combined with the absence of *sbe1a* mutant band identified homozygous *Sbe1a* alleles (lane 1), whereas, the presence of *sbe1a* mutant band combined with the absence of *Sbe1a* band identified homozygous *sbe1a* mutant alleles (lane 3). The presence of both bands in two PCR screenings identified heterozygous *Sbe1a/sbe1a* alleles (lane 2). The same rule of identification applies for *Sbe2a* (Table 2.1). Detection of *Sbe2a* alleles used primers 2A2/2A32 (Blauth et al. 2001), and detection of *sbe2a* alleles using primers 2A2/*Mu*TIR9242 (Blauth et al. 2001). Detection of *Ae* and *ae* alleles was achieved in one PCR screening using primers *ae*6279F/*ae*7675R (Fig. 2.1, Table 2.1). Three different fragments (0.5 kb, 0.9 kb, 1.4 kb) were available in the screening results. The presence of all the three fragments identified heterozygous *Ae/ae* alleles (lane 5), the presence of a 1.4 kb fragment identified homozygous *Ae* alleles (lane 4), and the presence of a 0.5 kb fragment identified homozygous *ae* mutant alleles (lane 6).

For each plant, five different PCR screenings were conducted to detect alleles of *Sbe1a*, *sbe1a*, *Sbe2a*, *sbe2a*, and *Ae/ae*, respectively (Table 2.1). When PCR results identify homozygous alleles of *Sbe1a/Sbe1a*, *Sbe2a/Sbe2a*, and *Ae/Ae*, the plant will be referred as homozygous Wt. When PCR results identify homozygous mutant alleles of *sbe1a/sbe1a*, and homozygous Wt alleles of *Sbe2a/Sbe2a* and *Ae/Ae*, the plant will be referred as *sbe1a* mutant, and the Wt alleles will not be mentioned.

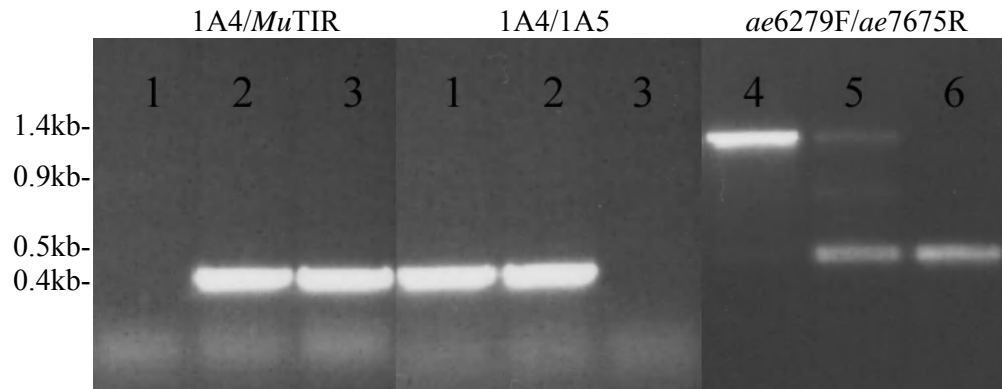


Figure 2.1 Gel electrophoresis of PCR amplification products. Numbers indicate specific sample. 1A4 and 1A5 are pair of primers used for detecting *Sbe1a* alleles; and 1A4 and *MuTIR* are pair of primers used for detecting *sbe1a* alleles (Blauth et al. 2002). *ae6279F* and *ae7675R* are pair of primers used for detecting both *Ae* and *ae* alleles. Band in Lane 1, 2, or 3 detects *Sbe1a* alleles, *Sbe1a/sbe1a* alleles, and *sbe1a* alleles, respectively. Band in Lane 4, 5, or 6 detects *Ae* alleles, *Ae/ae* alleles, and *ae* alleles, respectively.

Table 2.1 PCR Primers for genotyping the maize *sbe* mutants used in this study. Specific primer pairs were created for both the Wt and *Mu* insertional alleles of *sbe1a* and *sbe2a* (Blauth et al. 2002; 2001). The *Ae* primer pair results in a codominant amplification product thus only one pair was used.

<b>Genotype</b>	<b>Primer Pair 1</b>	<b>Fragment size(s) 1</b>	<b>Primer Pair 2</b>	<b>Fragment Size(s) 2</b>
<i>Sbe1a/Sbe1a</i>	1A4/1A5	0.4 kb	1A4/ <i>Mu</i> TIR9242	none
<i>Sbe1a/sbe1a</i>	1A4/1A5	0.4 kb	1A4/ <i>Mu</i> TIR9242	0.4 kb
<i>sbe1a/sbe1a</i>	1A4/1A5	none	1A4/ <i>Mu</i> TIR9242	0.4 kb
<i>Sbe2a/Sbe2a</i>	2A2/2A32	0.5 kb	2A2/ <i>Mu</i> TIR9242	none
<i>Sbe2a/sbe2a</i>	2A2/2A32	0.5 kb	2A2/ <i>Mu</i> TIR9242	0.5 kb
<i>sbe2a/sbe2a</i>	2A2/2A32	none	2A2/ <i>Mu</i> TIR9242	0.5 kb
<i>Ae/Ae</i>	<i>ae</i> 6279F/ <i>ae</i> 7675R	1.4 kb		
<i>Ae/ae</i>	<i>ae</i> 6279F/ <i>ae</i> 7675R	0.5 kb, 0.9 kb, 1.4 kb		
<i>ae/ae</i>	<i>ae</i> 6279F/ <i>ae</i> 7675R	0.5 kb		

The same rule of nomenclature applies for other *sbe* single and double mutants used in this thesis. The detected Wt and mutant plants were self-pollinated to produce ears for endosperm analysis.

### **2.3 Generation of Segregating Populations for Endosperm Analysis**

The initial idea of this continuing line of research was to study endosperm starch from the maize *sbe* single mutants, all the combinations of double mutants, and the triple mutant. In order to compare starch material from highly similar genetic background, a strategy that was chosen entailed generating homozygous sibling plants from the same segregating population to obtain ears for endosperm analysis.

In the previous breeding conducted by Blauth et al. (2001; 2002), plants determined to contain *Mu* insertions within *Sbe1a* or *Sbe2a* gene were backcrossed either 3 or 2 times to the W64A background (a commonly used inbred line for research), and homozygotes were selected via PCR (Fig. 2.2). A seed population segregating for all the three *sbe* genes, referred to as the 3-gene segregating population, was available from subsequent breeding by Dr. Marna Yandea-Nelson in the summer of 2006 (Fig. 2.3a). The progeny from this population were self-pollinated, and the homozygotes were selected via PCR for endosperm analysis (Fig. 2.3a). Theoretically, all the single, double, and triple homozygous *sbe* mutant combinations would be identified from the selfed progeny of this population. However, all the *sbe2a*-containing plants had severe leaf senescence which significantly compromised the plants' fitness and reduced their fertility. Consequently, only a very limited number of *sbe2a*-containing homozygous kernels were generated from this population (Fig. 2.3a), and this was insufficient for three biological replications.

**a. *sbe1a* Breeding by Blauth et al. (2002)**

Genotype	Pollination Date	Back Crossing
TUSC F <sub>1</sub> for <i>sbe1a</i>		
⊗		
↓		
W64A × 97250*	02/1997	BC1 for <i>sbe1a</i>
↓		
W64A × 97310*	08/1997	BC2 for <i>sbe1a</i>
↓		
W64A × 98038*	11/1997	BC3 for <i>sbe1a</i>
↓		
98132*		

\*97250, 97310, 98038, and 98132 were identified as *sbe1a* via PCR. 98132 was used for generating the segregating populations used in this thesis.

**b. *sbe2a* Breeding by Blauth et al. (2001)**

Genotype	Pollination Date	Back Crossing
TUSC F <sub>1</sub> for <i>sbe2a</i>		
⊗		
↓		
W64A × 98025*	11/1997	BC1 for <i>sbe2a</i>
↓		
W64A × 98133*	03/1998	BC2 for <i>sbe2a</i>
↓		
98159*		

\*98025, 98133, and 98159 were identified as *sbe2a* via PCR. 98159 was used for the segregating populations used in this thesis.

Figure 2.2 Pedigree of *sbe* mutants: A description of the breeding work by Blauth et al. (2002; 2001). ⊗ refers to selfed pollination; x refers to hybridization between two different genotypes; ↓ refers to the process of generating progeny population. TUSC F<sub>1</sub> refers to plants containing a *Mu* insertion in *Sbe1a* or *Sbe2a* gene obtained from the Trait Utility System for Corn (TUSC) performed by Pioneer Hi-bred International as a collaborative effort with PSU. Numbers under genotype category indicate the codes for specific segregating progeny.

Genotype	Pollination Date	Back Crossing
98132 ( <i>sbe1a</i> ) × 98159 ( <i>sbe2a</i> )	07/1999	BC4 for <i>sbe1a</i> ; BC3 for <i>sbe2a</i>
↓		
99050		
⊗	11/1999	
↓		
99052 × <i>ae</i> (W64A)*	04/2000	BC5 for <i>sbe1a</i> ; BC4 for <i>sbe2a</i>
↓		
044, 049, 051, 055		
⊗	08/2000	
↓		
00-Summer-87-2, 00-55		
⊗	08/2006	
↓		
06-1082, 1088-1090 (various heterozygotes identified via PCR)		
<b>Referred to as the 3-gene segregating population</b>		
⊗	08/2007	
↓		
07-1001-1009, 1114, 1115 (various homozygotes selected via PCR)		

**Outcome:** An ample number (>10) of full ears for homozygous Wt, *sbe1a*, *ae* and *sbe1a ae*, 2 small ears for homozygous *sbe1a sbe2a*. 1 small ear for homozygous *sbe2a ae*, and no ear for homozygous *sbe2a*.

\* *ae* has been backcrossed to W64A background numerous times (n>6), and is considered to be equal to W64A background.

Figure 2.3a. Pedigree of *sbe* mutants: Attempt to produce a population segregating for all three *sbe* genes, using seed population bred by Blauth et al. (2002; 2001). The meanings of the symbols are the same as in Fig. 2.2.

Genotype	Pollination Date	Back Crossing
98132 ( <i>sbe1a</i> ) × 98159 ( <i>sbe2a</i> )	07/1999	BC4 for <i>sbe1a</i> ; BC3 for <i>sbe2a</i>
↓		
99050		
⊗	11/1999	
↓		
99052		
⊗	08/2006	
↓		
06-1045, 1047, 1048 (various heterozygotes identified via PCR)		
<b>Referred to as the 2-gene segregating population</b>		
⊗	08/2007	
↓		
07-1053-1082 (various homozygotes selected via PCR)		

**Outcome:** An ample numbers (>10) of ears for homozygous Wt, *sbe1a*, *sbe2a*, and *sbe1a sbe2a*. Ears obtained for *sbe2a* and *sbe1a sbe2a* were smaller than others.

Figure 2.3b. Pedigree of *sbe* mutants: Attempt to produce a population segregating for *sbe1a* and *sbe2a* genes, using seed population bred by Blauth et al. (2002; 2001). The meanings of the symbols are the same as in Fig. 2.2.

No *sbe2a*-containing plants from this population grew well, however, sufficient seed stock was obtained in the form of homozygous ears of Wt, *sbe1a*, *ae*, and *sbe1a ae*.

In order to generate sufficient *sbe2a*-containing kernels, a second strategy was employed. A seed population, segregating specifically for *sbe1a* and *sbe2a* genes, was created, referred to as the 2-gene segregating population. Its progeny were selfed, and homozygotes were selected for endosperm analysis (Fig. 2.3b). An adequate amount of homozygous ears of Wt, *sbe1a*, *sbe2a*, and *sbe1a sbe2a* was generated from this population. However, a much lower-than-expected frequency of *sbe2a ae* double homozygous mutant was observed in the selfed progeny.

Additionally the triple homozygous mutant (*sbe1a sbe2a ae*) was reproducibly not present, possibly due to a close linkage of *sbe1a* and *ae* genes and subsequent lack of segregation (personal communication, Dr. Marna Yandea-Nelson). This observation is consistent with the previous study (Yao et al. 2003, see details in 1.2.3.2, p13).

In the progeny of the 3-gene segregating population, *sbe1a* and *sbe2a* have been backcrossed 5 times and 4 times, respectively, as shown by the pedigree (Fig. 2.3a); *ae* has been backcrossed numerous times according to previous records. In the progeny of the 2-gene segregating population, *sbe1a* and *sbe2a* have been backcrossed 4 times and 3 times, respectively, as shown by the pedigree (Fig. 2.3b). Due to differences in the number of backcrosses, the progeny from the two populations may have slightly different genetic background. By conventional standards, in the combined genotypes the amount of genetic background that is coming from sources other than W64A would be equivalent to the least number of backcrossed of any of the parents. For this case, progeny from the 3-gene segregating population is considered to be a 4<sup>th</sup> backcrossed generation and share approximately 93.8% ( $1 - \frac{1}{2^4}$ ) of the W64A background, progeny from the 2-gene segregating

population is considered to be a 3<sup>rd</sup> backcrossed generation and share approximately 87.5% ( $1 - \frac{1}{2^3}$ ) of the W64A background. Thus, the 2-gene segregating population shared approximately 6% less of the W64A background than the 3-gene segregating population. To avoid the confounding factor caused by the possible differences in genetic background of these two populations, comparisons were performed within each population from segregating sibling seeds. These comparisons would reduce the potential genetic differences between individuals to a minimum possibility without several additional years of backcrossing (which is now in progress). For each genotype, endosperm starch was extracted from three different ears from three plants and maintained as distinct samples (biological replications) and noted as B1, B2, and B3.

The research plants in this study were grown during summer in 2007 at The Pennsylvania State University Horticultural Research Farm (Rock Springs, PA), and during fall and spring in 2006 and 2007 under standard greenhouse conditions with supplemental lighting on a 14-hr-day/10-hr-night cycle.

## **2.4 Endosperm Starch Extraction**

For each biological replication, maize kernels (~5 g) were randomly picked from a sample ear and were used for starch extraction according to the method of Boyer et al. (1976) with slight modifications as described by Yao et al. (2003). The kernels were treated in a steeping solution (0.02M NaAc, 0.01M HgCl<sub>2</sub>, pH 6.5) and prepared as described in Yao et al. (2002). The extraction was done at room temperature. The endosperm was homogenized repeatedly (3 times) in a Waring blender with 50 mL of 0.05M NaCl for 2 min intervals, passed through 105- $\mu$ m mesh nylon cloth screen, and rinsed with 100 mL of 0.05M NaCl. The fibrous material not

passing through the screen was further homogenized with a Tissumizer (Model SDT 1810; Tekmar) at 20,000 rpm for 1 min in 50 mL of 0.05M NaCl. The homogenized slurry was then shaken at 300 rpm for 1 hr, filtered, and rinsed repeatedly for maximum release of starch granules. The starch was purified by 12 extractions with a mixture of 0.05M NaCl aqueous solution and toluene (3:1, v/v) to remove the protein. For each protein extraction, the mixture was shaken at 300 rpm for 1 hr, allowed to stand until the starch precipitated, and then separated by centrifugation ( $1,100 \times g$ , 20 min). The purified starch was then washed with deionized water (4 times), 95% ethanol (twice), and acetone (once) before being dried at 22°C for 24 hr.

## **2.5 Starch Digestibility Analysis**

### **2.5.1 Resistant Starch Determination**

The official method for *in vitro* resistant starch (RS) determination (AOAC 2002.02, AACC 32-40) was employed, as scaled-down and modified for direct analysis of the digestion supernatant for total carbohydrate (Evans and Thompson 2008). The modification allowed analysis of digestion time-course for small starch samples (~20mg). For RS determination, after the 16 hr digestion step at 37°C with porcine pancreatic  $\alpha$ -amylase (PPA) and amyloglucosidase (AMG) (enzymes from RS Assay Kit, Cat.No. K-RSTAR, Megazyme International Ireland, Ltd.), the sample tube was removed from the water bath and to an aliquot of each sample was added 1 volume of 95% (v/v) ethanol with 0.5% (w/v) EDTA. After centrifugation ( $1,500 \times g$ , 10 min), the supernatant was analyzed in duplicate for total carbohydrate using the phenol sulfuric acid method (Dubois et al. 1956). The percent non-digested starch (% NDS) was calculated from this data and is the basis for the calculation of the RS value.

### 2.5.2 Digestion Time-Course Analysis

Digestion time-course analysis was performed for Wt and *sbe1a* starch from the 2-gene segregating population. For determination of digestion time-course, the starch samples were digested as described above. An aliquot was removed at approximately 30 sec, 3 min, 6 min, 15 min, 30 min, 1 hr, 2 hr, 3 hr, 4 hr, 5 hr, 7 hr, 10 hr, 13 hr, and twice at 16 hr, and added to 1 volume of ethanol/EDTA solution to ensure immediate deactivation of the enzymes. After centrifugation the supernatants were analyzed for total carbohydrate as described above.

Digestion time-course was analyzed following the method developed by Rees (2008) to obtain kinetic data. A “Double, 5 parameter” regression model in SigmaPlot (Systat Software, Inc.) was selected to fit the data using the double exponential decay equation:

$$y = y_0 + S_1 e^{-k_1 x} + S_2 e^{-k_2 x}$$

where  $y$  is % NDS,  $x$  is the time,  $y_0$  is the  $y$ -value that the model asymptotically approaches,  $S_1$  and  $S_2$  are the concentrations of the two different substrate components, and  $k_1$  and  $k_2$  are the reaction rate constants for the decay of the two different components. The units for  $y_0$ ,  $S_1$ , and  $S_2$  were % of initial starch, and the units for the rate constants were  $\text{min}^{-1}$ . After running the regression program, the software gives three possible completion status messages depending on how well the model fits the data:

- (1) Converged, tolerance satisfied.
- (2) Converged, tolerance satisfied. Parameter may not be valid. Array numerically singular on final iteration.
- (3) Didn't converge, exceeded maximum number of iterations.

The data were kept for further regression analysis if message 1 or 2 resulted, and were

discarded if message 3 resulted.

Digestion time-course analysis was performed for three biological replications per genotype. For each biological replication, two technical replications were performed. If both sets of data “converged” using the model (message 1 or 2), no further analyses were performed. If message 3 appeared, a new technical replication was done until the data “converged.” The status of the technical replication is shown in Table 2.2.

The data from the two “converged” technical replications for each biological replication were combined, and the software program was run on the combined data. For all samples, the regression model fit for the combined data completed with convergence (Message 1), and generated valid parameters for analysis (Table 2.2). Using the combined data, values for 5 parameters in the equation were determined for each biological replication (Table 2.2). A mean and standard deviation of the 5 parameters for each genotype was then calculated, and comparisons among genotypes were made by one-way ANOVA analysis (see Table 3.1).

## **2.6 Starch Molecular Structure Analysis**

### **2.6.1 Preparation of Non-Granular Starch and Starch Fractions**

Preparation of non-granular (NG) starch and starch fractions followed the method of Klucinec and Thompson (1998) with a slight modification in sample size. Granular starches (~2 g, dry weight) were dispersed in 40 mL of 90% dimethyl sulfoxide (DMSO) by heating the mixtures in a boiling water bath with constant stirring for 3 hr. Following dispersion, 4 volumes of ethanol were added and the mixture was then centrifuged at  $6,500 \times g$  for 15 min at 4°C. The pellets were washed with 95% ethanol (twice) and acetone (once) before being dried at 50°C for 24 hr.

Table 2.2 Kinetics of digestion of the resistant starch assay: Process for obtaining two technical replications for each biological replication for analysis of Wt and *sbe1a* starch.

Starch	Converge (Y/N) <sup>1</sup>	y <sub>0</sub> (%)	S <sub>1</sub> (%)	k <sub>1</sub> (x 10 <sup>2</sup> min <sup>-1</sup> )	S <sub>2</sub> (%)	k <sub>2</sub> (x 10 <sup>3</sup> min <sup>-1</sup> )
Wt-B1, 1	Y	1.52	76.46	1.6	20	4.53
Wt-B1, 2	Y?	-95.24	83.48	1.42	110.9	0.14
Wt-B1,combined	Y	-3.92	84.1	1.46	18.33	1.21
Wt-B2, 1	Y	-0.8	89.13	1.47	9.91	1.43
Wt-B2, 2	N	-1536	86.78	1.7	1548	0.01
Wt-B2, 3	Y	-10.97	90.06	1.32	18.57	0.37
Wt-B2,1&3combined	Y	-4.25	89.89	1.38	12.28	0.72
Wt-B3, 1	N	-28050	81.41	1.47	28070	0
Wt-B3, 2	N	-2845	87.29	1.22	2856	0
Wt-B3, 3	Y	-3.05	73.04	1.6	28.32	1.7
Wt-B3, 4	Y?	-4191	92.44	1.14	4198	0
Wt-B3,3&4combined	Y	-8.05	83.65	1.31	23.01	0.89
<i>sbe1a</i> -B1, 1	Y	13.15	53.83	1.78	31.79	4.14
<i>sbe1a</i> -B1, 2	Y	12.85	61.23	1.68	23.72	2.96
<i>sbe1a</i> -B1,combined	Y	13.06	58.21	1.71	27.01	3.52
<i>sbe1a</i> -B2, 1	Y	18.05	24.49	3.02	54.62	7.22
<i>sbe1a</i> -B2, 2	Y	10.38	69.69	1.68	17.69	1.08
<i>sbe1a</i> -B2,combined	Y	16.78	57.87	1.77	22.63	3.81
<i>sbe1a</i> -B3, 1	Y	-32.03	63.48	1.9	65.91	0.34
<i>sbe1a</i> -B3, 2	Y	14.52	56.22	1.97	27.66	4.4
<i>sbe1a</i> -B3,combined	Y	11.21	63.31	1.85	23.3	1.8

<sup>1</sup> Y represents "Converged, tolerance satisfied."

Y? represents "Converged, tolerance satisfied. Parameter may not be valid."

Array numerically singular on final iteration."

N represents "Didn't converge, exceeded maximum number of iterations."

The dried NG starch was stored under desiccation ( $\text{CaSO}_4$ ).

For fractionation, NG starch (~1.5 g) was re-dispersed in 42 mL of 90% DMSO; then, 7 volumes of an aqueous mixture of 6% 1-butanol and 6% isoamyl alcohol was added to the dispersion. The mixtures were stirred and placed in a 95°C water bath for 1 hr, after which the entire system was insulated and allowed to cool to ~30°C for at least 18 hr. After cooling, the mixtures were gently agitated to re-suspend any precipitated starch and then centrifuged at  $10,000 \times g$  for 15 min at 4°C. The supernatants were saved. The precipitate was re-precipitated with the mixture of isoamyl alcohol and 1-butanol twice more, as described above. The supernatants from the three precipitation procedures were combined, and referred to as the amylopectin fraction. The secondary precipitate was dispersed in 42 mL of 90% DMSO and then mixed with 7 volumes of 6% 1-butanol. This mixture was heated, cooled, and centrifuged as described above. The supernatant from this step is referred to as the intermediate material fraction. The final precipitate, designated as the amylose fraction, was dispersed in 30 mL of 90% DMSO, precipitated by 95% ethanol, washed, dried and stored under desiccation, as described for the preparation of NG starch. The amylopectin and intermediate material fractions in aqueous alcohol mixtures were concentrated using a rotary evaporator, and then precipitated with ethanol, washed, dried, and stored as described above.

### **2.6.2 Iodine Binding Analysis of Starch Molecules**

The blue value and  $\lambda_{\text{max}}$  of NG starch and starch fractions were determined according to the procedures in Klucinec and Thompson (1998) with slight modifications in sample size. Starch samples (8 mg) were dispersed in 2 mL of DMSO containing 10% 6M urea (UDMSO) by heating in a boiling water bath for 3 hr

with intermittent vortexing. A 1-mL aliquot of each sample was placed in a 100-mL volumetric flask, to which approximately 95 mL of deionized water and 2 mL of an aqueous I<sub>2</sub>-KI solution (0.2% I<sub>2</sub> and 2% KI, w/v) were added. The mixture was brought to 100 mL with deionized water, mixed immediately, and stored in darkness for 15 minutes before spectrophotometric measurements (UltraSpec 3000; Pharmacia Biotech; Cambridge, England) were made. Blank solutions were made identically but without starch. Absorbance spectra were measured from 500 to 800 nm. The blue value of the starch was defined as the absorbance at 635 nm. The  $\lambda_{\max}$  was the wavelength of the maximum absorbance value over the range of wavelengths examined. Duplicate determinations were conducted for each starch sample.

### 2.6.3 Sepharose CL-2B Chromatography of Intact Molecules

Starch fractions were separated by chromatography on a Sepharose CL-2B column using gravity flow according to the procedures in Klucinec and Thompson (1998). The mobile phase in the system was 0.01M sodium hydroxide containing 0.02% (w/v) sodium azide. Starch samples (15 mg) were dispersed in 1 mL of 90% DMSO, diluted with 5 mL of mobile phase, filtered through a 5- $\mu$ m membrane, and then loaded onto the column using a sample applicator. The flow rate was adjusted to 20–30 mL/hr. For each sample, 500 mL of eluent was collected as 5-mL fractions using a fraction collector. Total carbohydrate and iodine binding analysis of 5-mL fractions followed the procedures in Klucinec and Thompson (1998). The void volume and salt volume of the column were determined for a mixture of 1 mg of *wx* starch and 1 mg of glucose, and were used for converting sample elution volumes to capacity factors ( $k'$ ) (Yau 1969).

#### 2.6.4 Preparation of Resistant Starch

For preparation of RS for subsequent analysis, 100 mg of starch was digested as described in 2.5.1. The isolation of RS followed the Megazyme RS assay procedure (Cat.No. K-RSTAR; Megazyme) at room temperature. After 16 hr, 1 volume of ethanol (99%) was added to the sample with vigorous vortexing. The mixture was then centrifuged at  $1,500 \times g$  for 10 min. Supernatant was carefully decanted; the pellet was re-suspended in 2 mL of 50% ethanol with vigorous vortexing, mixed with a further 6 mL of 50% ethanol, and centrifuged at  $1,500 \times g$  for 10 min. This suspension and centrifugation step was repeated once more, and the pellets were dried at 22°C for 24 hr.

#### 2.6.5 $\beta$ -Amylolysis of Amylopectin and Debranching of $\beta$ -Dextrins

$\beta$ -Dextrins were prepared by the method of Xia and Thompson (2006) with slight modifications in sample size. Amylopectin samples (48 mg) were dispersed in 480  $\mu$ L of 90% DMSO by heating in a boiling water bath for 10 min. To the dispersion, warm sodium acetate buffer (3.52 mL, 50°C; 0.02M, pH 6.0) was added. The mixture was heated in a boiling water bath for 10 min and cooled to 50°C. A 200- $\mu$ L aliquot of a  $\beta$ -amylase (from barley, Cat.No. E-BARBL; Megazyme) solution (250 U/mL (activity reported is as determined by manufacturer), 0.02M sodium acetate, pH 6.0) was added, and the samples were incubated at 50°C with constant agitation (200 strokes/min). At approximately 10 min, 30 min, 1 hr, 2 hr, 6 hr, and 24 hr, a 0.5-mL aliquot of sample was removed and heated in a boiling water bath for 10 min to stop the reaction. The procedures for precipitating  $\beta$ -dextrins and debranching  $\beta$ -dextrins by successive action of isoamylase (from *Pseudomonas* sp., Cat.No. E-ISAMY; Megazyme) and pullulanase (from *Klebsiella planticola*, Cat.No. E-PULKP;

Megazyme) were the same as used previously for  $\beta$ -limit dextrans ( $\beta$ -LDs) (Klucinec and Thompson 2002).

#### **2.6.6 Preparation of Isoamylase Debranched and Isoamylase plus Pullulanase Debranched $\beta$ -Limit Dextrans from Amylopectin and Amylose Fractions**

The preparation and debranching of  $\beta$ -LDs followed the procedures in Klucinec and Thompson (2002) with slight modifications in sample size. After the  $\beta$ -LDs were debranched with isoamylase for 24 hr, a 30- $\mu$ L aliquot of the digested solution was added to 270  $\mu$ L of DMSO and reserved for analysis by high-performance size-exclusion chromatography (HPSEC). Then the  $\beta$ -LDs were further debranched with pullulanase for 24 h, afterwards another 30- $\mu$ L aliquot of the digested solution was added to 270  $\mu$ L of DMSO for HPSEC analysis.

#### **2.6.7 High-Performance Chromatography of Debranched Molecules**

Debranching of NG starch, starch fractions, and RS followed the procedures in Klucinec and Thompson (1998). Debranching of  $\beta$ -dextrans and  $\beta$ -LDs followed the procedures in Klucinec and Thompson (2002). Debranched samples were desalted and subjected to HPSEC analysis, as described by Xia (2005). Except for the replacement of a new injector (Model 7725i; Rheodyne) the HPSEC system and the conditions of the separation were the same as those previously used (Klucinec and Thompson 1998). To construct a trinomial standard curve, maltose (DP 2), maltotriose (DP 3), maltoheptaose (DP 7), and three pullulan standards, P-5 (MW  $5.8 \times 10^3$ ,  $\sim$ DP 36), P-10 (MW  $1.22 \times 10^4$ ,  $\sim$ DP 75), and P-20 (MW  $2.37 \times 10^4$ ,  $\sim$ DP 146) were used. DPs from the standard curve, according to eluted time, are indicated on each chromatogram. DPs greater than 146 are shown only as estimates of starch

chain length. The chromatographic area of the refractive index response was normalized to equal total mass for all samples.

## **2.7 Starch Granular Structure Analysis**

All the microscopy work was performed for native starch and residual starch after RS digestion, at the Electron Microscopy Facility at PSU with the assistance from Ms. Missy Hazen.

### **2.7.1 Light Microscopy**

Bright field and polarized light microscopy were performed using a light microscope (BX51; Olympus) with an attached digital camera (Spot II RT; Diagnostic Instruments). 5 mg of native starch sample was mixed with 0.5 mL of deionized water in a micro-centrifuge tube. For the resistant starch samples, the supernatant was removed after centrifugation of digestion solution (see 2.2.3.1) and 20  $\mu$ L of deionized water was added to the pellets to disperse the sample. To examine the sample under the microscope, 20  $\mu$ L of the dispersed sample was added to a glass slide, and a cover slip was fixed over the sample with fingernail polish. Examination of iodine-stained starch followed the method in Evans and Thompson (2004). 20  $\mu$ L of iodine solution (0.08%  $I_2$ , 0.12% KI) was placed onto 20  $\mu$ L of the dispersed sample to give a final  $I_2$  concentration of 0.04%. In order to compare birefringence between granules, the camera's automatic exposure function turned off, and the exposure was set the same for all samples. The same sample field was examined under bright field and polarized light.

Heterogeneity of iodine staining was evaluated quantitatively. Differentially iodine-stained starch granules were classified into two categories, dark or light stained

granules, and were sorted visually by five individual evaluators who were not otherwise involved in the research. A sample micrograph was chosen from a portion of a micrograph for *sbe1a* granules, and granules were selected for use as standards to demonstrate the difference between dark and light stained granules for the evaluators. Four micrographs for each genotype (Wt or *sbe1a*) were used for sorting. The evaluators were then given those eight micrographs, unlabeled and in the randomized order, and asked to sort the granules into two categories. The proportion of dark granules for each micrograph was calculated based on the sorting results from all five evaluators, and a mean proportion was obtained for each micrograph. For each genotype, a mean was calculated from the means of the four micrographs. Comparison between two genotypes was made by one-way ANOVA.

### **2.7.2 Scanning Electron Microscopy**

A thin layer of starch sample was applied to double-sided sticky carbon tape on a specimen stub, and sputter-coated with 10 nm Au/Pd (BAL-TEC SCD 050; US-TechnoTrade). Samples were then examined using a scanning electron microscope (JSM-5400; JEOL Ltd.) at an accelerating voltage of 20 keV and at different magnification levels (1,500 ×, 3,500 ×, and 10,000 ×). For image collection, lower magnification was first employed to examine the whole view of samples, and higher magnification was then used to focus on sample areas that were representative overall.

### **2.7.3 Transmission Electron Microscopy**

Starch samples were stained and embedded in Eponate for TEM according to the methods in Planchot et al. (1995) and Rees (2008). Ultrathin (60–90 nm) sections of the embedded samples were obtained using an LKB III-8800 ultramicrotome

(Leica, Deerfield, IL), collected onto carbon-coated formvar-grids, and imaged with a transmission electron microscope (1200EXII; JEOL Ltd) at an accelerating voltage of 80 kV. Collected images were chosen as representative of the total population of samples, as described in 2.7.2.

## 2.8 Kernel Germination Assay

A kernel germination assay was performed according to the method in Dinges et al. (2003) with slight modifications. Mature, dried maize kernels were surface-sterilized by immersion in 15 mL of 1% sodium hypochlorite for 5 min and then washed three times with deionized water. 15 kernels from each of 3 ears for each genotype were placed in Petri dishes containing three layers of moist Whatman paper and incubated at 30°C in the dark. The length of each coleoptile was measured by a ruler on successive days throughout the 11-day incubation period. To measure the amount of endosperm starch remaining, the roots, coleoptiles, embryo, and pericarps were removed from 2 kernels at days 1, 6, 8, and 11. The remaining endosperm was ground with a mortar and pestle on ice. The powdered tissue was washed into a tube with deionized water and homogenized with a Tissumizer (Model SDT 1810; Tekmar) at 20,000 rpm for 1 min. The ground tissue was washed with deionized water, centrifuged at  $1500 \times g$  for 10 min, and suspended in 3 mL of deionized water. For calculating the dry weight of samples, 1 mL of this suspension was dried at 70°C overnight and weighed. The remaining 2 mL of the suspension was boiled for 30 min, and the total glucan polysaccharide in the solubilized solution was quantified in triplicates, using a commercial assay kit that measures glucose released after digestion with  $\alpha$ -amylase and amyloglucosidase (Cat.No. K-TSTA; Megazyme). The quantified starch content was normalized against the dry weight for comparison

between genotypes.

## 2.9 References-Chapter 2

- Blauth, S.L., Kim, K., Klucinec, J.D., Shannon, J.C., Thompson, D.B., and Gultinan, M.J. (2002). Identification of Mutator insertional mutants of starch branching enzyme 1 (sbe1) in *Zea mays* L. *Plant Mol. Biol.* 48, 287-297.
- Blauth, S.L., Yao, Y., Klucinec, J.D., Shannon, J.C., Thompson, D.B., and Gultinan, M.J. (2001). Identification of Mutator insertional mutants of starch-branching enzyme 2a in corn. *Plant Physiol.* 125, 1396-1405.
- Boyer, C.D., Daniels, R.R., and Shannon, J.C. (1976). Abnormal starch granule formation in *Zea mays* L. endosperms possessing the *amylose-extender* mutant. *Crop Sci.* 16, 298-301.
- Commission on Plant Gene Nomenclature. (1993). A nomenclature for sequenced plant genes. *Plant Mol. Biol. Reprtr.* 11, 291-312.
- Dellaporta, S. (1994). Plant DNA miniprep and microprep: versions 2.1-2.3. In: M. Freeling and V. Walbot (Eds.) *The Maize Handbook*, Springer-Verlag, New York, pp. 522-525.
- Dinges, J.R., Colleoni, C., James, M.G., and Myers, A.M. (2003). Mutational analysis of the pullulanase-type debranching enzyme of maize indicates multiple functions in starch metabolism. *Plant Cell* 15, 666-680.
- Dubois, M., Gilles, K. A., Hamilton, J. K., Rebers, P. A., and Smith, F. (1956). Colorimetric method for determination of sugars and related substances. *Anal. Chem.*, 28, 350-356.
- Evans, A. and Thompson, D.B. (2004). Resistance to  $\alpha$ -Amylase digestion in four active high-amylose maize starches *Cereal Chem.* 81, 31-37.
- Evans, A. and Thompson, B.D. (2008). Enzyme susceptibility of high-amylose starch precipitated from sodium hydroxide dispersions. *Cereal Chem.* 85, 480-487.
- Klucinec, J.D., and Thompson, D.B. (1998). Fractionation of high amylose maize starches by differential alcohol precipitation and chromatograph of the fractions. *Cereal Chem.* 75, 887-896.
- Klucinec, J.D., and Thompson, D.B. (2002). Note: Structure of amylopectins from *ae*-containing maize starches. *Cereal Chem.*, 79, 19-23.
- Planchot, V. P. Colonna, D.J. Gallant, and B. Bouchet. (1995). Extensive degradation of native starch granules by alpha-amylase from *Apergillus fumigatus*. *J. Cereal Sci.* 21, 163-171.

- Rees, E. (2008). Effect of a heat-moisture treatment on alpha-amylase susceptibility of high amylose maize starches. MS thesis. The Pennsylvania State University, University Park, PA.
- Xia, H. (2005). Branching pattern differences among amylopectins of several maize genotypes. MS thesis. The Pennsylvania State University, University Park, PA.
- Xia, H., and Thompson, D.B. (2006). Debranching of  $\beta$ -limit dextrins with isoamylase or pullulanase to explore the branching pattern of amylopectins from three maize genotypes. *Cereal Chem.* 83, 668-676.
- Yau, W.W. (1969). Steric exclusion and lateral diffusion in gel-permeation chromatography. *J. Polym. Sci. Part A-2* 7, 483-495.
- Yao, Y., Guiltinan, M.J., Shannon, J. C., and Thompson, D.B., (2002). Single kernel sampling method for maize starch analysis while maintaining kernel vitality. *Cereal Chem.*, 79, 757-762.
- Yao, Y., Thompson, D.B., and Guiltinan, M.J. (2003). Starch biosynthesis in Maize endosperm: in the absence of SBEIIb, the deficiency of SBEIIa leads to increased Amylopectin Branching. Presentation at 2003 AACC conference, Portland, OR.

## Chapter 3

# EFFECTS OF MAIZE SBEI DEFICIENCY ON ENDOSPERM STARCH STRUCTURE AND FUNCTION

### 3.1 Introduction and Objectives

Maize starch-branching enzyme (SBE) isoforms are known to influence starch structure and function. For example, the *ae* endosperm mutant, which is deficient in SBEIIb, has a profound effect on starch structure, leading to an increased amylose proportion and a reduced branching density of amylopectin (Garwood et al. 1976; Boyer et al. 1977; Boyer and Preiss 1981). Although no effect of SBEI deficiency alone on starch structure has been noted previously (Blauth et al. 2002; Yao et al. 2004), for endosperm starch deficient in SBEIIb, a further deficiency of SBEI increased branching of amylopectin (Yao et al. 2004). Using a small amount of starch obtained for different purpose, a preliminary test of endosperm starch digestibility for the *sbe1a* mutant showed that deficiency of SBEI caused a decreased susceptibility of the starch granules to pancreatic  $\alpha$ -amylase (Xia et al. 2007). This was the first indication of a function of SBEI alone in synthesis of endosperm starch. The likelihood that this functional difference had a basis in molecular structure justified further investigation of the function of the SBEI isoform by studying the structure and function of *sbe1a* mutant endosperm starch compared to Wt starch.

The objectives of this chapter were to determine digestion rate and extent using an *in vitro* resistant starch (RS) assay; to characterize molecular structure of the amylopectin and amylose fractions; to characterize granule structure for native starch and residual granule structure for RS after  $\alpha$ -amylase digestion, for a Wt and *sbe1a*

starch; to develop a hypothesis about how starch structure differences in the *sbe1a* mutant might cause decreased susceptibility to starch digestion; and to compare starch utilization and coleoptile growth for Wt and *sbe1a* seeds during germination. This information will provide insight into the functional significance of SBEI in the synthesis, hydrolysis, and utilization of maize endosperm starch.

## **3.2 Results**

### **3.2.1 Starch Digestibility**

A preliminary experiment indicated that the *sbe1a* mutant increased the RS value for endosperm starch. In order to have a definite determination of the effect of *sbe1a* on starch digestibility, three biological samples for both Wt and *sbe1a* generated from highly similar genetic background were used (see section 2.3), and both the digestion rate and extent were examined using an *in vitro* RS assay.

#### **3.2.1.1 Resistant Starch Value**

The experimental design followed a hierarchical nested order (Fig. 3.1), and the RS values of the three technical replications for each of the three biological replications were obtained (Table A.1, Appendix A). Determination of RS was based on the value averaged from three biological replications for each genotype. For each biological replication, the RS assay was conducted three times on separate days, considered as three technical replications. This experimental design had three sequentially nested sources of variability: genotype, biological replication, and technical replication. F-tests performed for a fully nested analysis of variance (ANOVA) (Table 3.1) showed that the effect of genotype was significant ( $p$ -value = 0.000), while the effect of biological replication was not ( $p$ -value = 0.334).

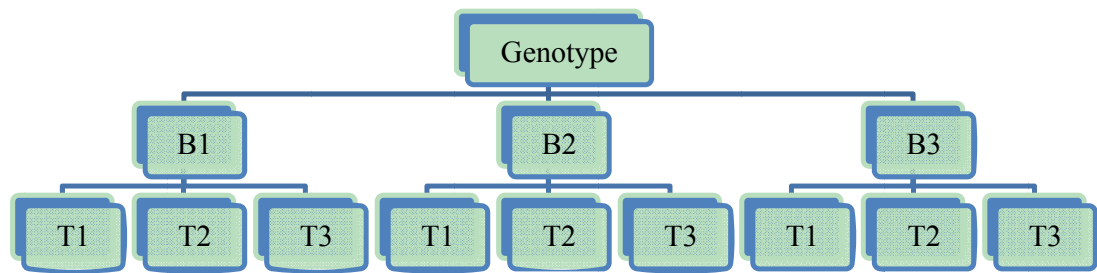


Figure 3.1 Hierarchical order of experimental design for resistant starch value determination. B1, B2, and B3 represent three biological replications, meaning that starch was extracted from three different ears from three plants. T1, T2, and T3 represent three technical replications for each biological replication.

The variance component estimated by nested ANOVA indicated that the variability attributable to genotype, biological replication, and technical replication was, respectively, 93.56, 0.54, and 5.90 percent, of the total variability (Table 3.1). The statistical results indicated that the RS values were reproducible among technical replications, indistinguishable among different biological samples, and dominantly influenced by the genotype effect. The RS values from the three technical replications were averaged for each biological replication, and the mean and standard deviation of the three biological replications for each genotype were then reported, and comparisons were made by one-way ANOVA (Table 3.2). The RS value was significantly higher in the *sbe1a* mutant starch (13.2%) as compared to Wt (1.6%).

#### **3.2.1.2 Digestion Time-Course Kinetics**

Analysis of digestion kinetics was based on the digestion time-course for RS determination. The kinetics of digestion was analyzed using a double-exponential decay fit, and five parameters from the model fit were obtained for Wt and *sbe1a* (Table 3.3). For graphic illustration of the component digestion data, the curves based on the combined data from two independent digestions on one biological replication are shown (Fig. 3.2). For each genotype, the curves for each of the three biological replications are shown (Fig. 3.3).

As depicted in Fig. 3.2, the time course of digestion between Wt and *sbe1a* mutant were different. Fig. 3.3 shows that the digestion pattern was similar among the three biological replications for each genotype. The value at 960 min (the time that defined the level of RS) was also similar among the three biological replications for each genotype, consistent with the analyses described in Table 3.1.

Table 3.1 Nested ANOVA results of resistant starch value versus the three sequentially nested factors of genotype, biological replication, and technical replication, for endosperm starch from Wt and *sbe1a* mutant.

Source	DF	SS	MS	F	P
Genotype	1	0.0606	0.0606	112.987	0.000
Biological rep	4	0.0021	0.0005	1.274	0.334
Technical rep	12	0.0051	0.0004		
Total	17	0.0678			

#### Variance Components

Source	Var	Comp.	% of	
			Total	StDev
Genotype	0.007	0.007	93.56	0.082
Biological rep	0.000	0.000	0.54	0.006
Technical rep	0.000	0.000	5.90	0.021
Total	0.007	0.007		0.084

#### Expected Mean Squares

1	Genotype	1.00(3) + 3.00(2) + 9.00(1)
2	Biological rep	1.00(3) + 3.00(2)
3	Technical rep	1.00(3)

Table 3.2 Resistant starch values for Wt and *sbe1a* mutant starch<sup>1</sup>.

<b>Starch Genotype</b>	<b>Resistant Starch Value (%)</b>
<b>Wt</b>	1.6 ± 0.5 <sup>a</sup>
<b><i>sbe1a</i></b>	13.2 ± 1.8 <sup>b</sup>

<sup>1</sup>Values are percentages of starch that was not digested. Values are expressed as mean ± standard deviation for three biological replications. Significant difference as determined by one-way ANOVA is indicated by different superscripts.

Table 3.3 Kinetics of digestion of the resistant starch assay for Wt and *sbe1a* mutant starch<sup>1</sup>.

<b>Starch</b>	<b><math>y_0</math> (%)</b>	<b><math>S_1</math> (%)</b>	<b><math>k_1</math> (min<sup>-1</sup>)</b>	<b><math>S_2</math> (%)</b>	<b><math>k_2</math> (min<sup>-1</sup>)</b>
<b>Wt</b>	$-5.4 \pm 2.3^a$	$85.9 \pm 3.5^b$	$1.4 \pm 0.1^a$ ( $\times 10^{-2}$ )	$17.9 \pm 5.4^a$	$0.9 \pm 0.2^a$ ( $\times 10^{-3}$ )
<b><i>sbe1a</i></b>	$13.7 \pm 2.8^b$	$59.8 \pm 3.0^a$	$1.8 \pm 0.1^b$ ( $\times 10^{-2}$ )	$24.3 \pm 2.4^a$	$3.0 \pm 1.1^b$ ( $\times 10^{-3}$ )

<sup>1</sup>Values are expressed as mean  $\pm$  standard deviation for three biological replications. Values for each biological replication were obtained from fit of combined data from two independent digestions. Significant differences in the same column, as determined by one-way ANOVA analysis, are indicated by different superscripts.

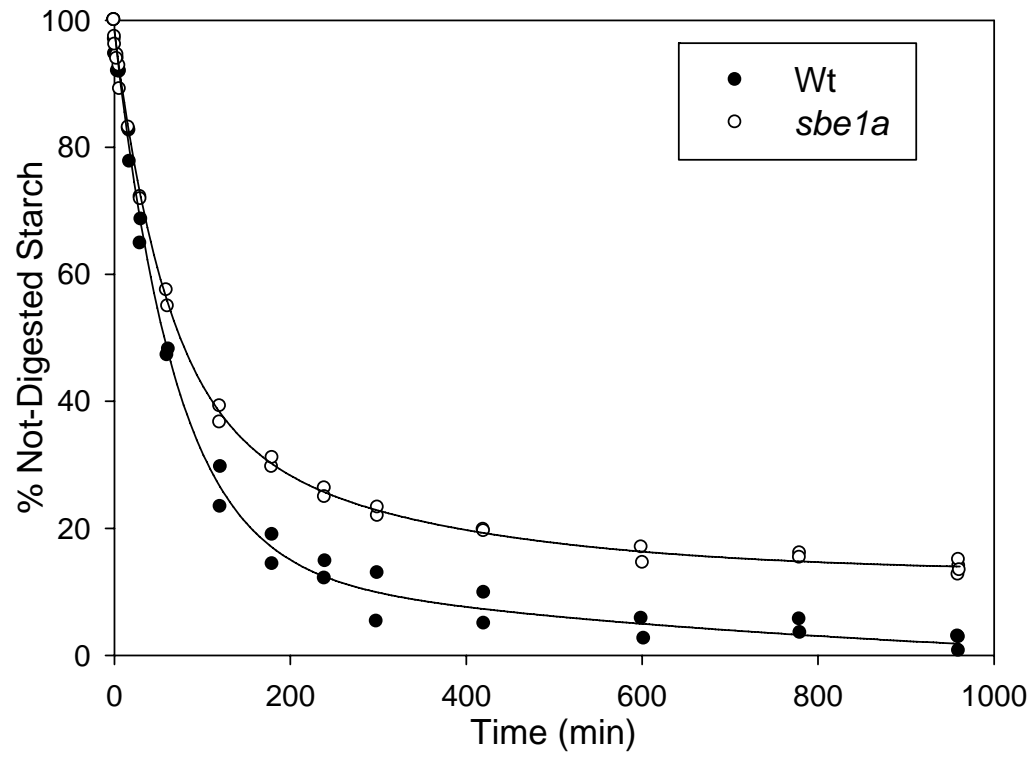


Figure 3.2 Time course of digestion of the resistant starch assay for Wt and *sbe1a* mutant starch from one biological replication. Curves shown are best fits of analysis of combined data from two independent digestions.

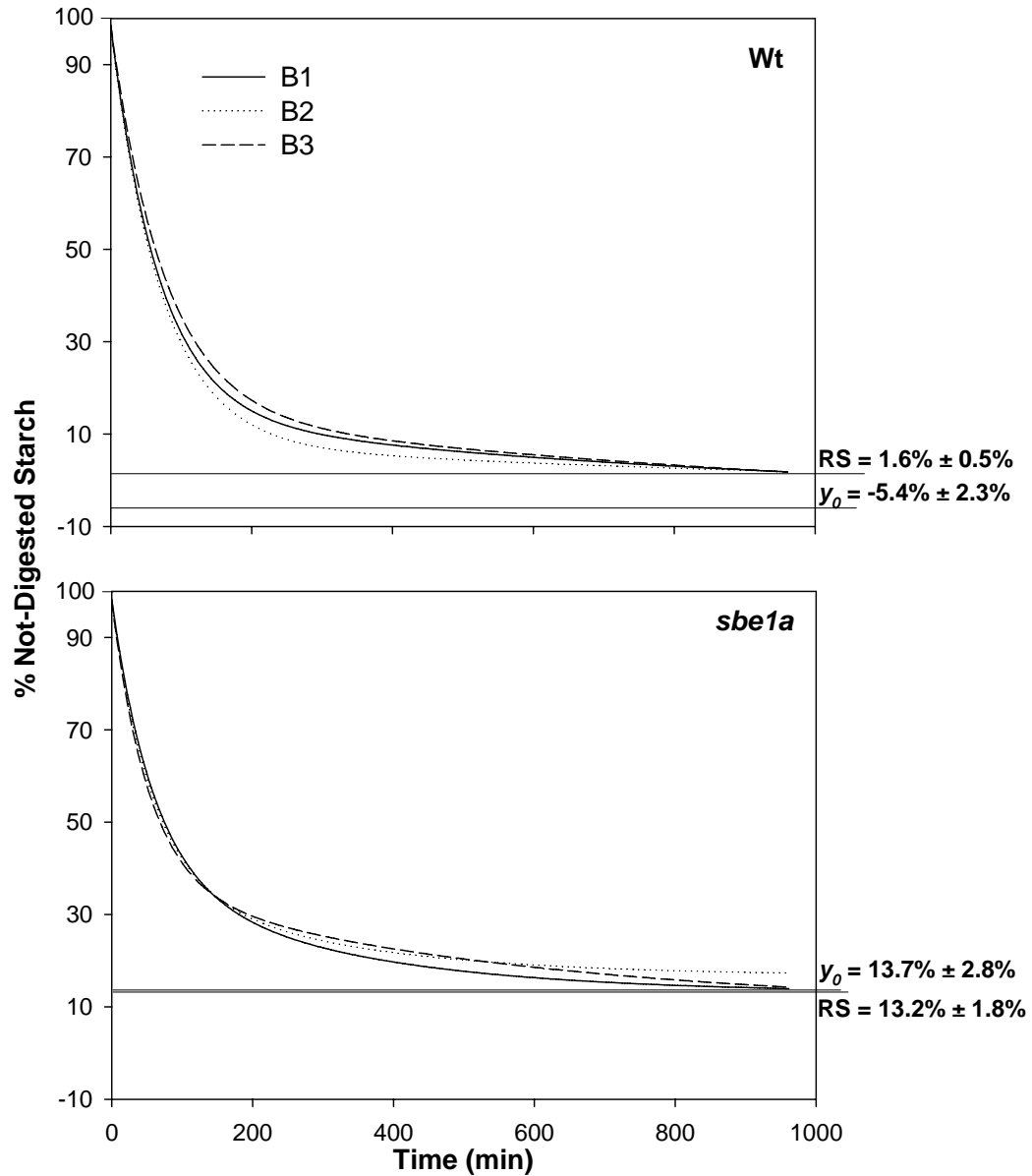


Figure 3.3 Best fit curves for digestion of the resistant starch assay for Wt (above) and *sbe1a* mutant (below) starch, using combined data from two independent digestions for each biological replication (B1, B2, B3). Mean and standard deviation of the parameters for each curve are presented in Table 3.3. The means and standard deviations for RS and  $y_0$  values (as reported in Table 3.2 and 3.3) are indicated for each starch.

A significantly higher  $y_0$  was found in *sbe1a* than for Wt, consistent with the higher RS value for this genotype (Table 3.2). The  $y_0$  was lower than the RS value for Wt starch, but the  $y_0$  and the RS value were similar for *sbe1a* starch (Table 3.2 & 3.3, Fig. 3.3). A significantly larger  $S_1$  value and a numerically smaller  $S_2$  value were observed for Wt than *sbe1a* (Table 3.3). The reaction rate constants for both components were smaller in Wt than *sbe1a*.

### 3.2.2 Starch Molecular Structure

I reasoned that if SBEI activity is important in determining starch digestibility, then an altered starch structure would also be observed in the *sbe1a* mutant. I further reasoned that the fundamental effect of altering an SBE activity would be to produce an altered branching pattern in starch, and the altered branching pattern may change the molecular structure of different fractions (amylopectin, amylose, and intermediate material) in starch. To study the effect of *sbe1a* on starch molecular structure, Wt and *sbe1a* starch were first fractionated, and the fine molecular structure of main fractions, amylopectin and amylose, was characterized.

#### 3.2.2.1 Starch Fractionation

For both genotypes, the total recovery from the fractionation procedure was above 90%. Amylopectin accounted for the largest component recovered from the fractionation, followed by amylose and intermediate material (Table 3.4). For all the starch fractions recovered, the proportion was not significantly different in *sbe1a* mutant from that in Wt.

Table 3.4 Recovery of starch fractions (% w/w) by differential alcohol precipitation from Wt and *sbe1a* mutant starch<sup>1</sup>.

<b>Starch Genotype</b>	<b>Total Recovery<sup>2</sup></b>	<b>Amylopectin<sup>3</sup></b>	<b>Amylose<sup>3</sup></b>	<b>Intermediate Material<sup>3</sup></b>
<b>Wt</b>	94.7 ± 1.2 <sup>a</sup>	72.8 ± 1.8 <sup>a</sup>	19.5 ± 2.3 <sup>a</sup>	7.7 ± 0.5 <sup>a</sup>
<b><i>sbe1a</i></b>	92.8 ± 2.7 <sup>a</sup>	71.5 ± 2.0 <sup>a</sup>	19.6 ± 0.8 <sup>a</sup>	8.9 ± 1.3 <sup>a</sup>

<sup>1</sup>Values are mean ± standard deviation based on fractionation results for three biological replications. Significant differences in the same column, as determined by one-way ANOVA, are indicated by different superscripts.

<sup>2</sup>Based on the sum of weights of recovered fractions divided by the starting weight of non-granular starch. Moisture content was assumed to be the same for all materials.

<sup>3</sup>Based on the weight of recovered fraction divided by the sum of the weights of the three recovered fractions.

### 3.2.2.2 Iodine Binding Properties of Non-Granular Starch and Starch Fractions

The non-granular (NG) starting material and the three fractions from Wt and *sbe1a* starch had similar iodine binding behaviors (Fig. 3.4). As is typically observed, the amylopectin from each genotype had the lowest absorbance at all wavelengths, the lowest  $\lambda_{\max}$ , and the lowest blue value. For each genotype, the amylose and intermediate material had almost overlapping absorbance curves, and both had the highest absorbance at all wavelengths, the highest  $\lambda_{\max}$ , and the highest blue value (Fig. 3.4, Table 3.5). The blue values and  $\lambda_{\max}$  were indistinguishable for the NG starch from both genotypes (Table 3.5). The blue values for the three starch fractions were indistinguishable for the two genotypes as well (Table 3.5). A slightly higher  $\lambda_{\max}$  was observed in *sbe1a* in each of the three starch fractions as compared to Wt (Table 3.5).

### 3.2.2.3 Size Distribution of Intact Amylopectin and Amylose Fractions

In order to examine the size distribution of intact molecules from the amylopectin and amylose fractions, the samples were separated by Sepharose CL-2B chromatography. The total carbohydrate elution profile, representing the mass response, and iodine binding  $\lambda_{\max}$ , correlating to the chain length (CL), are shown in Fig. 3.5. According to the methods in Klucinec and Thompson (1998), the chromatograms were divided into two regions: a region preceding  $k' = 0.2$ , representing material eluting near the void volume, and a region after  $k' = 0.2$  (Fig. 3.5a,b). The proportions of the two regions were calculated (Table 3.6). For both genotypes, a major proportion of the amylopectin (> 80%) eluted within the void volume region of the chromatogram, and had a  $\lambda_{\max}$  fluctuating around 550-560 nm.

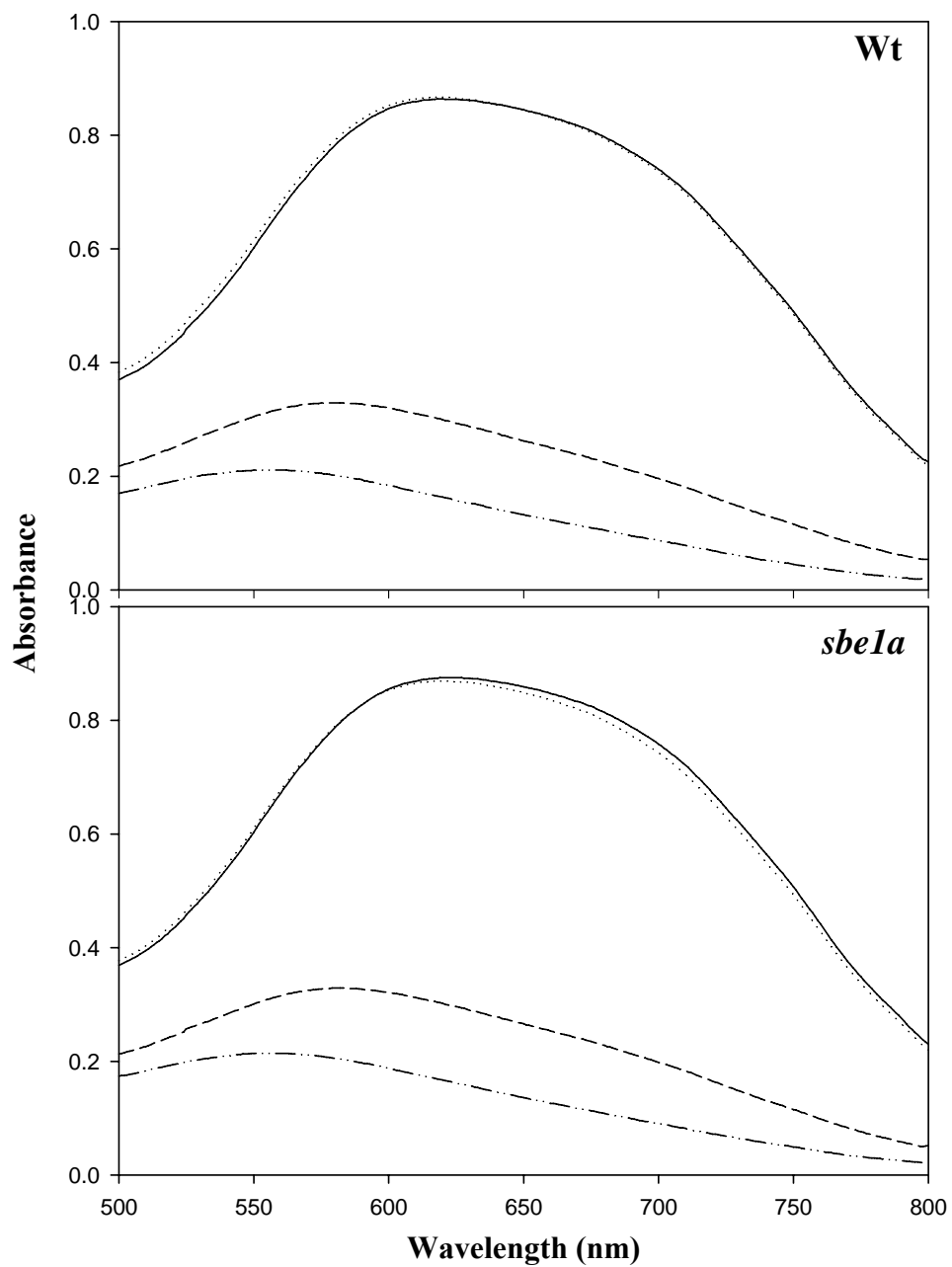


Figure 3.4 Iodine binding by non-granular starch and starch fractions obtained by differential alcohol precipitation from Wt and *sbel1* mutant starch<sup>1</sup>. Non-granular starches (---), amylopectin (- · - · -), intermediate material (·····), and amylose (—).

<sup>1</sup>Starch from one biological replication. See Table 3.5 for blue values and  $\lambda_{max}$  of starch samples.

Table 3.5 Iodine binding properties of non-granular starch and starch fractions recovered by differential alcohol precipitation from Wt and *sbe1a* mutant starch<sup>1</sup>.

Starch Samples	Blue Value <sup>2</sup>	$\lambda_{\max}$ <sup>3</sup>
<b>Non-granular Starch</b>		
Wt	0.28 ± 0.01 <sup>a</sup>	580.8 ± 0.5 <sup>a</sup>
<i>sbe1a</i>	0.28 ± 0.01 <sup>a</sup>	581.3 ± 0.4 <sup>a</sup>
<b>Amylopectin</b>		
Wt	0.15 ± 0.01 <sup>a</sup>	555.3 ± 0.7 <sup>a</sup>
<i>sbe1a</i>	0.15 ± 0.01 <sup>a</sup>	557.0 ± 0.1 <sup>b</sup>
<b>Amylose</b>		
Wt	0.86 ± 0.01 <sup>a</sup>	618.5 ± 0.8 <sup>a</sup>
<i>sbe1a</i>	0.87 ± 0.01 <sup>a</sup>	623.8 ± 0.5 <sup>b</sup>
<b>Intermediate Material</b>		
Wt	0.86 ± 0.01 <sup>a</sup>	618.5 ± 0.3 <sup>a</sup>
<i>sbe1a</i>	0.86 ± 0.00 <sup>a</sup>	619.5 ± 0.2 <sup>b</sup>

<sup>1</sup>Values are mean ± standard deviation based on two independent analyses for one biological replication. Significant differences within each category in the same column, as determined by one-way ANOVA, are indicated by different superscripts.

<sup>2</sup>Blue value is the absorbance of starch iodine mixture at 635 nm (Morrison and Laingelet 1983). See Fig. 3.4.

<sup>3</sup>Iodine binding wavelength maximum (Morrison and Laingelet 1983). See Fig. 3.4.

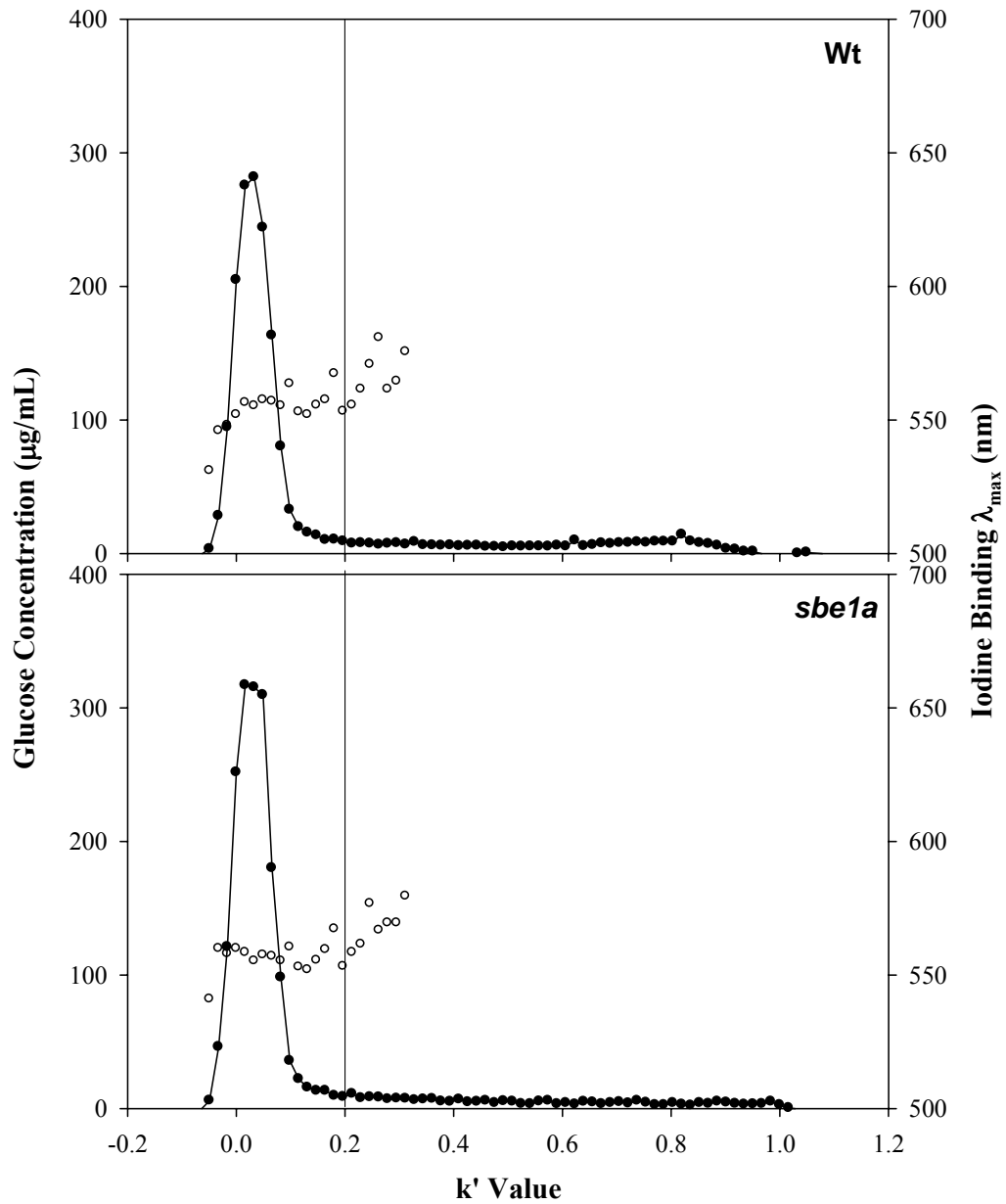


Figure 3.5a Size-exclusion chromatograms of amylopectin fraction from Wt and *sbe1a* mutant starch<sup>1</sup>. Line with filled dots refers to glucose concentration determined by sulfuric acid and phenol assay (Dubois et al. 1956) (uncorrected for 10% increase from hydrolyzed glucose); unfilled dots refer to iodine binding  $\lambda_{\max}$ .

<sup>1</sup>Starch from one biological replication.

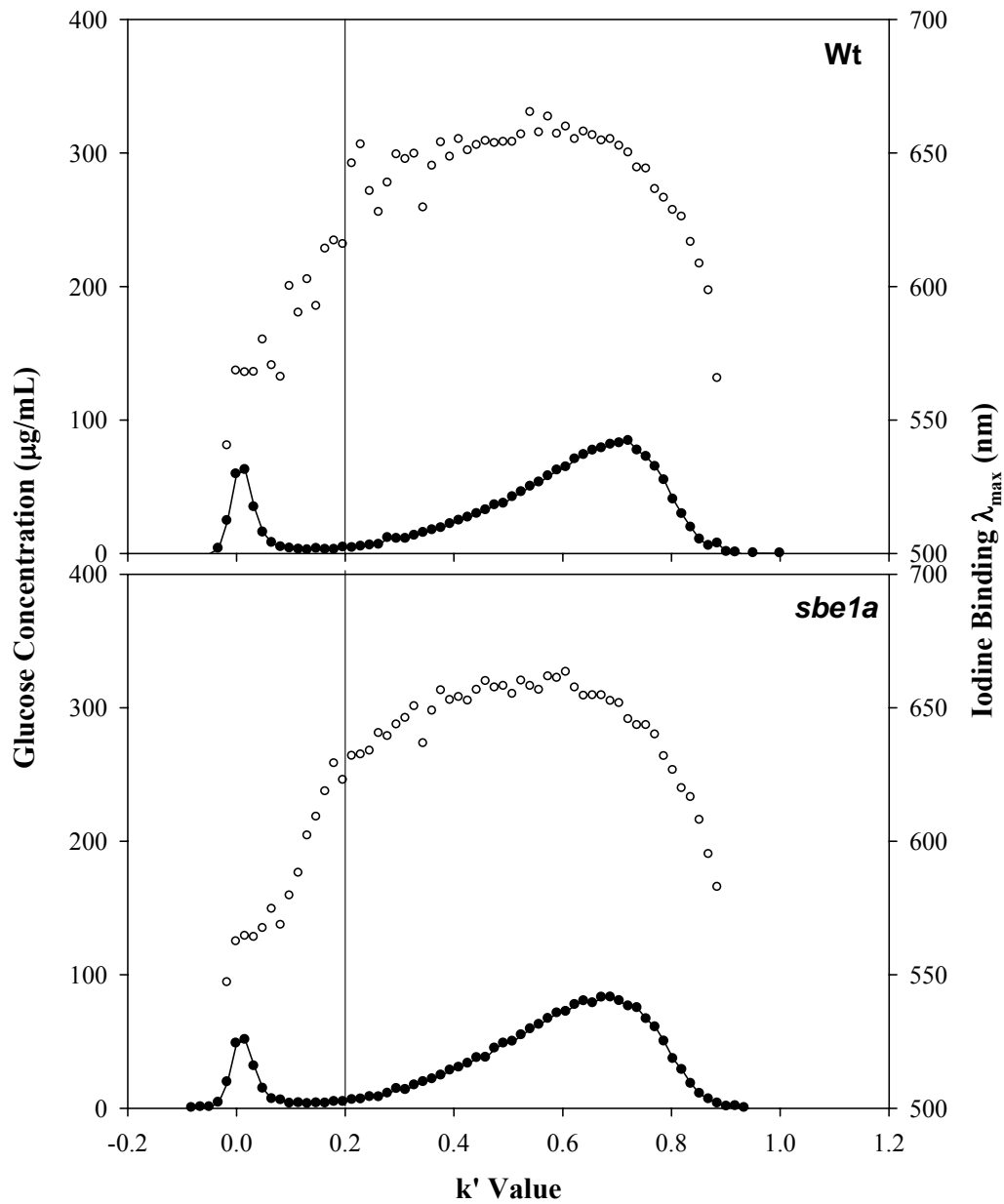


Figure 3.5b Size-exclusion chromatograms of amylose fraction from Wt and *sbe1a* mutant starch<sup>1</sup>. Line with filled dots refers to glucose concentration determined by sulfuric acid and phenol assay (Dubois et al. 1956) (uncorrected for 10% increase from hydrolyzed glucose); unfilled dots refer to iodine binding  $\lambda_{\max}$ .

<sup>1</sup>Starch from one biological replication.

Table 3.6 Partial chromatogram areas of amylopectin and amylose fractions from size-exclusion chromatography for Wt and *sbe1a* mutant starch<sup>1</sup>.

<b>Starch Sample</b>	<b>Starch Eluting (%)</b>	
	<b>Below <math>k' = 0.2</math></b>	<b>Above <math>k' = 0.2</math></b>
<b>Wt</b>		
Amylopectin	83	17
Amylose	12	88
<b><i>sbe1a</i></b>		
Amylopectin	88	12
Amylose	11	89

<sup>1</sup>Values are based on analysis for one biological replication. See Fig. 3.5 for chromatograms.

The proportion of the *sbe1a* amylopectin eluting after  $k' = 0.2$  was lower than for the Wt amylopectin (12% versus 17%, Table 3.6).

Amylose fractions from both genotypes had similar size distribution and iodine binding behavior (Table 3.6, Fig. 3.5b). Only a small proportion of the amylose eluted before  $k'$  of 0.1. These molecules had an iodine binding  $\lambda_{\max}$  of approximately 560 nm. The  $\lambda_{\max}$  of molecules eluting after  $k'$  of 0.1 increased rapidly, reaching a maximum of approximately 660 nm, and then decreased as the  $k'$  value approached 1.0. No difference was observed in the proportion of the regions below and above  $k'$  of 0.2 for both genotypes.

#### **3.2.2.4 Chain Length Distribution of Debranched Non-Granular Starch and Starch Fractions**

The chromatograms of each sample were divided into three regions for comparison (Fig. 3.6a,b). The division was based on the minima observed for debranched amylopectin from Wt, as in Klucinec and Thompson (1998). The adjusted proportions of region II and III allow the direct comparison of these regions excluding the influence of apparent contamination from amylose during the fractionation procedure.

By visual inspection, CL distribution of debranched NG starch and three starch fractions for both genotypes appeared similar (Fig. 3.6a,b). Proportions of chromatographic regions of all the starch samples were indistinguishable between both genotypes (Table 3.7). For both genotypes, region I, II, and III of the NG starch corresponded to approximately 28, 18, and 54% of the total area (Table 3.7). As is typically observed, for both genotypes, the proportion of region I followed the order amylose > intermediate material > NG starch > amylopectin (Table 3.7).

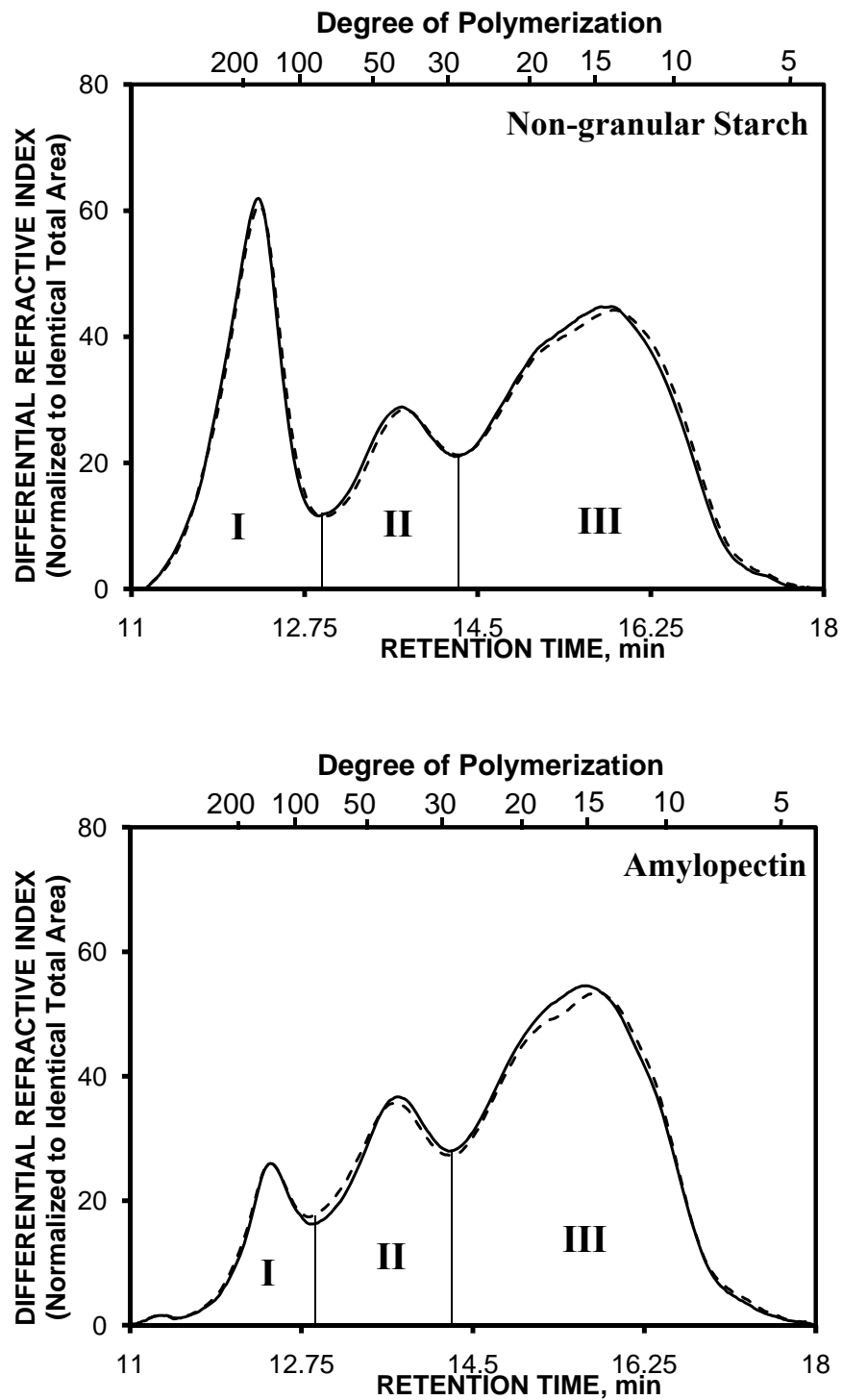


Figure 3.6a Chromatograms of isoamylase-debranched non-granular starch and amylopectin fractions from Wt (—) and *sbe1a* mutant (---) starch<sup>1</sup>.

<sup>1</sup>Representative chromatograms for starch from one biological replication. Proportions of region I, II, and III are presented in Table 3.7.

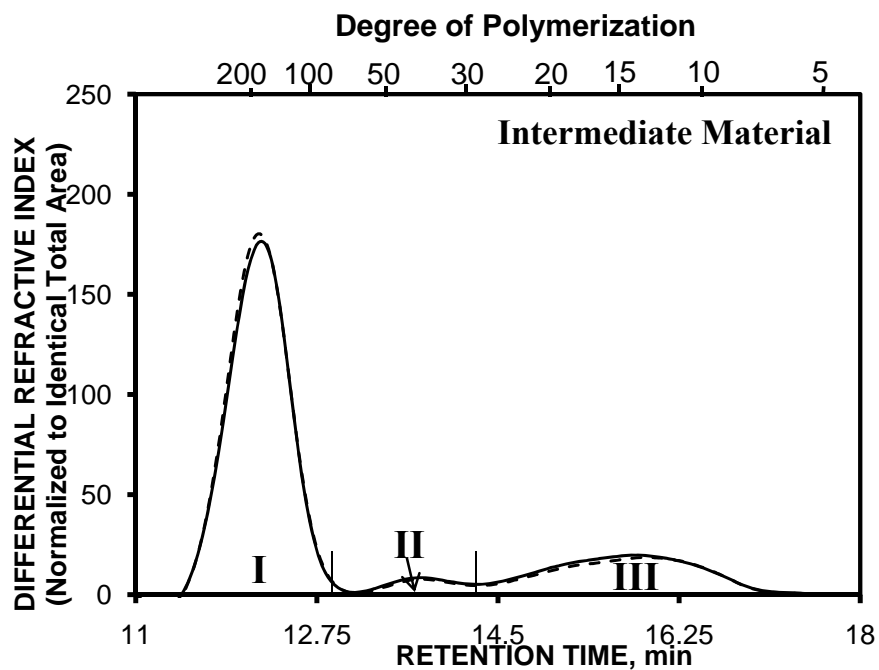
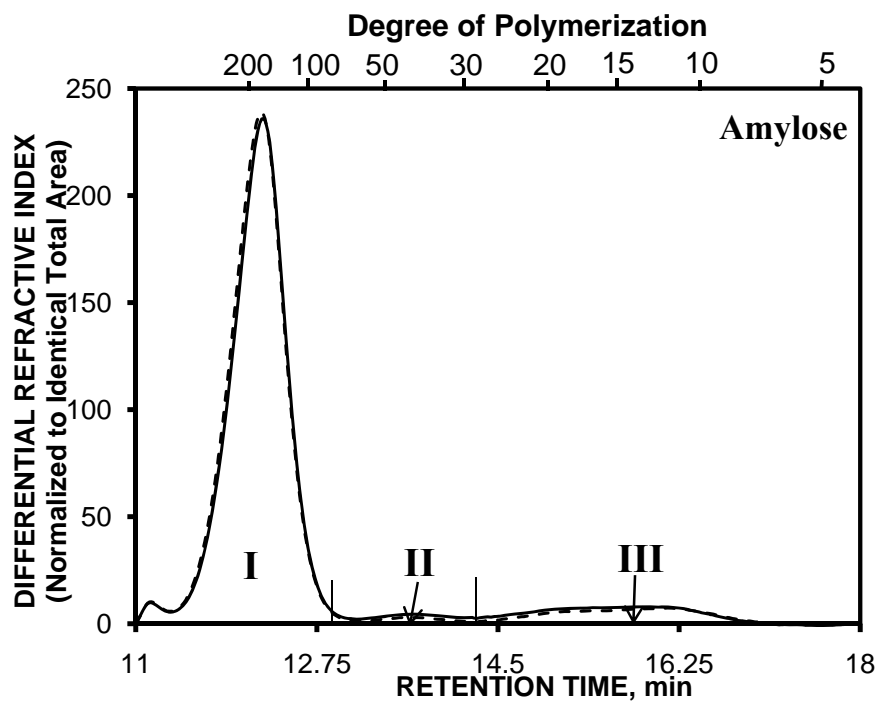


Figure 3.6b Chromatograms of isoamylase-debranched amylose and intermediate material fractions from Wt (—) and *sbe1a* mutant (---) starch<sup>1</sup>.

<sup>1</sup>Representative chromatograms for starch from one biological replication. Proportions of region I, II, and III are presented in Table 3.7.

Table 3.7 Chain length distribution of isoamylase-debranched non-granular starch and starch fractions from Wt and *sbe1a* mutant starch<sup>1</sup>.

Sample	Chromatographic Region <sup>2</sup>		
	I	II	III
<b>Non-granular Starch</b>			
<b>Wt</b>			
Weight %	27.4 ± 0.2 <sup>a</sup>	18.5 ± 0.5	54.1 ± 0.3
Adj Weight % <sup>3</sup>		25.5 ± 0.7 <sup>a</sup>	74.5 ± 0.7 <sup>a</sup>
<b><i>sbe1a</i></b>			
Weight %	27.9 ± 0.5 <sup>a</sup>	17.8 ± 0.1	54.3 ± 0.6
Adj Weight % <sup>3</sup>		24.6 ± 0.4 <sup>a</sup>	75.4 ± 0.4 <sup>a</sup>
<b>Amylopectin</b>			
<b>Wt</b>			
Weight %	9.7 ± 1.3 <sup>a</sup>	23.3 ± 0.5	67.0 ± 1.8
Adj Weight % <sup>3</sup>		25.8 ± 1.0 <sup>a</sup>	74.2 ± 1.0 <sup>a</sup>
<b><i>sbe1a</i></b>			
Weight %	10.8 ± 0.2 <sup>a</sup>	23.3 ± 0.8	65.9 ± 1.0
Adj Weight % <sup>3</sup>		26.1 ± 1.0 <sup>a</sup>	73.9 ± 1.0 <sup>a</sup>
<b>Amylose</b>			
<b>Wt</b>			
Weight %	86.9 ± 1.8 <sup>a</sup>	3.6 ± 1.0	9.4 ± 0.8
Adj Weight % <sup>3</sup>		27.5 ± 4.1 <sup>a</sup>	72.5 ± 4.1 <sup>a</sup>
<b><i>sbe1a</i></b>			
Weight %	89.8 ± 1.1 <sup>a</sup>	2.3 ± 0.7	8.0 ± 0.4
Adj Weight % <sup>3</sup>		21.8 ± 4.2 <sup>a</sup>	78.2 ± 4.2 <sup>a</sup>
<b>Intermediate Material</b>			
<b>Wt</b>			
Weight %	72.6 ± 1.5 <sup>a</sup>	6.3 ± 2.6	21.1 ± 1.1
Adj Weight % <sup>3</sup>		22.8 ± 8.1 <sup>a</sup>	77.2 ± 8.1 <sup>a</sup>
<b><i>sbe1a</i></b>			
Weight %	74.6 ± 1.4 <sup>a</sup>	5.9 ± 2.7	19.5 ± 1.3
Adj Weight % <sup>3</sup>		23.0 ± 9.3 <sup>a</sup>	77.0 ± 9.3 <sup>a</sup>

<sup>1</sup>Values are mean ± standard deviation based on two independent analyses for one biological replication. See Fig 3.6. Significant differences within each category in the same column, as determined by one-way ANOVA, are indicated by different superscripts.

<sup>2</sup>Regions were divided based on the minima observed for debranched amylopectin from wild-type starch, as in Klucinec and Thompson (1998).

<sup>3</sup>Adjusted weight percentage does not include the area from region I of the chromatogram.

### 3.2.2.5 Chain Length Distribution of Debranched Resistant Starch

The chromatograms of the debranched RS sample were divided into the same three regions (Fig. 3.7) as described in 3.2.2.4. Comparison of the proportions of the regions is shown in Table 3.8. The debranched RS from *sbe1a* had a slightly higher proportion of region I and a slightly lower proportion of region II than that from Wt (Table 3.8). By visually comparing the two chromatograms (Fig. 3.7), the CL distribution in region III for *sbe1a* was more towards smaller DP than that for Wt, even though the proportion of region III was indistinguishable between two genotypes (Table 3.8). In comparison to the respective native starch, there was an increase in the proportion of region II and a decrease in the proportion of region III for RS from both genotypes (Table 3.8). A decrease in the proportion of region I was also observed in the RS from Wt as compared to native starch, but not for *sbe1a* samples.

### 3.2.2.6 Starch Branching Pattern Exploration

#### 3.2.2.6.1 Time-Course of $\beta$ -Amylolysis of the Amylopectin Fraction Followed by Complete Debranching

For both genotypes, hydrolysis with  $\beta$ -amylase caused a dramatic change in CL distribution within the first 10 min (Fig. 3.8): A major increase was observed for  $DP \leq 7$ . For Wt, from 10 min to 24 hr of  $\beta$ -amylolysis, the change in the CL distribution was primarily a reduction of the DP 4 stubs and the simultaneous increase of the DP 2 stubs; however, no visible change was observed after 10 min for the *sbe1a* sample (Fig. 3.8).

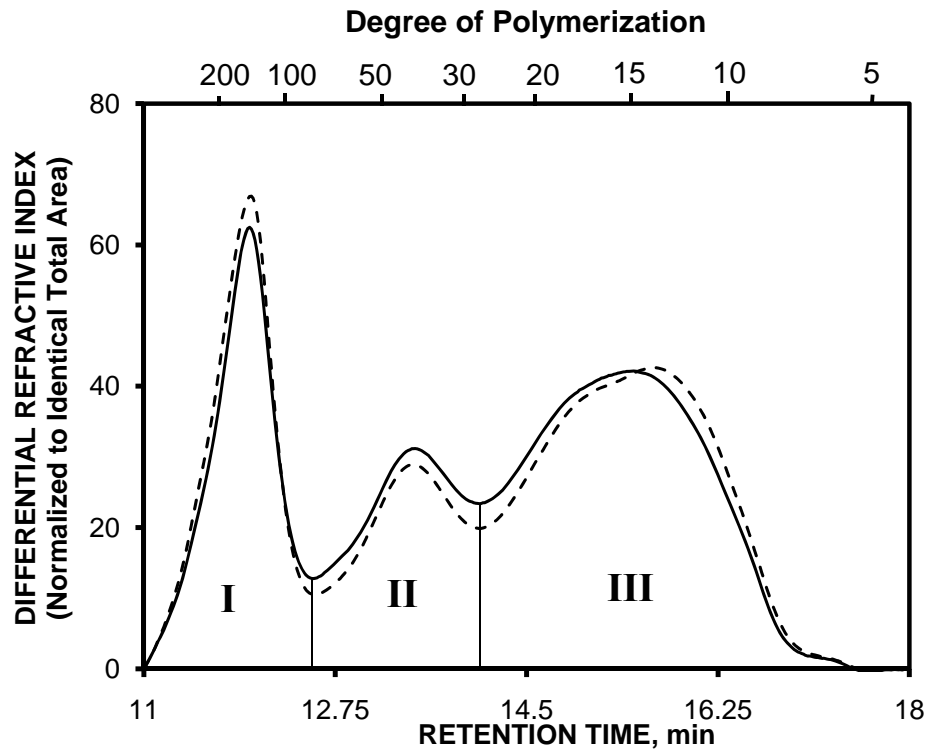


Figure 3.7 Chromatograms of isoamylase-debranched resistant starch from Wt (—) and *sbel1* mutant (---) starch<sup>1</sup>.

<sup>1</sup>Representative chromatograms for starch from one biological replication. Proportions of region I, II, and III are presented in Table 3.8.

Table 3.8 Chain length distribution of isoamylase-debranched native starch and resistant starch from Wt and *sbe1a* mutant starch<sup>1</sup>.

Sample	Chromatographic Region <sup>2</sup>		
	I	II	III
<b>Native Starch<sup>3</sup></b>			
Wt	27.4 ± 0.2 <sup>c</sup>	18.5 ± 0.5 <sup>b</sup>	54.1 ± 0.3 <sup>b</sup>
<i>sbe1a</i>	27.9 ± 0.5 <sup>b,c</sup>	17.8 ± 0.1 <sup>a</sup>	54.3 ± 0.6 <sup>b</sup>
<b>Resistant Starch</b>			
Wt	26.4 ± 0.5 <sup>a</sup>	21.3 ± 0.1 <sup>c</sup>	52.3 ± 0.5 <sup>a</sup>
<i>sbe1a</i>	28.2 ± 0.3 <sup>b</sup>	19.2 ± 0.4 <sup>b</sup>	52.6 ± 0.7 <sup>a</sup>

<sup>1</sup>Values are percentage by weight. Values are mean ± standard deviation based on two independent analyses for one biological replication. See Fig 3.7. Significant differences in the same column, as determined by one-way ANOVA, are indicated by different superscripts.

<sup>2</sup>Regions were divided based on the minima observed for debranched amylopectin from wild-type starch, as in Klucinec and Thompson (1998).

<sup>3</sup>Values are these for non-granular starch in Table 3.7.

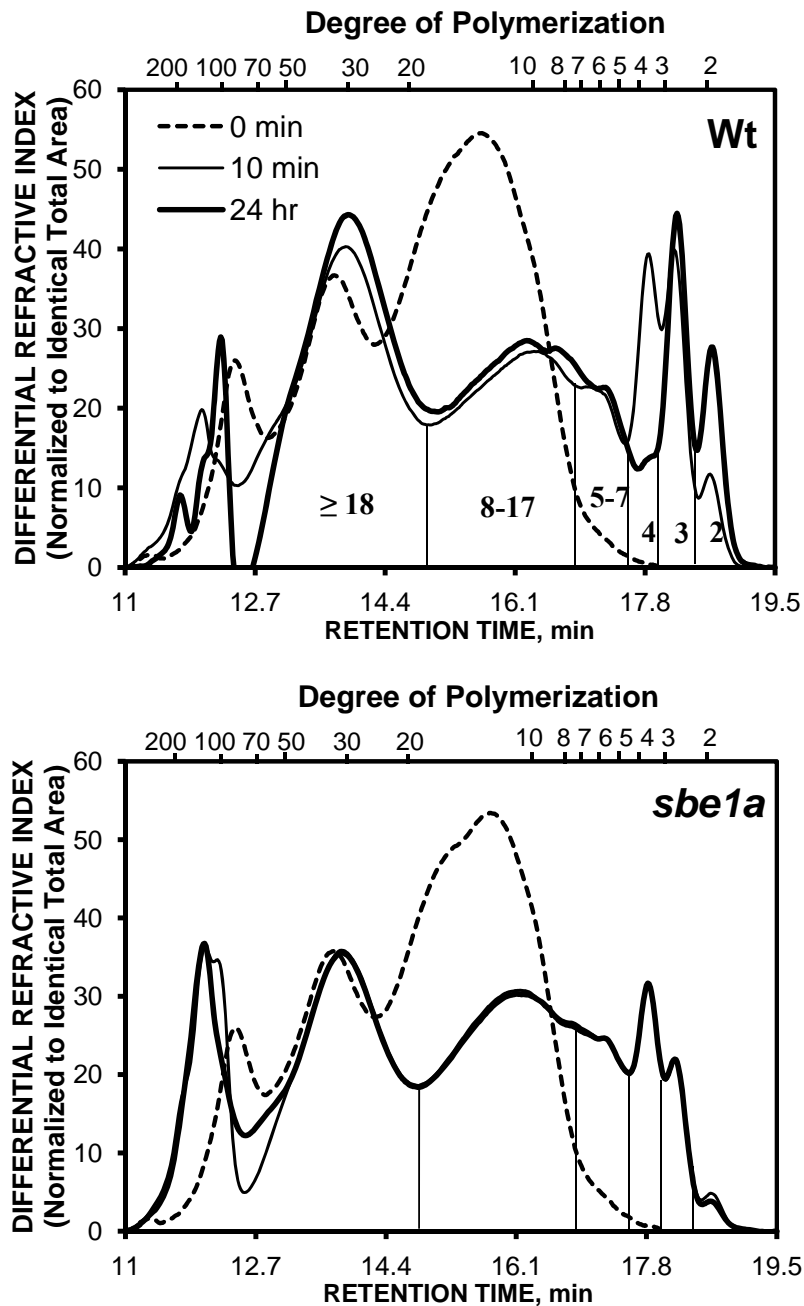


Figure 3.8 Chromatograms<sup>1</sup> of debranched<sup>2</sup>  $\beta$ -dextrins from amylopectin from Wt and *sbe1a* mutant starch<sup>3</sup> using  $\beta$ -amylase (250 U/mL).  $\beta$ -Amylolysis times and starch are indicated in the legend. Numbers indicate degree of polymerization.

<sup>1</sup>Chromatographic regions were divided as in Xia and Thompson (2006). Proportions of chains in each region are plotted in Fig. 3.9.

<sup>2</sup>Debranching was performed successively with isoamylase for 24 hr and pullulanase for 24 hr.

<sup>3</sup>Starch from one biological replication.

To measure the changes in the proportions of characteristic chains during the time-course of  $\beta$ -amylolysis, the chromatographic regions were divided according to Xia and Thompson (2006), and the proportion of chains in each region was plotted to follow the progress of  $\beta$ -amylolysis (Fig. 3.9). Within 10 min, for both genotypes, hydrolysis caused a decrease in the proportion of chains of DP  $\geq 18$  (a decrease of  $\sim 10\%$  for both) and of chains of DP 8-17 (a decrease of  $\sim 15\%$  for Wt,  $\sim 10\%$  for *sbe1a*), and an increase in the proportion of other chains (DP 5-7, DP 4, DP 3, and DP 2). The increase in the proportion of chains of DP 5-7 was greater for *sbe1a* than Wt, and the increase in the proportion of chains of DP 3 was less. After 10 min, the proportion of almost all the chains remained about the same, except for a gradual decrease in the DP 4 and a gradual increase in the DP 2 from Wt samples. At 24 hr of  $\beta$ -amylolysis, the *sbe1a* sample had a much smaller proportion of the DP 2 chains and a much larger proportion of the DP 4 chains than the Wt sample.

#### **3.2.2.6.2 Isoamylase-Debranched and Isoamylase-plus-Pullulanase-Debranched $\beta$ -Limit Dextrins from the Amylopectin Fraction**

The CL distribution of debranched  $\beta$ -limit dextrins ( $\beta$ -LDs) by isoamylase or by isoamylase plus pullulanase from the amylopectin fraction showed a different pattern for Wt and *sbe1a* starch (Fig. 3.10). For the purpose of quantitative comparison, the chromatographic regions were divided according to Xia and Thompson (2006), and the proportions of chains in each region were calculated (Table 3.9). The major difference between Wt and *sbe1a* was that the isoamylase-debranched  $\beta$ -LDs from *sbe1a* had a much larger DP 4 area and a much smaller DP 2 area. For both genotypes, the subsequent pullulanase debranching of the isoamylase-debranched  $\beta$ -LDs led to an evident increase in the DP 2 area (Fig. 3.10, Table 3.9).

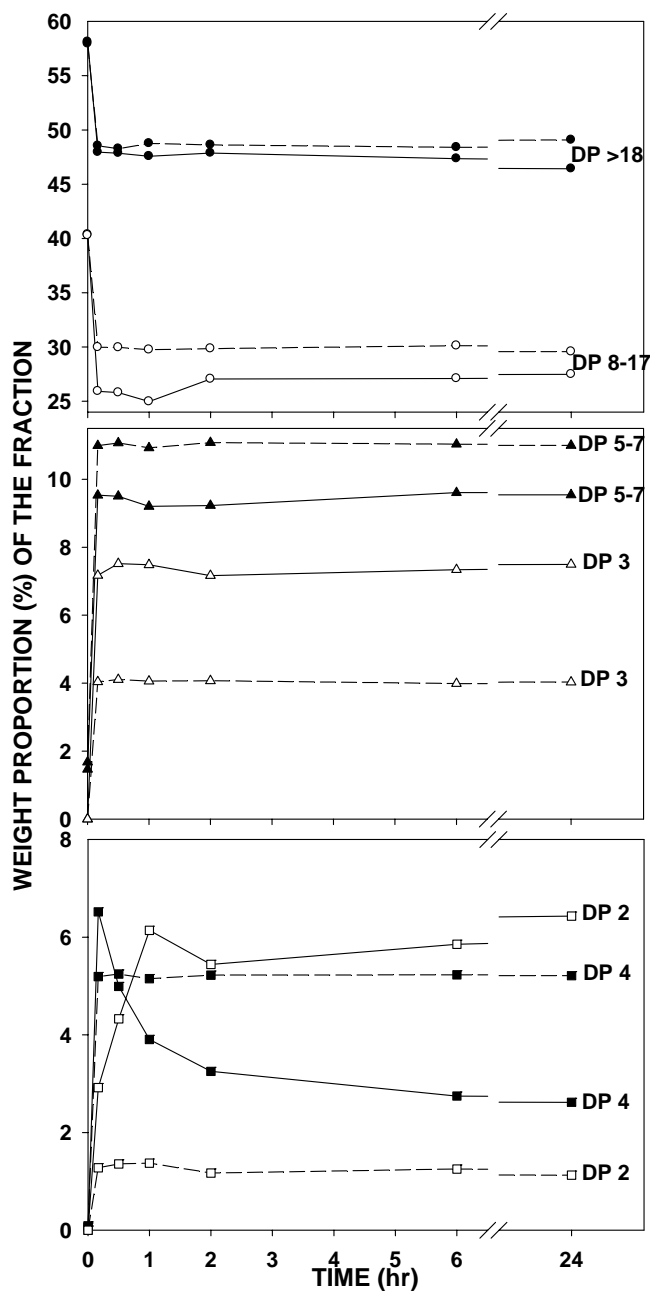


Figure 3.9 Proportions of chains<sup>1</sup> from debranched  $\beta$ -dextrins during time course of  $\beta$ -amylolysis of amylopectin from Wt (—) and *sbe1a* mutant (---) starch<sup>2</sup> using  $\beta$ -amylase (250 U/mL).

<sup>1</sup>Proportions of DP  $\geq 18$ , DP 8-17, DP 5-7, DP 4, DP 3 and DP 2 were calculated as the areas for DP  $\geq 17.5$ ,  $7.5 \leq \text{DP} \leq 17.5$ ,  $4.5 \leq \text{DP} \leq 7.5$ ,  $3.5 \leq \text{DP} \leq 4.5$ ,  $2.5 \leq \text{DP} \leq 3.5$ , and DP  $\leq 2.5$ , respectively, as in Xia and Thompson (2006). See Fig. 3.8 for original chromatograms. Values are percentage by weight.

<sup>2</sup>Starch from one biological replication.

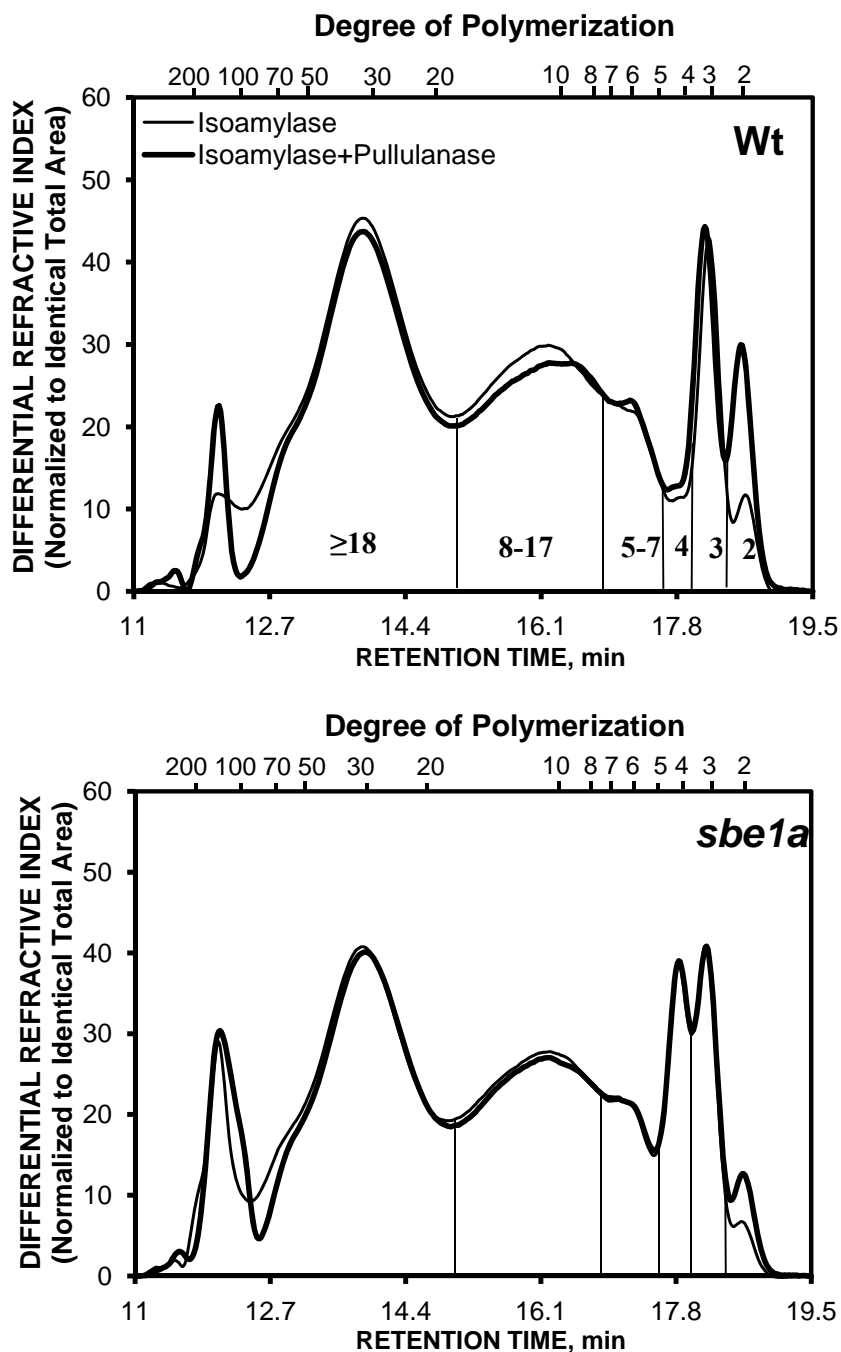


Figure 3.10 Chromatograms<sup>1</sup> of isoamylase-debranched and isoamylase-plus-pullulanase-debranched  $\beta$ -limit dextrans<sup>2</sup> from amylopectin fraction from Wt and *sbe1a* mutant starch<sup>3</sup>. Numbers indicate degree of polymerization.

<sup>1</sup>Chromatographic regions were divided as in Xia and Thompson (2006). Proportions of chains in each region are presented in Table 3.9.

<sup>2</sup> $\beta$ -limit dextrin was obtained after 3 times of 24-hr  $\beta$ -amylolysis on amylopectin.

<sup>3</sup>Representative chromatograms for starch from one biological replication.

Table 3.9 Chain length distribution of isoamylase-debranched and isoamylase-plus-pullulanase-debranched  $\beta$ -limit dextrans from the amylopectin fraction from Wt and *sbe1a* mutant starch<sup>1</sup>.

$\beta$ -Limit Dextrin from Amylopectin <sup>3</sup>	Chromatographic Region <sup>2</sup>						
	B <sub>L</sub> Chains	B <sub>S</sub> Chains		Bs or A chains	A chains		B <sub>S</sub> :B <sub>L</sub>
	DP $\geq$ 18	DP 8-17	DP 5-7	DP 4	DP 3	DP 2	
<b>Wt</b>							
Isoamylase	44.5 $\pm$ 7.2 <sup>a</sup>	34.2 $\pm$ 7.3 <sup>a</sup>	8.9 $\pm$ 0.3 <sup>b</sup>	2.5 $\pm$ 0.3 <sup>a</sup>	6.9 $\pm$ 0.3 <sup>a</sup>	3.1 $\pm$ 0.3 <sup>c</sup>	1.0 $\pm$ 0.3 <sup>a</sup>
Isoamylase, then pullulanase	42.0 $\pm$ 6.6 <sup>a</sup>	32.3 $\pm$ 6.6 <sup>a</sup>	9.5 $\pm$ 0.2 <sup>c</sup>	2.7 $\pm$ 0.3 <sup>a</sup>	7.2 $\pm$ 0.4 <sup>a</sup>	6.4 $\pm$ 0.4 <sup>d</sup>	1.0 $\pm$ 0.3 <sup>a</sup>
Increase by Pullulanase	-	-	0.6 $\pm$ 0.5 <sup>a</sup>	-	-	3.3 $\pm$ 0.1 <sup>c</sup>	-
<b><i>sbe1a</i></b>							
Isoamylase	44.0 $\pm$ 5.9 <sup>a</sup>	31.6 $\pm$ 6.4 <sup>a</sup>	9.5 $\pm$ 0.3 <sup>c</sup>	6.1 $\pm$ 0.6 <sup>b</sup>	6.8 $\pm$ 0.6 <sup>a</sup>	2.1 $\pm$ 0.3 <sup>b</sup>	1.0 $\pm$ 0.3 <sup>a</sup>
Isoamylase, then pullulanase	43.7 $\pm$ 5.1 <sup>a</sup>	30.6 $\pm$ 6.0 <sup>a</sup>	9.6 $\pm$ 0.4 <sup>c</sup>	6.1 $\pm$ 0.5 <sup>b</sup>	6.8 $\pm$ 0.7 <sup>a</sup>	3.2 $\pm$ 0.0 <sup>c</sup>	0.9 $\pm$ 0.3 <sup>a</sup>
Increase by Pullulanase	-	-	-	-	-	1.1 $\pm$ 0.3 <sup>a</sup>	-

<sup>1</sup>Values are percentage by weight. Values are mean  $\pm$  standard deviation based on two independent analyses for one biological replication. See Fig 3.10. Significant differences in the same column, as determined by one-way ANOVA with Fisher's LSD multiple comparison procedure, are indicated by different superscripts.

<sup>2</sup>Proportions of DP  $\geq$  18, DP 8-17, DP 5-7, DP 4, DP 3 and DP 2 were calculated as the areas for DP  $\geq$  17.5,  $7.5 \leq$  DP  $\leq$  17.5,  $4.5 \leq$  DP  $\leq$  7.5,  $3.5 \leq$  DP  $\leq$  4.5,  $2.5 \leq$  DP  $\leq$  3.5, and DP  $\leq$  2.5, respectively, as in Xia and Thompson (2006).

<sup>3</sup>The  $\beta$ -limit dextrans from amylopectin were either debranched by isoamylase, or by isoamylase plus pullulanase, indicated by "Isoamylase" and "Isoamylase, then pullulanase", respectively.

The increase in DP 2 stubs was smaller in *sbe1a* than in Wt (Table 3.9).

After isoamylase debranching only, the proportion of chains of DP 5-7 was slightly higher in the *sbe1a* sample than in the Wt sample. After subsequent pullulanase debranching, the proportion of chains of DP 5-7 increased slightly for the Wt sample, but stayed unchanged for the *sbe1a* sample (Table 3.9). The proportion of chains of DP 5-7 after pullulanase addition was indistinguishable between two genotypes (Table 3.9). Comparing *sbe1a* to Wt samples, there was no significant difference in the proportions of chains of DP  $\geq 18$ , DP 8-17, and DP 3, before and after pullulanase addition (Table 3.9). The ratio of  $B_S:B_L$  was also not distinguishable (Table 3.8).

### **3.2.2.6.3 Isoamylase-Debranched and Isoamylase-plus-Pullulanase-Debranched $\beta$ -Limit Dextrins from the Amylose Fraction**

The CL distribution of debranched  $\beta$ -LDs from the amylose fraction (Fig. 3.11) was analyzed using chromatographic regions (Table 3.10) divided as described above. The amylose from *sbe1a* resulted in a higher proportion of chains of DP  $\geq 100$  (Fig. 3.11, Table 3.10). *sbe1a* had lower proportions than Wt of chains of DP 18-99, DP 8-17, DP 3, and DP 2, before and after pullulanase addition (Table 3.10).

For both genotypes, the subsequent pullulanase debranching of isoamylase-debranched  $\beta$ -LDs led to an evident increase in both the DP 3 and DP 2 areas, and this increase was greater in *sbe1a* (Table 3.10). The subsequent pullulanase debranching also led to a decrease in chains around DP 8-9 for both genotypes (Fig. 3.11). This decrease was not reported in Table 3.10, due to the broad division of chromatographic regions. For *sbe1a* samples, there was a small increase by pullulanase in the proportions of DP 5-7 and DP 4 (not visible in Fig.3.11) (Table 3.10).

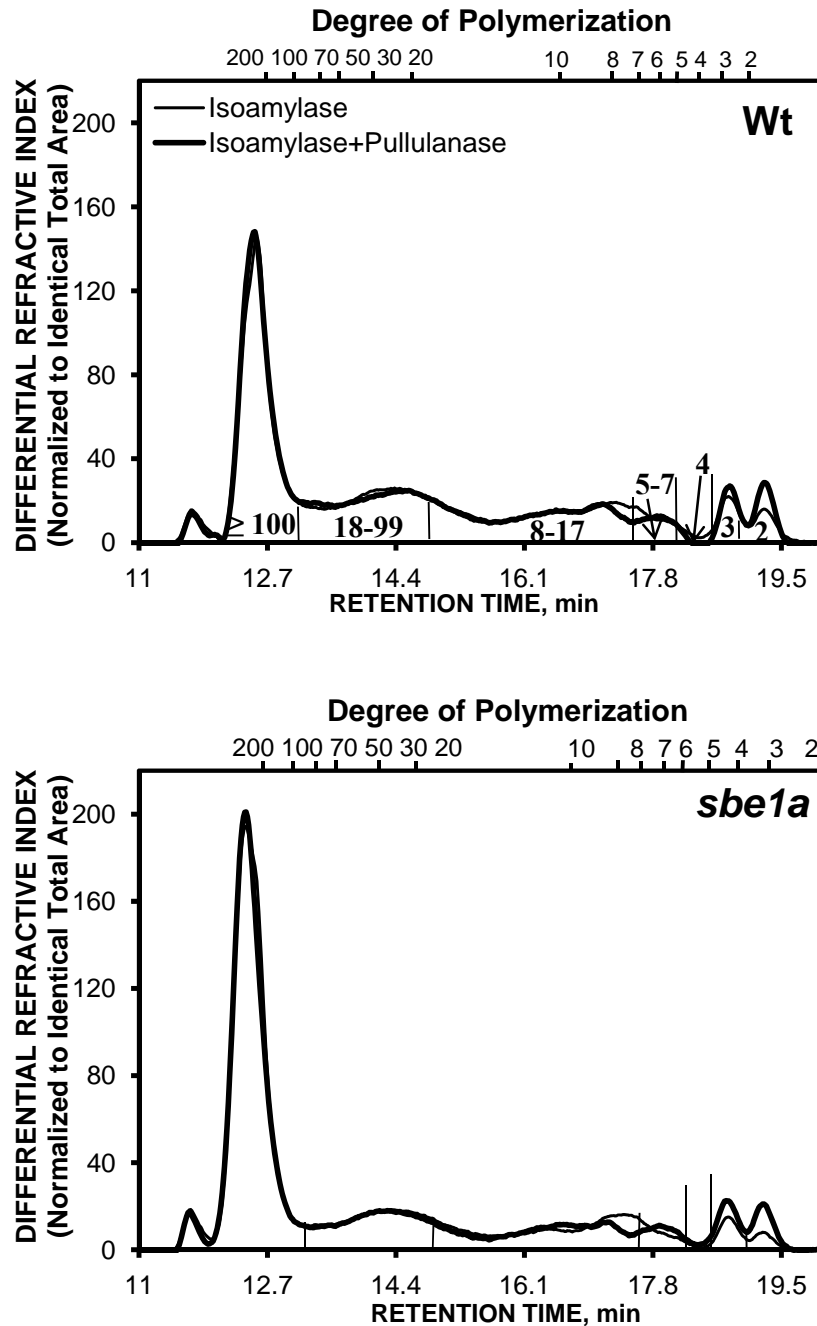


Figure 3.11 Chromatograms<sup>1</sup> of isoamylase-debranched and isoamylase-plus-pullulanase-debranched  $\beta$ -limit dextrins<sup>2</sup> from amylose fraction from Wt and *sbe1a* mutant starch<sup>3</sup>.

<sup>1</sup>Chromatographic regions were divided as in Xia and Thompson (2006). Proportions of chains in each region are presented in Table 3.10.

<sup>2</sup> $\beta$ -limit dextrin was obtained after 3 times of 24-hr  $\beta$ -amylolysis on amylopectin.

<sup>3</sup>Representative chromatograms for starch from one biological replication.

Table 3.10 Chain length distribution of isoamylase-debranched and isoamylase-plus-pullulanase-debranched  $\beta$ -limit dextrins from the amylose fraction from Wt and *sbe1a* mutant starch<sup>1</sup>.

<b><math>\beta</math>-Limit Dextrins from Amylose<sup>3</sup></b>	<b>Chromatographic Region<sup>2</sup></b>						
	<b>B<sub>L</sub> Chains</b>		<b>B<sub>S</sub> Chains</b>		<b>Bs or A chains</b>	<b>A chains</b>	
	<b>DP <math>\geq</math> 100</b>	<b>DP 18-99</b>	<b>DP 8-17</b>	<b>DP 5-7</b>	<b>DP 4</b>	<b>DP 3</b>	<b>DP 2</b>
<b>Wt</b>							
Isoamylase	40.3 $\pm$ 2.7 <sup>a</sup>	22.4 $\pm$ 0.9 <sup>b</sup>	23.5 $\pm$ 2.3 <sup>b</sup>	5.2 $\pm$ 0.5 <sup>d</sup>	1.1 $\pm$ 0.1 <sup>b</sup>	3.4 $\pm$ 0.1 <sup>d</sup>	4.1 $\pm$ 0.7 <sup>c</sup>
Isoamylase, then pullulanase	38.3 $\pm$ 5.8 <sup>a</sup>	23.5 $\pm$ 1.0 <sup>b</sup>	23.3 $\pm$ 2.7 <sup>b</sup>	4.8 $\pm$ 0.9 <sup>c,d</sup>	1.0 $\pm$ 0.8 <sup>b</sup>	3.9 $\pm$ 0.1 <sup>e</sup>	5.4 $\pm$ 0.5 <sup>d</sup>
Increase by pullulanase	-	-	-	-	-	0.4 $\pm$ 0.2 <sup>a</sup>	1.3 $\pm$ 0.2 <sup>a</sup>
<b><i>sbe1a</i></b>							
Isoamylase	57.3 $\pm$ 4.1 <sup>b</sup>	17.2 $\pm$ 1.5 <sup>a</sup>	17.3 $\pm$ 2.4 <sup>a</sup>	3.5 $\pm$ 0.3 <sup>b</sup>	0.6 $\pm$ 0.0 <sup>a</sup>	2.2 $\pm$ 0.0 <sup>c</sup>	2.0 $\pm$ 0.4 <sup>b</sup>
Isoamylase, then pullulanase	55.6 $\pm$ 3.4 <sup>b</sup>	16.2 $\pm$ 1.0 <sup>a</sup>	15.7 $\pm$ 2.5 <sup>a</sup>	4.0 $\pm$ 0.1 <sup>c</sup>	1.0 $\pm$ 0.2 <sup>b</sup>	3.2 $\pm$ 0.3 <sup>d</sup>	4.3 $\pm$ 0.3 <sup>c</sup>
Increase by pullulanase	-	-	-	0.6 $\pm$ 0.4 <sup>a</sup>	0.4 $\pm$ 0.2 <sup>a</sup>	0.9 $\pm$ 0.3 <sup>b</sup>	2.3 $\pm$ 0.1 <sup>b</sup>

<sup>1</sup>Values are percentage by weight. Values are mean  $\pm$  standard deviation based on two independent analyses for one biological replication. See Fig. 3.11. Significant differences in the same column, as determined by one-way ANOVA with Fisher's LSD multiple comparison procedure, are indicated by different superscripts.

<sup>2</sup>Proportions of DP  $\geq$  100, DP 18-99, DP 8-17, DP 5-7, DP 4, DP 3 and DP 2 were calculated as the areas for DP  $\geq$  99.5,  $17.5 \leq$  DP  $\leq$  99.5,  $7.5 \leq$  DP  $\leq$  17.5,  $4.5 \leq$  DP  $\leq$  7.5,  $3.5 \leq$  DP  $\leq$  4.5,  $2.5 \leq$  DP  $\leq$  3.5, and DP  $\leq$  2.5, respectively, as in Xia and Thompson (2006).

<sup>3</sup>The  $\beta$ -limit dextrins from amylose were either debranched by isoamylase, or by isoamylase plus pullulanase, indicated by "Isoamylase" and "Isoamylase, then pullulanase", respectively.

### 3.2.3 Starch Granular Structure

It is reasonable to hypothesize that if the *sbe1a* mutation results in the synthesis of starch with an altered branching pattern, then this difference might lead to a difference in starch granular structure. To study the effect of *sbe1a* on starch granular structure, various microscopic techniques were used to characterize the morphology of both the native starch granules and the residual starch granules after RS digestion for Wt and *sbe1a* starch.

#### 3.2.3.1 Light Microscopy

Light micrographs of native and resistant starch are shown in Fig. 3.12a,b. Prior to RS digestion (Fig. 3.12a), there was no apparent difference between Wt and *sbe1a* native starch in the granule size and shape, as well as in the degree of birefringence. Starch from both genotypes contained granules of different sizes (left pictures in Fig. 3.12a), and all the granules showed birefringence under polarized light regardless of the size (right pictures in Fig. 3.12a). After RS digestion (Fig. 3.12b), dramatic differences were observed between the two genotypes. The size of the residual granules was much smaller in Wt than in *sbe1a*. Only some very tiny pieces were left in Wt. In contrast, the morphology of the *sbe1a* residual granules showed great variation: some retained their basic shapes even though they were apparently not as intact as native granules, some barely kept their shapes, and others were broken into pieces. The Wt residual granules showed almost no birefringence, whereas many of the residual *sbe1a* granules showed some degree of birefringence, even though less intense than for the native granules. For some residual granules, the centers of the *sbe1a* residual granules appeared dark (see arrows in Fig.3.12b).

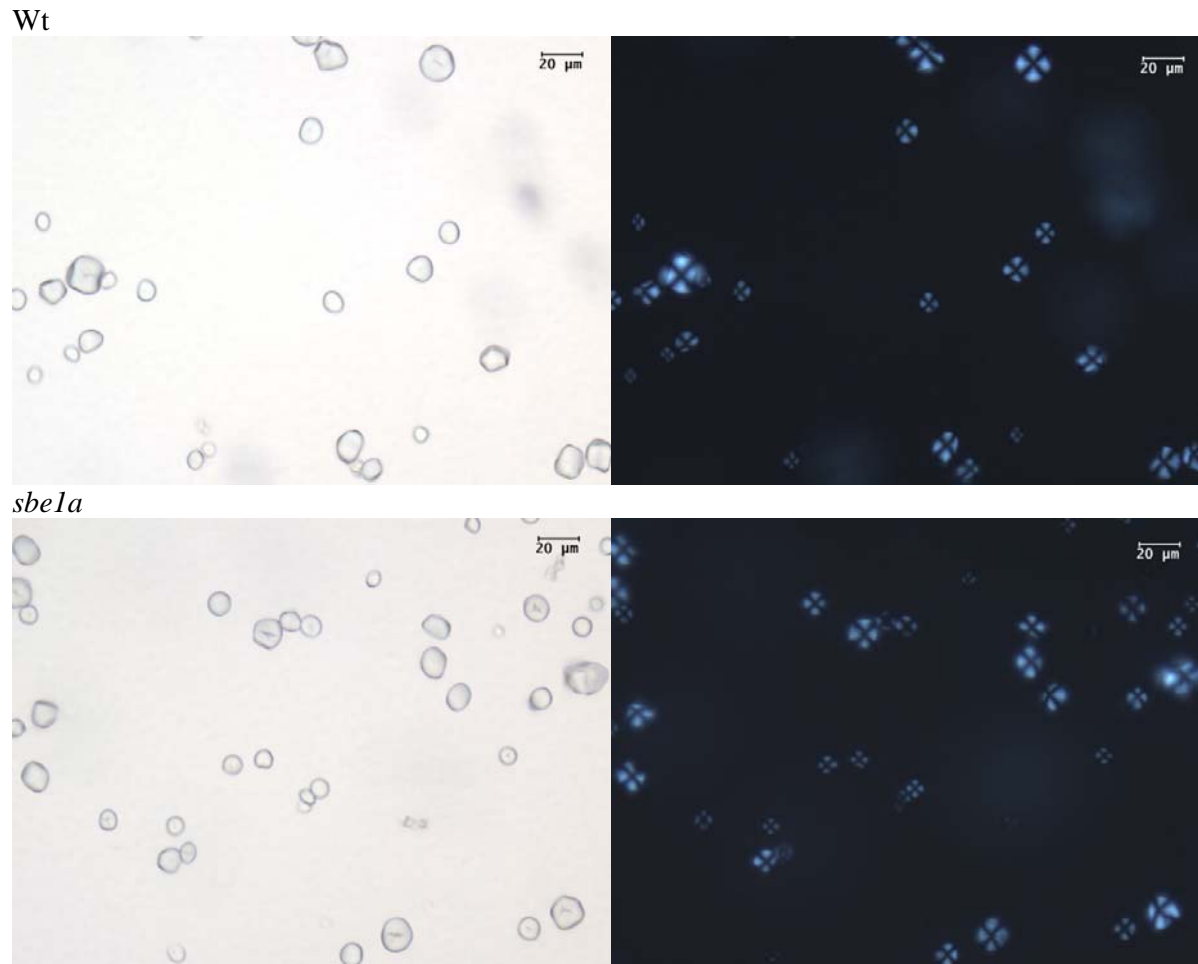


Figure 3.12a Bright field (left) and polarized light (right) micrographs of native starch from Wt and *sbel1* mutant.

Wt

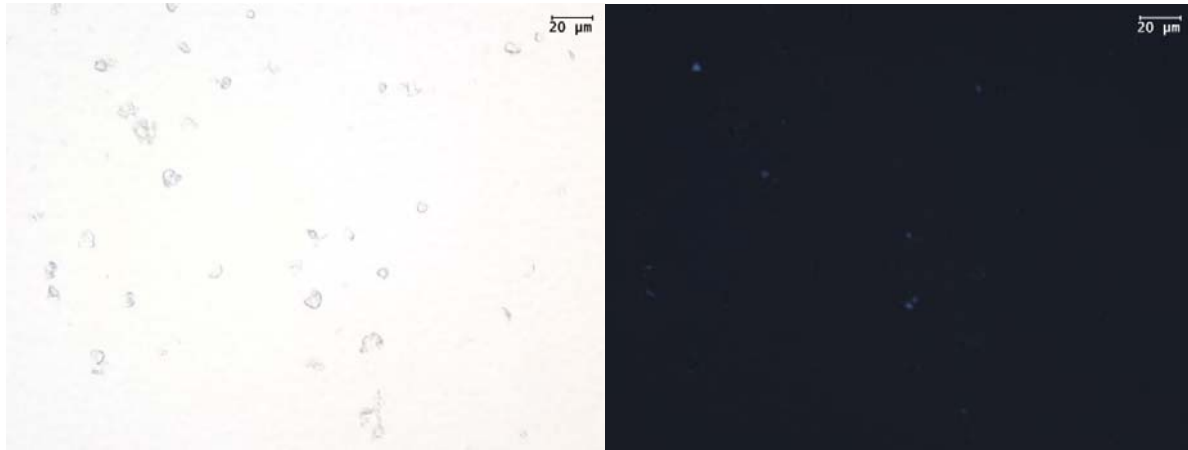
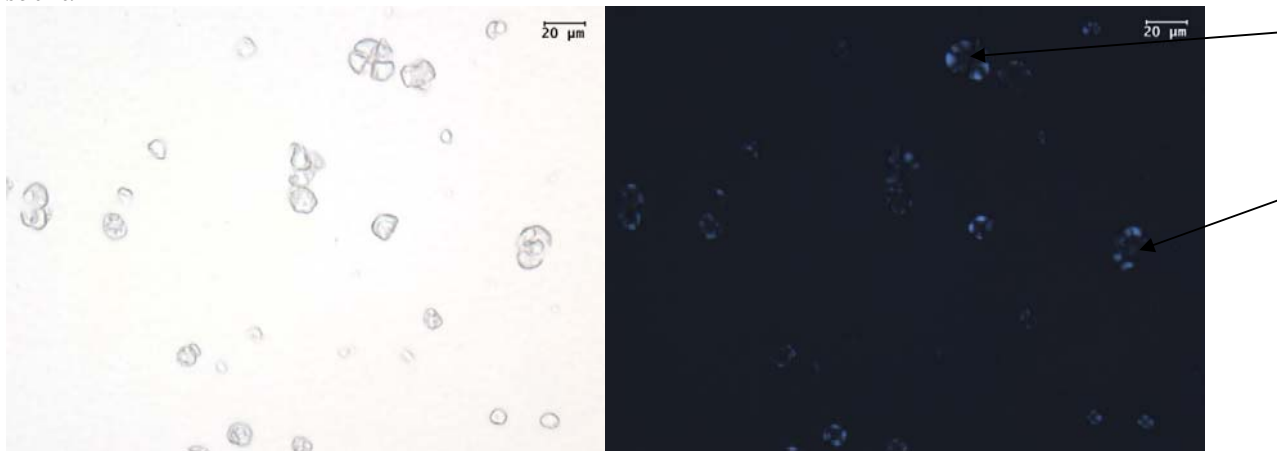
*sbe1a*

Figure 3.12b Bright field (left) and polarized light (right) micrographs of resistant starch from Wt and *sbe1a* mutant. Arrows point to residual granules with dark center.

Light micrographs of iodine-stained native and resistant starch are shown in Fig. 3.13a,b. For both genotypes, all native starch granules were stained blue, with a dark cross when viewed between a crossed polarizing lens pair (Fig. 3.13a). Under polarized light, *sbe1a* native starch showed more heterogeneity in staining (Fig. 3.13a). Some *sbe1a* granules were much darker stained and have a thicker dark cross than the others, whereas, Wt granules were stained to a similar degree (Fig. 3.13a). The respective darker-stained *sbe1a* granules seen under polarized light appeared somewhat darker when viewed in the bright field as well. The iodine-stained native granules were sorted into relatively dark and light granules by five volunteers not involved in this research. The sorting result showed that there were 24.3% and 8.7% of relatively dark-stained granules in *sbe1a* and Wt native starch, respectively. The value was significantly higher for *sbe1a* native granules ( $p$ -value = 0.006). When iodine-stained resistant starches were observed, the RS of Wt and *sbe1a* were not the same. The majority of Wt residual granules were not birefringent, but some *sbe1a* residual granules still had faint birefringence.

### 3.2.3.2 Scanning Electron Microscopy

Scanning electron micrographs of native and resistant starch are shown in Figs. 3.14-3.16. For each page, samples were first examined under a low magnification ( $1,500\times$ ) on a large scale ( $10\ \mu\text{m}$ ), and then interesting features within the same field were magnified ( $3,500\times$  or  $5,000\times$ ) and captured on smaller scales ( $5\ \mu\text{m}$  or  $1\ \mu\text{m}$ ). Additional micrographs that were taken not from the same field are shown in Appendix A (Fig. A.1-A.2).

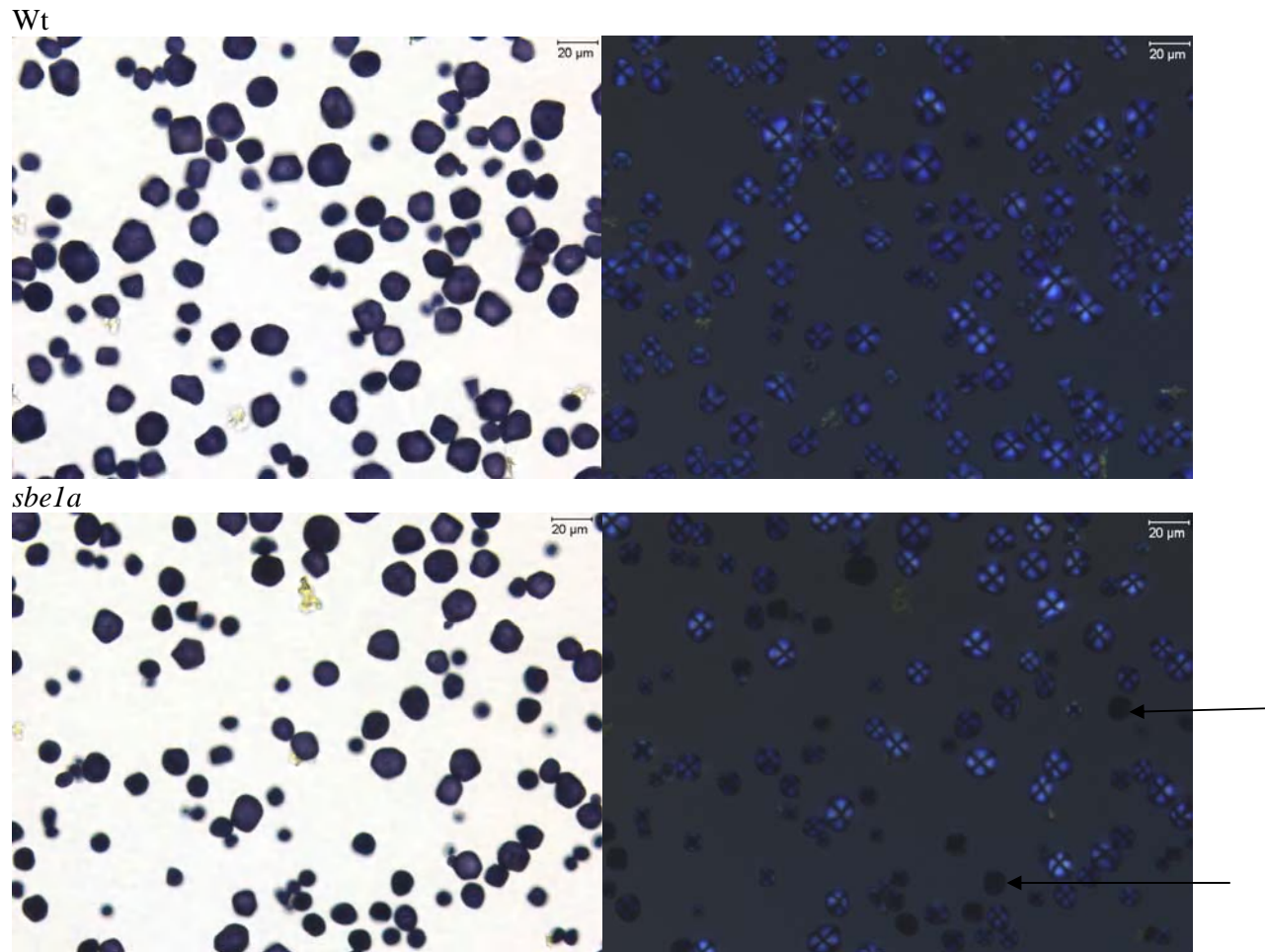


Figure 3.13a Bright field (left) and polarized light (right) micrographs of native starch from Wt and *sbe1a* mutant stained with 0.04% iodine and viewed within 5 min. Arrows point to dark stained granules.

Wt

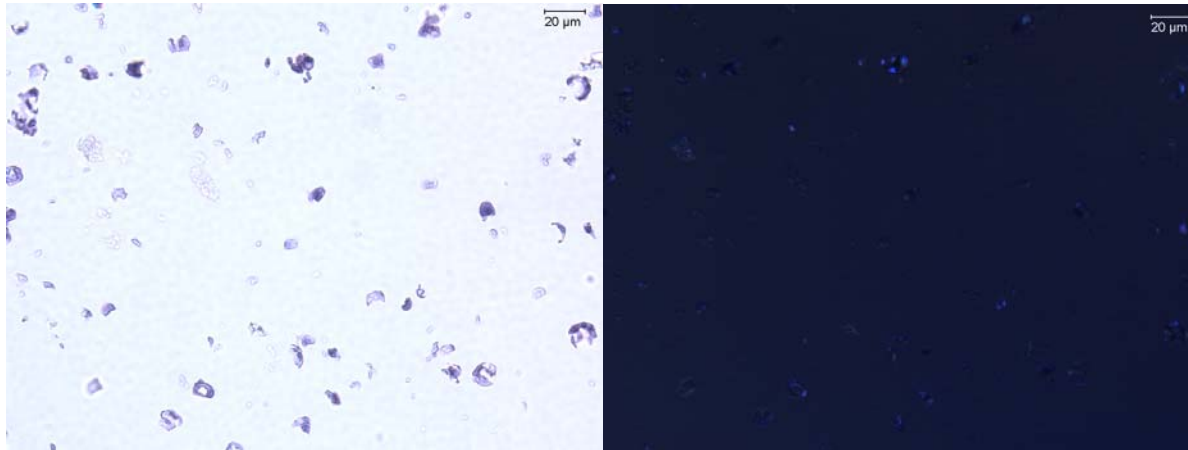
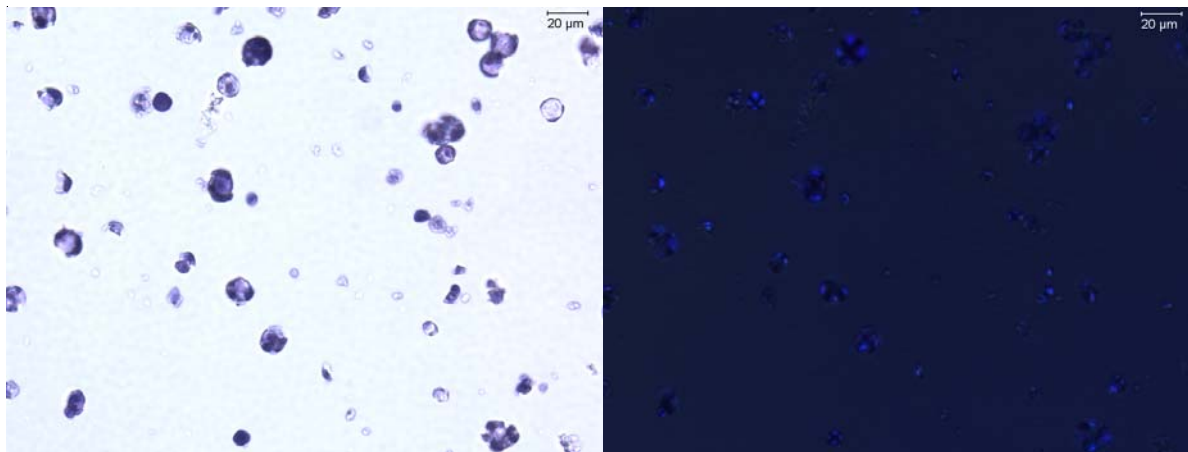
*sbe1a*

Figure 3.13b Bright field (left) and polarized light (right) micrographs of resistant starch from Wt and *sbe1a* mutant stained with 0.04% Iodine and viewed within 5 min.

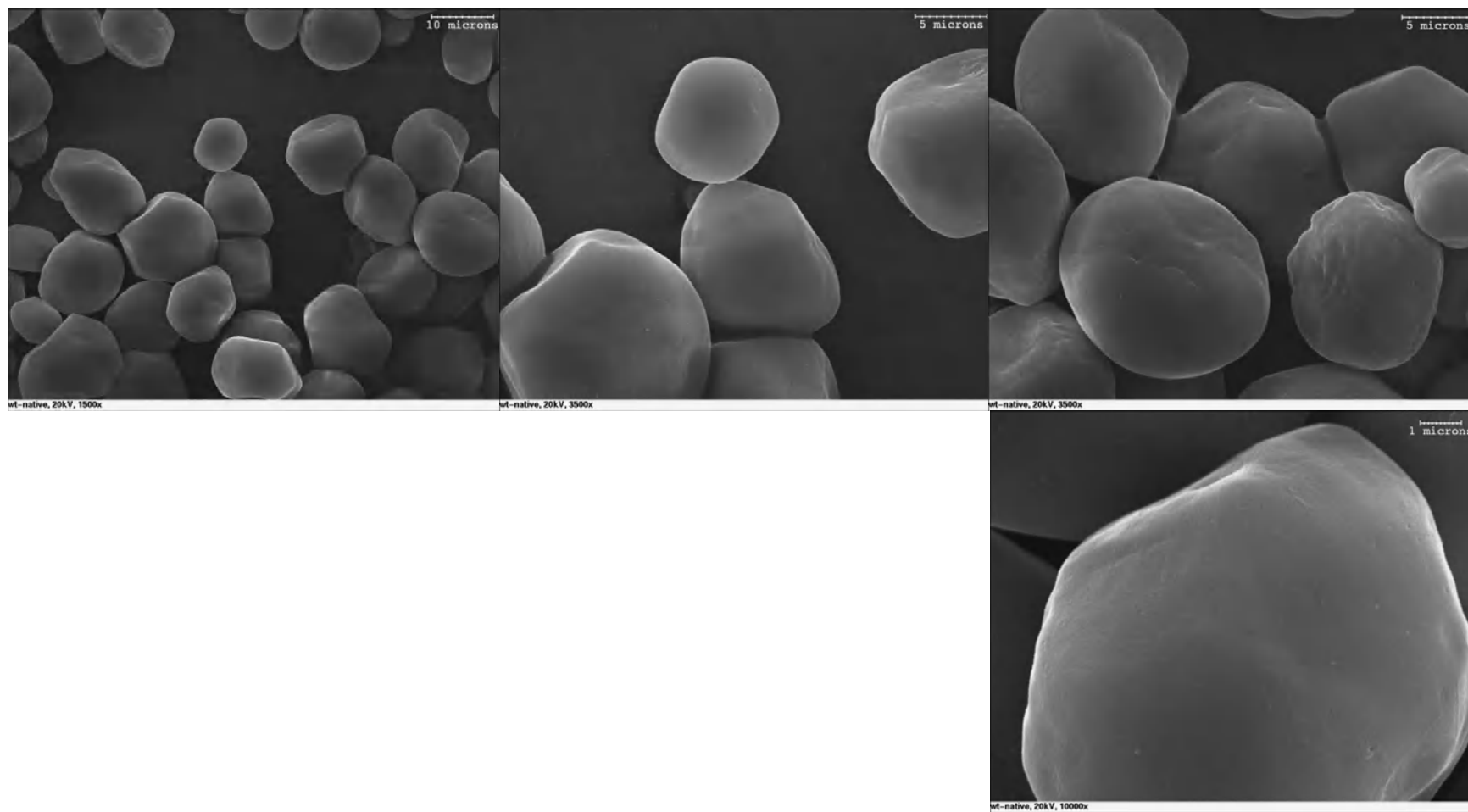


Figure 3.14a Scanning electron micrographs of Wt native starch. Scale bars represent 10  $\mu\text{m}$ , 5  $\mu\text{m}$ , or 1  $\mu\text{m}$  at the top of the graphs.

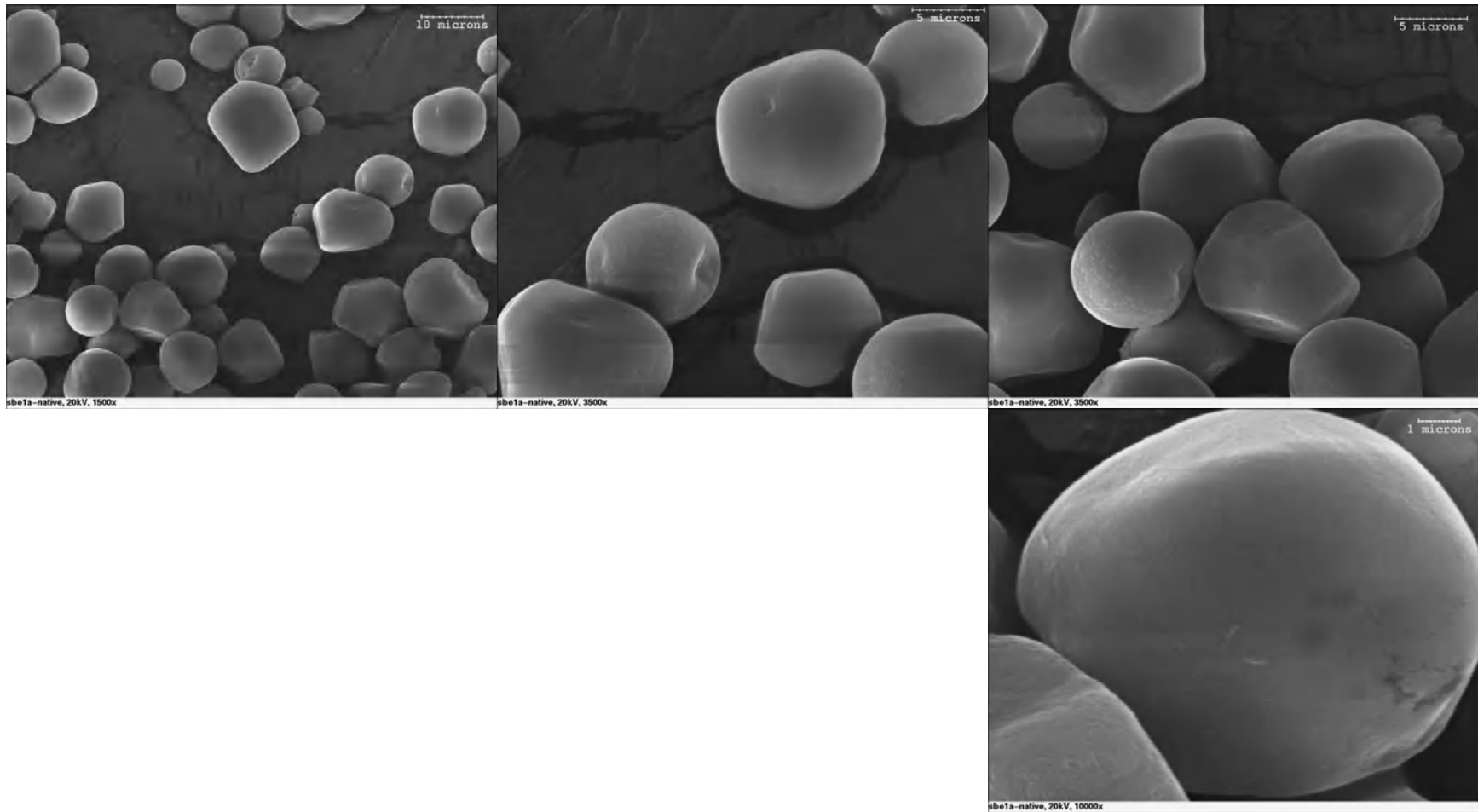


Figure 3.14b Scanning electron micrographs of *sbe1a* native starch. Scale bars represent 10  $\mu\text{m}$ , 5  $\mu\text{m}$ , or 1  $\mu\text{m}$  at the top of the graphs.

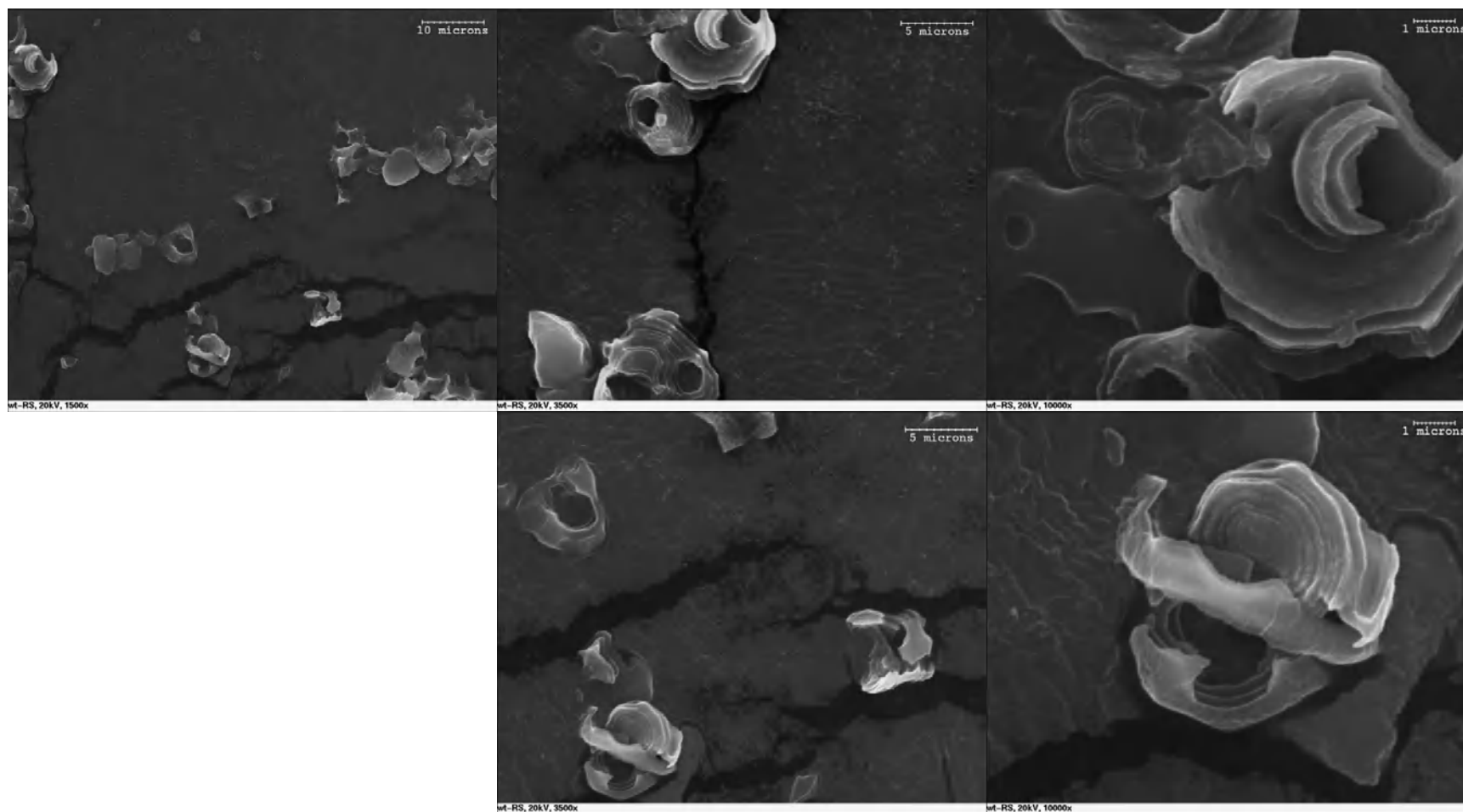


Figure 3.15 Scanning electron micrographs of Wt resistant starch. Scale bars represent 10  $\mu\text{m}$ , 5  $\mu\text{m}$ , or 1  $\mu\text{m}$  at the top of the graphs.

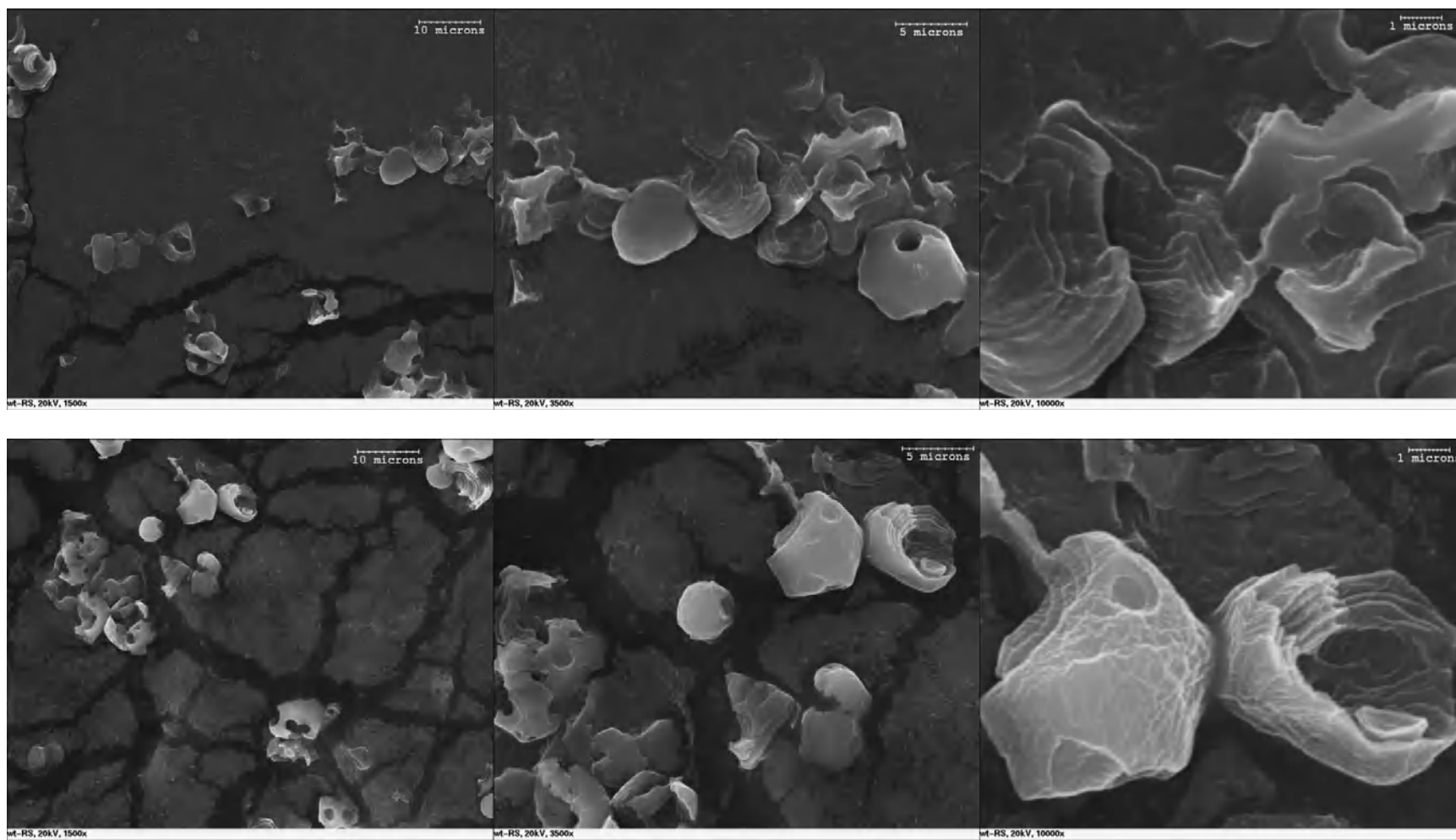


Figure 3.15(continued) Scanning electron micrographs of Wt resistant starch. Scale bars represent 10  $\mu\text{m}$ , 5  $\mu\text{m}$ , or 1  $\mu\text{m}$  at the top of the graphs.

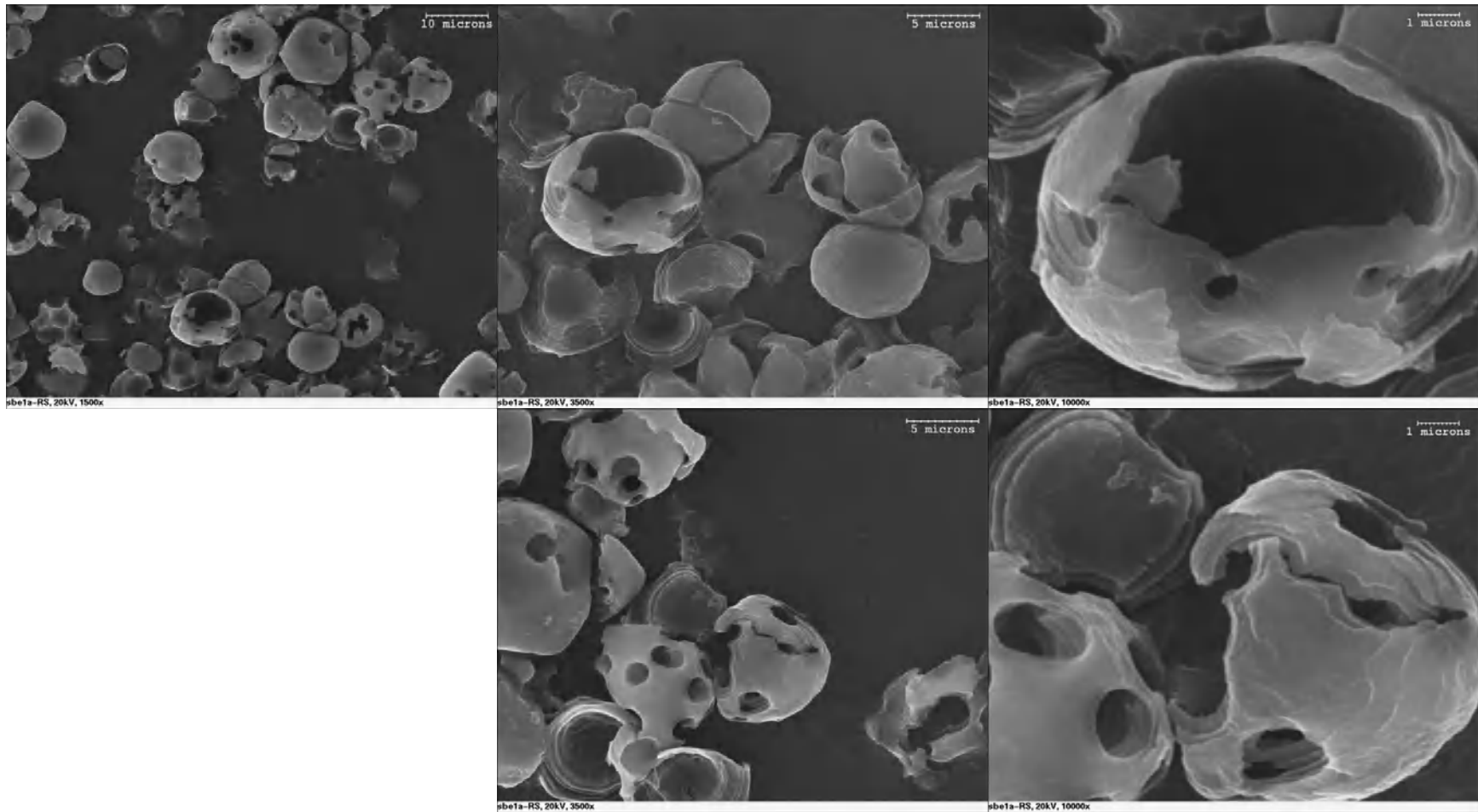


Figure 3.16 Scanning electron micrographs of *sbe1a* resistant starch. Scale bars represent 10  $\mu\text{m}$ , 5  $\mu\text{m}$ , or 1  $\mu\text{m}$  at the top of the graphs.

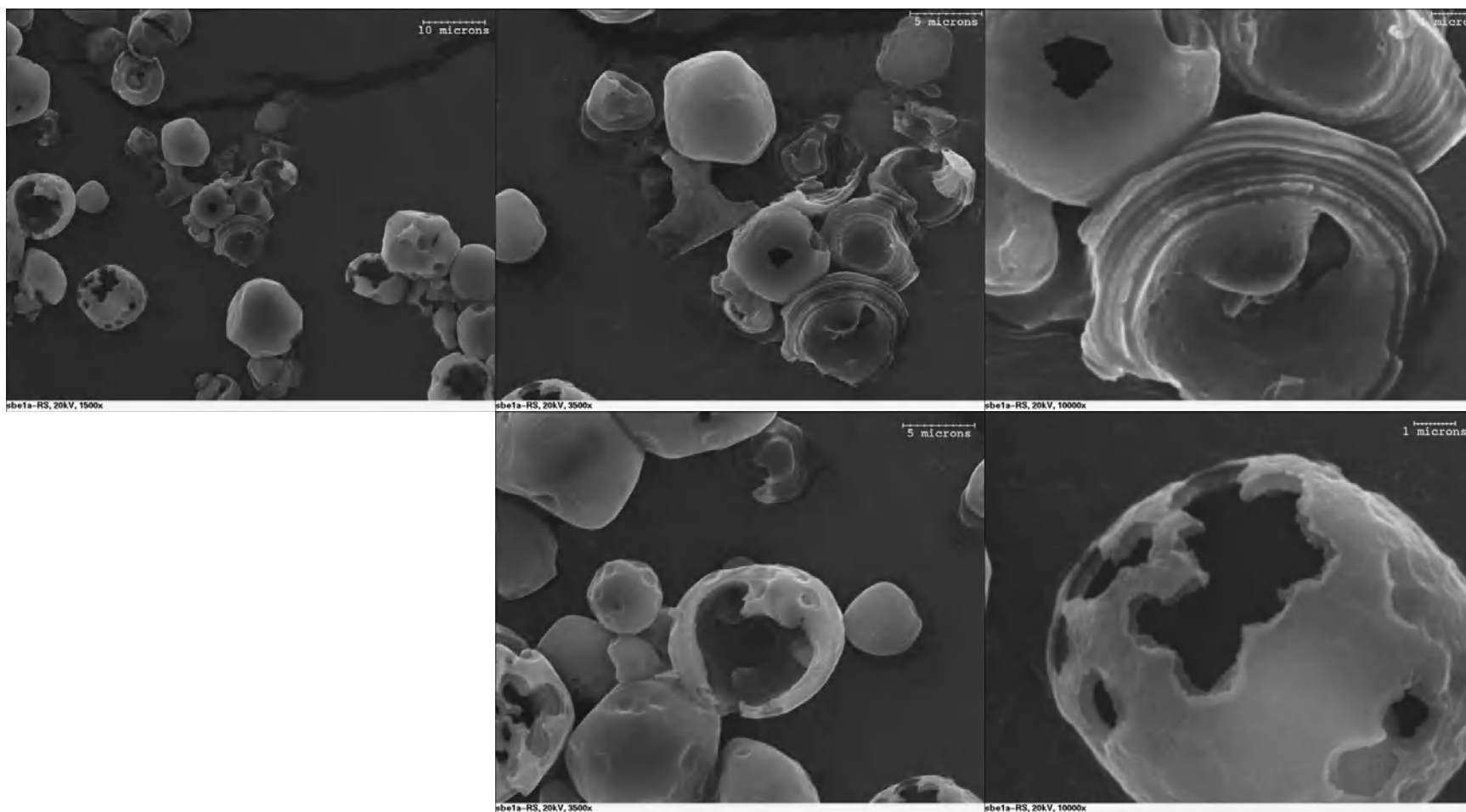


Figure 3.16 (continued) Scanning electron micrographs of *sbe1a* resistant starch. Scale bars represent 10  $\mu\text{m}$ , 5  $\mu\text{m}$ , or 1  $\mu\text{m}$  at the top of the graphs.

Fig. 3.14a,b show that native starch granules from Wt and *sbe1a* had similar morphology. Most native starch granules had a smooth surface, a near-spherical shape, and variable size. Some of the granules had indentations on the surface. The average granule diameter from a sample of 50 granules in the micrographs was 10.2  $\mu\text{m}$  for Wt and 9.8  $\mu\text{m}$  for *sbe1a*. These values were not statistically different ( $p$ -value = 0.586).

However, after RS digestion (Figs. 3.15-3.16), differences were observed between the granules synthesized by the two genotypes. More residual material in a field was seen in *sbe1a* samples (Fig. 3.16) than in Wt samples (Fig. 3.15). Samples of the *sbe1a* RS contained many residual granules with hollow interiors, whereas small fragments of residual granules were seen for Wt. There were distinct holes in the surface of many of the *sbe1a* residual granules. The morphology of the *sbe1a* RS showed wide variation, including pieces of granule fragments, fractured granules, shell-shaped granules, and almost intact granules; however, only small pieces of granule fragments were visible in the Wt RS. The most striking feature of Wt residual fragments was alternating layers, one being protruded and the other one being concaved. This feature was less evident in *sbe1a* samples.

### 3.2.3.3 Transmission Electron Microscopy

Transmission electron micrographs of native and resistant starch are shown in Figs. 3.17-3.18. Fig. 3.17a,b show that many native granule pieces had concentric rings. No apparent difference was observed between Wt and *sbe1a* granules. After RS digestion (Fig. 3.18a,b), only fragments of Wt residual granules were observed; but for *sbe1a* samples, as with the SEM analysis, the RS was heterogeneous. Some residual granules appeared to be intact, some were missing the interior part,

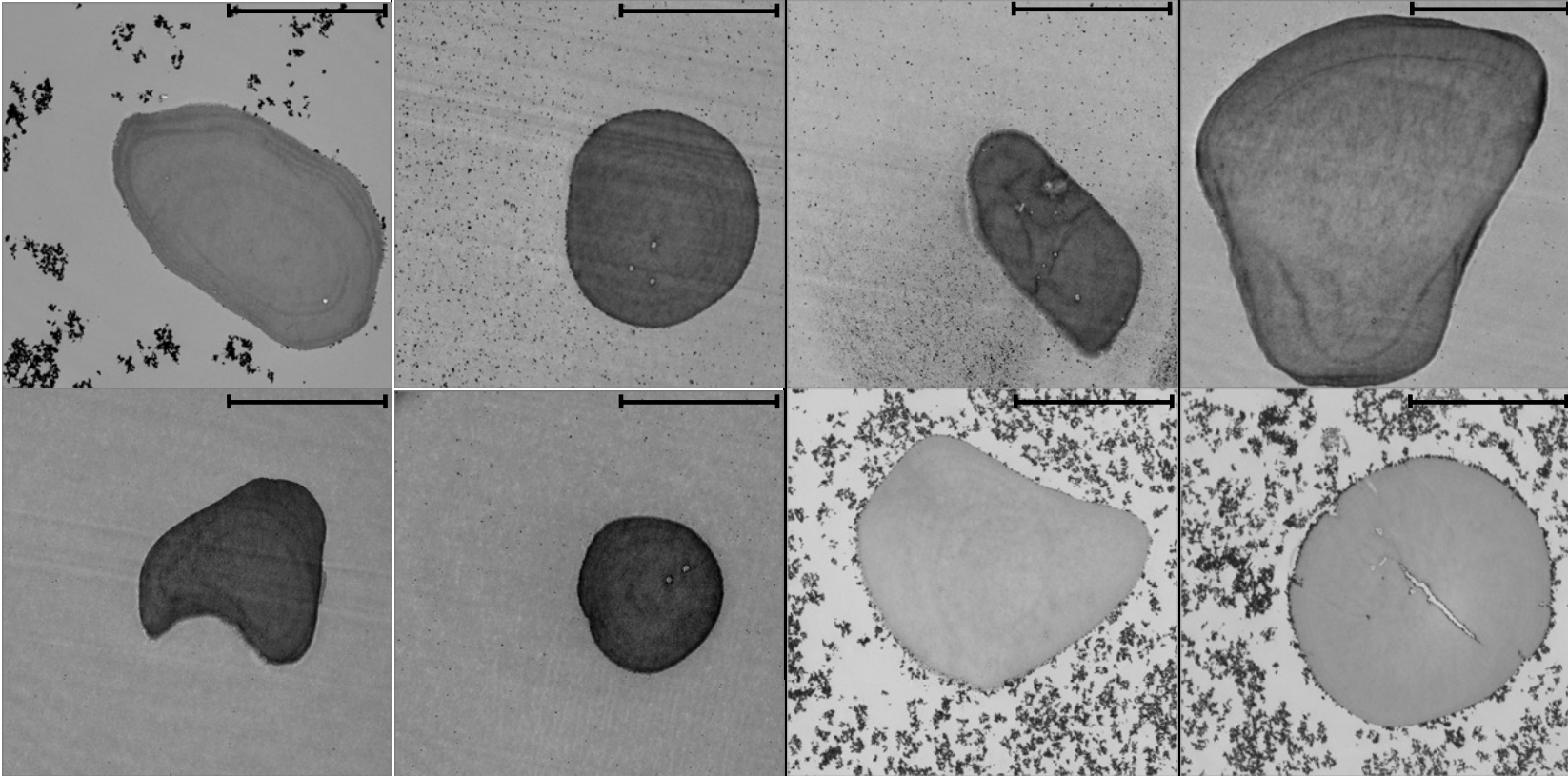


Figure 3.17a Transmission electron micrographs of Wt native starch. Scale bars represent 5  $\mu\text{m}$  at the top of the graphs.

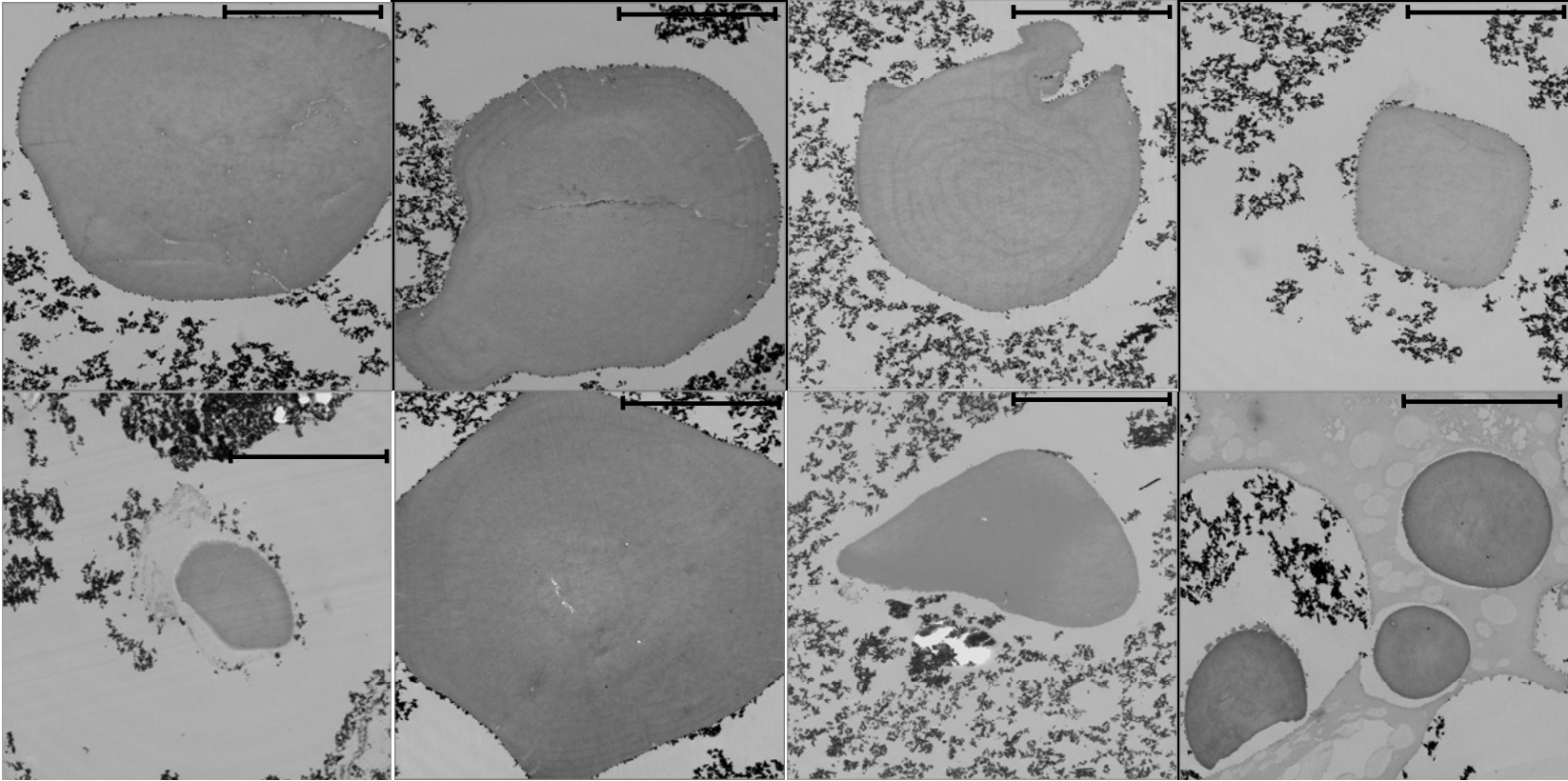


Figure 3.17b Transmission electron micrographs of *sbela* native starch. Scale bars represent 5 µm at the top of the graphs.

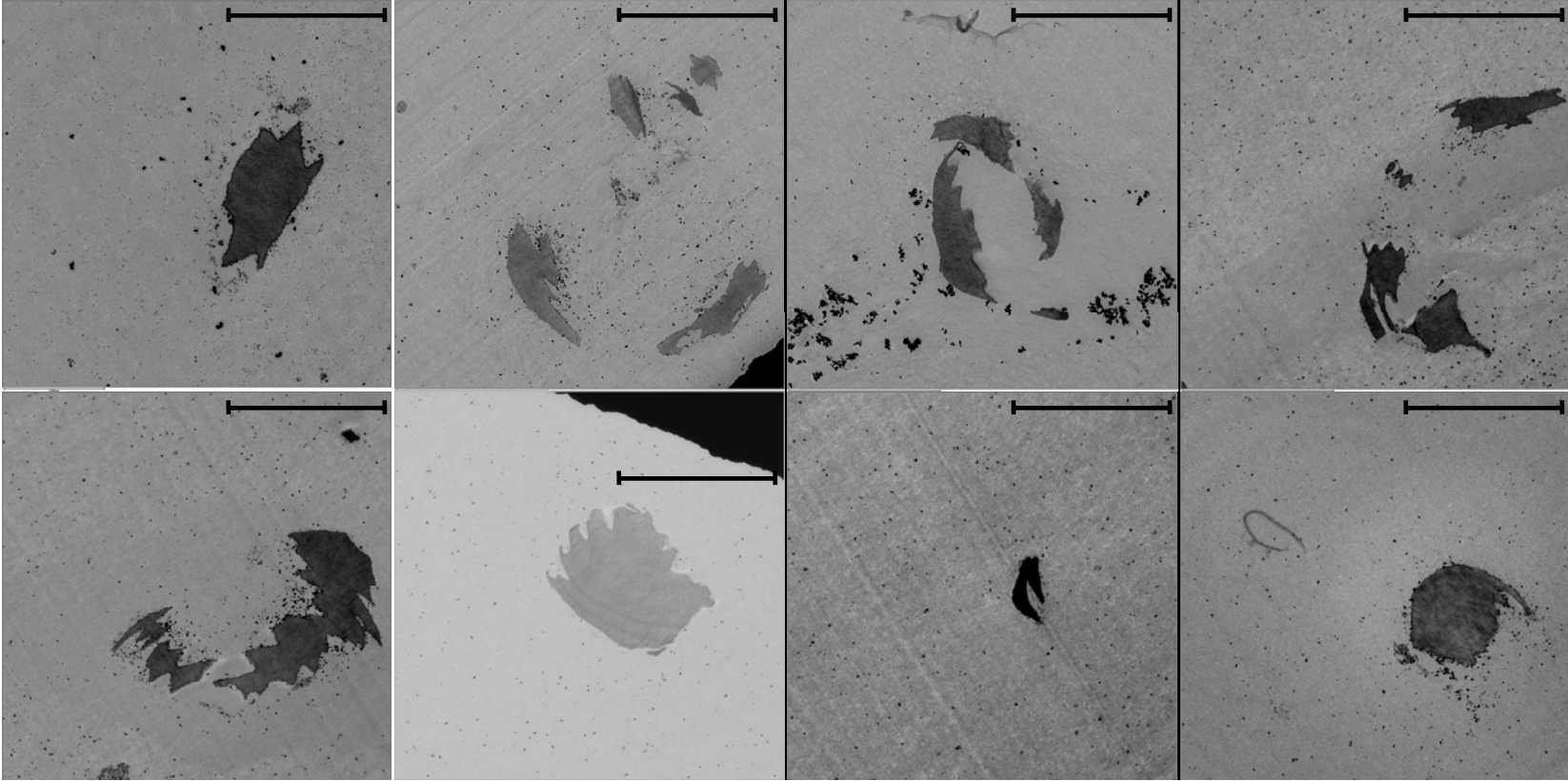


Figure 3.18a Transmission electron micrographs of Wt resistant starch. Scale bars represent 5  $\mu\text{m}$  at the top of the graphs.

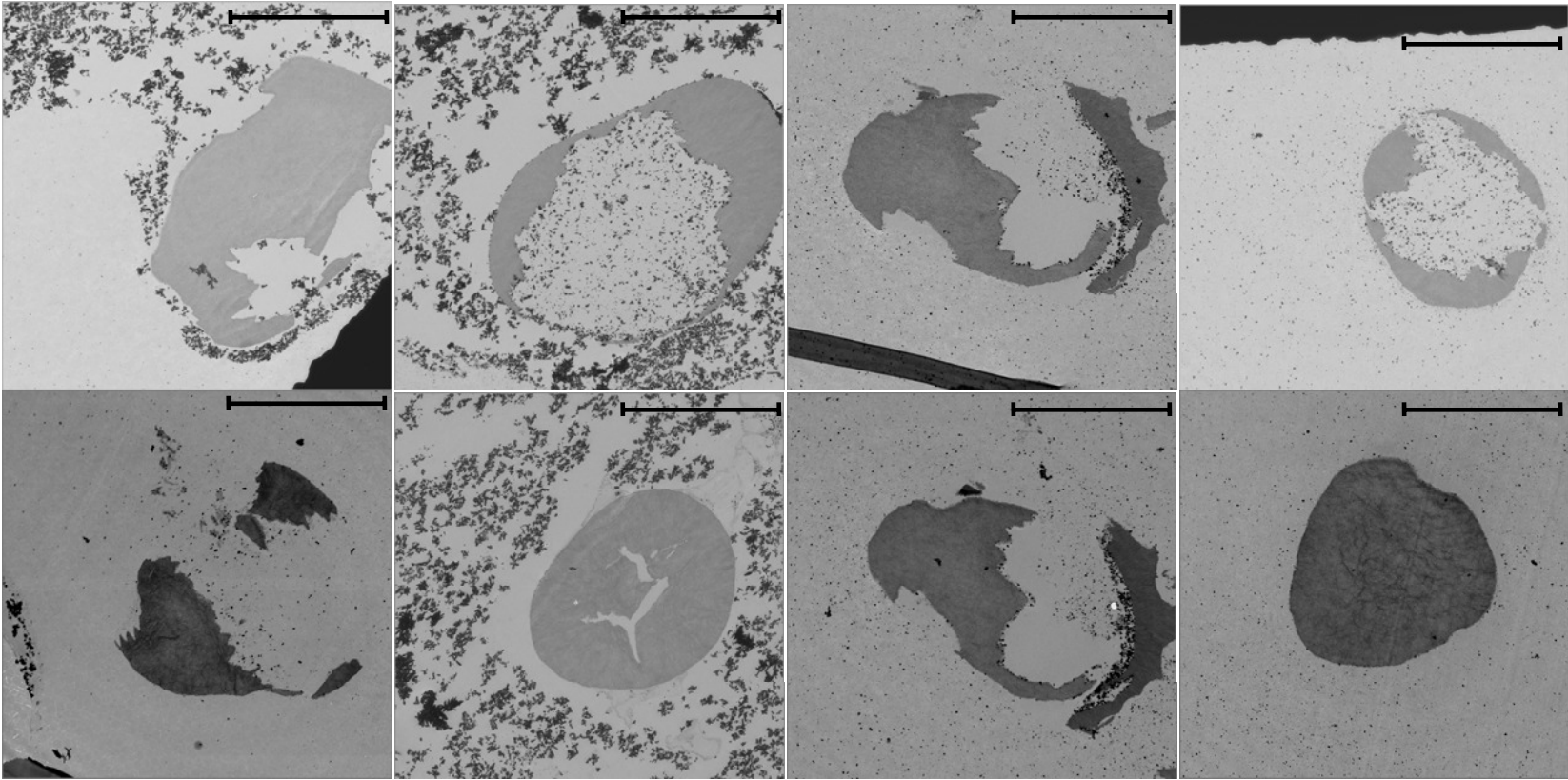


Figure 3.18b Transmission electron micrographs of *sbel1* resistant starch. Scale bars represent 5  $\mu\text{m}$  at the top of the graphs.

and others only had fragments left. The Wt fragments also showed evident alternating layers on the edge of the pieces, which was less evidently present in *sbe1a* samples.

### 3.2.4 Kernel Germination Analysis

As endosperm starch from the *sbe1a* mutant has a lower susceptibility to pancreatic  $\alpha$ -amylase, I reasoned that the *sbe1a* endosperm starch might be less readily utilized during kernel germination. To study the effect of *sbe1a* on kernel germination, starch utilization and coleoptile growth of Wt and *sbe1a* mutant kernels were examined.

All the kernels from three different ears of both Wt and *sbe1a* genotypes were germinated. The coleoptiles from some kernels started to emerge at Day 3 for both genotypes (Fig. 3.19). The coleoptile length of each genotype was measured daily over 11 days (Fig. 3.19). The average length of *sbe1a* coleoptiles was shorter as compared to Wt from Day 7 onwards (Fig. 3.19). One-way ANOVA analysis showed the growth differences were significant from Day 7-11.

To directly examine the starch utilization rate in germinating kernels, the amount of starch remaining in the endosperm was measured periodically (Fig. 3.20). For both genotypes, as expected, the endosperm starch content decreased over time (Fig. 3.20). On Days 6, 8, and 11, the starch content was higher in *sbe1a* germinating endosperm as compared to Wt. This trend is consistent with the reduced growth of *sbe1a* coleoptiles after Day 6.

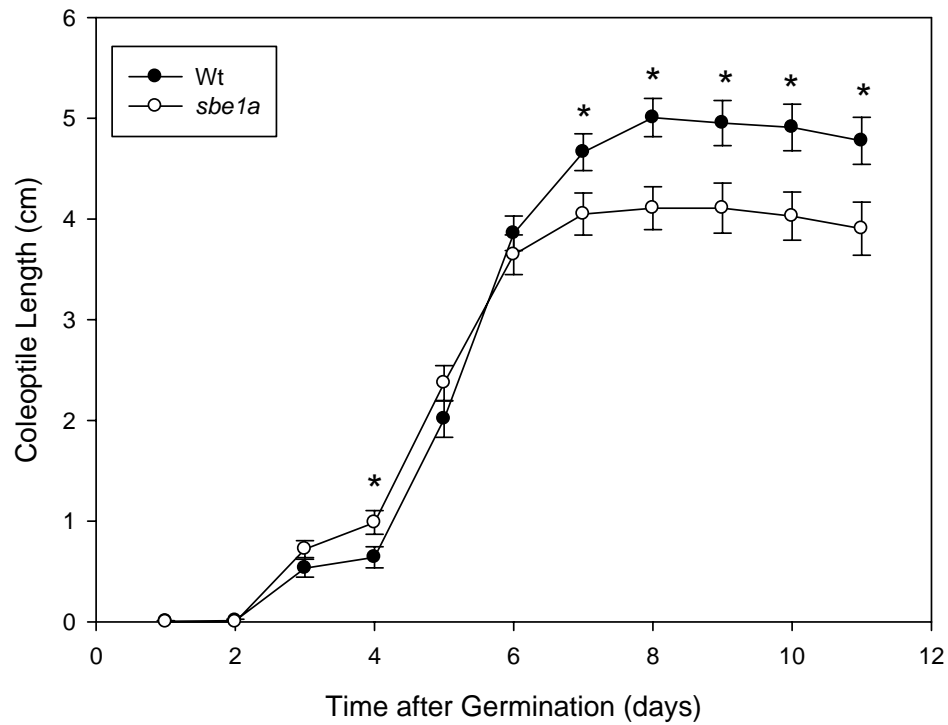


Figure 3.19 Germination of Wt and *sbe1a* mutant kernels: The lengths of the emerged coleoptiles were measured on successive days during the incubation period<sup>1</sup>.

<sup>1</sup>Each data point is mean  $\pm$  standard error of measurements of kernels from three biological replications. As 2 kernels were removed at Day 1, 6, 8, 11 for quantifying starch content, 15, 13, 11, and 9 kernels from three biological replications were used for coleoptile measurement Day 1, 2-6, 7-8, 9-11, respectively. Comparison between two genotypes for each day was made by one-way ANOVA analysis and a significant difference was marked by an asterisk ( $p < 0.05$ ).

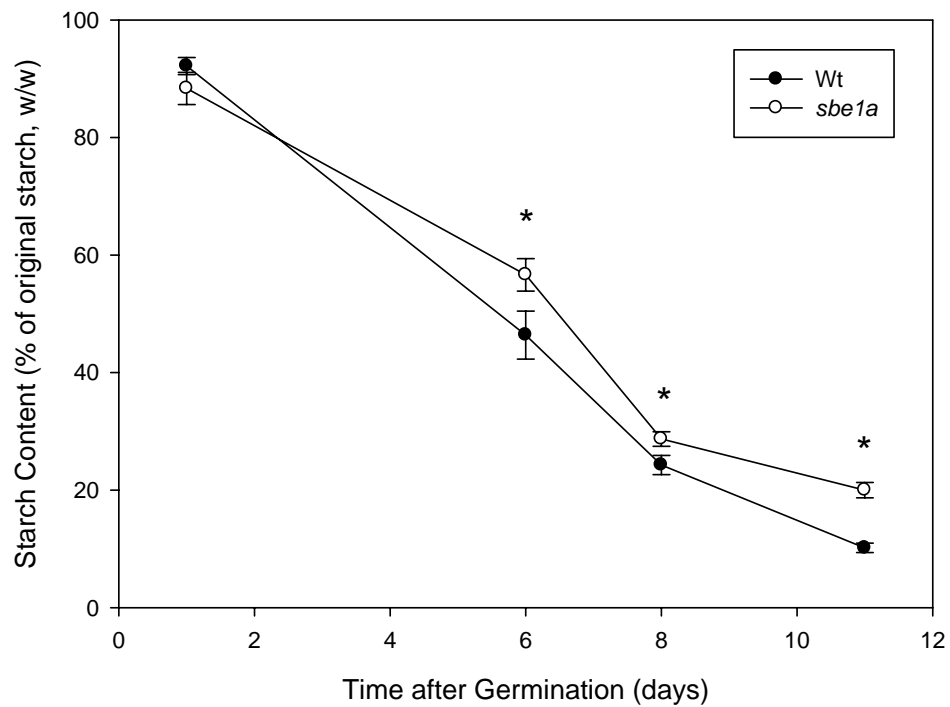


Figure 3.20 Germination of Wt and *sbe1a* mutant kernels: Starch content in the germinating endosperm was quantified at Day 1, 6, 8, 11, and percentage of starch content at each day against the dry weight of Day 1 kernels was plotted<sup>1</sup>.

<sup>1</sup>Each data point is mean  $\pm$  standard error of measurements of 2 kernels from three biological replications. At the same day, comparison between two genotypes was made by one-way ANOVA analysis and a significant difference was marked by an asterisk ( $p < 0.05$ ).

### 3.3 Discussion

#### 3.3.1 Starch Digestibility

Determination of RS values demonstrated that the *sbe1a* mutant results in a higher proportion of non-digested starch (13.2%) as compared to the Wt control (1.6%). Kinetic analysis, using a double exponential model fit, allows a quantitative comparison of the digestion time-course for Wt and *sbe1a* mutant starch.

Considering the high standard deviation, the  $y_0$  value for Wt starch is not much different than zero (Table 3.3). As the RS value for Wt starch is also close to zero (Table 3.2), the  $y_0$  value is in reasonable agreement with the RS value for Wt starch. For the *sbe1a* starch, the  $y_0$  and RS values are in very close agreement, so the RS value can be considered to be approximately the limit of digestion (Fig. 3.3).

The kinetic analysis for both genotypes is consistent with the presence of two starch components: a rapidly-digested substrate ( $S_1$ ), and a slowly-digested substrate ( $S_2$ ) (Rees 2008; Evans and Thompson 2008).  $S_1$  had a rate constant approximately 10-fold larger than  $S_2$  (Table 3.3). The two genotypes differ both in the proportions and the reaction rate constants for these two components. According to the fit, most of Wt starch (85.9%) was  $S_1$ , leaving a small portion (17.9%) to digest at a rate constant 10-fold smaller. For *sbe1a*, only a bit over half (59.8%) was  $S_1$ , with a reaction rate constant ( $1.8 \times 10^{-2} \text{ min}^{-1}$ ) slightly higher than that for Wt ( $1.4 \times 10^{-2} \text{ min}^{-1}$ ). A lower proportion of  $S_1$  in *sbe1a* indicates that *sbe1a* mutation has changed the starch structure to result in less of rapidly-digested component. The proportion of  $S_2$  for *sbe1a* was numerically higher than for Wt, but not statistically different (Table 3.2). The rate constant for  $S_2$  was higher for *sbe1a* than for Wt, indicating that for *sbe1a*, the starch in  $S_2$  is digested more quickly than  $S_2$  for Wt starch.

In the conventional standard for getting data to an exponential decay model,

the reaction needs to be monitored for at least five times the half-life,  $t_{1/2} = \ln 2 / k$ , where  $k$  is rate constant. For example, for  $k_1$  for  $S_1$  of Wt starch (Table 3.3), calculated from  $k_1$  the half-life would be 49.5 min, so the reaction would need to be monitored for 247.5 min to achieve good fit, well within the monitoring time (960 min) in this experiment. However, for  $k_2$  for  $S_2$  of Wt starch (Table 3.3), the half-life would be 770 min, so the reaction would need to be monitored for 3850 min to achieve good fit, far beyond the monitoring time (960 min) in this experiment. The half-life for  $S_1$  and  $S_2$  of *sbe1a* starch is in the same range as those of Wt starch. The longer half-life for  $S_2$  suggests that the data points collected in this experiment are not sufficient to obtain a good fit. Thus the values for parameters  $S_2$  and  $k_2$  should be interpreted with caution.

Using a different enzyme concentration and a different time period of digestion (120 min), the starch digestion time-course curve of Englyst et al. (1992) had similar shape as the digestion curves in this study. During 120 min of digestion, Englyst et al. (1992) differentiated rapidly digested starch (SDS) and slowly digested starch (RDS) using an arbitrary 20 min dividing line. Ao et al. (2007) used Englyst's method to study starch digestion and found that by increasing the branch density in starch to different degrees, the proportion of SDS decreased and the proportion of RDS increased accordingly. The study by Ao et al. suggests that branch density may be a cause for differences in starch digestibility. In the current work, a double exponential decay fit of the 960-min digestion data in contrast to Englyst's arbitrary choice of 20 min showed that less starch was rapidly digested in *sbe1a* as compared to Wt. The *sbe1a* mutation may alter starch digestibility by affecting starch branching structure.

### 3.3.2 Starch Molecular Structure

Because for both Wt and *sbe1a* starch, starch from the three biological replications have similar digestibility, it is reasonable to assume that starch structure is consistent between individuals of identical genotype. Based on this consideration, starch structural analysis was based on starch from one biological replication only.

The proportions of the three recovered starch fractions from differential alcohol precipitation were similar for Wt and *sbe1a* starch, and are consistent with proportions for commercial common corn starch as described in Klucinec and Thompson (1998). The results of iodine binding properties and size-exclusion chromatograms of the intact and debranched starch fractions indicate that amylopectin and amylose have been fractioned with some contamination for both Wt and *sbe1a* starch. Since the material eluting after  $k'$  of 0.2 may be considered to be largely classical amylose (Klucinec and Thompson 1998), the contamination of amylopectin with amylose was similar in Wt and *sbe1a* samples (Fig. 3.5b, Table 3.6), and is consistent with what was observed for fractionation of commercial common corn starch (Klucinec and Thompson 1998).

Iodine binding behavior for respective starch fractions from Wt and *sbe1a* was generally similar (Fig. 3.4), except that a slightly higher  $\lambda_{\max}$  was observed for the starch fractions from *sbe1a* as compared to those from Wt, suggesting that the chains involved in iodine binding are slightly longer from *sbe1a*. Nevertheless, the CL profiles of native starch molecules and starch fractions appeared very similar for Wt and *sbe1a* (Fig. 3.5 & 3.6). The similar CL profile seen for native starch molecules from Wt and *sbe1a* is consistent with the results in Blauth et al. (2002); and the similar CL profile seen for fractioned amylopectin molecules from Wt and *sbe1a* is consistent with the results in Yao et al. (2004), where they compared CL profiles for

amylopectins from *sbe1a wx* to *wx* and did not observe a difference.

Some small differences between the two genotypes were observed in the CL profile of their RS, as well as in the comparison of the CL profile of their RS to the respective native starch (Fig. 3.7, Table 3.8). Comparing RS to native starch, for Wt a decrease in the proportion of region I, considered to be mainly from amylose chains (Batey and Curtin 1996), and an increase in region II, were observed (Table 3.8). One explanation for this change in chain proportions from Wt could be that during digestion, a few long amylose or amylose-like chains have been hydrolyzed to produce chains of shorter CL that elute in region II. However, a decrease in proportion of region I was not evident in the RS from *sbe1a* as compared to the respective native starch. After  $\beta$ -amylolysis of amylose, more of the long chains ( $DP \geq 100$ ) remained in *sbe1a* as compared to Wt. As  $\beta$ -amylase cannot bypass branch points to hydrolyze starch chains, the higher proportion of the long chains of  $DP \geq 100$  remaining after  $\beta$ -amylase attack in *sbe1a* may indicate that the distribution of branch points on these long chains are closer to the non-reducing ends, so that the longer internal chains can escape  $\beta$ -amylase hydrolysis. It is possible that in a starch granule, a longer internal chain in amylose from *sbe1a* may be more favored for co-crystallization of the chains in amylopectin, rendering it less susceptible for  $\alpha$ -amylase attack.

Comparing the RS to the respective native starches, RS from both Wt and *sbe1a* had an increase in region II. The increase was larger in Wt, resulting in a lower proportion of region II in RS from *sbe1a* (Table 3.8, Fig. 3.7). If region II is considered to represent chains from long B chain residues in amylopectin (Hizukuri 1986; Klucinec and Thompson 1998), one explanation for a lower proportion of region II in RS from *sbe1a* is that perhaps the long B chains from *sbe1a* have longer

internal segments, rendering these chains readily hydrolyzed by  $\alpha$ -amylase. The hypothesis of longer internal segments in long B chains from *sbe1a* is consistent with a slightly higher  $\lambda_{\max}$  observed for amylopectin from *sbe1a* as compared to Wt. Chains in RS from both Wt and *sbe1a* had a small decrease in the proportion of region III as compared to the respective native starches (Table 3.8). If region III is considered to represent chains from short B chain or A chain residues (Hizukuri 1986), a decrease in the proportion of region III could be due to the hydrolysis of external chains from short B chains or A chains by  $\alpha$ -amylase. If short B chains or A chains are the major components of amylopectin crystalline regions, the decrease in region III could suggest a slight preference for attack on amylopectin crystalline regions by  $\alpha$ -amylase. As the decrease of region III was observed for both genotypes, this change during RS digestion was unaffected by the *sbe1a* mutation.

The differences in the chain proportions of RS and native starch were relatively small for both genotypes. The RS in this study is considered as type 2 RS according to the definition (Englyst et al. 1992). Evans and Thompson (2004) studied type 2 RS from high-amylose maize starch, and found that unlike type 3 RS, the CL profile of type 2 RS was to a great extent similar to that of the starting material. The current study is consistent with the observation of Evans and Thompson (2004).

Lee (1971) suggested there are two stages of  $\beta$ -amylolysis on amylopectin. In the first stage, most external chains are rapidly degraded; in the second stage, partly degraded chains of DP 4 are slowly and gradually hydrolyzed to DP 2 while the other chains remain the same. Xia and Thompson (2006) suggested that the proximal closely associated branch points may interfere with  $\beta$ -amylolysis in the second stage, and following the progress of  $\beta$ -amylolysis provides insight into amylopectin branching pattern. In the present study, over the 24-hr period of  $\beta$ -amylolysis, a rapid

degradation of chains of DP  $\geq 18$  and DP 8-17 were observed for both Wt and *sbe1a* samples (Fig. 3.8 & 3.9). A higher proportion of chains of DP 8-17, which is considered to be from a portion of short B chains (Klucinec and Thompson 2002), was degraded in Wt (a decrease of  $\sim 15\%$ ) than in *sbe1a* (a decrease of  $\sim 10\%$ ) (Fig. 3.9). As  $\beta$ -amylase cannot bypass branch points to hydrolyze starch chains, a plausible interpretation for the smaller degradation of DP 8-17 in *sbe1a* would be that the branches on some of these B chains lies closer to the non-reducing ends, so that the B chains would have slightly longer internal segments and shorter external chains, thus being less susceptible to  $\beta$ -amylase attack. The hypothesis of longer internal segments in B chains from *sbe1a* is consistent with the evidence obtained from the  $\lambda_{\max}$  and CL profile of RS for *sbe1a*.

In the second stage of  $\beta$ -amylolysis as Lee (1971) suggested, a slow reduction of DP 4 chains occurs. This slow reduction was observed in Wt samples over the period of 10 min to 24 hr but not in *sbe1a* samples (Fig. 3.8 & 3.9). Xia and Thompson (2006) argued that the rate of DP 4 reduction in the second stage of  $\beta$ -amylolysis might be a function of the branching pattern, as differences in the proportion of branch points would differentially limit access of the enzyme to glycosidic linkages. Amylopectin branching pattern models for both *sbe1a* and Wt are presented to account for this difference in  $\beta$ -amylase action on DP 4 stubs in *sbe1a* versus Wt (Fig. 3.21). Both models are consistent with the fast action of  $\beta$ -amylase in the first stage being not influenced by different branching patterns. However, the slow action of  $\beta$ -amylase in the second stage is differentiated in two models.

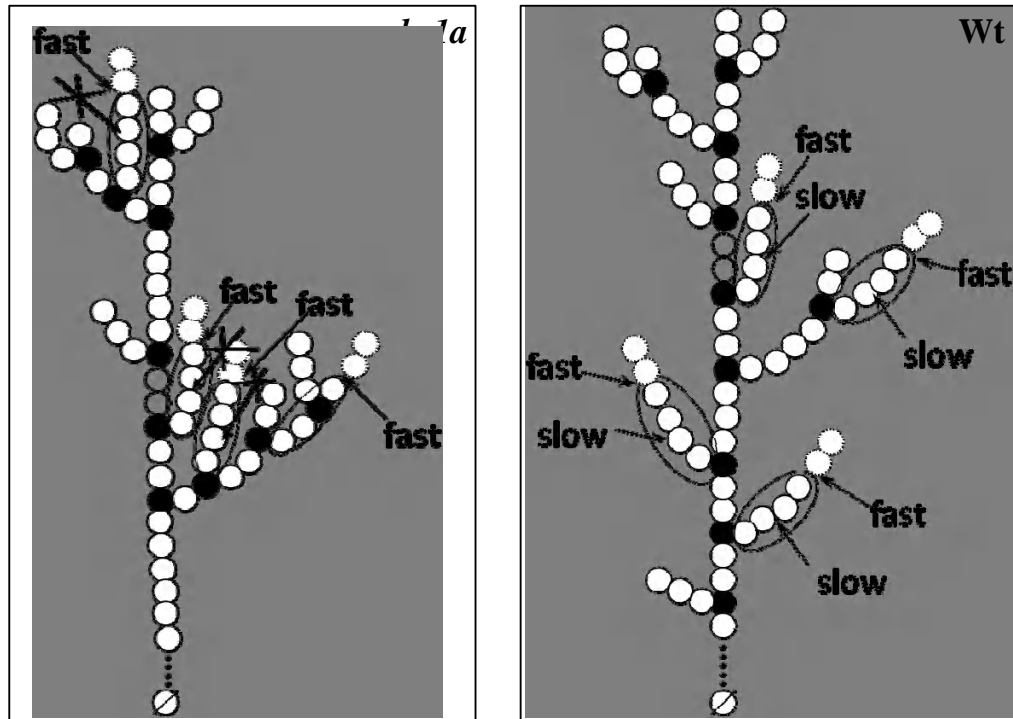


Figure 3.21 Branching pattern models for amylopectin from *sbe1a* and Wt starches. Shown are  $\beta$ -dextrins approaching the limit of digestion by  $\beta$ -amylase, with differences in the amount of DP 4 stubs. All circles indicate glucose units. Dotted line indicates more glucose units. Dotted circles indicate glucose hydrolyzed by  $\beta$ -amylase. Solid black circles indicate branch points. Circles with a slash indicate reducing ends. Circles in an ellipse indicate glucose units that would result in a DP 4 chain. Arrows indicate the action sites of  $\beta$ -amylase. Arrows with a cross indicates that action of  $\beta$ -amylase is prevented by closely associated branch points nearby. Fast and slow indicate the first and second stage of  $\beta$ -amylolysis, respectively.

In the model for *sbe1a*, DP 4 stubs would be difficult for  $\beta$ -amylase to split to DP 2 when the proximal closely associated branch points behave as a barrier against substrate binding to subsites of  $\beta$ -amylase; a small amount of DP 4 chains from residual B chains would also escape  $\beta$ -amylolysis. However, most of the DP 4 is from residual A chains. The incomplete hydrolysis of DP 4 in *sbe1a* suggests that in *sbe1a*, A chains are preferentially localized near another branch point, leading to 1) hindered hydrolysis of residual A chains of DP 4 to DP 2 due to steric hindrance, and 2) more residual B chains with DP 4 due to incidence of short internal segments (Fig. 3.21). In the model for Wt, the DP 4 stubs would be slowly hydrolyzed to DP 2, as there is less steric hindrance from proximal branch points. According to the two models, the limited extent of DP 4 hydrolysis in *sbe1a* samples would indicate a higher proportion of closely associated branch points in the amylopectin from *sbe1a*.

The restricted hydrolysis of the amylopectin from *sbe1a* persists after three successive 24-hr  $\beta$ -amylolysis treatments. The presence of a DP 4 peak (Fig. 3.10) indicates extreme difficulty of hydrolyzing these chains to accomplish the final step of  $\beta$ -amylolysis. After exhaustive  $\beta$ -amylolysis on amylopectin, different debranching strategies were used to separate the residual chains in the putative  $\beta$ -LDs. Isoamylase alone was able to debranch most of chains in  $\beta$ -LDs except for some of the DP 2 stubs in both genotypes. Those DP 2 stubs resistant to isoamylase debranching, however, can be hydrolyzed by pullulanase debranching. The DP 2 stubs released after subsequent pullulanase debranching were much fewer in *sbe1a* than in Wt (Fig. 3.10, Table 3.9). As DP 4 hydrolysis by  $\beta$ -amylase was restricted in *sbe1a*, the conversion of DP 4 to DP 2 was reduced, and thus fewer DP 2 stubs would be available in the  $\beta$ -LDs of *sbe1a*. Thus, the smaller increase in DP 2 stubs from *sbe1a* is the result of the restricted  $\beta$ -amylolysis on DP 4 chains, and would also be a function of a higher

proportion of closely associated branch points in the amylopectin.

For the Wt sample, the subsequent pullulanase debranching released not only DP 2 stubs, but also generated some new DP 5-7 chains, which may have been originally closely associated with DP 2 stubs (Table 3.9). This result is consistent with the previous suggestion (Xia and Thompson 2006) that subsequent pullulanase debranching can release some DP 5-7 chains which are originally closely associated with DP 2 stubs. However, no increase in DP 5-7 was observed for *sbe1a* after subsequent pullulanase debranching. As there were far fewer DP 2 stubs in the *sbe1a* sample, there may not be structures consisting of closely associated DP 5-7 chains with DP 2 stubs; instead, there may be structures consisting of closely associated DP 5-7 chains with DP 4 chains. No DP 4 increase was evident after subsequent pullulanase debranching (Fig. 3.10, Table 3.9), suggesting that isoamylase is able to debranch all the DP 4 chains. Thus, the DP 5-7 chains associated with DP 4 in the *sbe1a* sample can be released after isoamylase debranching, and no additional DP 5-7 chains can be released after subsequent pullulanase debranching. Lack of increase in DP 5-7 may be another function of the restricted DP 4 hydrolysis and indicates a higher proportion of closely associated branch points in the amylopectin from *sbe1a*.

As the CL profile is highly similar for amylopectin from Wt and *sbe1a* (Fig. 3.6a) and the average branching density can be obtained from the reciprocal of average CL, the average branching density is similar in two amylopectins. Coupled with the evidence obtained from residual DP 4 stubs after  $\beta$ -amylolysis and subsequent debranching on  $\beta$ -LDs, I suggest that the effect of *sbe1a* mutation is to increase the local concentration of branch points but not to influence the overall amount of branch points in amylopectin. Further, evidence from  $\lambda_{\max}$ , CL profile of RS, and long B chain degradation by  $\beta$ -amylase leads to a hypothesis that long B

chains from *sbe1a* have longer internal segments, which is consistent with more concentrated local branching in *sbe1a*.

By analyzing the CL distribution of  $\beta$ -LDs from amylopectin from *sbe1a wx* and *wx*, Yao et al. (2004) did not observe an effect of *sbe1a* mutation on amylopectin branching in the *wx* background. This apparent inconsistency with current finding suggests that the amylopectin from *sbe1a wx* may be different than the amylopectin fractionated from *sbe1a*. That amylopectin might have a different structure in the *wx* background has been observed for the amylopectin from *ae wx* and the amylopectin fractionated from *ae* in commercial starches (Klucinec and Thompson 2002). As the *wx* mutant is deficient in granule-bound starch synthase (GBSS), the synthesis of amylopectin may be influenced without the presence of GBSS in the *wx* mutant. In preliminary work by Xia (2005), following time course of  $\beta$ -amylolysis of *sbe1a wx* and *wx* suggested that slightly more DP 4 stubs remained in *sbe1a wx* (Fig.1.5). Even though the difference of DP 4 stubs between *sbe1a wx* and *wx* is not as large as the difference between amylopectin from *sbe1a* and Wt, the work reported by Xia (2005) suggests that there may well be a small effect of *sbe1a* mutation on amylopectin branching in the *wx* mutant, regardless of the possible difference in amylopectin synthesis in the *wx* mutant. The disagreement of the work of Xia (2005) and Yao et al. (2004) suggests that studying the progress of  $\beta$ -amylolysis can reveal the nuances of molecular structure difference which is not observed by studying CL distribution of  $\beta$ -LDs only.

To study the fine structure of amylose, exhaustive  $\beta$ -amylolysis and subsequent isoamylase and pullulanase debranching were also applied to the amylose fraction from Wt and *sbe1a*. Despite a similar CL profile observed for amylose from the two genotypes (Fig. 3.6b), the CL distribution after  $\beta$ -amylolysis showed

differences for Wt and *sbe1a* (Fig. 3.11). A higher proportion of long chains of DP  $\geq$  100 and lower proportion of other chains (DP < 100) was observed in *sbe1a* (Table 3.10). As the proportion of chains of DP  $\geq$  100 was not different for intact amylose from the two genotypes (Fig. 3.6b), the lower proportion of some of these chains found in  $\beta$ -LDs of amylose from Wt can be explained by a greater susceptibility of some of these chains to  $\beta$ -amylase as compared to longer chains from *sbe1a*. Consequently, the degradation of more chains of DP  $\geq$  100 resulted in a higher proportion of chains of DP < 100 in Wt as compared to *sbe1a*. As discussed earlier in this section, the higher proportion of the long chains of DP  $\geq$  100 remaining after  $\beta$ -amylase attack on amylose of *sbe1a* may indicate that the distribution of branch points on these long chains are closer to the non-reducing ends, so that the longer internal chains can escape  $\beta$ -amylase hydrolysis.

Pullulanase debranching subsequent to isoamylase debranching on  $\beta$ -LDs from amylose for both genotypes led to an increase in both DP 2 and DP 3 and a greater increase in DP 2 than DP 3 (Table 3.10). For  $\beta$ -LD from amylopectin, all of the DP 3 and some of the DP 2 are debranched by isoamylase. Unlike  $\beta$ -LD from amylopectin, for  $\beta$ -LD from amylose, some DP 3 chains are not debranched by isoamylase for both genotypes. Comparing *sbe1a* to Wt, more of DP 2 and DP 3 chains are not debranched by isoamylase in  $\beta$ -LD from *sbe1a* amylose, resulting in a greater increase by subsequent debranching in both DP 2 and DP 3 for *sbe1a* (Table 3.10). As the structures escaping isoamylase debranching may have closely associated branch points and those structures can be debranched by pullulanase (Xia and Thompson 2006), a greater increase in both DP 2 and DP 3 by pullulanase may suggest a higher proportion of these structures resistant to isoamylase in amylose from *sbe1a*. Amylose branching pattern models for both *sbe1a* and Wt are presented (Fig.

3.22) to account for the difference in isoamylase action on  $\beta$ -LD in *sbe1a* versus Wt. In the model for *sbe1a*, A chains are preferentially attached by branch points close to each other, leading to hindered isoamylase debranching of residual A chains of DP 2 and DP 3. In the model for Wt, A chains are not as preferentially attached by branch points close to each other as those in *sbe1a*, leading to hindered isoamylase debranching of some DP 2 and DP 3 stubs but not as many as in *sbe1a*. The two models account for a greater increase in DP 2 or DP 3 by pullulanase observed for *sbe1a*. These two models are consistent with the idea that the A chains in the *sbe1a* amylose are more preferentially attached by branch points close to each other, leading to a structure of closely associated branch points more prevalent in *sbe1a*.

The evidence that amylose for *sbe1a* has 1) longer internal chains and 2) A chains attached by branch points close to each other, can be used to create an overall model for amylose branching patterns of *sbe1a* and Wt (Fig. 3.23). The models are drawn taking into account the evidence in this study that the CL profile is highly similar for amylose from Wt and *sbe1a* (Fig. 3.6b) and the evidence in literature that ~50% of amylose molecules are branched and ~5-6 branches exist per molecule (Takeda et al. 1987). According to the proposed model, for *sbe1a*, A chains are closer to each other, and the location of the chains tends to be more towards non-reducing end. For Wt, A chains are farther from each other, and the location of the chains is more random and thus more distributed over the long chain. Evidence from  $\lambda_{\max}$  suggests amylose from *sbe1a* has longer internal segments than amylose from Wt, which is consistent with the amylose models proposed in Fig. 3.23.

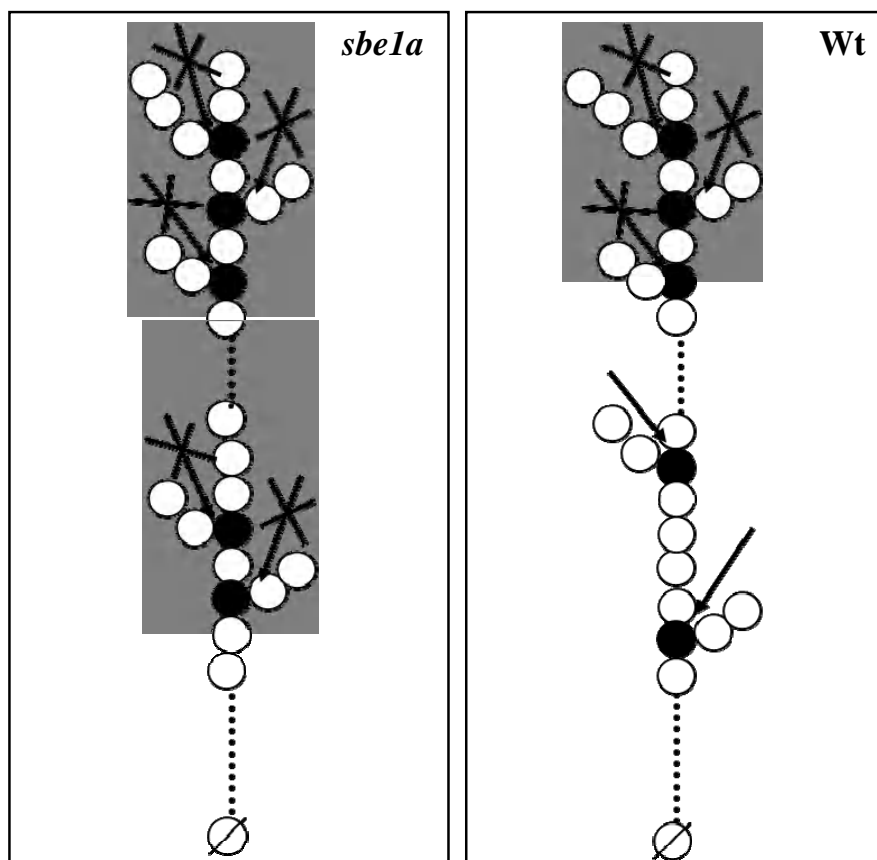


Figure 3.22 Branching pattern models for amylose from *sbe1a* and Wt starches. Shown are  $\beta$ -limit dextrans that are consistent with difference in action of isoamylase. All circles indicate glucose units. Dotted lines indicate more glucose units. Solid black circles indicate branch points. Circles with a slash indicate reducing ends. Arrows indicate the action sites of isoamylase. Arrows with a cross indicates that action of isoamylase is prevented by closely associated branch points nearby.

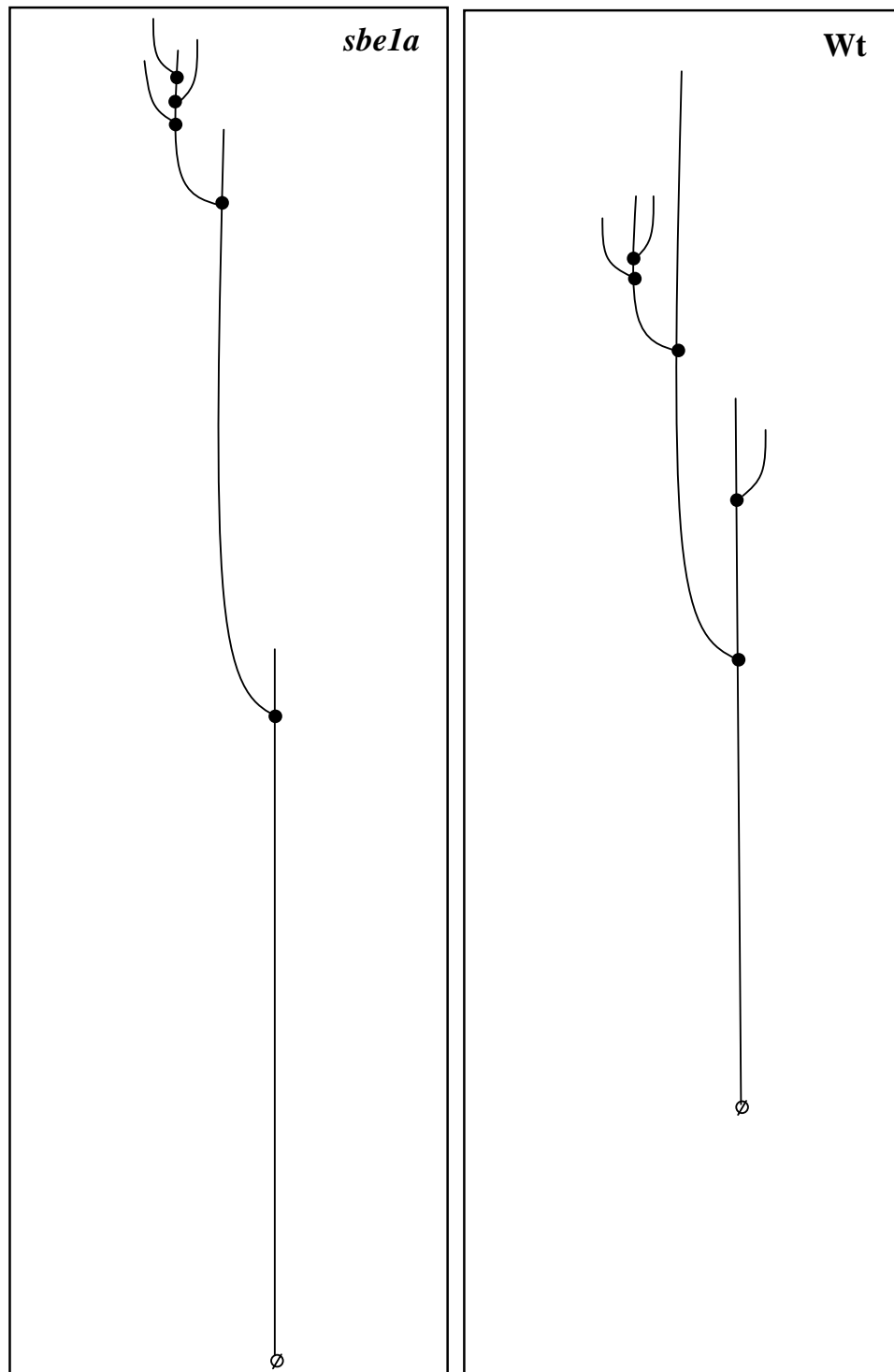


Figure 3.23 Proposed overall amylose branching pattern models for *sbela* and *Wt* starches, consistent with the differences in actions of  $\beta$ -amylase and isoamylase. All lines indicate glucose chains. Solid black circles indicate branch points. Circles with a slash indicate reducing ends.

### 3.3.3 Starch Granular Structure

Of the three microscopic techniques employed to observe granular structure before and after RS digestion, scanning electron microscopy (SEM) gives the most revealing view of starch ultra-structure after digestion. The micrographs from light microscopy (LM) and transmission electron microscopy (TEM) are supplementary to the observations from SEM. LM is helpful that it describes possible heterogeneity of native and digested granules. TEM reveals the interior structure of the residual granules which is invisible by SEM in some cases. A combination of the three microscopic techniques helps to comprehensively visualize granular structure at different levels.

Prior to RS digestion, the native starch granules from Wt and *sbe1a* appear similar in size, shape, degree of birefringence, and morphology, consistent with the similarity seen for *wx* and *sbe1a wx* granules (Li et al. 2007). Consistent with the RS measurement, micrographs for RS from all the three techniques showed that more residual material in a field was observed in *sbe1a* starch than Wt after RS digestion (Fig. 3.12-3.18). Under polarized LM (Fig. 3.12b), almost all the digested Wt granules had lost their birefringence; while for *sbe1a*, many digested granules had managed to maintain their birefringence in the peripheral area of the granules but lost birefringence in the center, which indicates that the center area of the digested *sbe1a* granules is either gone or no longer crystalline enough to show birefringence. The presence of a hollow interior in the digested *sbe1a* granules was confirmed by SEM (Fig. 3.16), indicating a greater resistance of the exterior portion of the granule. These observations suggest that the digestion pattern for *sbe1a* granules is initiated with an intrusion from the granule surface into the interior, followed by hydrolysis from the interior to the exterior.

Most of the Wt RS was small granule fragments. However, the *sbe1a* RS showed variations in morphology, from small fragments to almost intact granules. The difference in digestion of individual granules may be due to heterogeneity of the native granules, as heterogeneity is indicated by different degrees of iodine staining of the native granules (24.3% of them are more dark stained than the others) (Fig. 3.13a). SEM revealed the presence of resistant layers in the Wt residual fragments (Fig. 3.15). This evidence is also shown by TEM, where the sliced granules from Wt showed evident alternating layers (Fig. 3.18a); these layers were less evidently present in the *sbe1a* samples (Fig. 3.18b). The alternating layers probably reflect the residual growth rings after digestion. As more than 98% of Wt starch was digested, these residual rings in the Wt RS may represent the most resistant portion for digestion.

By observing the *sbe1a* RS by SEM (Fig. 3.16), one may roughly estimate that, for the recovered granules, approximately 40% of granule content has escaped digestion. However the RS value for *sbe1a* starch is approximately 13%. Therefore, some of the *sbe1a* granules must have been digested completely. The heterogeneity found among *sbe1a* granules (Fig. 3.13a) may account for different degree of digestion of individual granules. Thus, it can be reasoned that the micrographs of the *sbe1a* RS disproportionately represent the more resistant granules.

A distinct feature of the *sbe1a* RS is the presence of holes on the surface of the peripheral area. These holes are possibly from the enlargement of the surface pores in native granules by  $\alpha$ -amylase hydrolysis (Zhang et al. 2006). The presence of these holes on the shell is consistent with previous studies that digestion of normal granules starts with surface pores and proceeds to channels in granules that provide access for  $\alpha$ -amylase to hydrolyze the interior material (Leach and Schoch 1961; Valetudie et al. 1993; Herbert et al. 1996; Li et al. 2004). It is reasonable to hypothesize that if these

holes continue to grow on the granule surface, the granule would eventually become fragmented. Zhang et al. (2006) showed that holes on the surface of normal maize starch were visible after 40 min of pancreatic  $\alpha$ -amylase digestion; but after 120 min of digestion, most of the holes disappeared due to fragmentation of starch granules. In the current study, the presence of remaining shells with holes in the *sbe1a* RS represents difficulty in digestion by  $\alpha$ -amylase. Neither holes nor shells were observed in the Wt RS, indicating a more complete digestion.

As observed under microscopy, the Wt RS are mostly residual rings, and the *sbe1a* RS are mostly residual peripheral regions, suggesting that granules of the original starch are different for Wt and *sbe1a*. From the kinetic analysis, the digestion of *sbe1a* starch reached a plateau by 16 hr, suggesting the RS from *sbe1a* cannot be further digested. When the RS is observed by SEM, one can conclude that some of the peripheral region in *sbe1a* cannot be further digested. It is unclear what accounts for the resistance from the peripheral region to  $\alpha$ -amylase digestion. Based on the evidence from  $\lambda_{\max}$  as well as amylose branching pattern, a longer internal chain amylose from *sbe1a* may be more favored for co-crystallization of the chains in amylopectin, rendering it less susceptible for  $\alpha$ -amylase attack. Enrichment of amylose has been found by some to exist toward the granule peripheral region (Morrison and Gadan 1987; Atkin et al. 1999). A hypothesis for the greater resistance from the peripheral region in *sbe1a* is that the peripheral region may be rich of amylose favored for co-crystallization with amylopectin to increase the enzyme resistance. Alternatively, the granule organization such as the crystalline structure of the peripheral region in *sbe1a* may be different than the other regions in granule, rendering it more resistant to  $\alpha$ -amylase attack.

Microscopy evidence also shows that some *sbe1a* granules have been

completely digested, while others have been digested to different degrees. Thus, what is digested in *sbe1a* could be whole granules or partial granules in different regions. This kind of variation in what is digested does not seem to apply for Wt starch, as most of the Wt granules has been completely digested except for some residual rings. The possible difference in digested portion between *sbe1a* and Wt starches is consistent with the observed different kinetic parameters for the digested components ( $S_1$  and  $S_2$ ) for *sbe1a* and Wt starches (Table 3.3). However, microscopy evidence from current study only focused on RS, which cannot explain the differences in digested components.

According to Gao et al. (1996), the expression of *Sbe1a* mRNA levels peaked later than for *Sbe2* (including *Sbe2a* and *Sbe2b*) mRNA in the developing endosperm. If the SBE enzymatic activities are reflected by the *Sbe* mRNA levels during endosperm development, the differential expression of the *Sbe1a* and *Sbe2* genes suggests that SBEI activity may play a more important role during the later stage of starch synthesis in endosperm. Thus, deficiency of SBEI in the *sbe1a* mutant would have a greater influence on starch molecular structures synthesized later during development. A reasonable speculation is that most of the later-synthesized molecular structures would be deposited in the peripheral regions of *sbe1a* granules. SEM showed that the peripheral regions were more resistant to  $\alpha$ -amylase digestion in *sbe1a* granules. It is possible that a more ordered molecular structure in the peripheral regions may have resulted from deficiency of SBEI. However, no direct evidence was obtained in the current study about whether the molecular structure in the peripheral regions was different in *sbe1a*.

As high-amylose starch, mostly *ae*-type, is known for high resistance to  $\alpha$ -amylase digestion, partially digested granules from this source have been extensively

examined by microscopy (Gallant et al. 1992; Planchot et al. 1995; Evans and Thompson 2004; Rees 2008). The RS from *sbe1a* granules is different than that from *ae*-type starch. Unlike the intact surface appearance of RS from most *ae*-type granules, for the *sbe1a* RS, distinct holes are often present on the resistant peripheral layer, and growth rings as represented by alternating layers are visible underneath some of the distinct holes. The holes and rings are not common in RS from *ae*-type starch. A thin, corroded outermost layer was often seen in the RS from high-amylose starch (Evans and Thompson 2004; Rees 2008), which was not visible in the *sbe1a* RS. Despite the intact external appearance of RS from most high-amylose granules, the digested granules usually have a hollow interior that often contains radially oriented channels originated from the granule center, best visible by TEM (Evans and Thompson 2004; Rees 2008). No such channels were observed in the *sbe1a* RS by TEM (Fig. 3.18b). The kinetic analysis of the digestion of some high-amylose starch showed that the limit of digestion ( $y_0$ ) is always smaller than RS value (Rees 2008). However for *sbe1a*,  $y_0$  is very close to the RS value (Fig.3.3). The difference between  $y_0$  and RS value for high-amylose starch indicates a difference in the nature of what is quantified as RS than for *sbe1a*. All the observed differences suggest a different digestion pattern for *sbe1a* as compared to high-amylose starch granules.

### 3.3.4 Structural Basis for Decreased Digestibility of *sbe1a* Starch

Visual evidence from microscopy suggests that a resistant peripheral layer accounts for the decreased digestibility of *sbe1a* starch. In order to understand the granule resistance to  $\alpha$ -amylase digestion, the molecular structures of fractionated amylopectin and amylose from native starch granule were characterized by following  $\beta$ -amylolysis as well as by stepwise debranching  $\beta$ -dextrins using isoamylase and

pullulanase. Investigation of amylopectin branching pattern suggests that the *sbe1a* amylopectin has a higher proportion of closely associated branch points due to preferentially localized A chains with another branch points. The other structural evidence for amylopectin suggests that long B chains from *sbe1a* have longer internal segments, consistent with more concentrated local branching in *sbe1a*. Investigation of amylose branching pattern suggests that the *sbe1a* amylose has a higher proportion of closely associated branch points due to more of localized A chains, and the location of the chains is not random and more towards non-reducing end. The other structural evidence for amylose suggests that amylose chains from *sbe1a* have longer internal segments, consistent with the amylose branching pattern model for *sbe1a*. Given all the evidence from molecular structure analysis, a plausible speculation is that in an *sbe1a* starch granule, longer internal segment in both amylopectin and amylose chains may be more favored for co-crystallization, and the prevalence of closely associated branch points on both amylopectin and amylose may cause steric hindrance for  $\alpha$ -amylase action; this type of branching pattern in *sbe1a* may result in a more resistant starch granule to  $\alpha$ -amylase digestion. It is possible that these differences are localized to peripheral region.

An attempt to obtain direct evidence for granule resistance was made through characterizing the CL profile of RS and comparing it to CL profile of native starch. Although generally similar CL distributions were observed for RS and native starch from *sbe1a* (Table 3.8), the observed small differences suggest that amylose chains in *sbe1a* are less hydrolyzed during  $\alpha$ -amylase digestion, consistent with the hypothesis that amylose chains may be more favored for co-crystallization with amylopectin in *sbe1a*, rendering these amylose chains less hydrolyzed. Enrichment of amylose has been found by some to exist toward the granule peripheral region (Morrison and

Gadan 1987; Atkin et al. 1999). It can be reasoned that the resistant peripheral region in the *sbe1a* RS may be rich of these amylose chains involved in co-crystallization with amylopectin. Due to the small amount of RS recovered after digestion, the branching pattern of RS was not investigated. It is possible that the branching pattern might differ between the RS and the digested portion of *sbe1a* starch, and this difference might also account for the decreased digestibility of the peripheral region in *sbe1a* granule.

### 3.3.5 Starch Utilization during Kernel Germination

*In vitro* enzyme hydrolysis of Wt and *sbe1a* starch by pancreatic  $\alpha$ -amylase revealed decreased susceptibility of the *sbe1a* starch. A kernel germination test of Wt and *sbe1a* seeds showed that germinating *sbe1a* kernels exhibited a slower rate of coleoptile growth and an accordingly decreased rate of starch hydrolysis, suggesting an *in vivo* functional effect of SBEI deficiency.

A plant  $\alpha$ -amylase is considered to be responsible for attacking the starch granule and initiating starch hydrolysis in germinating cereal endosperm (Smith et al. 2005). Starch hydrolysis continues by the action of limit dextrinase,  $\alpha$ -amylase,  $\beta$ -amylase, and  $\alpha$ -glucosidase to produce maltose and glucose for plant utilization (Smith et al. 2005). The observed reduction in starch hydrolysis during the later stages of germination raises the possibility that continued hydrolysis of  $\alpha$ -amylase-hydrolyzed glucans might also be hindered in the *sbe1a* mutant. The altered carbon metabolism could then cause a deficiency in general plant growth characteristics such as coleoptile length. A reasonable speculation is that deficiency in starch utilization of *sbe1a* seeds may be due to an altered starch branching pattern caused by the deficiency of SBEI. Even though the deficiency in starch utilization of *sbe1a* seeds is

not substantial, it would provide a very powerful selection pressure for SBEI isoform in nature. For a plant growing in the wild under marginal conditions, competing with other plants for nutrients or other resources, this compromised utilization would limit the growth and reproductive fitness of a plant. Therefore, SBEI activity may provide an important advantage for synthesizing starch that is maximally efficient for energy transduction for normal plant growth and development.

### 3.4 References-Chapter 3

- Ao, Z., Simsek, S., Zhang, G., Venkatachalam, M., Reuhs, B.L., Hamaker, B.R. (2007). Starch with slow digestion property produced by altering its chain-length, branch density and crystalline structure. *J. Agri. Food. Chem.* 55, 4540-4547.
- Atkin, N.J., Cheng, S.L., Abeysekera, R.M. and Robards, A.W. (1999). Localisation of amylose and amylopectin in starch granules using enzyme-gold labelling. *Starch/Stärke*, 51, 163-172.
- Batey I.L., Curtin B.M. (1996). Measurement of amylose/amylopectin ratio by high-performance liquid chromatography. *Starch/Stärke*, 48: 338-344.
- Blauth, S.L., Kim, K., Klucinec, J.D., Shannon, J.C., Thompson, D.B., Guiltinan, M.J. (2002). Identification of Mutator insertional mutants of starch branching enzyme 1 (*sbe1*) in *Zea mays* L. *Plant. Mol. Biol.* 48, 287-297.
- Boyer, C. D., Daniels, R. R. and Shannon, J. C. (1977). Starch granule (amyloplast) development in endosperm of several *Zea mays* L. genotypes affecting kernel polysaccharides. *Amer. J. Bot.*, 64, 50-56.
- Boyer, C. D. and Preiss, J. (1978). Multiple forms of (1,4)- $\alpha$ -D-glucan-6-glucosyl transferase from developing *Zea Mays* L. kernels. *Carbohydr. Res.*, 61, 321-334.
- Dubois, M., Gilles, K. A., Hamilton, J. K., Rebers, P. A., and Smith, F. (1956). Colorimetric method for determination of sugars and related substances. *Anal. Chem.*, 28, 350-356.
- Englyst, H. N., Kingman, S. M. and Cummings, J. H. (1992). Classification and measurement of nutritionally important starch fractions. *Eur. J. Clin. Nutr.* 46, S33-S50.
- Evans, A. and Thompson, D.B. (2004). Resistance to  $\alpha$ -Amylase digestion in four native high-amylose maize starches. *Cereal Chem.* 81, 31-37.

- Evans, A. and Thompson, D.B. (2008). Enzyme susceptibility of high-amylose starch precipitated from sodium hydroxide dispersions. *Cereal Chem.* 85, 480–487.
- Gallant, D.J., Bouchet, B., Buleon, A., and Perez, S. (1992). Physical characteristics of starch granules and susceptibility to enzymatic degradation. *Eur. J. Clin.*
- Gao, M., Fisher, D.K., Kim, K.N., Shannon, J.C., and Guiltinan, M.J. (1996). Evolutionary conservation and expression patterns of maize starch branching enzyme I and IIb genes suggests isoform specialization. *Plant Mol. Biol.*, 30, 1223-1232.
- Garwood, D.L., Shannon, J.C., and Creech, R.G. (1976). Starches of endosperms possessing different alleles at the *amylose-extender* locus in *Zea mays* L. *Cereal Chem.* 53, 355-364.
- Helbert, W., Schülein, M., & Henrissat, B. (1996). Electron microscopic investigation of the diffusion of *Bacillus licheniformis*  $\alpha$ -amylase into corn starch granules. *Int. J. Biol. Macromol.*, 19, 165–169.
- Hizukuri, S. (1986). Polymodal distribution of the chain lengths of amylopectins, and its significance. *Carbohydr. Res.*, 147, 342-347.
- Klucinec, J.D., and Thompson, D.B. (1998). Fractionation of high amylose maize starches by differential alcohol precipitation and chromatograph of the fractions. *Cereal Chem.* 75, 887-896.
- Klucinec, J.D., and Thompson, D.B. (2002). Note: Structure of amylopectins from *ae*-containing maize starches. *Cereal Chem.*, 79, 19-23.
- Leach, H. W., & Schoch, T. J. (1961). Structure of the starch granule. II. Action of various amylase on granular starches. *Cereal Chem.*, 38, 34–46.
- Lee, E. Y. C. (1971). The action of sweet potato  $\beta$ -amylase on glycogen and amylopectin: formation of a novel limit dextrin. *Arch. Biochem. Biophys.*, 146, 488-492.
- Li, J.H., Thompson, D.B., and Guiltinan, M. (2007). Mutation of the maize *sbe1a* and *ae* genes alters morphology and physical behavior of *wx*-type endosperm starch granules. *Carbohydr. Res.* 342, 2619–2627.
- Li, J.H., Vasanthan, T., Hoover, R., Rossnagel, B.G. (2004). Starch from hull-less barley: V. In-vitro susceptibility of waxy, normal, and high-amylose starches towards hydrolysis by alpha-amylases and amyloglucosidase. *Food Chem.*, 84, 621–632.
- Morrison, W.R. and Gadan, H.J. (1987). The amylose content of starch granules in developing wheat endosperm. *J. Cereal Sci.* 5, 263-275.
- Morrison, W.R., and Laignelet, B. (1983). An improved colorimetric procedure

for determining apparent and total amylose in cereal and other starches. *J. Cereal Sci.* 1, 9-20.

- Planchot, V., Colonna, P., Gallant, D.J., and Bouchet, B. (1995). Extensive degradation of native starch granules by alpha-amylase from *Apergillus fumigatus*. *J Cereal Sci.* 21, 163-171.
- Rees, E. (2008). Effect of a heat-moisture treatment on alpha-amylase susceptibility of high amylose maize starches. MS thesis. The Pennsylvania State University, University Park, PA.
- Smith, A.M, Zeeman, S.C., and Smith, S.M. (2005). Starch Degradation. *Annu. Rev. Plant Biol.* 56, 73-98.
- Takeda, Y., Hizukuri, S., Takeda, C. Suzuki, A. (1987). Structures of branched molecules of amyloses of various origins, and molar fractions of branched and unbranched molecules. *Carbohydr. Res.* 165, 139-145.
- Valetudie, J. C., Colonna, P., Bouchet, B., Gallant, D. J. (1993). Hydrolysis of tropical tuber starches by bacterial and pancreatic  $\alpha$ -amylases. *Starch/Stärke*, 45, 270-276.
- Xia, H. (2005). Branching pattern differences among amylopectins of several maize genotypes. MS thesis. The Pennsylvania State University, University Park, PA.
- Xia, H. Yandeau-Nelson, M., Gultinan, M.J., Thompson, D.B. (2007). SBE maize endosperm mutations are associated with different levels of resistant starch. Presentation at 2007 AACCC conference, Starch Round Table, San Antonio, Texas.
- Xia, H., and Thompson, D.B. (2006). Debranching of  $\beta$ -limit dextrans with isoamylase or pullulanase to explore the branching pattern of amylopectins from three maize genotypes. *Cereal Chem.* 83, 668-676.
- Yao, Y., Thompson, D.B., and Gultinan, M.J. (2004). Maize starch branching enzyme (SBE) isoforms and amylopectin structure: in the absence of SBEIIb, the future absence of SBEIa leads to increased branching. *Plant Physiol.*, 106, 293-316.
- Zhang, G., Ao, Z., Hamaker, B. R. (2006). Slow digestion property of native cereal starches. *Biomacromolecules*, 7, 3252-3258.

## Chapter 4

# EFFECTS OF DEFICIENCY OF MAIZE SBEs ALONE AND IN COMBINATION ON ENDOSPERM STARCH DIGESTIBILITY AND MOLECULAR STRUCTURE

### 4.1 Introduction and Objectives

Effects of deficiency of one or more maize starch-branching enzyme (SBE) isoforms on endosperm starch structure have been studied through the use of *sbe* mutants differing in SBE isoform activities (Table 4.1). In an analysis of starch isolated from kernels from *sbe2a* and *ae* mutant combinations, Yao et al. (2003) suggested that a deficiency of SBEIIa increases amylopectin branching only when SBEIIb is deficient. By comparing starch from *sbe1a* and *ae* mutant combinations (all in a *wx* background), Yao et al. (2004) suggested similarly that a deficiency of SBEIa increases amylopectin branching only when SBEIIb is also deficient. Granular structural differences were also seen between *sbe1a ae* and *ae* endosperm starch in a *wx* background (Li et al. 2007). It can be reasoned from these studies that some type of interactions occur among individual SBE isoforms and/or their biochemical activities.

Prior to the present research, *sbe1a* and *sbe2a* mutant combinations have not been studied (Table 4.1). In this chapter, effects of these mutants on starch structure are described.

Table 4.1 Various *sbe* mutants differing in SBE isoform activities.

<b>Genotype</b>	<b>Deficient SBE Isoform(s)</b>	<b>Remaining SBE Isoform(s)</b>
Wt <sup>1,2</sup>	None	SBEIa, SBEIIa, SBEIIb
<i>sbe1a</i> <sup>1</sup>	SBEIa	SBEIIa, SBEIIb
<i>sbe2a</i> <sup>2</sup>	SBEIIa	SBEIa, SBEIIb
<i>ae</i> <sup>1,2</sup>	SBEIIb	SBEIa, SBEIIa
<i>sbe1a sbe2a</i>	SBEIa, SBEIIa	SBEIIb
<i>sbe1a ae</i> <sup>1</sup>	SBEIa, SBEIIb	SBEIIa
<i>sbe2a ae</i> <sup>2</sup>	SBEIIa, SBEIIb	SBEIa

<sup>1</sup>Mutants studied in Yao et al. (2004) and Li et al. (2007).

<sup>2</sup>Mutants studied in Yao et al. (2003).

A high resistant starch (RS) value has been routinely observed for the *ae* mutant (Richardson et al. 2000). As documented in Chapter 3 of this thesis, an *sbe1a* mutant caused a decreased digestibility of starch granules to pancreatic  $\alpha$ -amylase compared to Wt. Thus, it is of interest to ask whether there might be effects of *sbe2a* mutant and of other *sbe* mutant combinations on starch digestibility.

Due to the compromised growth of the *sbe2a* mutant, it was not possible to examine starch from homozygous mutant lines, which would not be of comparable size or vigor during seed development. Therefore, for the present study, homozygous Wt, *sbe1a*, *ae*, and *sbe1a ae* starch was isolated from kernels produced on siblings from one segregating population, and homozygous Wt, *sbe1a*, *sbe2a*, and *sbe1a sbe2a* starch was generated from siblings in a second segregating population. The genetic crosses and scheme are described in Chapter 2 in more detail (see 2.3). In this way, any differential maternal effect on seed development was eliminated as a variable in these experiments. Because an insufficient amount of *sbe2a ae* starch was generated, a study of *sbe2a* and *ae* mutant combinations (Wt, *sbe2a*, *ae*, and *sbe2a ae*) was impossible.

The objectives of this chapter were to characterize RS values and starch molecular structure of *sbe* mutant starches differing in SBE isoform activities. Comparisons were made respectively within two groups: among Wt, *sbe1a*, *ae*, and *sbe1a ae* starches, and among Wt, *sbe1a*, *sbe2a*, and *sbe1a sbe2a* starches. As starch structure of the *sbe1a* and *ae* combinations including chain length (CL) profiles of amylopectins and respective  $\beta$ -limit dextrins ( $\beta$ -LDs) has already been characterized (Yao et al. 2004; Li et al. 2007), the research described in this chapter will focus on molecular structure analysis of *sbe1a* and *sbe2a* mutant combinations.

## 4.2 Results

### 4.2.1 Resistant Starch Value

The experimental design for determination of RS values followed a hierarchical nested order as described in 3.2.1.1 (Fig. 3.1), and RS values of the three technical replications for each of the three biological replications were obtained (Table A.1 & A.2, Appendix A).

Nested ANOVA was performed on the RS values for three biological replications of homozygous Wt, *sbe1a*, *sbe2a*, and *sbe1a sbe2a* starch from the 2-gene segregating population. (The comparison of RS from Wt and *sbe1a* starch has been presented in 3.2.1.1.) For statistical analysis of the four genotypes together, F-tests showed that the effect of genotype was significant ( $p$ -value = 0.001). One-way ANOVA showed that the RS values were in the order  $sbe1a > sbe1a sbe2a > sbe2a \approx$  Wt (Table 4.2). The RS value of *sbe2a* (3.4%) was numerically higher than Wt (1.5%), but not significantly different. Two-way ANOVA of the effects of *sbe1a* and *sbe2a* on RS value showed that there was a significant main effect of *sbe1a* ( $p$ -value = 0.000), but not of *sbe2a* ( $p$ -value = 0.348), and that there was a significant interaction of *sbe1a* and *sbe2a* ( $p$ -value = 0.048).

For three biological replications of homozygous Wt, *sbe1a*, *ae*, and *sbe1a ae* starch from the 3-gene segregating population, Nested ANOVA was also performed on the RS values. F-tests showed that the effect of genotype was significant ( $p$ -value = 0.000). One-way ANOVA showed that the RS values were in the order  $sbe1a ae > ae > sbe1a >$  Wt (Table 4.3). The *ae* effect on the RS value is much stronger than the *sbe1a* effect, as indicated by a much higher RS value (74.7% versus 7.5%).

Table 4.2 Resistant starch values for starch from mutant combinations of *sbe1a* and *sbe2a* (Wt, *sbe1a*, *sbe2a*, and *sbe1a sbe2a*)<sup>1</sup>.

<b>Genotype</b>	<b>Resistant Starch Value (%)</b>
<b>Wt</b>	1.5 ± 0.5 <sup>a</sup>
<b><i>sbe1a</i></b>	13.2 ± 1.8 <sup>c</sup>
<b><i>sbe2a</i></b>	3.4 ± 1.2 <sup>a</sup>
<b><i>sbe1a sbe2a</i></b>	8.5 ± 4.3 <sup>b</sup>

<sup>1</sup>Values are percentages of starch that was not digested. Values are expressed as mean ± standard deviation for three biological replications from the 2-gene segregating population. Significant differences as determined by one-way ANOVA with Fisher's LSD multiple comparison procedure are indicated by different superscripts.

Table 4.3 Resistant starch values for starch from mutant combinations of *sbe1a* and *ae* (Wt, *sbe1a*, *ae*, and *sbe1a ae*)<sup>1</sup>.

<b>Genotype</b>	<b>Resistant Starch Value (%)</b>
<b>Wt</b>	2.0 ± 0.1 <sup>a</sup>
<b><i>sbe1a</i></b>	7.5 ± 2.3 <sup>b</sup>
<b><i>ae</i></b>	74.7 ± 0.6 <sup>c</sup>
<b><i>sbe1a ae</i></b>	77.7 ± 1.7 <sup>d</sup>

<sup>1</sup>Values are percentages of starch that was not digested. Values are expressed as mean ± standard deviation for three biological replications from the 3-gene segregating population. Significant differences as determined by one-way ANOVA with Fisher's LSD multiple comparison procedure are indicated by different superscripts.

Two-way ANOVA of the effects of *sbe1a* and *ae* on RS value showed that there were significant main effects of *sbe1a* ( $p$ -value = 0.001) and *ae* ( $p$ -value = 0.000), but there was no significant interaction of *sbe1a* and *ae* ( $p$ -value = 0.171).

## 4.2.2 Starch Molecular Structure

### 4.2.2.1 Starch Fractionation

Starch from Wt, *sbe1a*, *sbe2a*, and *sbe1a sbe2a* was fractionated into amylopectin, amylose, and intermediate material. For all the genotypes, the total recovery from the fractionation procedure was above 94%. Amylopectin accounted for the largest proportion recovered from the fractionation, followed by amylose and intermediate material (Table 4.4). The proportion for the three recovered starch fractions appeared similar among the four genotypes, except that *sbe2a* had a slightly higher proportion of amylose and a slightly lower proportion of intermediate material from the result of one fractionation (Table 4.4).

### 4.2.2.2 Iodine Binding Properties of Non-Granular Starch and Starch Fractions

The non-granular (NG) starting material and starch fractions from Wt, *sbe1a*, *sbe2a*, and *sbe1a sbe2a* had similar iodine binding properties (Fig. 4.1a,b), except that the intermediate material from *sbe2a* had a much lower iodine binding behavior than that from the other genotypes (Fig. 4.1b). The blue value and  $\lambda_{\max}$  for the NG starch and starch fractions are shown in Table 4.5. The  $\lambda_{\max}$  for the amylopectin from *sbe1a* was slightly higher than the others (Table 4.5). As is typically observed, the amylopectin from each starch had the weakest iodine binding behaviors (Table 4.5).

Table 4.4 Recovery of starch fractions (% w/w) by differential alcohol precipitation from Wt, *sbe1a*, *sbe2a*, and *sbe1a sbe2a* starch<sup>1</sup>.

<b>Starch</b>	<b>Total Recovery<sup>2</sup></b>	<b>Amylopectin<sup>3</sup></b>	<b>Amylose<sup>3</sup></b>	<b>Intermediate Material<sup>3</sup></b>
Wt	94.7	74.9	16.9	8.2
<i>sbe1a</i>	95.7	73.6	18.7	7.7
<i>sbe2a</i>	94.4	73.1	20.5	6.5
<i>sbe1a sbe2a</i>	94.6	73.4	17.5	9.1

<sup>1</sup>Values are from one fractionation of one biological replication from the 2-gene segregating population. Values for Wt and *sbe1a* were presented in Table 3.4 as well.

<sup>2</sup>Based on the sum of weights of recovered fractions divided by the starting weight of non-granular starch. Moisture content was assumed to be the same for all materials.

<sup>3</sup>Based on the weight of recovered fraction divided by the sum of the weights of the three recovered fractions.

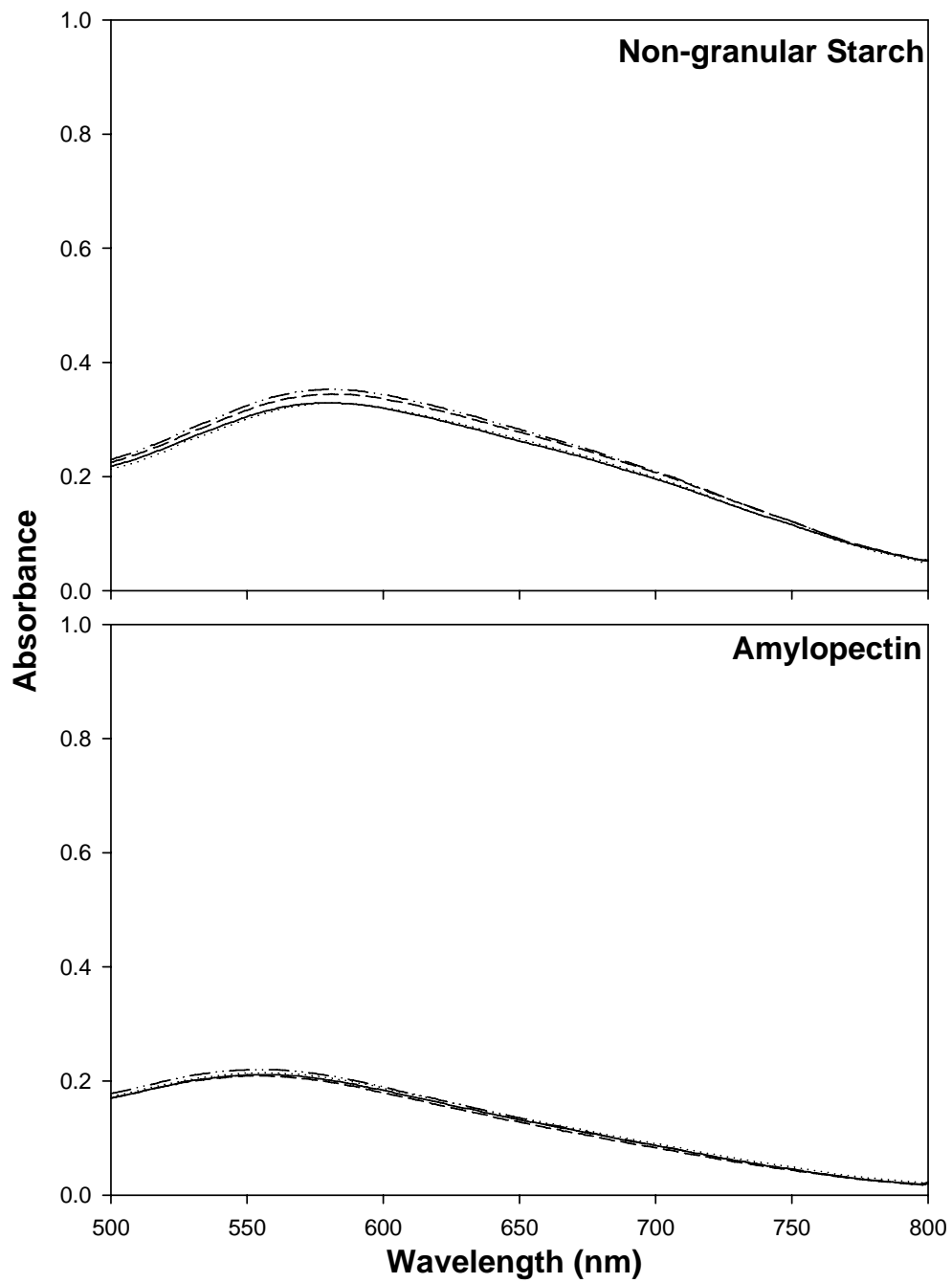


Figure 4.1a Iodine binding by non-granular starch and amylopectin fraction obtained by differential alcohol precipitation from Wt (—), *sbe1a* (·····), *sbe2a* (---), and *sbe1a sbe2a* (- · - ·) starch<sup>1</sup>.

<sup>1</sup>Starch from one biological replication from the 2-gene segregating population. See Table 4.5 for blue values and  $\lambda_{max}$ .

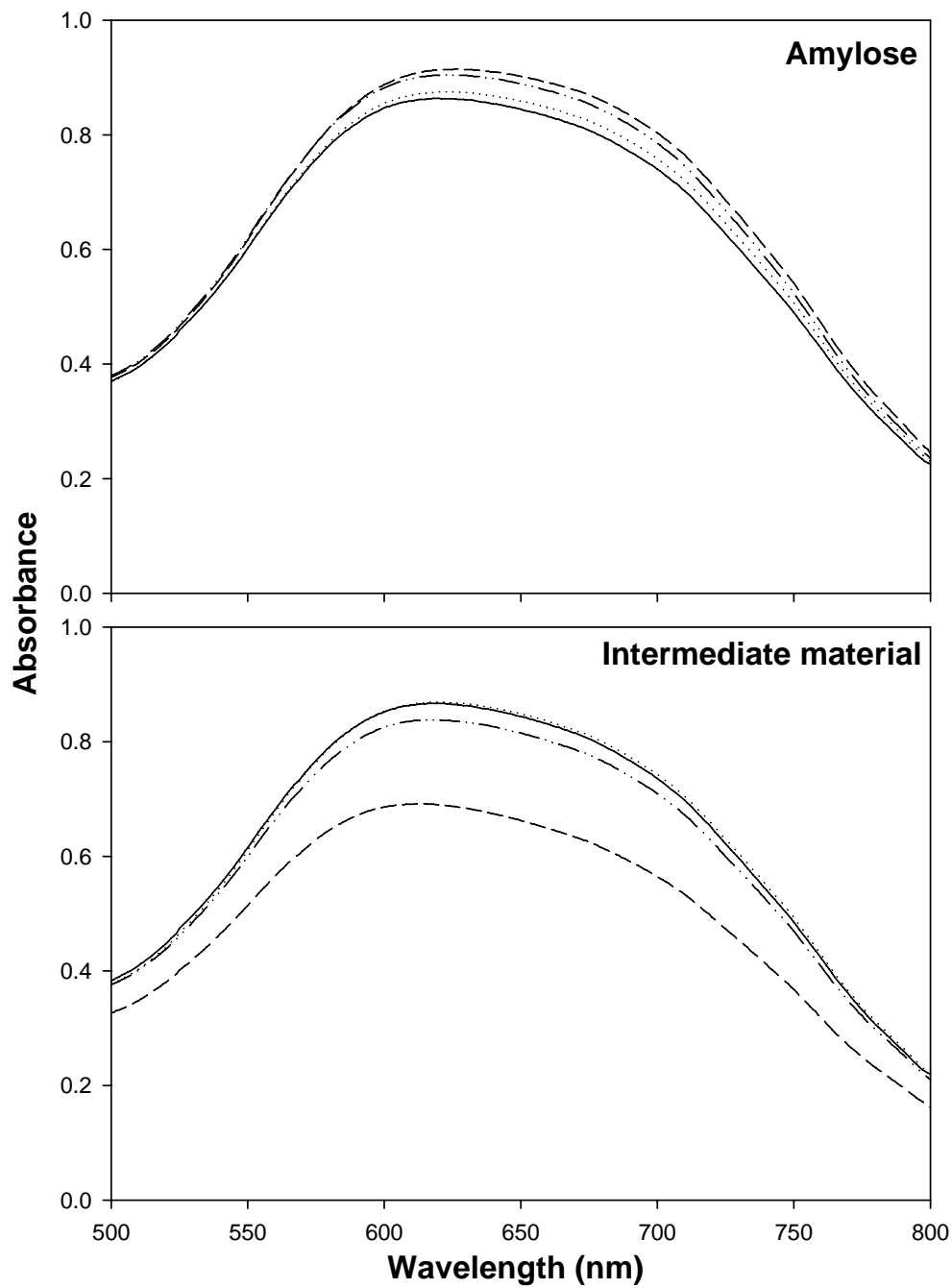


Figure 4.1b Iodine binding by amylose and intermediate material fractions obtained by differential alcohol precipitation from Wt (—), *sbe1a* (·····), *sbe2a* (---), and *sbe1a sbe2a* (- · - ·) starch<sup>1</sup>.

<sup>1</sup>Starch from one biological replication from the 2-gene segregating population. See Table 4.5 for blue values and  $\lambda_{max}$ .

Table 4.5 Iodine binding properties of non-granular starch and starch fractions recovered by differential alcohol precipitation from Wt, *sbe1a*, *sbe2a*, and *sbe1a sbe2a* starch<sup>1</sup>.

Starch Samples	Blue Value <sup>2</sup>	$\lambda_{\max}$ <sup>3</sup>
<b>Non-granular Starch</b>		
Wt	0.28 ± 0.01 <sup>a</sup>	580.8 ± 0.5 <sup>a</sup>
<i>sbe1a</i>	0.28 ± 0.01 <sup>a</sup>	581.3 ± 0.4 <sup>a</sup>
<i>sbe2a</i>	0.30 ± 0.02 <sup>a</sup>	581.0 ± 0.0 <sup>a</sup>
<i>sbe1a sbe2a</i>	0.30 ± 0.04 <sup>a</sup>	581.8 ± 0.3 <sup>a</sup>
<b>Amylopectin</b>		
Wt	0.15 ± 0.01 <sup>a</sup>	555.3 ± 0.7 <sup>a</sup>
<i>sbe1a</i>	0.15 ± 0.01 <sup>a</sup>	557.0 ± 0.1 <sup>b</sup>
<i>sbe2a</i>	0.14 ± 0.02 <sup>a</sup>	554.9 ± 0.8 <sup>a</sup>
<i>sbe1a sbe2a</i>	0.15 ± 0.01 <sup>a</sup>	554.3 ± 0.9 <sup>a</sup>
<b>Amylose</b>		
Wt	0.86 ± 0.01 <sup>a</sup>	618.5 ± 0.8 <sup>a</sup>
<i>sbe1a</i>	0.87 ± 0.01 <sup>a</sup>	623.8 ± 0.5 <sup>b</sup>
<i>sbe2a</i>	0.91 ± 0.00 <sup>b</sup>	626.8 ± 0.6 <sup>c</sup>
<i>sbe1a sbe2a</i>	0.90 ± 0.01 <sup>b</sup>	623.3 ± 0.4 <sup>b</sup>
<b>Intermediate Material</b>		
Wt	0.86 ± 0.01 <sup>b,c</sup>	618.5 ± 0.3 <sup>a</sup>
<i>sbe1a</i>	0.86 ± 0.00 <sup>c</sup>	619.5 ± 0.2 <sup>b</sup>
<i>sbe2a</i>	0.68 ± 0.01 <sup>a</sup>	612.0 ± 1.0 <sup>a,b</sup>
<i>sbe1a sbe2a</i>	0.83 ± 0.02 <sup>b</sup>	618.5 ± 0.1 <sup>a</sup>

<sup>1</sup>Values are mean ± standard deviation based on two independent analyses for one biological replication from the 2-gene segregating population. Values for Wt and *sbe1a* were presented in Table 3.5 as well. Significant differences within NG starch or starch fractions in the same column, as determined by one-way ANOVA with Fisher's LSD multiple comparison procedure, are indicated by different superscripts.

<sup>2</sup>Blue value is the absorbance of starch iodine mixture at 635 nm (Morrison and Laingelet 1983). See Fig. 4.1.

<sup>3</sup>Iodine binding wavelength maximum (Morrison and Laingelet 1983). See Fig. 4.1.

The NG starch from Wt, *sbe1a*, *ae*, and *sbe1a ae* had considerably different iodine binding behaviors (Fig. 4.2, Table 4.6). The NG starch from *sbe1a ae* and *ae* had much higher absorbance at all wavelengths, higher  $\lambda_{\max}$ , and higher blue value than that from Wt and *sbe1a*. The iodine binding properties of Wt and *sbe1a* were similar. *sbe1a ae* had a higher absorbance than *ae* at all wavelengths.

#### 4.2.2.3 Size Distribution of Intact Amylopectin and Amylose Fractions

In order to examine the size distribution of intact molecules from the amylopectin and amylose fractions, the samples were separated by Sepharose CL-2B chromatography. The total carbohydrate elution profile, representing the mass response, and iodine binding  $\lambda_{\max}$ , correlating to the CL, are shown in Fig. 4.3 for *sbe2a* and *sbe1a sbe2a* samples and in Fig. 3.5 for Wt and *sbe1a* samples. The chromatograms were similar among the four genotypes. The proportions of the region near the void volume preceding  $k' = 0.2$  and the region after  $k' = 0.2$  were calculated (Table 4.7), according to the methods in Klucinec and Thompson (1998).

For all genotypes, > 80% of the amylopectin eluted within the void volume region of the chromatogram, and had a  $\lambda_{\max}$  fluctuating around 550-560 nm (Table 4.7, Fig. 3.5a & 4.3a). Small differences were observed for the proportion of the amylopectin eluting after  $k'$  of 0.2 among the four genotypes (Table 4.7).

The amylose fractions from the four genotypes had similar size distribution (Table 4.7, Fig. 3.5b & 4.3b). Only a small proportion of the amylose eluted before  $k'$  of 0.1, with an iodine binding  $\lambda_{\max}$  of approximately 560 nm. The  $\lambda_{\max}$  of molecules eluting after  $k'$  of 0.1 increased rapidly, reaching a maximum of approximately 660 nm, and then decreased as the  $k'$  value approached 1.0. No difference was observed in the proportion of the regions below and above  $k'$  of 0.2 for the four genotypes.

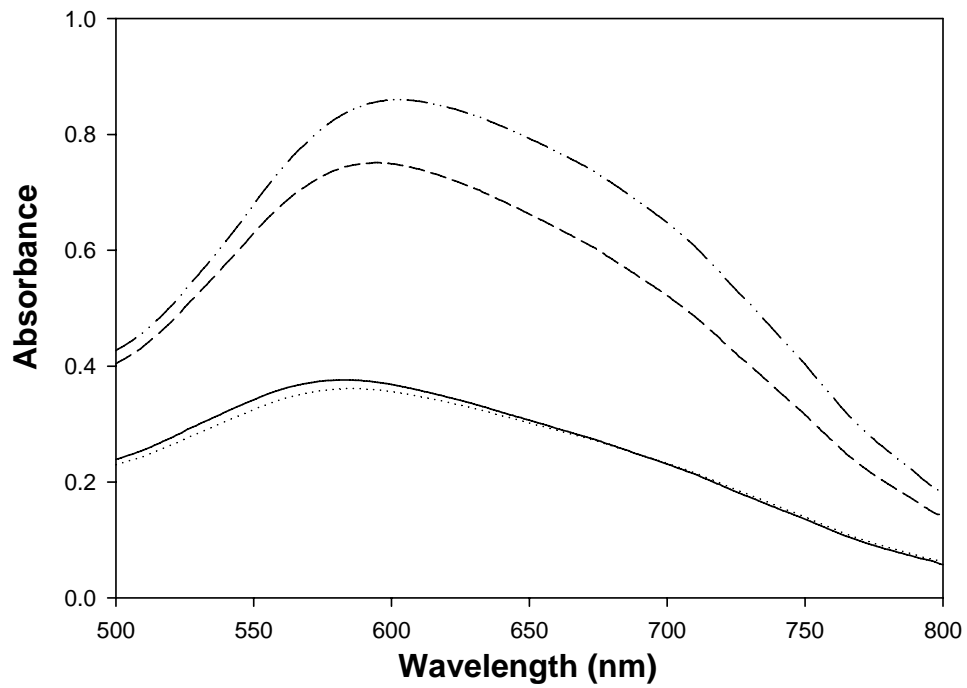


Figure 4.2 Iodine binding by non-granular starch from Wt (—), *sbe1a* (·····), *ae* (---), and *sbe1a ae* (- · - · -) starch<sup>1</sup>.

<sup>1</sup>Starch from one biological replication from the 3-gene segregating population. See Table 4.6 for blue values and  $\lambda_{max}$ .

Table 4.6 Iodine binding properties of non-granular starch from Wt, *sbe1a*, *ae*, and *sbe1a ae* starch<sup>1</sup>.

<b>Non-granular Starch</b>	<b>Blue Value<sup>2</sup></b>	<b><math>\lambda_{\max}</math> (nm)<sup>3</sup></b>
<b>Wt</b>	0.33 ± 0.01 <sup>a</sup>	580.5 ± 0.7 <sup>a</sup>
<b><i>sbe1a</i></b>	0.32 ± 0.01 <sup>a</sup>	582.3 ± 1.1 <sup>a</sup>
<b><i>ae</i></b>	0.70 ± 0.02 <sup>b</sup>	593.5 ± 0.0 <sup>b</sup>
<b><i>sbe1a ae</i></b>	0.82 ± 0.04 <sup>c</sup>	600.0 ± 0.7 <sup>c</sup>

<sup>1</sup>Values are mean ± standard deviation based on two independent analyses for one biological replication from the 3-gene segregating population. Significant differences in the same column, as determined by one-way ANOVA with Fisher's LSD multiple comparison procedure, are indicated by different superscripts.

<sup>2</sup>Blue value is the absorbance of starch iodine mixture at 635 nm (Morrison and Laingelet 1983). See Fig. 4.2.

<sup>3</sup>Iodine binding wavelength maximum (Morrison and Laingelet 1983). See Fig. 4.2.

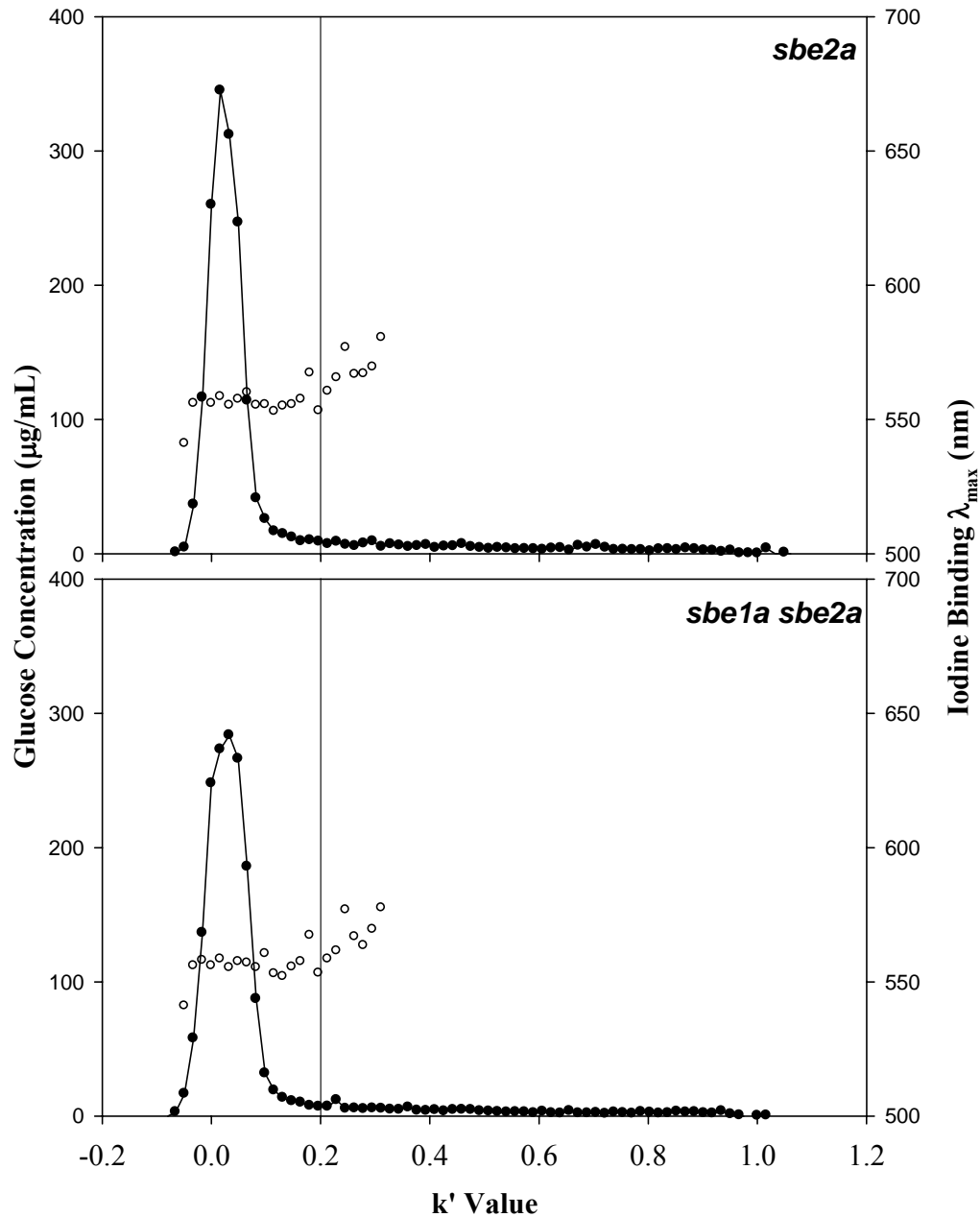


Figure 4.3a Size-exclusion chromatograms of amylopectin fraction from *sbe2a* and *sbe1a sbe2a* starch<sup>1</sup>. Lines with filled dots refer to glucose concentration determined by sulfuric acid and phenol assay (Dubois et al. 1956) (uncorrected for 10% increase from hydrolyzed glucose); unfilled dots refer to iodine binding  $\lambda_{\max}$ .

<sup>1</sup>Starch from one biological replication from the 2-gene segregating population. See Fig. 3.5a for chromatograms for *Wt* and *sbe1a* starch.

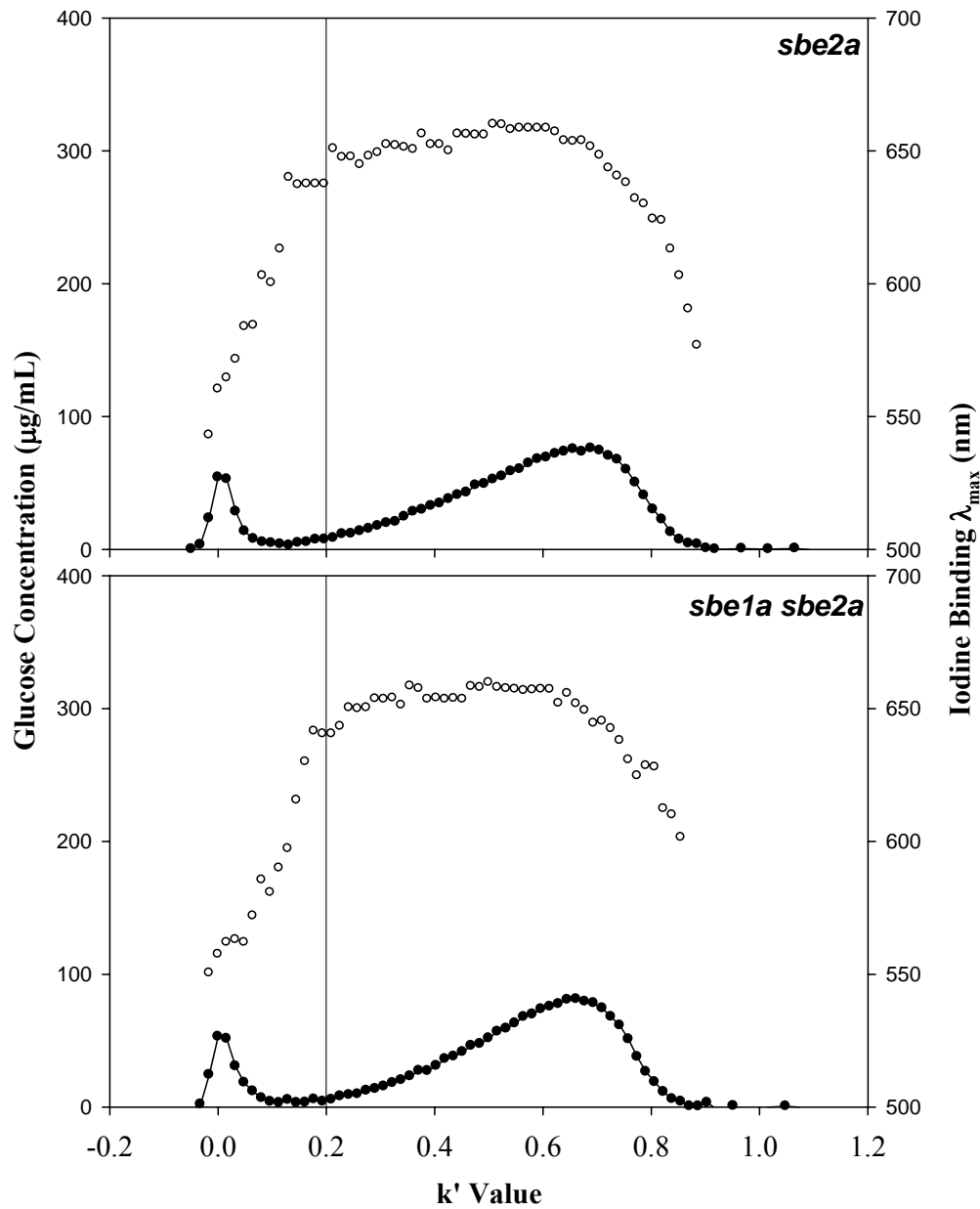


Figure 4.3b Size-exclusion chromatograms of amylose fraction from *sbe2a* and *sbe1a sbe2a* starch<sup>1</sup>. Line with filled dots refers to glucose concentration determined by sulfuric acid and phenol assay (Dubois et al. 1956) (uncorrected for 10% increase from hydrolyzed glucose); unfilled dots refer to iodine binding  $\lambda_{\max}$ .

<sup>1</sup>Starch from one biological sample from 2-gene segregating population. See Fig. 3.5b for chromatograms for *Wt* and *sbe1a* starch.

Table 4.7 Partial chromatogram areas of amylopectin and amylose fractions from size-exclusion chromatography for Wt, *sbe1a*, *sbe2a*, and *sbe1a sbe2a* starch<sup>1</sup>.

Starch Sample	Starch Eluting (%)	
	Below $k' = 0.2$	Above $k' = 0.2$
<b>Wt</b>		
Amylopectin	83	17
Amylose	12	88
<b><i>sbe1a</i></b>		
Amylopectin	88	12
Amylose	11	89
<b><i>sbe2a</i></b>		
Amylopectin	88	12
Amylose	11	89
<b><i>sbe1a sbe2a</i></b>		
Amylopectin	91	9
Amylose	12	88

<sup>1</sup>Values are based on analysis for one biological sample from the 2-gene segregating population. Values for Wt and *sbe1a* were presented in Table 3.6 as well. See Fig. 3.6 & 4.3 for chromatograms.

#### 4.2.2.4 Chain Length Distribution of Debranched Non-Granular Starch and Starch Fractions

The division of chromatograms and the calculation of each region (Fig. 4.4a,b) were as described in 3.2.2.4, according to Klucinec and Thompson (1998). By visual inspection, CL distribution of debranched NG starch and three starch fractions for Wt, *sbe1a*, *sbe2a*, and *sbe1a sbe2a* starch appeared similar (Fig. 4.4a,b), except that the intermediate material from *sbe2a* had a lower proportion in the region I (Fig. 4.4b), which is likely originated from amylose (Batey and Curtin 1996). Proportions of chromatographic regions of NG starch and three starch fractions are shown in Table 4.8. Only small differences were observed in these proportions among the four genotypes, other than that the intermediate material from *sbe2a* had a lower proportion of region I as compared to the other three genotypes (Table 4.8b).

The CL distribution of the debranched NG starch for Wt, *sbe1a*, *ae*, and *sbe1a ae* starch is shown in Fig. 4.5. No differences were observed between Wt and *sbe1a*. Substantial differences were observed by comparing the Wt and *sbe1a* starch to the *ae* or to *sbe1a ae* starch. Both the *ae* and *sbe1a ae* starch had higher proportions of region I and II and a lower proportion of region III than that from Wt and *sbe1a* starch (Fig. 4.5, Table 4.9). *sbe1a ae* starch had a higher proportion of region I and lower proportions of region II and III than *ae* (Fig. 4.5, Table 4.9).

#### 4.2.2.5 Chain Length Distribution of Debranched Resistant Starch

The chromatograms of debranched RS samples were divided into three regions (Figs. 4.6 & 4.7), as described in 3.2.2.4. The calculated proportions of each region are shown in Table 4.9 & 4.10.

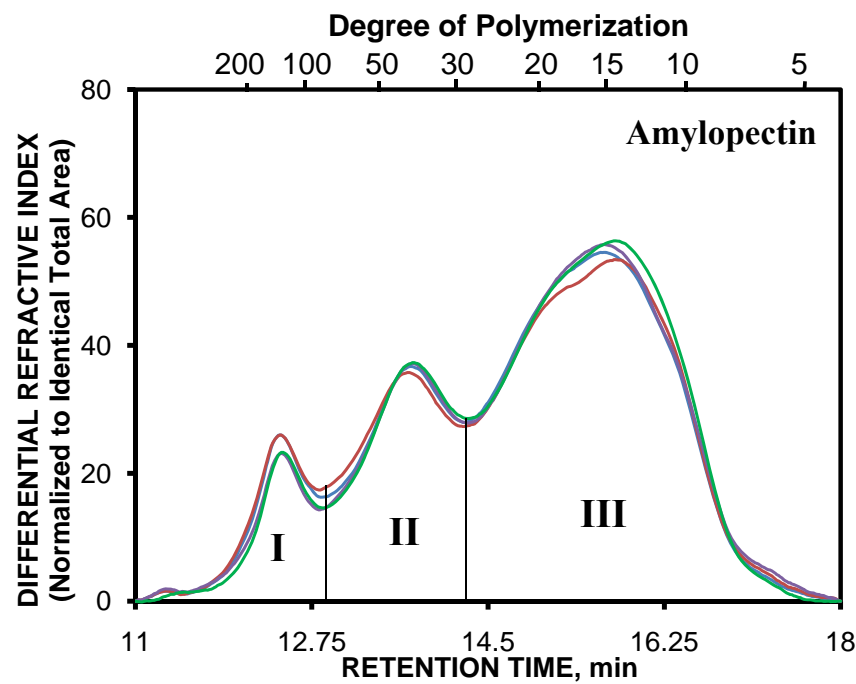
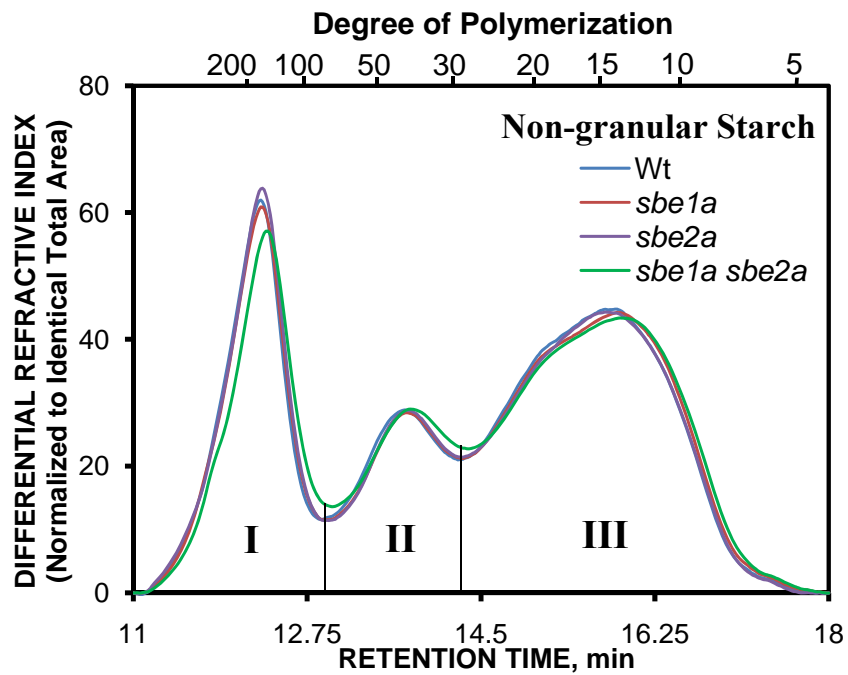


Figure 4.4a Chromatograms of isoamylase-debranched non-granular starch and amylopectin fractions from Wt, *sbe1a*, *sbe2a*, and *sbe1a sbe2a* starch<sup>1</sup>.

<sup>1</sup>Representative chromatograms for starch from one biological replication from the 2-gene segregating population. Proportions of region I, II, and III are presented in Table 4.8a. The chromatograms for Wt and *sbe1a* are also shown in Fig. 3.6a.

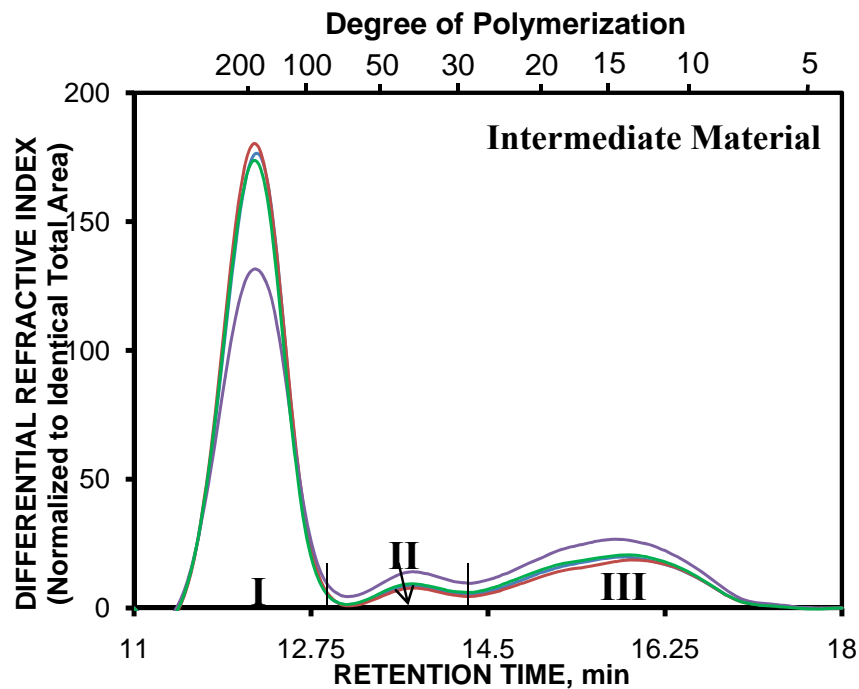
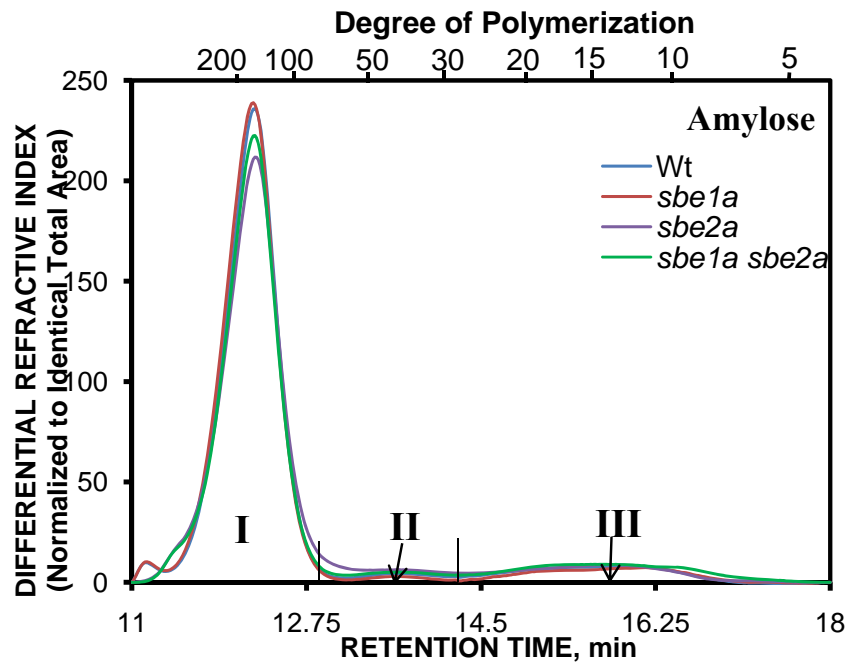


Figure 4.4b Chromatograms of isoamylase-debranched amylose and intermediate material fractions from Wt, *sbe1a*, *sbe2a*, and *sbe1a sbe2a* starch<sup>1</sup>.

<sup>1</sup>Representative chromatograms for starch from one biological replication from the 2-gene segregating population. Proportions of region I, II, and III are presented in Table 4.8b. The chromatograms for Wt and *sbe1a* are also shown in Fig. 3.6b.

Table 4.8a Chain length distribution of isoamylase-debranched non-granular starch and amylopectin fraction from Wt, *sbe1a*, *sbe2a*, and *sbe1a sbe2a* starch<sup>1</sup>.

Sample	Chromatographic Region <sup>2</sup>		
	I	II	III
<b>Non-granular Starch</b>			
<b>Wt</b>			
Weight %	27.4 ± 0.2 <sup>b</sup>	18.5 ± 0.5	54.1 ± 0.3
Adj Weight % <sup>3</sup>		25.5 ± 0.7 <sup>a</sup>	74.5 ± 0.7 <sup>a</sup>
<b><i>sbe1a</i></b>			
Weight %	27.9 ± 0.5 <sup>b</sup>	17.8 ± 0.1	54.3 ± 0.6
Adj Weight % <sup>3</sup>		24.6 ± 0.4 <sup>a</sup>	75.4 ± 0.4 <sup>a</sup>
<b><i>sbe2a</i></b>			
Weight %	28.4 ± 0.2 <sup>b</sup>	18.0 ± 0.3	53.6 ± 0.1
Adj Weight % <sup>3</sup>		25.1 ± 0.3 <sup>a</sup>	74.9 ± 0.3 <sup>a</sup>
<b><i>sbe1a sbe2a</i></b>			
Weight %	26.5 ± 0.5 <sup>a</sup>	18.8 ± 0.2	54.7 ± 0.7
Adj Weight % <sup>3</sup>		25.5 ± 0.4 <sup>a</sup>	74.5 ± 0.4 <sup>a</sup>
<b>Amylopectin</b>			
<b>Wt</b>			
Weight %	9.7 ± 1.3 <sup>a,b</sup>	23.3 ± 0.5	67.0 ± 1.8
Adj Weight % <sup>3</sup>		25.8 ± 1.0 <sup>a</sup>	74.2 ± 1.0 <sup>a</sup>
<b><i>sbe1a</i></b>			
Weight %	10.8 ± 0.2 <sup>b</sup>	23.3 ± 0.8	65.9 ± 1.0
Adj Weight % <sup>3</sup>		26.1 ± 1.0 <sup>a</sup>	73.9 ± 1.0 <sup>a</sup>
<b><i>sbe2a</i></b>			
Weight %	8.9 ± 0.8 <sup>a</sup>	23.0 ± 0.7	68.1 ± 1.5
Adj Weight % <sup>3</sup>		25.2 ± 1.0 <sup>a</sup>	74.8 ± 1.0 <sup>a</sup>
<b><i>sbe1a sbe2a</i></b>			
Weight %	9.1 ± 0.2 <sup>a</sup>	23.5 ± 0.0	67.4 ± 0.2
Adj Weight % <sup>3</sup>		25.9 ± 0.1 <sup>a</sup>	74.1 ± 0.1 <sup>a</sup>

<sup>1</sup>Values are mean ± standard deviation based on two independent analyses for one biological replication from the 2-gene segregating population. See Fig 4.4a. The values for Wt and *sbe1a* are also shown in Table 3.7 & 3.8. Significant differences within each category in the same column, as determined by one-way ANOVA with Fisher's LSD multiple comparison procedure, are indicated by different superscripts.

<sup>2</sup>Regions were divided based on the minima observed for debranched amylopectin from wild-type starch, as in Klucinec and Thompson (1998).

<sup>3</sup>Adjusted weight percentage does not include the area from region I of the chromatogram.

Table 4.8b Chain length distribution of isoamylase-debranched amylose and intermediate material fractions from Wt, *sbe1a*, *sbe2a*, and *sbe1a sbe2a* starch<sup>1</sup>.

Sample	Chromatographic Region <sup>2</sup>		
	I	II	III
<b>Amylose</b>			
<b>Wt</b>			
Weight %	86.9 ± 1.8 <sup>a,b</sup>	3.6 ± 1.0	9.4 ± 0.8
Adj Weight % <sup>3</sup>		27.5 ± 4.1 <sup>a</sup>	72.5 ± 4.1 <sup>b</sup>
<b><i>sbe1a</i></b>			
Weight %	89.8 ± 1.1 <sup>b</sup>	2.3 ± 0.7	8.0 ± 0.4
Adj Weight % <sup>3</sup>		21.8 ± 4.2 <sup>a</sup>	78.2 ± 4.2 <sup>b</sup>
<b><i>sbe2a</i></b>			
Weight %	86.2 ± 2.3 <sup>a</sup>	4.8 ± 0.9	8.9 ± 1.3
Adj Weight % <sup>3</sup>		35.0 ± 1.1 <sup>b</sup>	65.0 ± 1.1 <sup>a</sup>
<b><i>sbe1a sbe2a</i></b>			
Weight %	84.7 ± 1.4 <sup>a</sup>	4.7 ± 0.8	10.6 ± 2.2
Adj Weight % <sup>3</sup>		30.8 ± 8.1 <sup>a,b</sup>	69.2 ± 8.1 <sup>a,b</sup>
<b>Intermediate Material</b>			
<b>Wt</b>			
Weight %	72.6 ± 1.5 <sup>b,c</sup>	6.3 ± 2.6	21.1 ± 1.1
Adj Weight % <sup>3</sup>		22.8 ± 8.1 <sup>a</sup>	77.2 ± 8.1 <sup>a</sup>
<b><i>sbe1a</i></b>			
Weight %	74.6 ± 1.4 <sup>c</sup>	5.9 ± 2.7	19.5 ± 1.3
Adj Weight % <sup>3</sup>		23.0 ± 9.3 <sup>a</sup>	77.0 ± 9.3 <sup>a</sup>
<b><i>sbe2a</i></b>			
Weight %	60.9 ± 0.4 <sup>a</sup>	9.9 ± 2.4	29.2 ± 2.0
Adj Weight % <sup>3</sup>		25.3 ± 5.8 <sup>a</sup>	74.7 ± 5.8 <sup>a</sup>
<b><i>sbe1a sbe2a</i></b>			
Weight %	70.1 ± 2.6 <sup>b</sup>	7.2 ± 3.2	22.7 ± 0.6
Adj Weight % <sup>3</sup>		23.8 ± 8.6 <sup>a</sup>	76.2 ± 8.6 <sup>a</sup>

<sup>1</sup>Values are mean ± standard deviation based on two independent analyses for one biological sample from the 2-gene segregating population. See Fig 4.4b. The values for Wt and *sbe1a* are also shown in Table 3.7. Significant differences within each category in the same column, as determined by one-way ANOVA with Fisher's LSD multiple comparison procedure, are indicated by different superscripts.

<sup>2</sup>Regions were divided based on the minima observed for debranched amylopectin from wild-type starch, as in Klucinec and Thompson (1998).

<sup>3</sup>Adjusted weight percentage does not include the area from region I of the chromatogram.

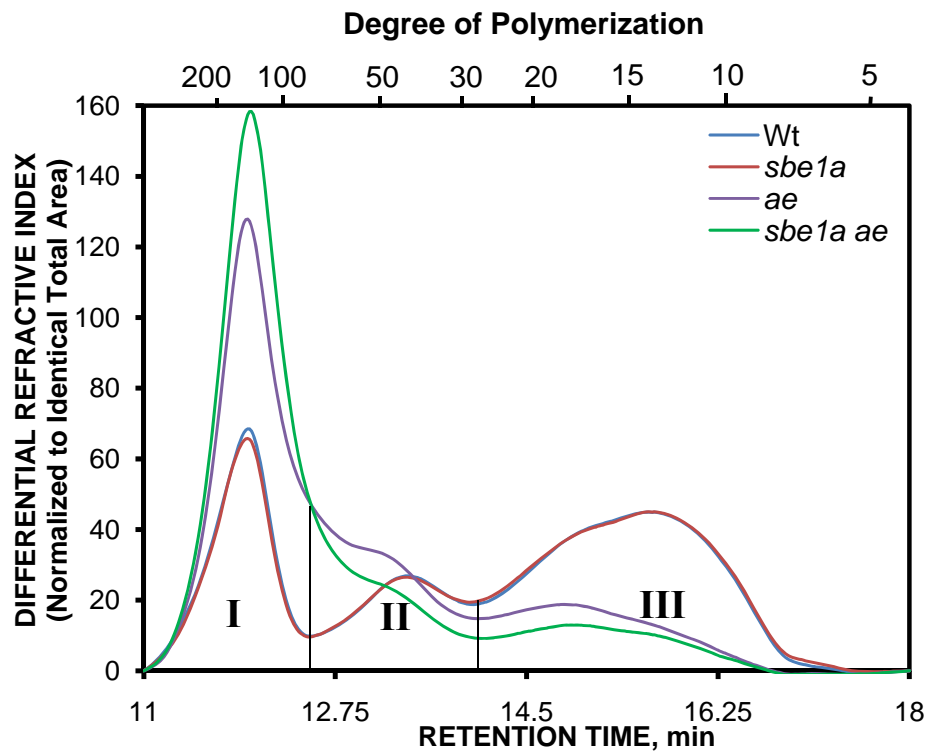


Figure 4.5 Chromatograms of isoamylase-debranched non-granular starch from Wt, *sbe1a*, *ae*, and *sbe1a ae* starch<sup>1</sup>.

<sup>1</sup>Representative chromatograms for starch from one biological replication from the 3-gene segregating population. Proportions of region I, II, and III are presented in Table 4.9.

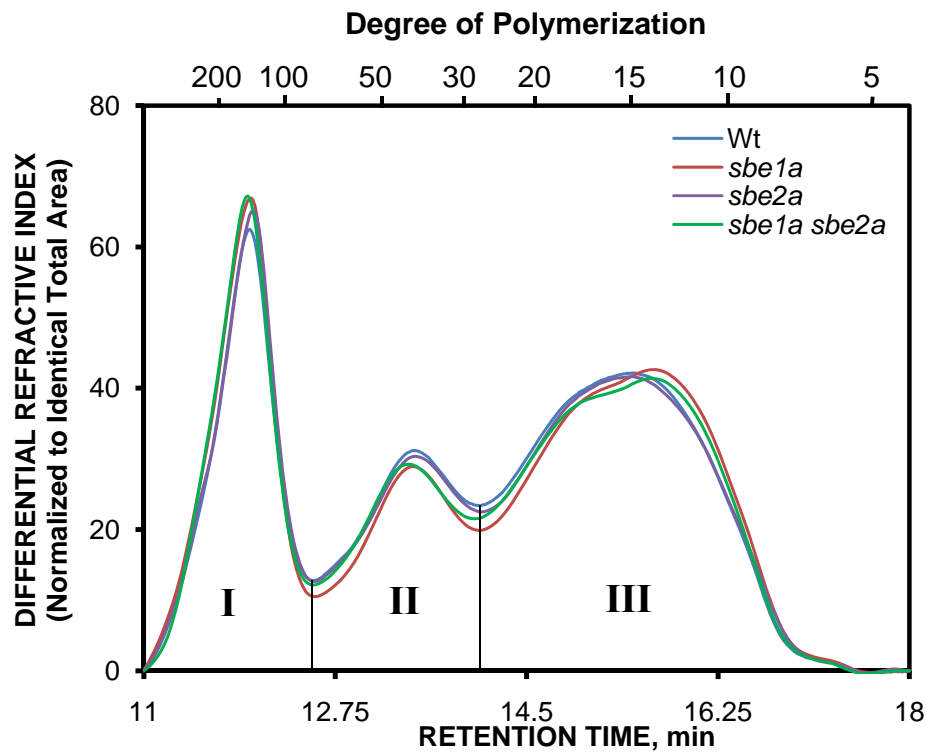


Figure 4.6 Chromatograms of isoamylase-debranched resistant starch from Wt, *sbe1a*, *sbe2a*, and *sbe1a sbe2a* starch<sup>1</sup>.

<sup>1</sup>Representative chromatograms for starch from one biological replication from the 2-gene segregating population. Proportions of region I, II, and III are presented in Table 4.9. The chromatograms for Wt and *sbe1a* are also shown in Fig. 3.7.

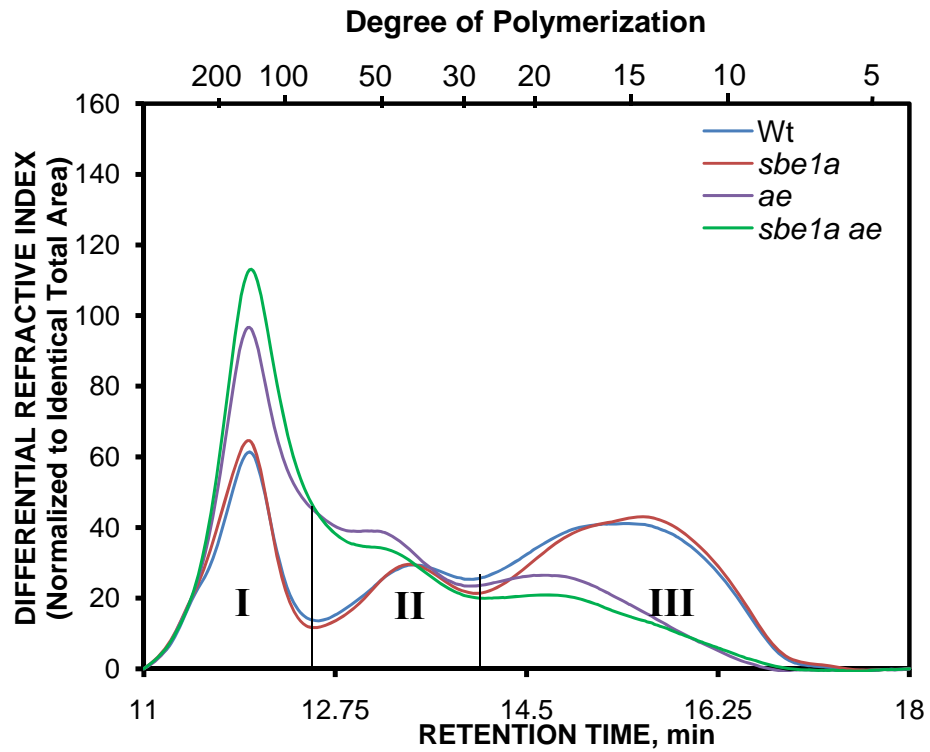


Figure 4.7 Chromatograms of isoamylase-debranched resistant starch from Wt, *sbe1a*, *ae*, and *sbe1a ae* starch<sup>1</sup>.

<sup>1</sup>Representative chromatograms for starch from one biological replication from the 3-gene segregating population. Proportions of region I, II, and III are presented in Table 4.10.

Table 4.9 Chain length distribution of isoamylase-debranched native starch and resistant starch from Wt, *sbe1a*, *sbe2a*, and *sbe1a sbe2a* starch<sup>1</sup>.

Sample	Chromatographic Region <sup>2</sup>		
	I	II	III
<b>Native Starch<sup>3</sup></b>			
Wt	27.4 ± 0.2 <sup>b</sup>	18.5 ± 0.5 <sup>b,c</sup>	54.1 ± 0.3 <sup>c</sup>
<i>sbe1a</i>	27.9 ± 0.5 <sup>b,c</sup>	17.8 ± 0.1 <sup>a</sup>	54.3 ± 0.6 <sup>b,c</sup>
<i>sbe2a</i>	28.4 ± 0.2 <sup>c</sup>	18.0 ± 0.3 <sup>a,b</sup>	53.6 ± 0.1 <sup>b</sup>
<i>sbe1a sbe2a</i>	26.5 ± 0.5 <sup>a</sup>	18.8 ± 0.2 <sup>b,c</sup>	54.7 ± 0.7 <sup>c</sup>
<b>Resistant Starch</b>			
Wt	26.4 ± 0.5 <sup>a</sup>	21.3 ± 0.1 <sup>f</sup>	52.3 ± 0.5 <sup>a</sup>
<i>sbe1a</i>	28.2 ± 0.3 <sup>c</sup>	19.2 ± 0.4 <sup>c</sup>	52.6 ± 0.7 <sup>a</sup>
<i>sbe2a</i>	27.2 ± 0.4 <sup>a,b</sup>	20.9 ± 0.2 <sup>e</sup>	51.8 ± 0.7 <sup>a</sup>
<i>sbe1a sbe2a</i>	27.5 ± 0.1 <sup>b</sup>	20.2 ± 0.2 <sup>d</sup>	52.3 ± 0.1 <sup>a</sup>

<sup>1</sup>Values are percentage by weight. Values are mean ± standard deviation based on two independent analyses for one biological replication from the 2-gene segregating population. See Fig 4.4a & 4.6. The values for Wt and *sbe1a* are also shown in Table 3.8. Significant differences in the same column, as determined by one-way ANOVA with Fisher's LSD multiple comparison procedure, are indicated by different superscripts.

<sup>2</sup>Regions were divided based on the minima observed for debranched amylopectin from wild-type starch, as in Klucinec and Thompson (1998).

<sup>3</sup>Values are these for non-granular starch in Table 4.8a.

Table 4.10 Chain length distribution of isoamylase-debranched native starch and resistant starch from Wt, *sbela*, *ae*, and *sbela ae* starch<sup>1</sup>.

Sample	Chromatographic Region <sup>2</sup>		
	I	II	III
<b>Native Starch<sup>3</sup></b>			
Wt	28.3 ± 1.0 <sup>a</sup>	18.0 ± 0.1 <sup>a</sup>	53.7 ± 1.0 <sup>d</sup>
<i>sbela</i>	27.3 ± 1.1 <sup>a</sup>	18.5 ± 0.7 <sup>a</sup>	54.2 ± 1.8 <sup>d</sup>
<i>ae</i>	53.7 ± 1.2 <sup>d</sup>	25.2 ± 0.9 <sup>d</sup>	21.1 ± 2.2 <sup>b</sup>
<i>sbela ae</i>	64.3 ± 3.3 <sup>e</sup>	19.8 ± 0.0 <sup>b</sup>	15.9 ± 3.3 <sup>a</sup>
<b>Resistant Starch</b>			
Wt	26.9 ± 1.1 <sup>a</sup>	22.0 ± 1.1 <sup>c</sup>	51.1 ± 2.2 <sup>d</sup>
<i>sbela</i>	27.8 ± 0.9 <sup>a</sup>	19.7 ± 0.4 <sup>b</sup>	52.5 ± 0.5 <sup>d</sup>
<i>ae</i>	44.0 ± 0.4 <sup>b</sup>	30.0 ± 0.8 <sup>f</sup>	26.0 ± 0.3 <sup>c</sup>
<i>sbela ae</i>	50.5 ± 0.6 <sup>c</sup>	27.4 ± 0.7 <sup>e</sup>	22.0 ± 0.1 <sup>b</sup>

<sup>1</sup>Values are percentage by weight. Values are mean ± standard deviation based on two independent analyses for one biological replication from the 3-gene segregating population. See Fig 4.5 & 4.7. Significant differences in the same column, as determined by one-way ANOVA with Fisher's LSD multiple comparison procedure, are indicated by different superscripts.

<sup>2</sup>Regions were divided based on the minima observed for debranched amylopectin from wild-type starch, as in Klucinec and Thompson (1998).

<sup>3</sup>Values are these for non-granular starch in Fig. 4.5.

Comparison among the RS from Wt, *sbe1a*, *sbe2a*, and *sbe1a sbe2a* showed that CL distribution of the RS from the four genotypes was similar (Fig. 4.6).

Although the CL distribution in region III for *sbe1a* and *sbe1a sbe2a* seemed to be shifted towards a smaller DP than that for Wt and *sbe2a* (Fig. 4.6), the calculated proportion of region III was indistinguishable among the four genotypes (Table 4.9).

Comparison of CL distribution of the RS to the respective native starch from Wt, *sbe1a*, *sbe2a*, and *sbe1a sbe2a* is shown in Table 4.9. For the RS from each genotype, the proportion of region II was higher, and the proportion of region III was lower. The proportion of region I was lower for the RS from Wt and *sbe2a*, but not for the RS from *sbe1a*. The proportion of region I was higher for the RS from *sbe1a sbe2a*.

In contrast to the comparison among the RS from Wt, *sbe1a*, *sbe2a*, and *sbe1a sbe2a*, comparison among the RS from Wt, *sbe1a*, *ae*, and *sbe1a ae* showed a large difference in the CL distribution of the RS from the four genotypes (Fig. 4.7, Table 4.10). A large difference was also observed between *ae*-type starch (*ae* and *sbe1a ae*) and non-*ae*-type starch (Wt and *sbe1a*). A smaller difference was observed between *ae* and *sbe1a ae*, and between Wt and *sbe1a*.

Comparison of CL distribution of RS to respective native starch from Wt, *sbe1a*, *ae*, and *sbe1a ae* is shown in Table 4.10. The proportion of region II was higher for the RS from each genotype. The proportion of region I was lower and the proportion of region III was higher for the RS from *ae* and *sbe1a ae*, but not for the RS from Wt and *sbe1a*.

#### 4.2.2.6 Isoamylase-Debranched and Isoamylase-plus-Pullulanase-Debranched $\beta$ -Limit Dextrins from the Amylopectin Fraction of *sbe1a* and *sbe2a* Mutant Combinations

The CL distributions of the debranched  $\beta$ -LDs from the amylopectin fraction for Wt, *sbe1a*, *sbe2a*, and *sbe1a sbe2a* starch are shown in Fig. 3.10 & 4.8. The chromatographic regions were divided according to Xia and Thompson (2006), and the proportions of chains in each region were calculated (Table 4.11). The most important difference was observed in the proportion of DP 4 chains from the debranched  $\beta$ -LDs, which was in the order *sbe1a* > *sbe1a sbe2a* > Wt  $\approx$  *sbe2a* (Table 4.11). For each genotype, the subsequent pullulanase debranching on the isoamylase-debranched  $\beta$ -LDs led to an increase in the DP 2 area (Fig. 3.10 & 4.8). The increase in DP 2 stubs was in the order Wt  $\approx$  *sbe2a* > *sbe1a sbe2a* > *sbe1a* (Table 4.11).

After subsequent pullulanase debranching, the proportion of chains of DP 5-7 had a small increase for the Wt, *sbe2a*, and *sbe1a sbe2a* samples, but stayed unchanged for the *sbe1a* sample (Table 4.11). Among the four genotypes, there was no significant difference in the proportions of chains of DP  $\geq$  18, DP 8-17, and DP 3, before and after pullulanase addition (Table 4.11). The ratio of B<sub>S</sub>:B<sub>L</sub> was not different among the four genotypes as well (Table 4.11).

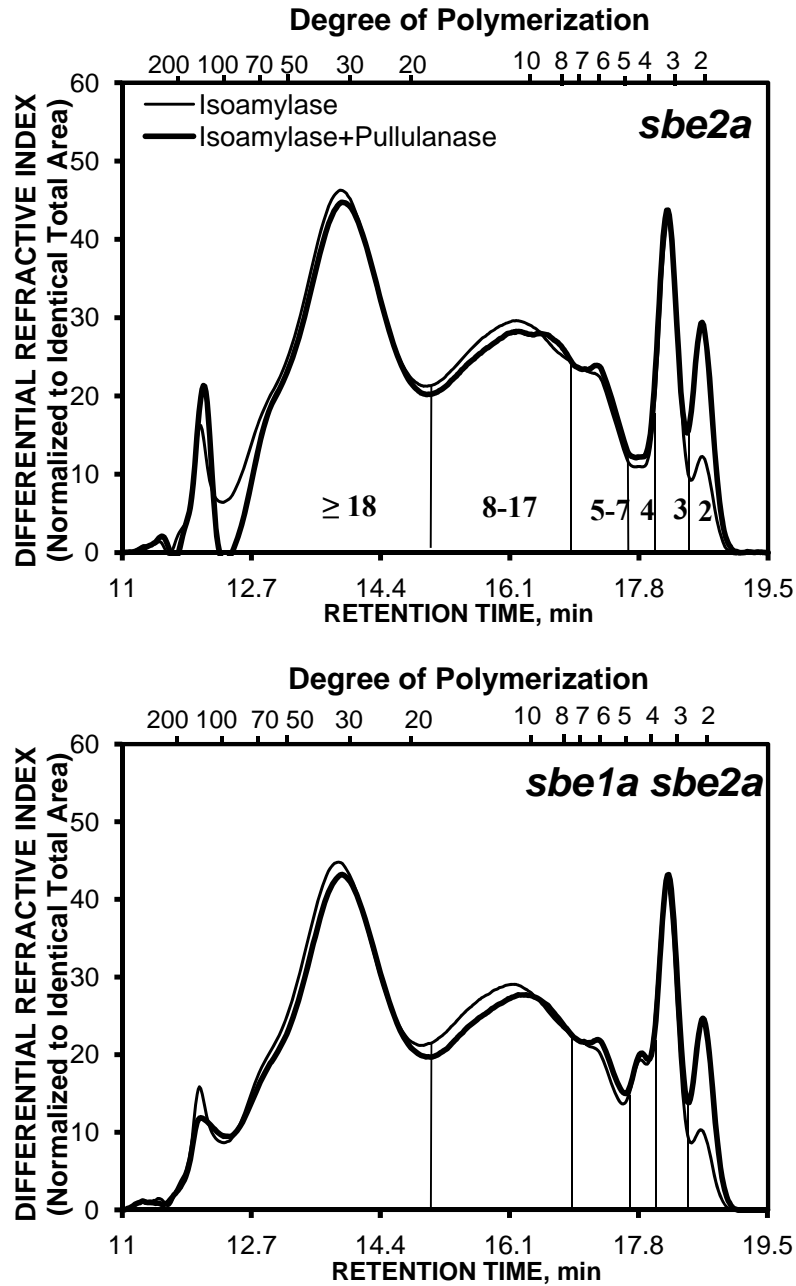


Figure 4.8 Chromatograms<sup>1</sup> of isoamylase-debranched and isoamylase-plus-pullulanase-debranched  $\beta$ -limit dextrans<sup>2</sup> from amylopectin fraction from *sbe2a* and *sbe1a sbe2a* starch<sup>3</sup>. Numbers indicate degree of polymerization.

<sup>1</sup>Chromatographic regions were divided as in Xia and Thompson (2006). Proportions of chains in each region are presented in Table 4.11.

<sup>2</sup> $\beta$ -limit dextrin was obtained after 3 times of 24-hr  $\beta$ -amylolysis on amylopectin.

<sup>3</sup>Representative chromatograms for starch from one biological replication from the 2-gene segregating population. See Fig. 3.10 for chromatograms for *Wt* and *sbe1a* starch.

Table 4.11 Chain length distribution of isoamylase-debranched and isoamylase-plus-pullulanase-debranched  $\beta$ -limit dextrins from the amylopectin fraction from Wt, *sbe1a*, *sbe2a*, and *sbe1a sbe2a* starch<sup>1</sup>.

<b>β-Limit Dextrin from Amylopectin<sup>3</sup></b>	<b>Chromatographic Region<sup>2</sup></b>						
	<b>B<sub>L</sub> Chains</b>	<b>B<sub>S</sub> Chains</b>		<b>Bs or A chains</b>	<b>A chains</b>		<b>B<sub>S</sub>:B<sub>L</sub></b>
	<b>DP ≥ 18</b>	<b>DP 8-17</b>	<b>DP 5-7</b>	<b>DP 4</b>	<b>DP 3</b>	<b>DP 2</b>	
<b>Wt</b>							
Isoamylase	44.5 ± 7.2 <sup>a</sup>	34.2 ± 7.3 <sup>a</sup>	8.9 ± 0.3 <sup>b</sup>	2.5 ± 0.3 <sup>a</sup>	6.9 ± 0.3 <sup>a</sup>	3.1 ± 0.3 <sup>c,d</sup>	1.0 ± 0.3 <sup>a</sup>
Isoamylase, then pullulanase	42.0 ± 6.6 <sup>a</sup>	32.3 ± 6.6 <sup>a</sup>	9.5 ± 0.2 <sup>c</sup>	2.7 ± 0.3 <sup>a</sup>	7.2 ± 0.4 <sup>a</sup>	6.4 ± 0.4 <sup>f</sup>	1.0 ± 0.3 <sup>a</sup>
Increase by Pullulanase	-	-	0.6 ± 0.5 <sup>a</sup>	-	-	3.3 ± 0.1 <sup>d</sup>	-
<b><i>sbe1a</i></b>							
Isoamylase	44.0 ± 5.9 <sup>a</sup>	31.6 ± 6.4 <sup>a</sup>	9.5 ± 0.3 <sup>c</sup>	6.1 ± 0.6 <sup>c</sup>	6.8 ± 0.6 <sup>a</sup>	2.1 ± 0.3 <sup>b</sup>	1.0 ± 0.3 <sup>a</sup>
Isoamylase, then pullulanase	43.7 ± 5.1 <sup>a</sup>	30.6 ± 6.0 <sup>a</sup>	9.6 ± 0.4 <sup>c</sup>	6.1 ± 0.5 <sup>c</sup>	6.8 ± 0.7 <sup>a</sup>	3.2 ± 0.0 <sup>d</sup>	0.9 ± 0.3 <sup>a</sup>
Increase by Pullulanase	-	-	-	-	-	1.1 ± 0.3 <sup>a</sup>	-
<b><i>sbe2a</i></b>							
Isoamylase	44.2 ± 6.2 <sup>a</sup>	33.5 ± 7.1 <sup>a</sup>	9.6 ± 0.2 <sup>c</sup>	2.5 ± 0.3 <sup>a</sup>	6.8 ± 0.4 <sup>a</sup>	3.2 ± 0.3 <sup>c,d</sup>	1.0 ± 0.3 <sup>a</sup>
Isoamylase, then pullulanase	41.6 ± 5.6 <sup>a</sup>	32.8 ± 6.2 <sup>a</sup>	9.9 ± 0.2 <sup>c</sup>	2.6 ± 0.2 <sup>a</sup>	7.2 ± 0.3 <sup>a</sup>	6.3 ± 0.2 <sup>f</sup>	1.1 ± 0.3 <sup>a</sup>
Increase by Pullulanase	-	-	0.4 ± 0.2 <sup>a</sup>	-	-	3.2 ± 0.1 <sup>d</sup>	-
<b><i>sbe1a sbe2a</i></b>							
Isoamylase	44.3 ± 5.5 <sup>a</sup>	33.0 ± 5.4 <sup>a</sup>	8.7 ± 0.3 <sup>b</sup>	3.7 ± 0.2 <sup>b</sup>	6.9 ± 0.5 <sup>a</sup>	2.8 ± 0.2 <sup>c</sup>	1.0 ± 0.3 <sup>a</sup>
Isoamylase, then pullulanase	42.4 ± 6.4 <sup>a</sup>	32.0 ± 5.8 <sup>a</sup>	9.3 ± 0.1 <sup>c</sup>	3.8 ± 0.3 <sup>b</sup>	7.2 ± 0.5 <sup>a</sup>	5.7 ± 0.1 <sup>e</sup>	1.0 ± 0.2 <sup>a</sup>
Increase by Pullulanase	-	-	0.5 ± 0.3 <sup>a</sup>	-	-	2.8 ± 0.2 <sup>c</sup>	-

<sup>1</sup>Values are percentage by weight. Values are mean ± standard deviation based on two independent analyses for one biological replication from the 2-gene segregating population. See Fig 3.10 for *Wt* and *sbe1a* and Fig 4.8 for *sbe2a* and *sbe1a sbe2a* starch. In the same column, significant differences among the four genotypes, as determined by one-way ANOVA with Fisher's LSD multiple comparison procedure, are indicated by different superscripts.

<sup>2</sup>Proportions of DP ≥ 18, DP 8-17, DP 5-7, DP 4, DP 3 and DP 2 were calculated as the areas for DP ≥ 17.5, 7.5 ≤ DP ≤ 17.5, 4.5 ≤ DP ≤ 7.5, 3.5 ≤ DP ≤ 4.5, 2.5 ≤ DP ≤ 3.5, and DP ≤ 2.5, respectively, as in Xia and Thompson (2006).

<sup>3</sup>The β-limit dextrins from amylopectin were either debranched by isoamylase, or by isoamylase plus pullulanase, indicated by "Isoamylase" and "Isoamylase, then pullulanase", respectively.

## 4.3 Discussion

### 4.3.1 Resistant Starch Values for Maize Endosperm Starch of *sbe1a* and *sbe2a* Mutant Combinations and of *sbe1a* and *ae* Mutant Combinations

A major effect of *ae* on the RS value was observed in comparisons among *sbe1a* and *ae* mutant combinations, confirming previous work (Richardson et al. 2000). A main effect of *sbe1a* on RS value and a significant difference between *sbe1a* and Wt were observed for comparisons among *sbe1a* and *sbe2a* mutant combinations, and also for comparisons among *sbe1a* and *ae* mutant combinations. This is substantial confirmation of our first report of an *sbe1a* effect alone (see Chapter 3). Neither a main effect of *sbe2a*, nor a significant difference between *sbe2a* and Wt, was observed in these comparisons. The lack of effect of SBEIIa deficiency suggests a minor function of SBEIIa than SBEIIb or SBEIa.

The significant main effects of both *sbe1a* and *ae*, and the lack of significant interaction of the effects of *sbe1a* and *ae* on RS value shows that the effect of *sbe1a* (deficient of SBEIa) and the effect of *ae* (deficient of SBEIIb) on RS value are independent. In contrast, the significant main effect of *sbe1a* but not *sbe2a*, and the significant interaction the effects of *sbe1a* and *sbe2a* on RS value shows that the effect of *sbe1a* (deficient of SBEIa) and the effect of *sbe2a* (deficient of SBEIIa) on RS value are not independent. The lack of independence among one set of mutant combinations but not among the other set suggests the possibility that SBE isoforms interact differently with other SBEs or with other starch synthetic enzymes.

Different RS values were observed for *sbe1a* mutant (13.2% versus 7.5%) (Table 4.2 & 4.3) in these two sets of mutant combinations generated from two different segregating populations. As mentioned in Chapter 2, the 2-gene segregating population shares approximately 6% less of the W64A background than the 3-gene

segregating population (see section 2.3). A higher RS value for an *sbe1a* mutant might be associated with the less share of the W64A background. Differences in the function and structure of other maize mutant starch were reported among the same mutant but in a different background (Li and Corke 1999). It is likely that an effect of *sbe1a* on starch digestion varies according to genetic background.

#### **4.3.2 Molecular Structure for Maize Endosperm Starch of *sbe1a* and *sbe2a* Mutant Combinations**

Although effects of *sbe1a* and *sbe2a* mutant combinations RS value are observed, there was little difference in the iodine binding behavior or in the CL distribution of the NG starch and starch fractions for these genotypes, as only a minor effect of *sbe2a* was observed. Although the intermediate material from *sbe2a* had a lower iodine binding behavior (Fig. 4.1b) and a lower proportion of long chains in region I (Fig. 4.4b), a relatively lower proportion of the intermediate material was fractionated from the *sbe2a* starch (Table 4.4). The differences in the proportion of intermediate material fractionated could reflect the *in vivo* situation, but it is also possible that the fractionation recovery was somehow influenced by the genotype.

Blue value has been used to evaluate amylose content in starch (Morrison and Laignelet 1983; Daniels 2003). The indistinguishable blue value observed for the NG starch from the four genotypes (Table 4.5) suggests similar amylose content. The region I in the CL distribution of the NG starch is considered to be from amylose (Batey and Curtin 1996) and has also been used to estimate amylose content in starch (Fig. 4.4a). Based on this argument, the amylose content is similar among the four genotypes except for a slightly lower proportion in *sbe1a sbe2a* (Table 4.8a).

Some small differences among Wt, *sbe1a*, *sbe2a*, and *sbe1a sbe2a* starch were

observed in the CL profile of their RS, as well as in the comparison of the CL profile of their RS to native starch (Table 4.9). As region II and region III are considered to represent chains mainly from long B chains and short B or A chains, respectively (Hizukuri 1986), an increase in region II could mean less degradation of long B chains during RS digestion as compared to other chains, and a decrease in region III could mean more degradation of short B or A chains as compared to other chains. This change during RS digestion suggests that short B or A chains are preferentially involved in the vulnerable region for  $\alpha$ -amylase attack. That such a change was observed for all the four genotypes suggests a common structural feature unaffected by either *sbe1a* or *sbe2a* mutation.

Comparing RS to respective native starch, the change in the proportion of region I was relatively small and was not the same for each genotype. Not much information can be concluded from this observation.

Effects of *sbe1a* and *sbe2a* mutant combinations were observed on the molecular structure of the putative  $\beta$ -LDs from amylopectin. For the debranched  $\beta$ -LDs, the *sbe1a* sample had a highest proportion of DP 4 followed by *sbe1a sbe2a*, and then by Wt and *sbe2a* (Table 4.11). As discussed in 3.3.2 and shown in Fig. 3.21, the limited extent of DP 4 hydrolysis by  $\beta$ -amylase is consistent with a higher proportion of closely associated branch points in this amylopectin. Based on this interpretation, the frequency of closely associated branch points would be in the order *sbe1a* > *sbe1a sbe2a* > Wt  $\approx$  *sbe2a*, indicating an effect of *sbe1a* along but no effect of *sbe2a* alone on branching pattern. The *sbe1a sbe2a* effect is less evident than the *sbe1a* effect, similar to the statistical interaction observed for RS values from these mutations. Thus, for *sbe1a* and *sbe2a* mutant combinations, the effects on amylopectin branching pattern are consistent with the RS values.

For the isoamylase-debranched  $\beta$ -LDs, a different extent of DP 2 increase after the subsequent pullulanase treatment was observed among the four genotypes (Table 4.11). The extent of the DP 2 increase was in the opposite order as the proportion of the DP 4 in the four genotypes (Table 4.11). As discussed in 3.3.2, the smaller increase in DP 2 stubs is interpreted to be the result of the restricted  $\beta$ -amylolysis on DP 4 chains, and would also be a function of a higher proportion of closely associated branch points in amylopectin (Xia and Thompson 2006). The different extent of the DP 2 increase in the four genotypes is consistent with the observed effects of *sbe1a* and *sbe2a* mutant combinations on amylopectin branching pattern. As discussed in 3.3.2, the lack of increase in DP 5-7 is associated with a restricted DP 4 hydrolysis. That there is no increase in DP 5-7 observed for *sbe1a* (Table 4.11) is further evidence for an effect of *sbe1a* alone on amylopectin branching pattern.

#### **4.3.3 Molecular Structure for Maize Endosperm Starch of *sbe1a* and *ae* Mutant Combinations**

The dominant *ae* effect and the additive *sbe1a* effect to the *ae* effect seen for RS values were also observed in the iodine binding behavior and CL distribution of the NG starches. No effect of *sbe1a* alone was observed by iodine binding. *ae* and *sbe1a ae* had a much stronger iodine binding behavior than Wt and *sbe1a* (Fig. 4.2), indicating that longer chains were involved in helical inclusion complexes with iodine. The CL distribution of *ae* and *sbe1a ae* starch showed a much higher proportion of region I, which has been used to estimate amylose content (Batey and Curtin 1996), as compared to Wt and *sbe1a* starch (Fig. 4.7, Table 4.10). This evidence is consistent with the routinely observed high amylose content in *ae*-type starches. Between the *ae* and *sbe1a ae* starch, *sbe1a ae* had a stronger iodine binding

behavior and a higher proportion of region I, suggesting that *sbe1a* in the presence of *ae* further increases the proportion of amylose chains above what is produced by *ae*. It is possible that the higher proportion of amylose in *sbe1a ae* than in *ae* may contribute to increased granule enzymatic resistance, and result in a higher RS value for the *sbe1a ae* starch as observed.

Although an effect of *sbe1a* on amylose content is observed in the presence of *ae*, the amylose content in *sbe1a* was not higher than in Wt (Fig. 4.7, Table 4.10). For amylose content, an effect of *sbe1a* was observed only in the presence of *ae*; there was no effect of *sbe1a* alone. The interaction of the effects of *sbe1a* and *ae* on amylose content may suggest possible interactions of SBEs with granule-bond starch synthase, the enzyme elongates amylose chains. Similar to amylose content, for amylopectin from a *wx* background, an effect of *sbe1a* on amylopectin branching was observed only in the presence of *ae* (Yao et al. 2004). However, for amylopectin from a non-*wx* background (as discussed in Chapter 3), an effect of *sbe1a* alone on amylopectin branching was observed. The presence of *ae* was not required to observe the effect of *sbe1a* on amylopectin branching. Comparisons of RS values show no statistically significant interaction of the effects of *sbe1a* and *ae*. The molecular basis for the independent effects of *sbe1a* and *ae* on RS values is not explained by the apparent interaction regarding amylose content. Thus branching pattern may be a more likely explanation for RS values.

Differences in the CL distribution before and after the  $\alpha$ -amylase digestion were observed among Wt, *sbe1a*, *ae*, and *sbe1a ae* starch. A major decrease in the chains in region I was observed for the RS compared to native starch for the *ae* and *sbe1a ae* starch, but not for the Wt and *sbe1a* starch (Table 4.10). As chains in region I are considered to be from amylose or amylose-like chains, for the *ae* and *sbe1a ae*

starch, the regions rich in amylose seem to be somewhat more susceptible to  $\alpha$ -amylase attack. This change was not observed by Evans and Thompson (2004) for a commercial high-amylose maize starch, which had relatively similar CL profile for the RS and the respective native starch. A somewhat greater degradation of chains in region I was observed for *sbela ae* (a decrease of ~14%), as compared to *ae* (a decrease of ~10%) (Table 4.10). This observation suggests that the amylose chains in *sbela ae* are organized so as to be more susceptible to  $\alpha$ -amylase.

An increase in the proportion of region II and III was also observed in the RS from *ae* and *sbela ae* as compared to native starch. This increase could result from the degradation of amylose chains in region I, producing chains of shorter length that eluted in region II and III. A lower proportion of region II (in undigested starch, this fraction is considered to be from long B chains in amylopectin) was observed for the RS from *sbela* as compared to the RS from Wt, and the proportion of region I and III was similar between the two RS (Table 4.10). Assuming that region II comes from long B chains, this observation suggests that the susceptibility of the long B chains relative to other chains is greater in *sbela* as compared to Wt, resulting in fewer residual long B chains relative to other chains in the *sbela* RS. This observation is consistent with the hypothesis developed in Chapter 3 that the *sbela* mutant may have longer internal segments on the long B chains, as these would be more susceptible to  $\alpha$ -amylase attack.

#### **4.3.4 Effects of Deficiency of Maize SBEs Alone and In Combination on Endosperm Starch Digestibility and Molecular Structure**

Comparisons of RS values among two sets of mutant combinations both show a main effect of *sbela* and a significant difference between *sbela* and Wt. This study

substantially confirms our first report of an effect of *sbe1a* alone in Chapter 3. For *sbe1a* and *sbe2a* mutant combinations, the effects of *sbe1a* and *sbe2a* on both RS values and amylopectin branching are not independent. In contrast, for *sbe1a* and *ae* mutant combinations, the effects of *sbe1a* and *ae* on RS values are independent, but the effects of *sbe1a* and *ae* on amylose content are not independent. The complexity of dependence of the effects of *sbe* mutants suggest the possible interactions between SBEs or other starch synthetic enzymes.

#### 4.4 References-Chapter 4

- Batey I.L., Curtin B.M. (1996). Measurement of amylose/amylopectin ratio by high-performance liquid chromatography. *Starch/Stärke*, 48: 338-344.
- Daniels, H.E. (2003). Granule swelling, homoglucan leaching, and thermal analysis of selected maize starches as influenced by native lipid. MS thesis. The Pennsylvania State University, University Park, PA.
- Dubois, M., Gilles, K. A., Hamilton, J. K., Rebers, P. A., and Smith, F. (1956). Colorimetric method for determination of sugars and related substances. *Anal. Chem.*, 28, 350-356.
- Evans, A. and Thompson, D.B. (2004). Resistance to  $\alpha$ -Amylase digestion in four native high-amylose maize starches *Cereal Chem.* 81, 31–37.
- Hizukuri, S. (1986). Polymodal distribution of the chain lengths of amylopectins, and its significance. *Carbohydr. Res.*, 147, 342-347.
- Klucinec, J.D., and Thompson, D.B. (1998). Fractionation of high amylose maize starches by differential alcohol precipitation and chromatograph of the fractions. *Cereal Chem.* 75, 887-896.
- Li, J. and Corke, H. (1999). Physicochemical properties of normal and low-amylose Job's Tears (*Coix lachryma-jobi* L.) starch. *Cereal Chem.* 76, 413-416.
- Li, J.H., Thompson, D.B., and Gultinan, M. (2007). Mutation of the maize *sbe1a* and *ae* genes alters morphology and physical behavior of wx-type endosperm starch granules. *Carbohydr. Res.* 342, 2619–2627.
- Morrison, W.R., and Laignelet, B. (1983). An improved colorimetric procedure for determining apparent and total amylose in cereal and other starches. *J. Cereal Sci.* 1, 9-20.

- Richardson, P.H., Jeffcoat R., and Shi, Y.-C. (2000). High-amylose starches: from biosynthesis to their use as food ingredients. *MRS Bulletin*. 25, 20–24.
- Xia, H., and Thompson D.B. (2006). Debranching of  $\beta$ -limit dextrans with isoamylase or pullulanase to explore the branching pattern of amylopectins from three maize genotypes. *Cereal Chem.* 83, 668-676.
- Yao, Y., Thompson, D.B., Gultinan, M. (2003). Starch biosynthesis in maize endosperm: in the absence of SBEIIb, the deficiency of SBEIIa leads to increased amylopectin branching. Presentation at 2003 AACC conference, Portland, OR.
- Yao, Y., Thompson, D.B., Gultinan, M. (2004). Maize starch branching enzyme (SBE) isoforms and amylopectin structure: in the absence of SBEIIb, the future absence of SBEIa leads to increased branching. *Plant Physiol.*, 106, 293-316.

## Chapter 5

### CONCLUSIONS AND FUTURE WORK

#### 5.1 Conclusions

##### 5.1.1 Effects of Maize SBE Isoforms on Endosperm Starch Structure

Because there are subtle differences in amino acid sequences of the different isoforms and differences in their expression profiles during plant development, it is reasonable to expect that each isoform would have different biochemical activities that together act to produce starch structure for optimal usage by the plant. This hypothesis is supported by *in vitro* data (Guan and Preiss 1993; Takeda et al. 1993) and by evolutionary evidence based on gene conservation (Gao et al. 1996; Morell et al. 1997; Rahman et al. 2001; Xu and Messing 2008; Comparot-Moss and Denyer K. 2009). To investigate this hypothesis, our group has utilized a reverse genetics approach, in which null mutations for each SBE isoform were identified and also combined in multiple mutant combinations. In this thesis, I undertook a detailed structural and functional analysis of starch isolated from the *sbe* single null mutants and several combinations of null mutants. The effects of the various *sbe* mutant combinations reported in Chapters 3 and 4 are ultimately to be understood in terms of differences in SBE activity. The analysis of *sbe* mutants in this thesis has provided a new understanding of effects of SBE isoforms on starch structure as well as on starch digestion, as summarized in this section and next section (5.1.2).

Evidence for pairwise genotype comparisons from the current study as well as from previous studies (Blauth et al. 2001; 2002; Yao et al. 2003; 2004) of starch structure of *sbe* mutants is summarized in Table 5.1.

Table 5.1 Evidence of effects of maize SBE isoforms on endosperm starch structure. Pairwise comparisons indicate the effect of the presence of a particular SBE isoform. Figures and tables listed are for results described in this thesis. Ref.1, 2, 3, and 4 represent Blauth et al. (2001), Blauth et al. (2002), Yao et al. (2003) and Yao et al. (2004), respectively. Numbers 1-9 indicate nine important pairwise comparisons that differed only in terms of the absence or presence of a single SBE isoform. The outcomes for each of the nine comparisons are listed in the footnote, described as the effect of the presence of the isoform as compared to its absence in that comparison. These nine comparisons are further elaborated in the discussion in this Chapter. “NA” indicates that endosperm starch for a particular genotype comparison was not available for study.

Present SBE Isoform(s) (Genotype)	I IIa IIb (Wt)	IIa IIb ( <i>sbe1a</i> )	I IIb ( <i>sbe2a</i> )	I IIa ( <i>ae</i> )	IIb ( <i>sbe1a sbe2a</i> )	IIa ( <i>sbe1a ae</i> )	I ( <i>sbe2a ae</i> )	None ( <i>sbe1a sbe2a ae</i> )
I IIa IIb (Wt)								
IIa IIb ( <i>sbe1a</i> )	<b>(1)</b> (Fig.3.5, 3.6, 3.8-3.11, 4.5, Ref.2, 4)							
I IIb ( <i>sbe2a</i> )	<b>(4)</b> (Table 4.7-4.9, 4.11, Fig. 4.4, Ref.1, 3)	(Table 4.7-4.9, 4.11, Fig.4.4)						
I IIa ( <i>ae</i> )	<b>(7)</b> (Fig.4.5, Ref.3, 4)	(Fig.4.5, Ref.4)	(Ref.3)					
IIb ( <i>sbe1a sbe2a</i> )	(Table 4.7-4.9, 4.11, Fig.4.4)	<b>(5)</b> (Table 4.7- 4.9, 4.11, Fig.4.4)	<b>(2)</b> (Table 4.7- 4.9, 4.11, Fig.4.4)	NA				
IIa ( <i>sbe1a ae</i> )	(Fig.4.5, Ref.4)	<b>(8)</b> (Fig.4.5, Ref.4)	NA	<b>(3)</b> (Fig.4.5, Ref.4)	NA			
I ( <i>sbe2a ae</i> )	(Ref.3)	NA	<b>(9)</b> (Ref.3)	<b>(6)</b> (Ref.3)	NA	NA		
None ( <i>sbe1a sbe2a ae</i> )	NA	NA	NA	NA	NA	NA	NA	

- (1) Effect of SBEI in the presence of SBEIIa and IIb is to create less locally clustered branch points in both amylopectin and amylose.
- (2) Effect of SBEI in the presence of SBEIIb is to create less locally clustered branch points in amylopectin.
- (3) Effect of SBEI in the presence of SBEIIa is to create less clustered branch points in amylopectin and to decrease amylose content.
- (4) No effect of SBEIIa in the presence of SBEI and IIb was observed.
- (5) Effect of SBEIIa in the presence of SBEIIb is to create more locally clustered branch points in amylopectin.

- (6) Effect of SBEIIa in the presence of SBEI is to create less clustered branch points in amylopectin.
- (7) Effect of SBEIIb in the presence of SBEI and IIa is to create more clustered branch points in amylopectin and to decrease amylose content.
- (8) Effect of SBEIIb in the presence of SBEIIa is to create more clustered branch points in amylopectin and to decrease amylose content.
- (9) Effect of SBEIIb in the presence of SBEI is to create more clustered branch points in amylopectin.

These pairwise comparisons allow inferences about the effect of the presence of an individual SBE isoform on starch structure. For SBEI, comparison (1) of Wt versus *sbe1a* allows us to examine the effect of SBEI in the presence of SBEIIa and SBEIIb, comparison (2) of *sbe2a* versus *sbe1a sbe2a* allows us to examine the effect of SBEI in the presence of SBEIIb, and comparison (3) of *ae* versus *sbe1a ae* allows us to examine effect of SBEI in the presence of SBEIIa. For SBEIIa, comparison (4) of Wt versus *sbe2a* allows us to examine the effect of SBEIIa in the presence of SBEI and IIb, comparison (5) of *sbe1a* versus *sbe1a sbe2a* allows us to examine the effect of SBEIIa in the presence of SBEIIb, and comparison (6) of *ae* versus *sbe2a ae* allows us to examine the effect of SBEIIa in the presence of SBEI. For SBEIIb, comparison (7) of Wt versus *ae* allows us to examine the effect of SBEIIb in the presence of SBEI and IIa, comparison (8) of *sbe1a* versus *sbe1a ae* allows us to examine the effect of SBEIIb in the presence of SBEIIa, and comparison (9) of *sbe2a* versus *sbe2a ae* allows us to examine the effect of SBEIIb in the presence of SBEI.

Inferences about the effect of SBEI are described in this paragraph.

Exhaustive  $\beta$ -amylolysis on amylopectin showed that a much smaller proportion of DP 4 chains remained after hydrolysis when SBEI was present than when it was absent in the presence of SBEIIa and SBEIIb in comparison (1). This is the first report of an effect of the *sbe1a* mutation alone, meaning the absence of SBEI only. I interpret this to indicate that these DP 4 chains resist  $\beta$ -amylolysis because of steric hindrance caused by clusters of closely associated branch points (see section 3.3.2). Similar to comparison (1), a smaller proportion of DP 4 chains remained after  $\beta$ -amylolysis when SBEI was present than when it was absent in the presence of SBEIIb in comparison (2). Given that the similar chain length profile observed for Wt, *sbe1a*, *sbe2a* and *sbe1a sbe2a*, the total amount of branch points in each starch can be

interpreted as similar. From comparisons (1) and (2) together, we can infer that when SBEIIb is present, SBEI acts to create branch points that are less locally clustered. For comparison (3), the results by Yao et al. (2004) show that in the *wx* background, less branching was observed when SBEI was present than when it was absent in the presence of SBEIIa. From comparison (3), we can infer that when SBEIIb is absent, SBEI acts to create branch points that are less clustered. Taken comparisons (1) (2) (3) together, we can infer that the effect of SBEI is to create branch points that are less clustered, either locally or overall, depending on the presence of SBEIIb.

Inferences about the effect of SBEIIa are described in this paragraph. In comparison (4), no effect of SBEIIa was observed when both SBEI and SBEIIb are present. However, in comparison (5), a higher proportion of DP 4 chains remained upon an exhaustive  $\beta$ -amylolysis when SBEIIa was present than when it was absent in the presence of SBEIIb. By the reasoning described above, we can infer from comparison (5) that when only SBEIIb is present, SBEIIa acts to increase branch points that are more locally clustered. Similar to the comparison (3), for comparison (6), the results by Yao et al. (2003) show that less amylopectin branching was observed when SBEIIa was present than when it was absent in the presence of SBEI. From comparison (6), we can infer that when SBEIIb is absent, SBEIIa acts to create branch points that are less clustered. While this interpretation seems inconsistent with the observations made with comparison (5), it is similar to the results observed with comparison (3). From currently available evidence, it is impossible to distinguish the mechanism by which this might occur. One hypothesis to explain this mechanism would be that when SBEIIb is absent, SBEI or SBEIIa proteins could reciprocally inhibit activity of the other SBE, directly limiting the number of branch points synthesized in the *ae* mutant when both SBEI and SBEIIa are present. Alternatively,

SBEI or SBEIIa might interact with other starch synthetic enzymes to influence the synthesis of branch points. Possible functional interactions between the SBE isoforms and between SBE isoforms and other starch synthetic enzymes are elaborated in section below (5.1.3). Considering comparisons (4) (5) (6) together, we can infer that the effect of SBEIIa is dependent on the presence of other SBEs: when both SBEI and IIb are present, no effect of SBEIIa is observed; when only SBEIIb is present, the effect of SBEIIa is to create branch points that are more locally clustered; when SBEIIb is absent, SBEI and SBEIIa may have reciprocally inhibitory effects on synthesis of branch points.

Inferences about the effect of SBEIIb are described in this paragraph. Comparisons (7) (8) (9) all indicate that the effect of SBEIIb is to create branch points that are more clustered, regardless of the presence of other individual SBEs.

### **5.1.2 Effects of Maize SBE Isoforms on Endosperm Starch Digestion**

Evidence for pairwise genotype comparisons of resistant starch (RS) values of *sbe* mutants is summarized in Table 5.2. Using the same nine comparisons as in Table 5.1, we can make inferences about the effect of individual SBE isoform activities on starch digestion. Due to the lack of starch material, evidence for comparisons (6) and (9) was not obtained. For SBEI, comparisons (1) (2) (3) all show that the effect of SBEI is to decrease the RS value, regardless of the presence of other SBEs. For SBEIIa, comparison (4) did not reveal an effect of SBEIIa on the RS value when both SBEI and IIb are present. However, comparison (5) indicates that the effect of SBEIIa is to increase the RS value when only SBEIIb is present. For SBEIIb, comparisons (7) and (8) both indicate that the effect of SBEIIb is to decrease the RS value to a great extent, regardless of the presence of other individual SBE.

Table 5.2 Evidence of effects of maize SBE isoforms on endosperm starch digestion. Pairwise comparisons indicate the effect of the presence of a particular SBE isoform. Tables listed are for results described in this thesis. Numbers 1-9 indicate nine important pairwise comparisons that differed only in terms of the absence or presence of a single SBE isoform. Comparisons (6) and (9) are not available for study. The outcomes for each of the seven comparisons are listed in the footnote, described as the effect of the presence of the isoform as compared to its absence in that comparison. These nine comparisons are further elaborated in the discussion in this Chapter. “NA” indicates that endosperm starch for a particular genotype comparison was not available for study.

Present SBE Isoform(s) (Genotype)	I IIa IIb (Wt)	IIa IIb ( <i>sbe1a</i> )	I IIb ( <i>sbe2a</i> )	I IIa ( <i>ae</i> )	IIb ( <i>sbe1a sbe2a</i> )	IIa ( <i>sbe1a ae</i> )	I ( <i>sbe2a ae</i> )	None ( <i>sbe1a sbe2a ae</i> )
I IIa IIb (Wt)								
IIa IIb ( <i>sbe1a</i> )	<b>(1)</b> (Table 4.2, 4.3)							
I IIb ( <i>sbe2a</i> )	<b>(4)</b> (Table 4.2)	(Table 4.2)						
I IIa ( <i>ae</i> )	<b>(7)</b> (Table 4.3)	(Table 4.3)	NA					
IIb ( <i>sbe1a sbe2a</i> )	(Table 4.2)	<b>(5)</b> (Table 4.2)	<b>(2)</b> (Table 4.2)	NA				
IIa ( <i>sbe1a ae</i> )	(Table 4.3)	<b>(8)</b> (Table 4.3)	NA	<b>(3)</b> (Table 4.3)	NA			
I ( <i>sbe2a ae</i> )	NA	NA	<b>(9)</b> NA	<b>(6)</b> NA	NA	NA		
None ( <i>sbe1a sbe2a ae</i> )	NA	NA	NA	NA	NA	NA	NA	

- (1) Effect of SBEI in the presence of SBEIIa and IIb is to decrease the RS value.  
(2) Effect of SBEI in the presence of SBEIIb is to decrease the RS value.  
(3) Effect of SBEI in the presence of SBEIIa is to decrease the RS value.  
(4) No effect of SBEIIa in the presence of SBEI and IIb was observed.  
(5) Effect of SBEIIa in the presence of SBEIIb is to increase the RS value.

- (7) Effect of SBEIIb in the presence of SBEI and IIa is to greatly decrease the RS value.
- (8) Effect of SBEIIb in the presence of SBEIIa is to greatly decrease the RS value.

From comparisons of RS values, we can infer that both SBEI and SBEIIb decrease starch resistance to  $\alpha$ -amylase digestion, independent of the presence of other SBEs; the effect of SBEIIa on starch digestion is observable when only SBEIIb is present, which is to increase starch resistance to digestion. The different RS values strongly suggest difference in starch structure. Inferences about the effects of SBEs on starch digestion are consistent with a primary effect of SBEIIb, a secondary but important effect of SBEI, and a secondary and minor effect of SBEIIa only in the presence of SBEIIb alone on starch structure.

Factorial analysis of RS values among *sbe1a* and *sbe2a* mutant combinations and among *sbe1a* and *ae* mutant combinations both show a main effect of *sbe1a* and a significant difference between *sbe1a* and Wt. This is substantial confirmation of an effect of *sbe1a* alone. For *sbe1a* and *sbe2a* mutant combinations, the effects of *sbe1a* and *sbe2a* on RS values are not independent. In contrast, for *sbe1a* and *ae* mutant combinations, the effects of *sbe1a* and *ae* on RS values are independent. Similar to statistical interaction, structural analysis of the mutant combinations indicates that the effects of *sbe1a* and *sbe2a* on amylopectin branching are not independent, and the effects of *sbe1a* and *ae* on amylose content are not independent. The complexity of dependence of the effects of *sbe* mutants suggest the possible interactions between SBEs or other starch synthetic enzymes.

### **5.1.3 Function of Maize SBE Isoforms in Starch Biosynthesis**

Of the three maize SBE isoforms, SBEIIb is known to be the dominant SBE in starch biosynthesis (Garwood et al. 1976; Boyer et al. 1977; Boyer and Preiss 1981). This previous work, combined with evidence as described above, leads to several hypotheses about the specific functions of the three maize SBE isoforms in

endosperm starch biosynthesis: 1) The SBEIIb protein is the dominant form of SBE, and is responsible for synthesizing branch points that are more clustered. 2) When SBEIIb is present, SBEI and IIa are responsible for modulating the branching pattern by synthesizing branch points that are less locally clustered and more locally clustered, respectively. 3) When SBEIIb is absent, SBEI and IIa may have reciprocal inhibitory function on synthesis of branch points.

It should be noted that analysis of the *sbe2a* mutation revealed that a visible phenotype of this mutation during plant development can be seen in leaves, which display regions of premature senescence (Blauth et al. 2001). Analogous to a strong phenotype of the *sbe2a* mutation in leaf, a strong phenotype of the *ae* mutation in endosperm is a striking wrinkled kernel phenotype. In endosperm, even though SBEIIa has a minor function on starch synthesis, it acts like SBEIIb to create branch points that are more clustered. In leaf, it appears that SBEIIa is the only important isoform expressed (Gao et al. 1996; Blauth et al. 2001), and its absence results in higher proportion of amylose in leaf similar to *ae* starch from endosperm (Blauth et al. 2001). These evidences suggest the function of SBEIIa in leaf is similar to the function of SBEIIb in endosperm. A detailed examination of SBE isoform functionality in different tissues such as pollen, root tips, and root and stem tissues have yet to be described.

Takeda et al. (1993) showed that the *in vitro* action of SBEI on amylose preferentially transferred longer chains than the action of SBEIIa and SBEIIb. Starting with an amylose chain, for a given amount of starch, the action of SBEI resulted in fewer branch points than either of the SBEII isoforms, consistent with our hypotheses that the function of SBEI is to create branch points that are less clustered and the function of SBEII is to create branch points that are more clustered.

Differences in SBE activity in *sbe* mutants could be simply due to the amount of a remaining SBE isoform or to biochemical or physical interactions that modulate the activities of an isoform. These interactions could entail allosteric effects of metabolites, or protein-protein interactions among starch synthetic enzymes. Pleiotropic reduction in SBE activity has been observed in several maize mutants of starch-debranching enzyme (DBE) or starch synthase (SS) (Boyer and Preiss 1979; 1981; Gao et al. 1998; Beatty et al. 1999; Nishi et al. 2001; Colleoni et al. 2003; Dinges et al. 2001; 2003; Tetlow et al. 2004). These studies suggested that a multi-protein starch synthesizing complex(s) could exist, and that interactions within these complexes could modulate the intricate structure of a developing starch granule.

Seo et al. (2002) found that when SBEs were heterologously expressed in a yeast system, SBEIIa and/or SBEIIb appear to act before SBEI on synthesizing glucan structure. The studies of Yao et al. (2003; 2004) suggest that in the absence of SBEIIb, a reciprocal inhibition exists between SBEI and SBEIIa, and that the presence of either SBEI or SBEIIa increases amylopectin branching as opposed to the presence of SBEI and SBEIIa together. The reciprocal inhibition between SBEI and SBEIIa suggests possible interactions between SBEs or other starch synthetic enzymes. In order to explain a reciprocal inhibition between SBEI and SBEIIa, one hypothesis based on the idea of Seo et al. (2002) is that the action of the SBEIIa isoform may result in a structure that is not a favorable substrate for SBEI. An alternative hypothesis based on predicted interactions between SBEI and SSI (Boyer and Preiss 1979) and between SBEIIa and SSII (Boyer and Preiss 1981) is that the action of SSs to extend chains may be enhanced with presence of either SBEI or SBEIIa; with both SBEI and SBEIIa, more of longer chains and thus less branching would be generated. A second alternative hypothesis based on predicted interactions

between SBEIIa and DBEs (Colleoni et al. 2003; Dinges et al. 2003; Tetlow et al. 2004) is that SBEIIa may act to stimulate DBEs to form a substrate structure not favorable for SBEI. The present work was not designed to explore these interactions. These and additional possible functional interactions of starch synthetic enzymes remain to be investigated.

#### **5.1.4 An Evolutionary Perspective on the Function of Maize SBE Isoforms**

Gene duplication and neo-functionalization are well known mechanisms by which specific genes can evolve to express different isoforms of enzymes with slightly specialized expression patterns or different enzymatic activities (Gingerich et al. 2007; Prokhnevsky et al. 2008; Saleh et al. 2008). With the evidence from current and previous work, we can infer that the an ancestral *Sbe* gene has duplicated at least twice during the evolution of maize, then evolved to express three SBE isoforms with highly specific functions in starch biosynthesis. The SBEIIa and SBEIIb genes are expressed predominantly in the leaves and endosperm, respectively (Gao et al. 1996). In maize endosperm, SBEIIb dominates in the synthesis of the branching pattern by increasing clustering of branch points, SBEI modulates the branching pattern by decreasing local clustering of branch points, and SBEIIa has at best a minor function compared to SBEIIb or SBEI. In maize leaf, SBEIIa acts like SBEIIb in endosperm, creating most of the branch points. Phylogenetic evidence suggests that the *Sbe2a* and *Sbe2b* genes arose in monocots through a gene duplication event that post-dates the divergence of dicots from monocots (Rahman et al. 2001), consistent with the distinct functions of SBEIIa and SBEIIb in different plant tissues in maize.

This thesis for the first time reports an effect of the SBEI isoform on endosperm starch. Previously there has been no report that a lack of this activity

resulted in an effect on either starch molecular structure or starch function. Molecular structure analysis suggests an important function of SBEI in modulating the branching pattern in normal starch by decreasing local clustering of amylopectin branch points. Thompson (2000) emphasized the non-random nature of the distribution of branch points in starch. A specific type of non-random branching pattern may be required to optimize both storage and hydrolysis. It is reasonable to hypothesize that alteration in the specific non-random branching pattern could lead to an altered granule organization, rendering it more or less favorable to the plant for storage and/or for enzyme hydrolysis during utilization. Our functional analysis in *in vitro* starch digestibility and in the germinating plant supports this hypothesis, and shows that deficiency of SBEI in endosperm starch results in a less readily digested granule and retarded starch utilization during germination.

Phylogenetic evidence supports a specific and important function of SBEI in plant development, as SBEI evolves prior to monocot-dicot divergence and is highly conserved between all monocot and dicot plants for over 140 million years (Chaw et al. 2004; Gao et al. 1996). Since starch storage and utilization are central to the plant energy balance and reproductive capacity, a change in SBE isoform activity provides a powerful selection pressure for development of new or more favorable alleles of SBE isoforms and would thus drive isoform specialization. The evidence presented in this thesis strongly supports the hypothesis that SBEI is required to synthesize endosperm starch granules that allow normal hydrolysis and utilization during germination. Considering plant survival in the wild, optimal germination vigor would be a strong evolutionary force to select for genotypes of plants with starch granules optimized for molecular structure that would lead to efficient storage and utilization. The reduced germination vigor of *sbe1a* mutant seeds observed in this study provides

powerful evidence for a specialized and important role of SBEI in plant development, consistent with the evolutionary conservation of SBEI in all higher plants.

## **5.2 Suggestions for Future Work**

### **5.2.1 Understanding of Structural Basis for Starch Digestibility**

#### **5.2.1.1 Extended Digestion of Starch**

Using a double-exponential decay fit, the kinetic analysis of the 16-hr digestion time-course in this study suggested two substrate components, one being digested faster than the other. As at least five times the half-life would be needed to obtain a robust fit for exponential decay, the data points collected within 16 hr (time defined for obtaining RS value) were less than ideal to obtain kinetic parameters for the slowly-digested component. For a better comparison of the kinetics of the slowly-digested components, it would be necessary to collect more data points beyond 16 hr until digestion proceeds to at least five times the half-life.

#### **5.2.1.2 Characterization of Starch Structure During Digestion**

The kinetic parameters for two digested components were shown to be different between Wt and *sbe1a* starch. However, there is no direct structural evidence to account for this difference. It might be possible to gain insight into the structure of digested components by examining both molecular and granular structures of partially digested starch at different time intervals during the digestion. In order to obtain enough partially digested starch for analysis, a scale up of the  $\alpha$ -amylase digestion would be required.

### **5.2.1.3 Characterization of Branching Pattern for Resistant Starch**

The current study suggests that an altered branching pattern in *sbe1a* native starch may result in a more resistant starch granule to  $\alpha$ -amylase digestion. However, no branching pattern evidence was obtained for the RS from *sbe1a*. Characterization of branching pattern for RS would address the question of whether the RS and the digested starch might have different branching pattern.

### **5.2.1.4 Characterization of Starch Structure and Digestion from Differentially Iodine-Stained Granules**

*sbe1a* starch granules exhibited a higher degree of heterogeneity than Wt granules by iodine staining. A question remains as to the nature of this observed granule heterogeneity. It may be possible to sort these differentially stained granules through a cell flow cytometer or by other means. It would be interesting to examine the starch structure and digestion of these differentially stained granules separately, and to understand the contribution of different granules from the same genotype to starch digestion.

### **5.2.2 Structural Analysis of Starch from Different Biological Replications**

As starch from three biological replications (three different plants) showed similar digestibility, this work assumed that starch structure among biological replications is similar as well. Based on this consideration, starch structural analysis presented in this thesis was based on starch from one biological replication. However, the possibility of potential differences in starch structure among the biological replications cannot be ruled out. Thus, it would be appropriate to examine starch structure from all the three biological replications.

### 5.2.3 Breeding Strategies for Generating All the Combinations of *sbe* Mutants In Isogenic Lines

Due to the compromised vigor of the *sbe2a* mutant, it was not possible to generate all the multiple mutant combinations in the same segregating population in the present work. Thus, the *sbe1a* and *sbe2a* mutant combinations and the *sbe1a* and *ae* mutant combinations were obtained in two segregating populations. Due to the different pedigree of the plants that were used to originally identify the *sbe* mutations (see 2.2.1.2), these two segregating populations may differ slightly in their genetic background. Comparisons between mutants from different segregating populations must be made with caution, understanding that genetic background differences might also contribute to any differences in starch structure observed. Due to a limited availability of the *sbe2a ae* mutant and an unavailability of the triple *sbe1a sbe2a ae* mutant, the present work could not examine the effect of SBEI alone and the effect of a complete absence of SBE activity. The research presented in this thesis on the *sbe1a* mutant revealed new knowledge of the effect of the SBEI isoform in the presence of SBEIIa and IIb on starch structure. In the future, it is possible that even more information can be gained by direct examination of the branching produced by SBEI alone in the *sbe2a ae* mutant and provide a better understanding for the function of SBEI in starch biosynthesis.

Two possible breeding strategies might be used in the future to generate sufficient *sbe2a*-containing plants-including homozygous *sbe2a*, *sbe1a sbe2a*, *sbe2a ae*, and the triple *sbe1a sbe2a ae* mutants-in a similar genetic background. One strategy could be used in the short term. It is to select homozygotes from a much larger seed source in the 3-gene segregating population to maximize the chance of generation of sufficient number of desired *sbe* mutant ears. The present work used

780 seeds from the 3-gene segregating population and obtained no ears for *sbe2a* and *sbe1a sbe2a ae*, 2 small ears (~20 kernels) for *sbe1a sbe2a*, and 1 small ear (~20 kernels) for *sbe2a ae*. At least 3 homozygous ears for each genotype would be needed for complete biological replication study. If the homozygote yield from these 780 seeds is representative, an increase of 3-fold or 2340 seeds, may produce 6 ears for *sbe1a sbe2a* and 3 ears for *sbe2a ae*. To account for any weather conditions that may worsen the health condition of *sbe2a*-containing plants, a suggested number of starting seeds would be at least 3000 seeds.

The other strategy could be used in the long term. It is to backcross the *sbe* mutant to the W64A background until at least six backcrosses are achieved. Regardless of which segregating population they come from, the homozygotes selected from the 6<sup>th</sup> or above generation would share more than 98% ( $1 - \frac{1}{2^6}$ ) of the W64A background, and can be considered to be isogenic by conventional standards. The selected homozygotes of all the possible *sbe* mutants could be self-pollinated to generate homozygous ears, which could be further used for generating more ears by selfing. No segregating population would be necessary in this strategy, eliminating the uncertainty of obtaining the specific genotype due to unequal segregation.

#### **5.2.4 Functions of Maize SBE Isoforms in Other Tissues**

The compromised health and reduced fertility of *sbe2a* mutant plants are associated with heavy senescence of leaf tissues (Blauth et al. 2001; Yao et al. 2003) and the slow pollen tube growth (personal communication, Dr. Marna Yandea-Nelson). Despite the minor function of SBEIIa in maize endosperm suggested in the present work, the compromised health of *sbe2a* mutants has raised a question about the function of SBEIIa in other maize tissues. The work of Blauth et al. (2001) found

that in the *sbe2a* mutation, leaf starch is largely linear material, and suggested the role of SBEIIa in leaf is similar to the role of SBEIIb in endosperm. This is consistent with the observation that the level of *Sbe2a* gene expression is highest in leaves, and the *Ae* gene is not expressed in leaf tissues (Gao et al. 1996; 1997). Furthermore, although *Sbe1* mRNA has been detected in leaves, no protein has ever been detected using antibodies and western blotting (Blauth et al. 2002).

The work of Blauth et al. (2001, 2002) also showed that there is a fundamental difference between the structure of Wt starch from endosperm and leaf. Based on chain length profiles of debranched whole starch (Fig. 5, Blauth et al. 2001; Fig. 6, Blauth et al. 2002), endosperm starch appears to have a higher proportion of amylose. Moreover, within the short chain fraction (likely from amylopectin), the molar ratio of A:B1 chains is much greater for endosperm starch than for leaf starch. As the physiological utility of the two starches differs, one might expect that leaf starch would be more readily digestible for rapid use in the daily transition to the dark cycle.

Preliminary results from leaf starch digestibility using the RS assay (Appendix B) showed that Wt leaf starch is unusually rapidly and completely broken down, and *sbe2a* leaf starch is poorly digested, with a RS value of about 50%. This poor digestibility may account for the severe disadvantage for the health of leaves in these plants. A somewhat diminished digestion of leaf starch for the *sbe1a* genotype, with a RS value of 12-25% was also observed. This result suggests that there may well be an influence of the *Sbe1a* gene on SBE activity in the leaf, even though no *Sbe1* protein has been detected in leaves (Blauth et al. 2002). Consequently, it would be worthwhile to compare in detail the structure of leaf starch for the Wt and the *sbe1a* genotype, and to further explore the structure of leaf starch in the *sbe2a* genotype, using the approaches described in the present work.

The observed differences in starch structure from transitory (leaf) versus storage (endosperm) tissues suggest that the specific function of individual maize SBE isoforms may be different in leaf and endosperm tissues. As an energy reserve for the plant, maize starch is present in many other tissues, such as pollen, stem, and roots, it is possible that the starch structure in these tissues differs as well, as demanded by the different physiological utility. It is tempting to hypothesize that the function of individual SBE isoforms may differ in various tissues for plant development. One interesting structure from the root tip contains specialized cells which contain large starch granules (starch statoliths) and plays a role in the mechanisms of root gravitropism (Sack 1991; 1997). A detailed characterization of molecular and granular starch structure from other tissues would be necessary to gain a complete understanding of the functions of maize SBEs in plant development.

#### **5.2.5 Interactions of Maize SBEs with Other Starch Synthetic Enzymes in Starch Biosynthesis**

A common theme in the regulation and function of many different types of proteins in cells involves biochemical and physical interactions among multiple proteins (Jones and Thornton 1995; 1996). These interactions can involve protein-protein physical interactions, protein modifications such as phosphorylation or glycosylation, and synergistic or negative effects between different proteins acting indirectly through biochemical pathways (Nooren and Thornton 2003). It is likely that interaction of the SBEs with other proteins involved in starch biosynthesis is a common feature among diverse plant species. Starch biosynthesis involves coordinated function of four types of enzymes: ADP-Glc pyrophosphorylase, SS, SBE, and DBE. One area not explored in this thesis is to address how SBEs coordinate

with other starch synthetic enzymes to synthesize the starch granule. For example, enzyme complexes may have different compositions of proteins (DBEs, SSs, etc.) in various *sbe* mutants as well as in various tissues (kernel versus leaf), and these different complexes could have large effects on resulting starch structure. Studies by others have begun to reveal these interactions: investigators have suggested that a multi-protein starch synthesizing complex(s) exist and that interactions within these complexes comprise the mechanisms for modulating the intricate structure of a developing starch granule (Gao et al. 1998; Beatty et al. 1999; Nishi et al. 2001; Seo et al. 2002; Colleoni et al. 2003; Dinges et al. 2001; 2003; Tetlow et al. 2004; 2008). Many approaches to study protein complexes have been developed. Co-immunoprecipitation of protein complexes using isoform specific antibodies is a powerful approach to begin to map out the participants in the complexes (Tetlow et al. 2004; 2008). An indirect approach would be to study zymograms of crude protein extracts from different *sbe* mutants to see if the present starch synthetic enzymes are affected by the lack of a specific interacting partner (Dinges et al. 2003; Yao et al. 2004).

### 5.3 References-Chapter 5

- Beatty, M.K., Rahman, A., Cao, H., Woodman, W., Lee, M., Myers, A.M., and James, M.G. (1999). Purification and molecular genetic characterization of ZPU1, a pullulanase-type starch-debranching enzyme from maize. *Plant Physiol.* 119, 255–266.
- Blauth, S. L., Kim, K., Klucinec, J., Shannon, J. C., Thompson, B.D. and Gultinan, M.J. (2002). Identification of mutator insertional mutants of starch branching enzyme 1 (*sbe1*) in *Zea mays* L. *Plant. Mol. Biol.* 48, 287-297.
- Blauth, S.L., Yao, Y., Klucinec, J.D., Shannon, J.C., Thompson, B.D. and Gultinan, M. J. (2001). Identification of mutator insertional mutants of starch-branching enzyme 2a in corn. *Plant Physiol.* 125, 1396-1405.
- Boyer, C. D., Daniels, R. R. and Shannon, J. C. (1977). Starch granule (amyloplast)

development in endosperm of several *Zea mays* L. genotypes affecting kernel polysaccharides. *Amer. J. Bot.*, 64, 50-56.

- Boyer, C. D., and Preiss, J. (1979). Properties of citrate-stimulated starch synthesis catalyzed by starch synthase I of developing maize kernels. *Plant Physiol.*, 64, 1039–1042.
- Boyer, C.D., and Preiss, J. (1981). Evidence for independent genetic control of the multiple forms of maize endosperm branching enzymes and starch synthases. *Plant Physiol.*, 67, 1141-1145.
- Chaw, S.M., Chang, C.C., Chen, H.L., Li, W.H. (2004). Dating the monocot-dicot divergence and the origin of core eudicots using whole chloroplast genomes. *J. Mol. Evol.* 58, 424–441.
- Colleoni, C., Myers, A.M., and James, M.G. (2003). One- and two-dimensional native PAGE activity gel analyses of maize endosperm proteins reveal functional interactions between specific starch metabolizing enzymes. *J. Appl. Glycosci.* 50, 207–212.
- Comparot-Moss, S. and Denyer K. (2009). The evolution of the starch biosynthetic pathway in cereals and other grasses. *J. Exp. Bot.* 60, 2481-2492.
- Dinges, J.R., Colleoni, C., James, M.G., and Myers, A.M. (2003). Mutational analysis of the pullulanase-type debranching enzyme of maize indicates multiple functions in starch metabolism. *Plant Cell* 15, 666–680.
- Dinges, J.R., Colleoni, C., Myers, A.M., and James, M.G. (2001). Molecular structure of three mutations at the maize *sugary1* locus and their allele-specific phenotypic effects. *Plant Physiol.* 125, 1406–1418.
- Gao, M., Fisher, D.K., Kim, K., Shannon, J.C. and Gultinan, M.J. (1996). Evolutionary conservation and expression patterns of maize starch branching enzyme I and IIb genes suggests isoform specialization. *Plant Mol. Biol.* 30, 1223-1232.
- Gao, M., Fisher, D.K., Kim, K., Shannon, J.C. and Gultinan, M.J. (1997). Independent genetic control of maize starch-branching enzymes IIa and IIb- isolation and characterization of a Sbe2a cDNA. *Plant Physiol.* 114, 69-78.
- Gao, M., Wanat, J., Stinard, P.S., James, M.G., and Myers, A.M. (1998). Characterization of dull1, a maize gene coding for a novel starch synthase. *Plant Cell* 10, 339–412
- Garwood, D.L., McArdle, F.J., Vanderslice, S.F., Shannon, J.C. (1976). Postharvest carbohydrate transformations and processed quality of high sugar maize genotypes. *J. Am. Soc. Hortic. Sci.* 101, 400–404.
- Gingerich, D.J., Hanada, K., Shiu, S.H., Vierstra, R.D. (2007). Large-scale, lineage-specific expansion of a bric-a-brac/tramtrack/broad complex ubiquitin-ligase

- gene family in rice. *Plant Cell*. 19, 2329–2348.
- Guan, H.P. and Preiss, J. (1993). Differentiation of the properties of the branching isozymes from maize (*Zea mays*). *Plant Physiol*. 102, 1269-1273.
- Jones, S. and Thornton, J.M. (1995). Protein-protein interactions: a review of protein dimer structures. *Prog. Biophys. Mol. Biol.* 63, 31-65.
- Jones, S. and Thornton, J.M. (1996). Principles of protein-protein interactions. *Proc. Natl Acad. Sci. USA*, 93, 13-20.
- Morell, M.K., Blennow, A., Kosar-Hashemi, B., Samuel, M.S. (1997). Differential expression and properties of starch branching enzyme isoforms in developing wheat endosperm. *Plant Physiol.*, 113, 201–208.
- Nishi, A., Nakamura, Y., Tanaka, N., and Satoh, H. (2001). Biochemical and genetic effects of amylose-extender mutation in rice endosperm. *Plant Physiol*. 127, 459–472.
- Nooren, M.A., and Thornton, J.M. (2003). Diversity of protein-protein interactions *The EMBO J.* 22, 3486-3492.
- Prokhnovsky, A.I., Peremyslov, V.V., Dolja, V.V. (2008). Overlapping functions of the four class XI myosins in Arabidopsis growth, root hair elongation, and organelle motility. *Proc. Natl. Acad. Sci.* 105, 19744–19749.
- Rahman, S., Regina, A., Li, Z., Mukai, Y., Yamamoto, M., Kosar-Hashemi, B., Abrahams, S., Morell, M.K. (2001). Comparison of starch-branching enzyme genes reveals evolutionary relationships among isoforms. Characterization of a gene for starch-branching enzyme IIa from wheat D genome donor *Aegilops tauschii*. *Plant Physiol*. 125, 1314–1324.
- Sack, F.D. (1991). Plant gravity sensing. *Int. Rev. Cytol.* 127, 193-252.
- Sack, F.D. (1997). Plastids and gravitropic sensing. *Planta* 203, S63-S68.
- Saleh, A., Alvarez-Venegas, R., Yilmaz, M., Le, O., Hou, G., Sadler, M., Al-Abdallat, A., Xia, Y., Lu, G., Ladunga, I., Avramova, Z. (2008). The Highly Similar *Arabidopsis* homologs of trithorax ATX1 and ATX2 encode proteins with divergent biochemical functions. *Plant Cell*. 20, 568–579.
- Seo, B.S., Kim, S., Scott, M.P., Singletary, G.W., Wong, K.S., James, M.G., Myers, A.M. (2002). Functional interactions between heterologously expressed starch-branching enzymes of maize and the glycogen synthases of Brewer's yeast. *Plant Physiol*. 128, 1189-1199.
- Takeda, Y., Guan, H., Preiss, J. (1993). Branching of amylose by the branching isozymes of maize endosperm. *Carbohydr. Res.* 240, 253–263.
- Tetlow, I.J., Wait, R., Lu, Z., Akkasaeng, R., Bowsher, C.G., Esposito, S., Kosar-

- Hashemi, B., Morell, M.K., and Emes, M.J. (2004). Protein phosphorylation in amyloplasts regulates starch branching enzyme activity and protein-protein interactions. *Plant Cell* 16, 694-708.
- Tetlow, I.J., Beisel, K.G., Cameron, S., Makhmoudova, A., Liu, F., Bresolin, N.S., Wait, R., Morell, M.K., Emes, M.J. (2008). Analysis of protein complexes in wheat amyloplasts reveals functional interactions among starch biosynthetic enzymes. *Plant Physiol.* 146, 1878 - 1891.
- Thompson, D.B. (2000). On the non-random nature of amylopectin branching. *Carbohydr. Polym.*, 40, 223-239.
- Xu, J.H. and Messing, J. (2008). Organization of the prolamin gene family provides insight into the evolution of the maize genome and gene duplication in grass species. *Proc. Natl. Acad. Sci.* 105, 14330–14335.
- Yao, Y., Thompson, D.B., and Guiltinan, M. (2003). Starch biosynthesis in Maize endosperm: in the absence of SBEIIb, the deficiency of SBEIIa leads to increased amylopectin branching. Presentation at 2003 AACC conference, Portland, OR.
- Yao, Y., Thompson, D.B., and Guiltinan, M. (2004). Maize starch branching enzyme (SBE) isoforms and amylopectin structure: in the absence of SBEIIb, the future absence of SBEIa leads to increased branching. *Plant Physiol.* 106, 293-316.

## **Appendix A**

### **ADDITIONAL FIGURES AND TABLES FOR CH3 & CH4**

Table A.1 Resistant starch values for Wt, *sbe1a*, *sbe2a*, and *sbe1a sbe2a* starch from the 2-gene segregating population.

Genotype	Resistant Starch Value (%)			
	Rep1	Rep2	Rep3	mean $\pm$ SD
Wt-B1	0.81	2.78	2.69	2.1 $\pm$ 1.1
<i>sbe1a</i> -B1	10.2	11.97	11.05	11.1 $\pm$ 0.9
<i>sbe2a</i> -B1	6.27	5.17	2.34	4.6 $\pm$ 2.0
<i>sbe1a sbe2a</i> -B1	6.96	5.28	6.07	6.1 $\pm$ 0.8
Wt-B2	0.37	1.81	0.86	1.0 $\pm$ 0.7
<i>sbe1a</i> -B2	13.9	16.78	11.71	14.1 $\pm$ 2.5
<i>sbe2a</i> -B2	0.61	1.88	4.27	2.3 $\pm$ 1.9
<i>sbe1a sbe2a</i> -B2	7.02	7.06	4.16	6.1 $\pm$ 1.7
Wt-B3	1.05	1.54	2.1	1.6 $\pm$ 0.5
<i>sbe1a</i> -B3	18.21	14.44	10.22	14.3 $\pm$ 4.0
<i>sbe2a</i> -B3	2.88	2.89	4.33	3.4 $\pm$ 0.8
<i>sbe1a sbe2a</i> -B3	15.48	12.24	12.67	13.5 $\pm$ 1.8

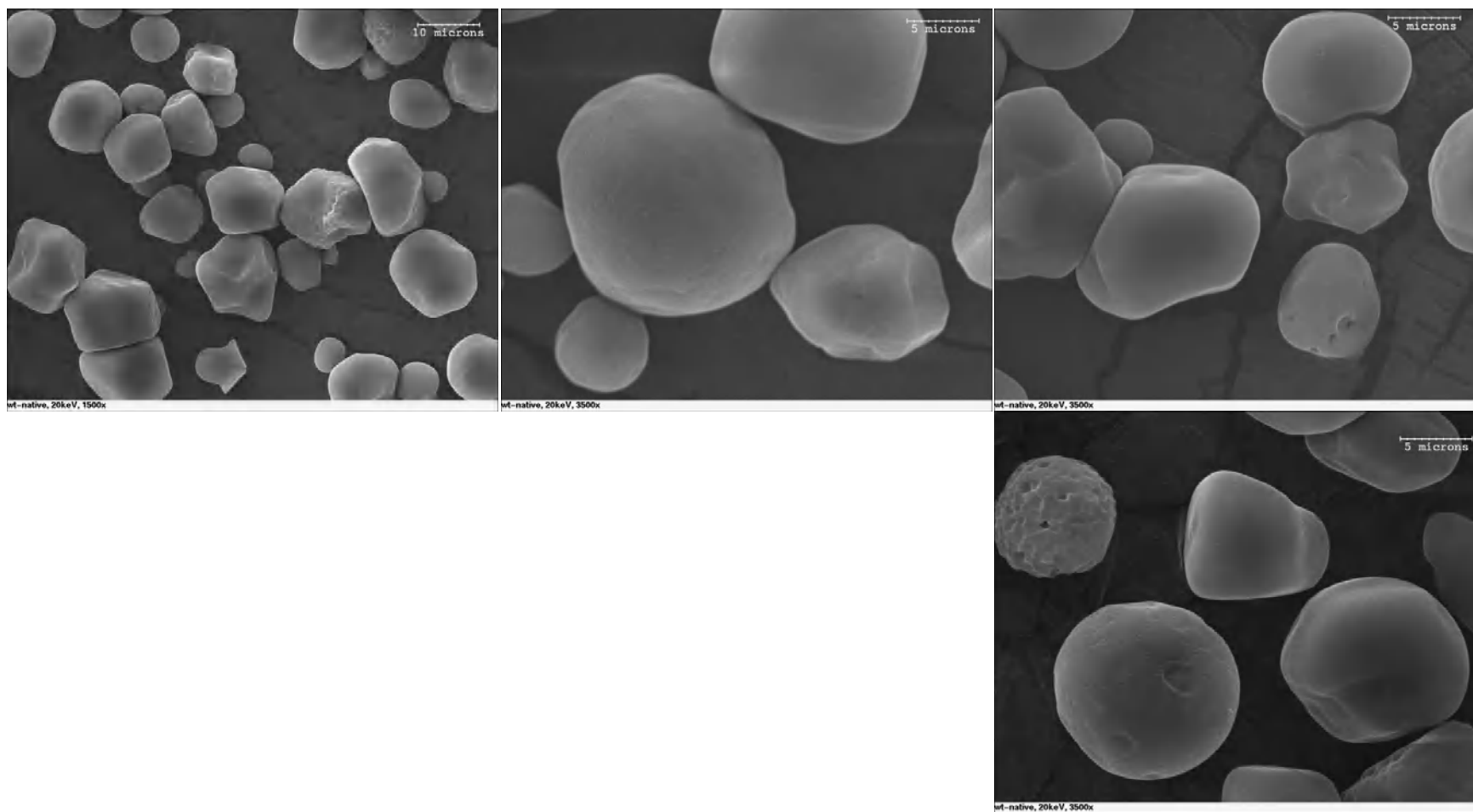


Figure A.1a. Additional scanning electron micrographs of Wt native starch. Scale bars represent 10  $\mu\text{m}$  or 5  $\mu\text{m}$  at the top of graphs. Not all are from the same original field.

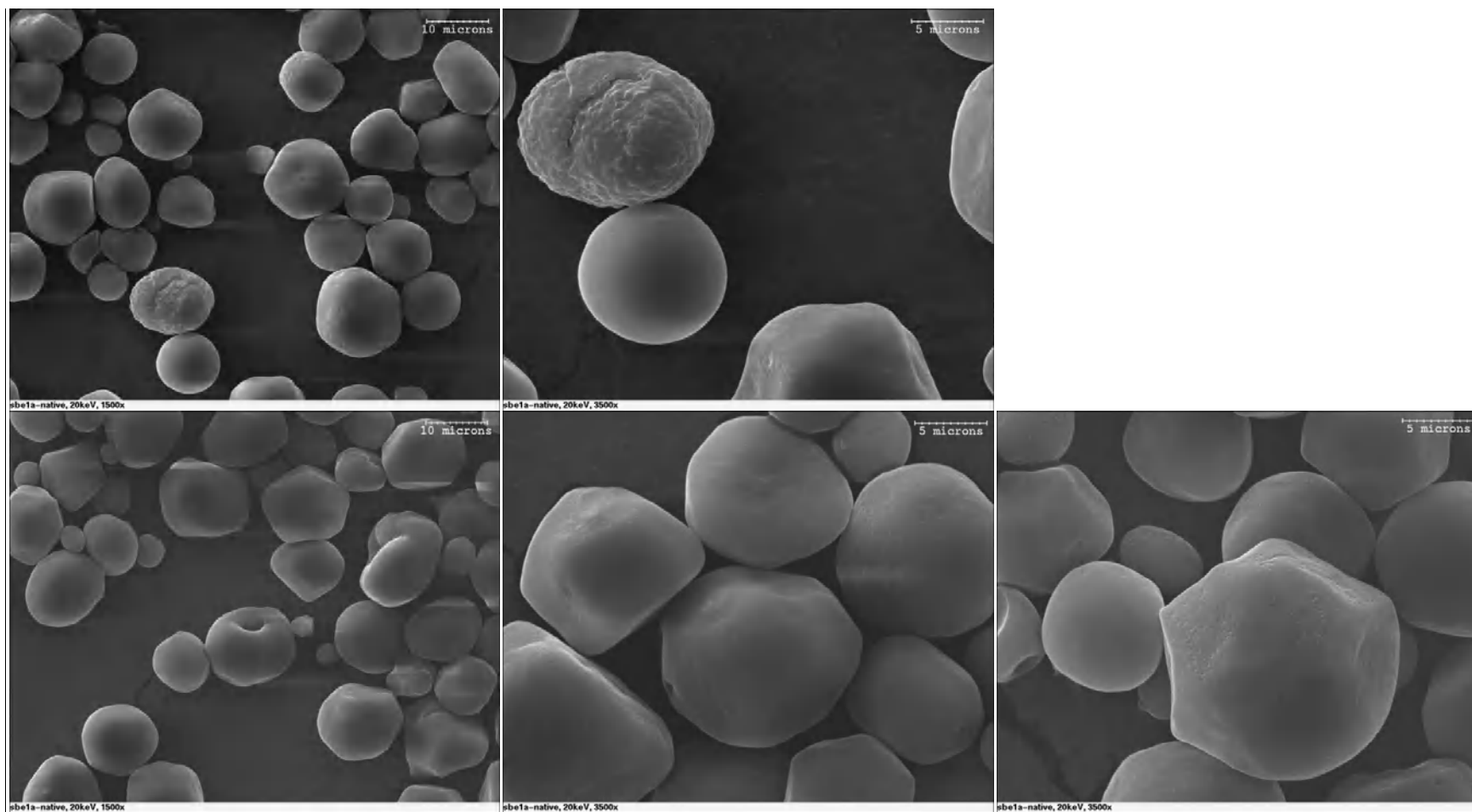


Figure A.1b. Additional scanning electron micrographs of *sbela* native starch. Scale bars represent 10  $\mu\text{m}$  or 5  $\mu\text{m}$  at the top of graphs. Not all are from the same original field.

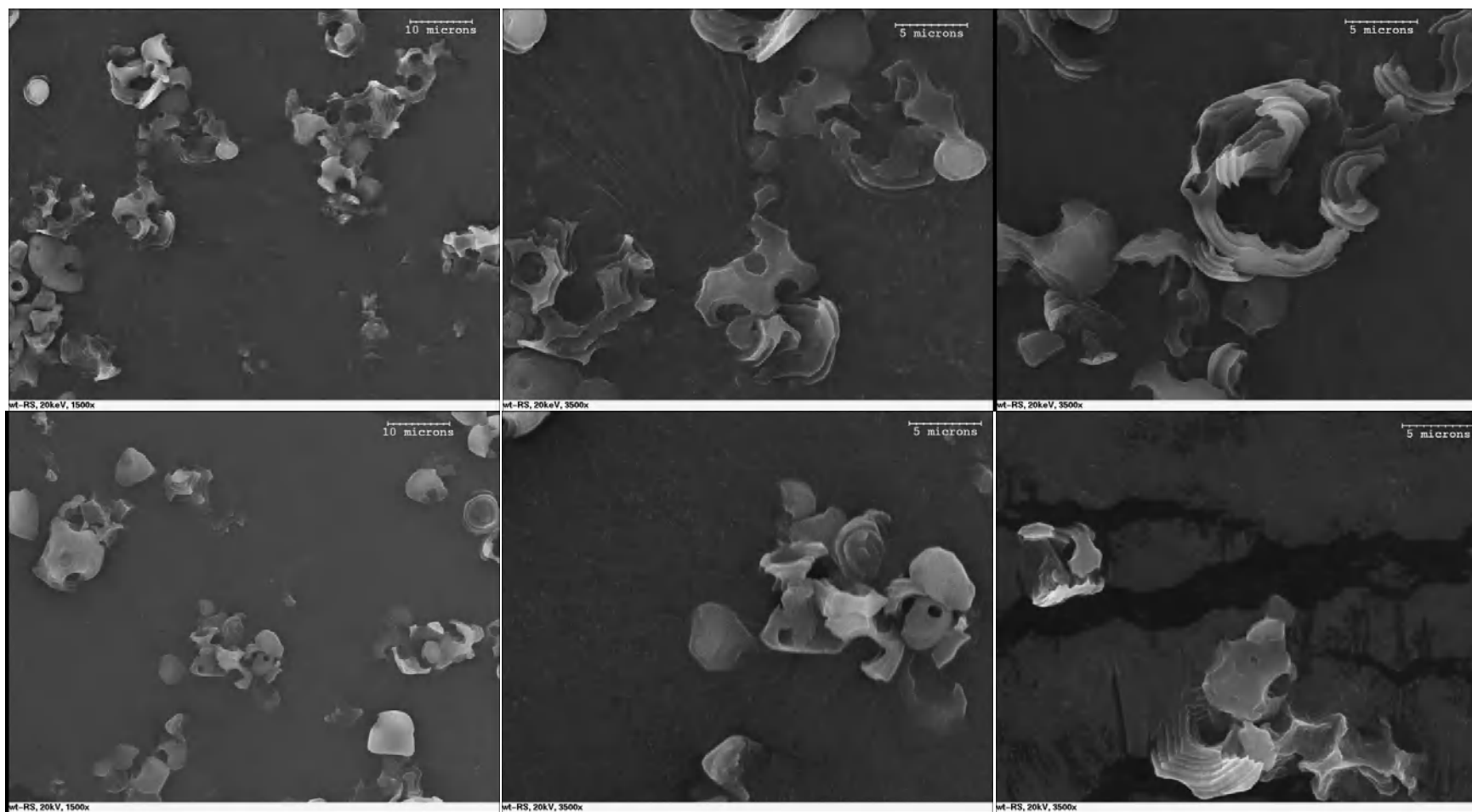


Figure A.2a. Additional scanning electron micrographs of Wt resistant starch. Scale bars represent 10  $\mu\text{m}$  or 5  $\mu\text{m}$  at the top of graphs. Not all are from the same original field.

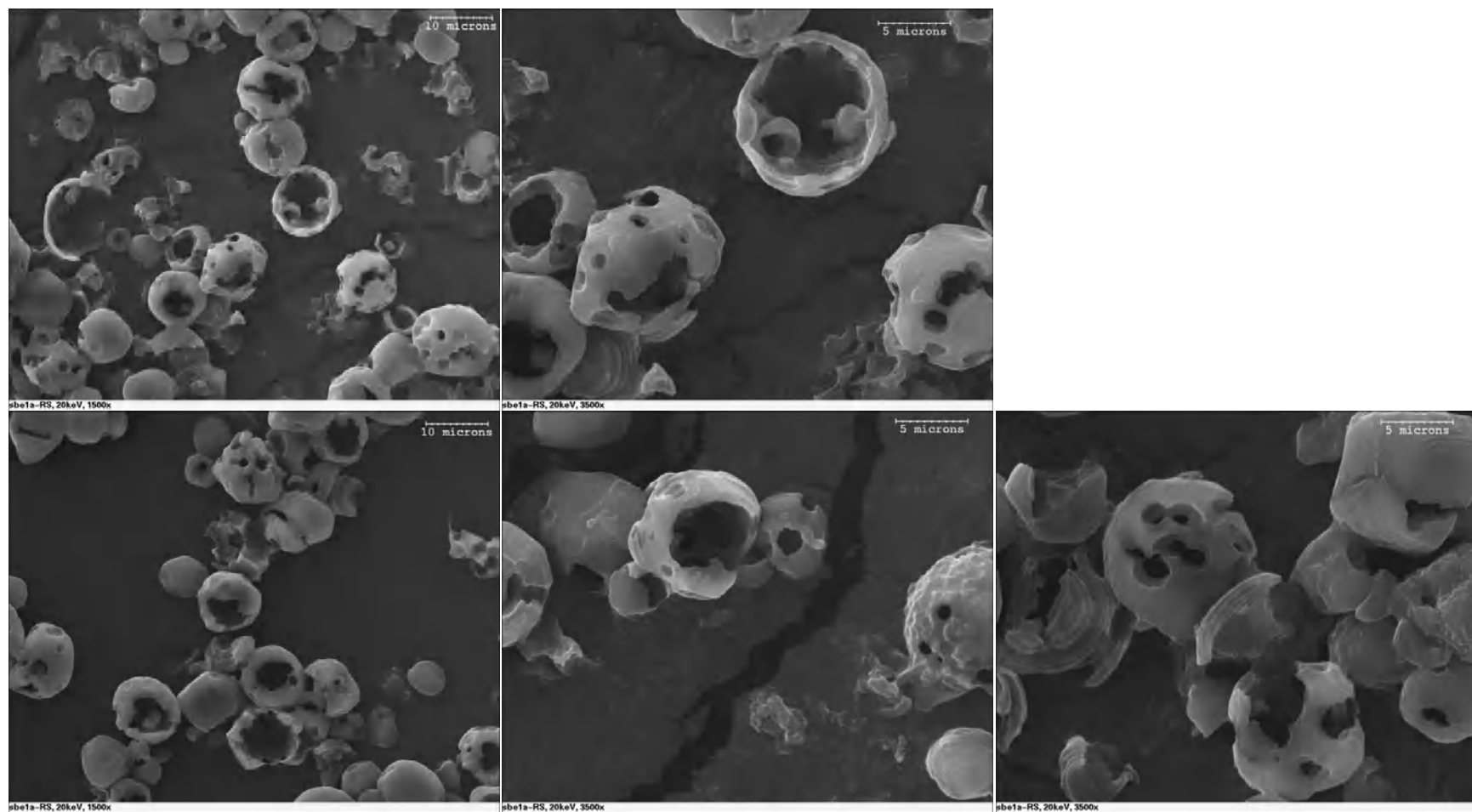


Figure A.2b. Additional scanning electron micrographs of *sbe1a* resistant starch. Scale bars represent 10  $\mu\text{m}$  or 5  $\mu\text{m}$  at the top of graphs. Not all are from the same original field.

Table A.2 Resistant starch values for Wt, *sbe1a*, *ae*, and *sbe1a ae* starch from the 3-gene segregating population.

Genotype	RS Value (%)			
	Rep1	Rep2	Rep3	mean $\pm$ SD
Wt-B1	0.71	3.46	1.54	1.9 $\pm$ 1.4
<i>sbe1a</i> -B1	4.48	5.22	5.19	5.0 $\pm$ 0.4
<i>ae</i> -B1	76.49	71.97	74.55	74.3 $\pm$ 2.3
<i>sbe1a ae</i> -B1	80.92	77.1	80	79.3 $\pm$ 2.0
Wt-B2	2.3	0.87	3.11	2.1 $\pm$ 1.1
<i>sbe1a</i> -B2	9.38	7.78	8.04	8.4 $\pm$ 0.9
<i>ae</i> -B2	75.24	77.8	73.21	75.4 $\pm$ 2.3
<i>sbe1a ae</i> -B2	78.13	78.46	76.79	77.8 $\pm$ 0.9
Wt-B3	0.5	3.11	2.52	2.0 $\pm$ 1.4
<i>sbe1a</i> -B3	10.07	9.11	8.54	9.2 $\pm$ 0.8
<i>ae</i> -B3	74.98	73.03	74.96	74.3 $\pm$ 1.1
<i>sbe1a ae</i> -B3	75.22	75.6	77.01	75.9 $\pm$ 0.9

**Appendix B**

**EFFECTS DEFICIENCY OF MAIZE SBEs ON LEAF  
STARCH DIGESTIBILITY AND GRANULAR  
STRUCTURE**

## B.1 Introduction and Objectives

Although reserve starch formed in amyloplasts of maize kernel endosperm has been widely studied, less attention has been paid to the transitory starch formed in maize leaf chloroplasts. In contrast to endosperm, which functions as a long-term storage sink for starch, leaves undergo starch synthesis and degradation in accordance with the diurnal cycle. During the light phase, photosynthesis results in the production of sugars that are transiently stored as starch within the chloroplast. During the dark phase, this transitory starch is degraded for use in leaf metabolism as well as for export to sink organs (reviewed in Zeeman et al. 2007). In wild type maize plants, the rate of starch degradation occurs throughout the night and is sufficient to consume approximately all of the starch accumulated from the previous day.

Maize starch-branching enzyme IIa (SBEIIa) is the major SBE isoform expressed in leaves and therefore is vital to leaf starch biosynthesis. Recently in our laboratory we observed that maize leaf starch which is deficient in SBEIIa activity appears to be poorly degraded during the night and remains at about the same levels as during the day (personal communication, Drs. Jihong Li and Marna Yandea-Nelson). We hypothesized that the rate and extent of starch degradation as well as the starch properties might be altered in the *sbe2a* mutant leaf tissue.

The main objectives of this preliminary study were to determine the susceptibility to porcine pancreatic  $\alpha$ -amylase and to characterize granule structure during  $\alpha$ -amylase digestion of starch synthesized in the *sbe2a* mutant leaves.

## B.2 Materials and Methods

### B.2.1 Plant germplasms and growth conditions

Maize leaves were harvested from plants 1 and 2 months after germination at the end of dark phase (7AM). Harvested leaves were from 1-month old *sbe2a wx* plant, 2-month old *sbe2a wx*, *sbe1a ae wx*, *sbe1a wx*, *ae wx*, and *wx* plants. All the maize plants were in the W64A inbred line background.

Plants were grown in a greenhouse with supplemental high-pressure sodium light under light intensity  $400\text{-}500 \mu\text{E m}^{-2} \text{s}^{-1}$  at a height of 3.5 feet, on a 16-h-day/8-h-night cycle, 60% humidity, and 27°C to 28°C in light period, 21°C to 22°C in dark period. Plants were grown in 5-gallon pots filled with Sungro SB300 soil-less mix supplemented with Osmocote 15-9-12 and Banrot fungicide.

### B.2.2 Leaf Starch Extraction

Leaf starch extraction was according to the method of Zeeman et al. (1998) with slight modifications. Maize leaves were flash-frozen in liquid nitrogen and ground into fine powder in a mortar and pestle in liquid nitrogen. The ground leaf powder was homogenized in extraction solution (100mM MOPS pH 7.2, 5mM EDTA, 10% (v/v) ethylene glycol) of five times the volumes of leaf powder, using a Tissumizer (Model SDT 1810; Tekmar) at 20,000 rpm for 3 times of 1 min at 4°C. The homogenate was filtered through 30 $\mu\text{m}$  nylon mesh cloth twice, rinsed with additional five volumes of extraction solution, and centrifuged ( $5,000 \times g$ , 15 min, 4°C). The pellet was re-suspended in five volumes of MOPS plus 0.5% (w/v) SDS. The starch was pelleted, washed three times more with MOPS plus SDS solution, four times with five volumes of deionized water, and once with ethanol and acetone. Starch was dried at room temperature in a flow hood for 24 hr.

### **B.2.3 Starch Digestibility Analysis**

The  $\alpha$ -amylase (EC 3.2.1.1) and amyloglucosidase (AMG, EC 3.2.1.3) used for determination of digestion rate and resistant starch (RS) value were part of the RS Determination Kit (K-RSTAR) obtained from Megazyme International (Ireland). Determination of RS value for leaf starch was the same as described in 2.5.1. Determination of the digestion time-course for leaf starch was according to 2.5.2, except that no aliquots were sampled from 2 hr to 16 hr.

Digestion time-course was analyzed following the method developed by Evans (2005) to obtain kinetic data. The enzyme reaction was considered to consist of two components with two separate substrates. A combination of two first-order decay reactions was used to describe the data for component 1 ( $\leq 30$  min) and component 2 ( $> 30$  min).

### **B.2.4 Scanning Electron Microscopy**

Scanning electron microscopy for leaf starch was the same as described in 2.2.5.1 and in 2.2.5.2, respectively.

## **B.3 Results**

### **B.3.1 Leaf Starch Digestibility**

The RS values for leaf starch are shown in Table 1. Due to the limited amount of leaf material, replicated analysis was only completed for the 2-month *sbe2a wx* leaf starch. Both the 1-month and 2-month old *sbe2a* leaf starch had a high RS value, comparable to the RS value (52%) of commercial high amylose maize starch (*aeVII*) (Evans 2005). In contrast, leaf starch from *wx* and *ae wx* mutants was digested completely after 16 hr.

For all leaf starches examined the digestion time-course was separated into two components: component 1 which has a rapidly-digested substrate, component 2 which has a slowly-digested substrate. From visual examination of the digestion plots, a digestion time of 30 min was chosen for defining component 1 and 2. The digestion time-course of leaf starch is shown in Fig. B.1. The regression fits of the component 1 for all starch and of the component 2 for *sbe2a wx* starch had  $R^2$  values greater than 0.8. However, the fits of the component 2 for *sbe1a wx* and *sbe1a ae wx* starch were not as good ( $R^2 = 0.5$  and  $0.6$  respectively), probably due to insufficient data points.

As extension of the linear fit of the component 1 for leaf starch from *ae wx* and *wx* overlapped the data points in the component 2, the linear fit of the component 2 was not necessary to be included (Fig. B.1). Both the component 1 and 2 of leaf starch from *ae wx* and *wx* were considered as rapidly-digested components.

The rate constants for component 1 of digestion increased in the order *sbe2a wx* < *sbe1a wx* < *sbe1a ae wx*  $\approx$  *ae wx* < *wx* (Fig. B.2). The 2-month *sbe2a wx* leaf starch had a higher rate constant for component 2 than that in the 1-month *sbe2a wx* (Fig. B.1). A portion of the *sbe2a wx* leaf starch exhibited a very fast digestion rate during the first 30 min; the remainder showed an extremely slow digestion rate (Fig. B.1). However, the digestion rate for *sbe2a wx* leaf starch during the first 30 min was much faster than for commercial endosperm *aeVII* starch (Fig. B.2).

Table B.1. Resistant starch values for maize leaf starch deficient in different SBE activities.

<b>Leaf Starch</b>	<b>Resistant Starch Value (%)</b>
<b>1-month <i>sbe2a wx</i></b>	51.9%
<b>2-month <i>sbe2a wx</i></b>	47.6% <sup>1</sup>
<b>2-month <i>sbe1a wx</i></b>	25.7%
<b>2-month <i>sbe1a ae wx</i></b>	12.8%
<b>2-month <i>ae wx</i></b>	N.D. <sup>2</sup>
<b>2-month <i>wx</i></b>	N.D. <sup>2</sup>

<sup>1</sup>Mean of three independent analyses; Standard deviation = 2.8%.

<sup>2</sup>non-detected: no starch left after digestion

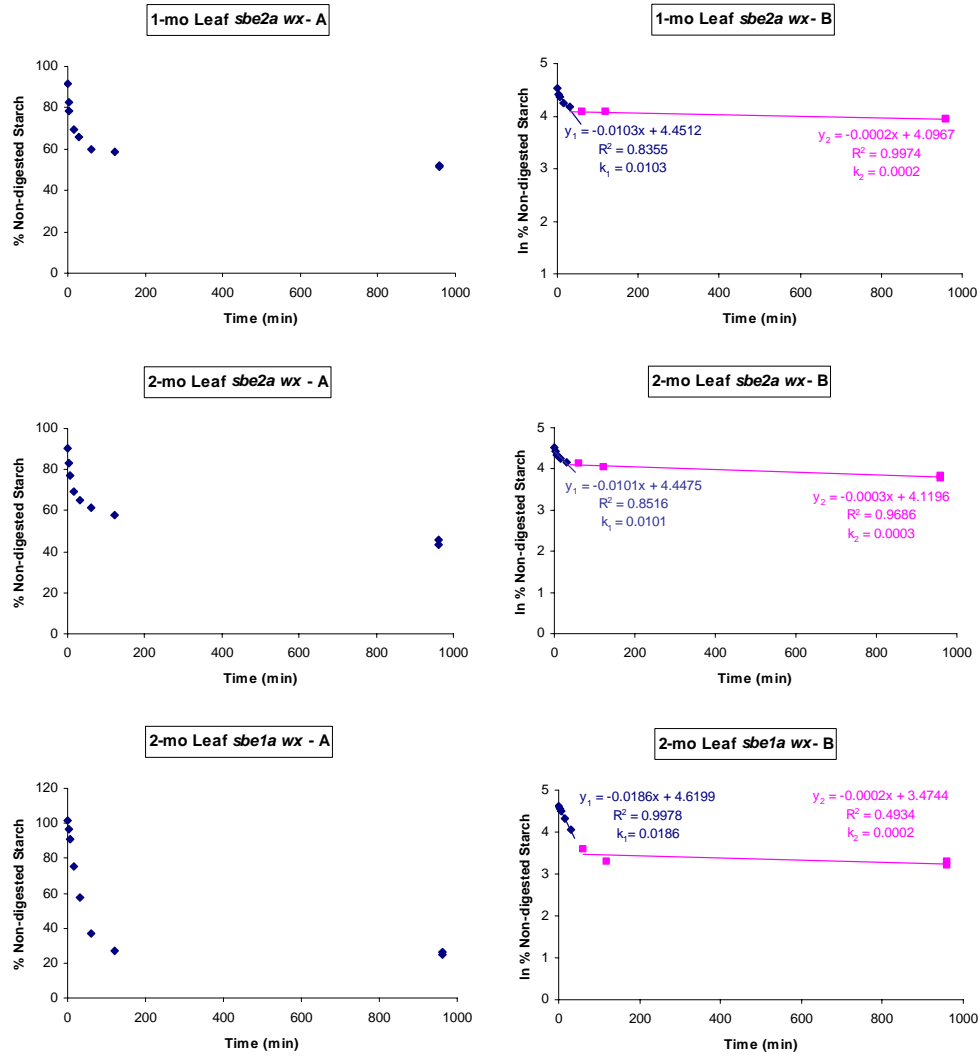


Fig. B.1. Digestion time-course for maize leaf starch deficient in different starch-branching enzyme activities.

A: Digestion time-course data.

B: Plot of ln % Non-digested starch (NDS) versus time. The lines are drawn to illustrate the linear regression fit applied to the two components of the digestion.

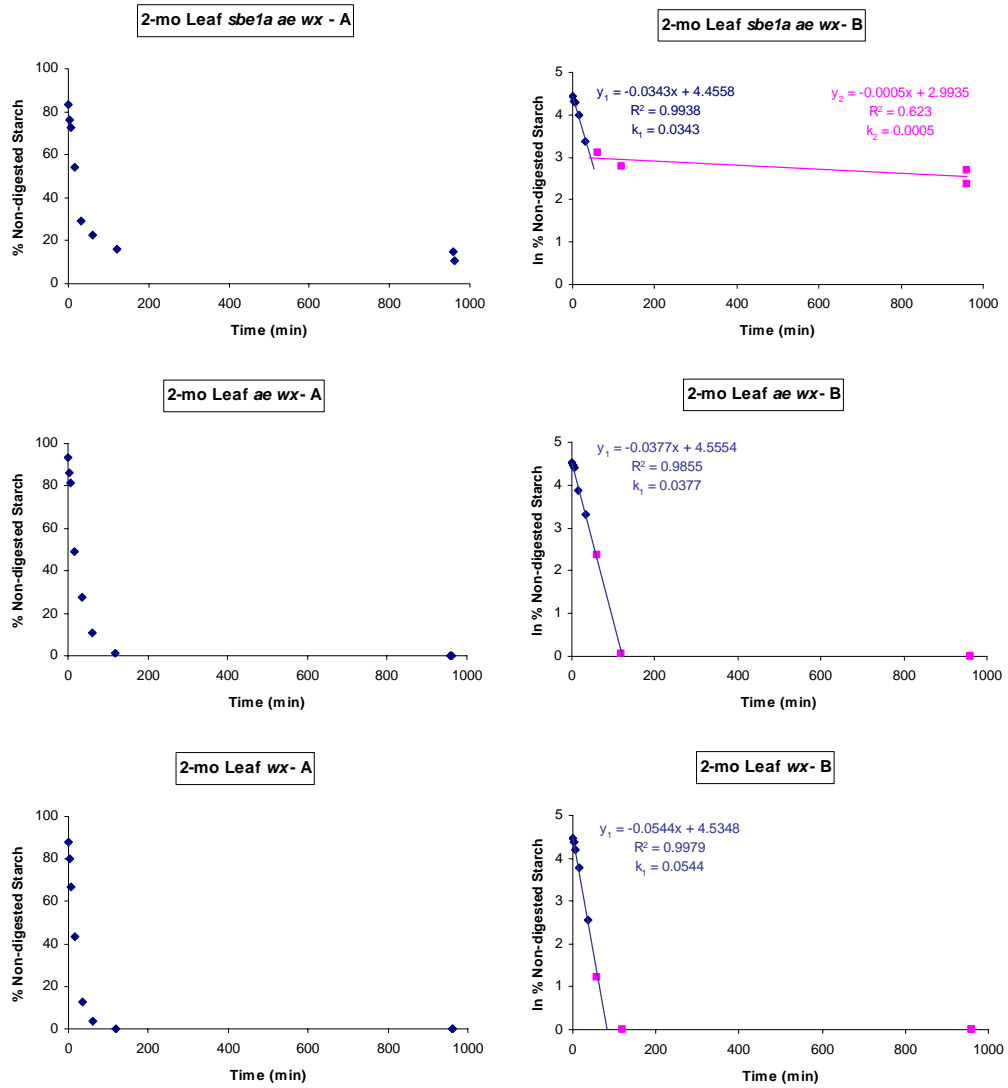


Fig. B.1 (continued) Digestion time-course for maize leaf starch deficient in different starch-branching enzyme activities.

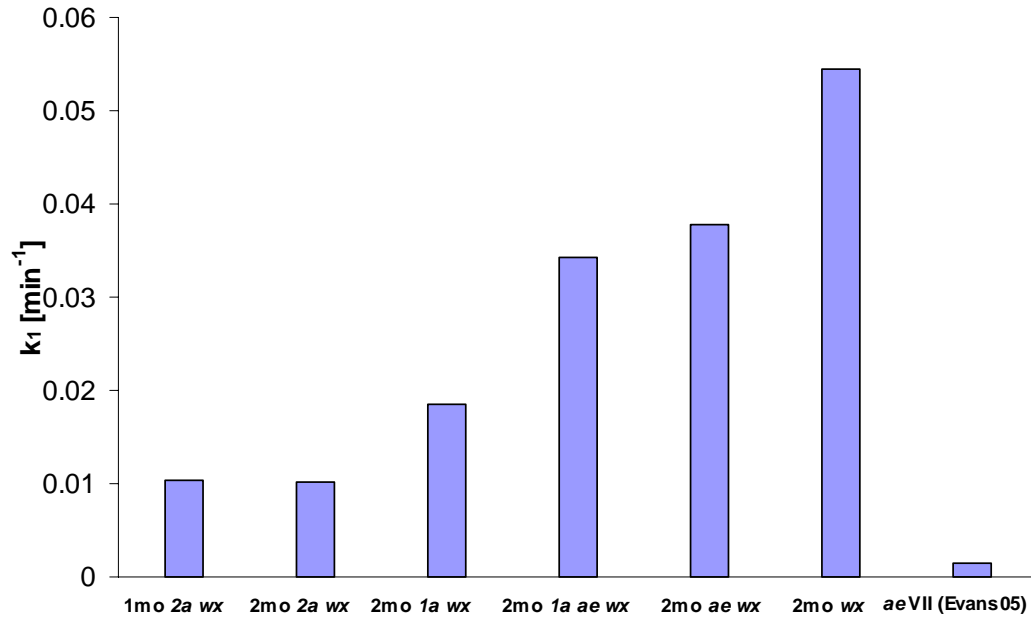


Fig. B.2 Digestion rate constants ( $k_1$ ) of component 1 for several maize leaf starch and *aeVII* starch ( $k_1$  of *aeVII* is adapted from Evans 2005).

### B.3.2 Leaf Starch Granular Structure

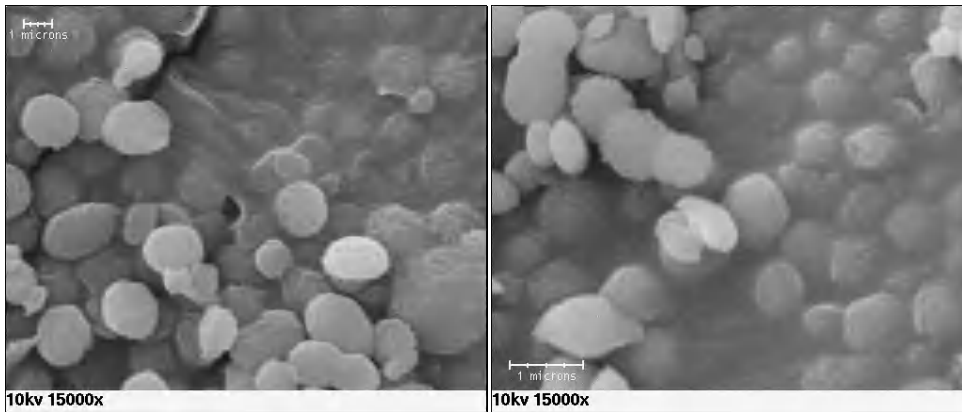
Scanning electron micrographs of native *sbe2a wx* and *sbe1a ae wx* leaf starches are shown in Fig. B.3. It should be noted that the size of leaf starch granule is much smaller from that of endosperm starch seen in this thesis, and that this size difference could also be a reason why leaf starch is digested faster than endosperm starch.

Leaf starch granules from *sbe1a ae wx* were lenticular-shaped. Leaf starch granules from *sbe2a wx* were also lenticular like, but were more round-shaped than *sbe1a ae wx* granules. Scanning electron micrographs of residual leaf starch digested by  $\alpha$ -amylase for 0.5 min, 2 hr, and 16 hr are shown in Fig. B.4, B.5, and B.6, respectively. No visible change was observed after 0.5 min of digestion for both genotypes (Fig. B.4). After 2 hr of digestion, *sbe1a ae wx* leaf starch lost its integrity and became solubilized; most of the *sbe2a wx* leaf starch granules appeared intact, only a few started to rupture (Fig. B.5). After 16 hr of digestion, *sbe1a ae wx* leaf starch granules only had some fragments left; but for *sbe2a wx*, most of the granules still appeared intact on surface, with occasionally fractured granules (Fig. B.6).

## B.4 Discussion

The work presented in this section demonstrates that *sbe2a* mutation leads to high RS in maize leaf blade tissue. Component 1 of 1-month and 2-month *sbe2a wx* leaf starch has similar fast digestion rate, but component 2 of the 1-month leaf starch has a slower rate than the 2-month leaf starch, resulting a higher RS value in 1-month *sbe2a wx* leaf starch. SBEIIa deficiency has a greater effect on maize leaf starch degradation for the 1-month plant than for the 2-month plant, indicating that the *sbe2a* mutation may affect starch synthesis differentially as the plant matures. Even though

*sbe2a wx*



*sbe1a ae wx*

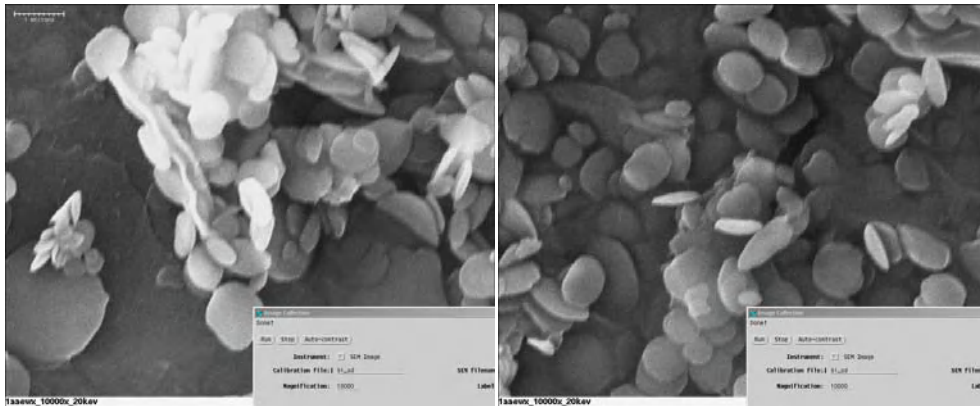
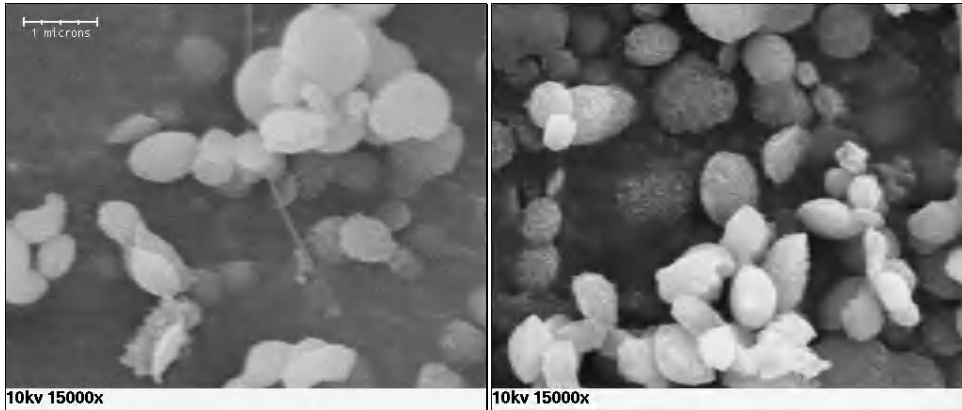


Fig. B.3 Scanning electron micrographs of native 2-month leaf starch from *sbe2a wx* and *sbe1a ae wx* mutant. Scale bars represent 1  $\mu$ m. Magnification used is indicated at the bottom of the graph.

*sbe2a wx*



*sbe1a ae wx*

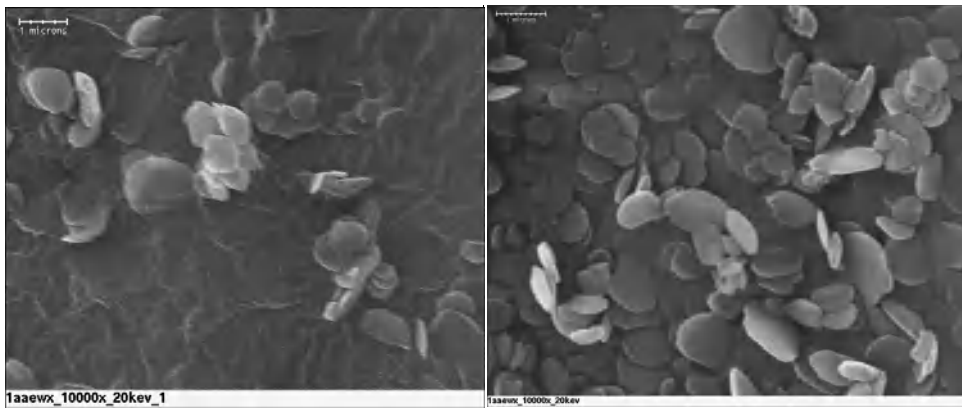


Fig. B.4 Scanning electron micrographs of residual 2-month leaf starch from *sbe2a wx* and *sbe1a ae wx* mutant, digested by  $\alpha$ -amylase for 0.5 min. Scale bars represent 1  $\mu$ m. Magnification used is indicated at the bottom of the graph.

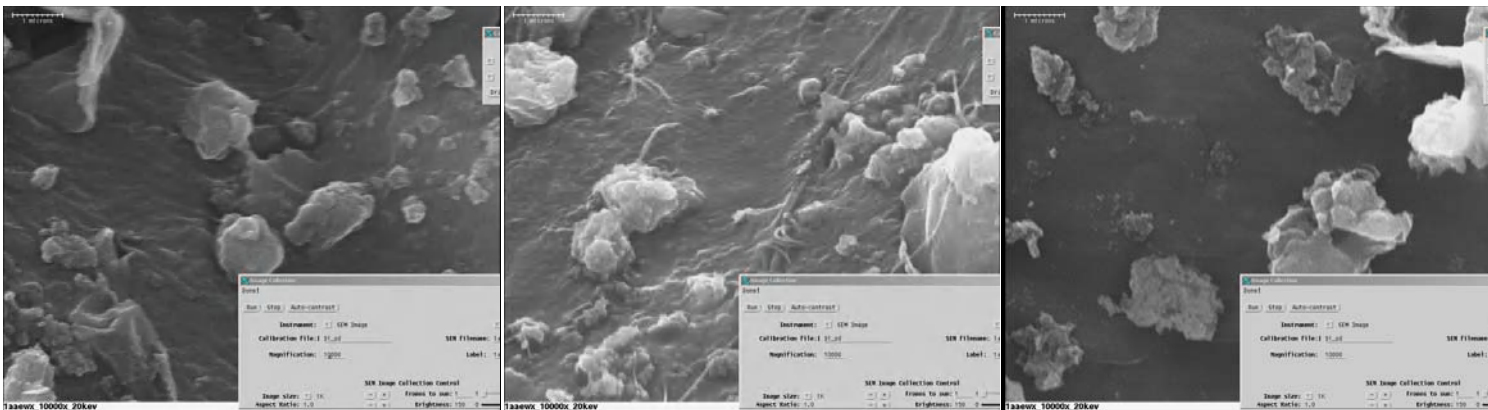
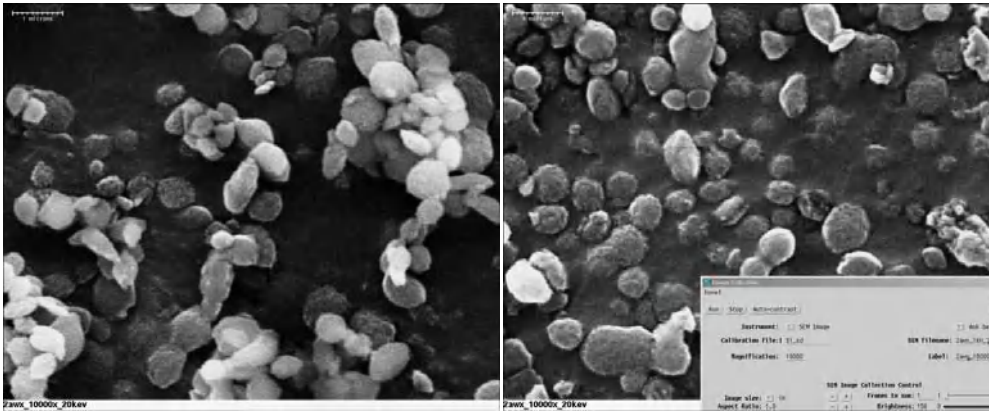
*sbe2a wx**sbe1a ae wx*

Fig. B.5 Scanning electron micrographs of residual 2-month leaf starch from *sbe2a wx* and *sbe1a ae wx* mutant, digested by  $\alpha$ -amylase for 2 hr. Scale bars represent 1  $\mu$ m. Magnification used is indicated at the bottom of the graph.

*sbe2a wx*



*sbe1a ae wx*

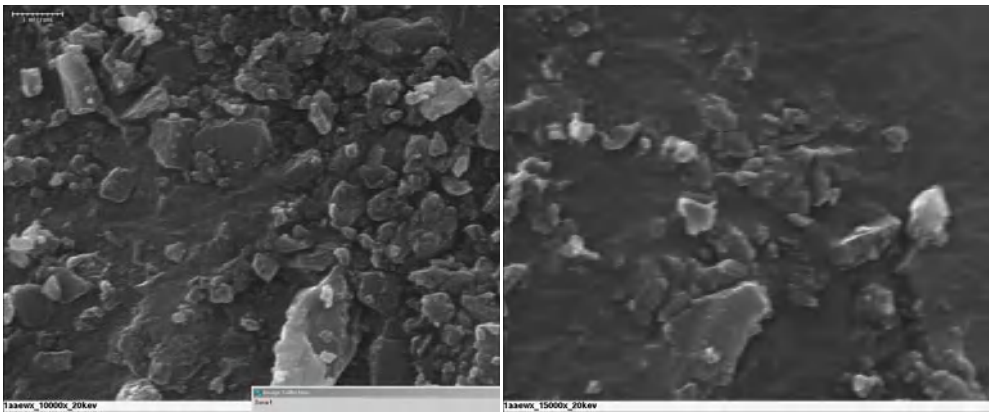


Fig. B.6 Scanning electron micrographs of residual 2-month leaf starch from *sbe2a wx* and *sbe1a ae wx* mutant, digested by  $\alpha$ -amylase for 16 hr. Scale bars represent 1  $\mu$ m. Magnification used is indicated at the bottom of the graph.

producing similar RS value as commercial *aeVII* starch, *sbe2a wx* leaf starch exhibits much faster digestion rate during the first 30 min. Leaf starch from *sbe2a wx* maize appears to be a unique combination of enzyme susceptibility and enzyme resistance.

Leaf starch from both *wx* and *ae wx* was rapidly and completely digested by 2 hr. This is not surprising since both of these genes are thought to be expressed specifically in the endosperm. However, for both *sbe1a wx* and *sbe1a ae wx*, leaf starch was only partially digested and contained appreciable RS. Thus, similar to its role in endosperm starch biosynthesis discussed in this thesis, SBEI seems to also play a minor supporting role in leaf starch synthesis.

Micrographs of the mutant starch revealed that the native leaf starch from *sbe2a wx* appears more round-shaped than that *sbe1a ae wx* starch. The morphology change of residual leaf starch during digestion was different for *sbe2a wx* from *sbe1a ae wx*. Most *sbe1a ae wx* leaf starch granules were disintegrated after 2 hr of digestion, but *sbe2a wx* leaf starch granules were still able to keep granule shape even after 16 hr digestion. These evidences suggest a fundamental difference in granule structure between *sbe2a wx* and *sbe1a ae wx* leaf starch. It is reasonable to speculate that the difference in the digestion pattern and the RS value for these two leaf starch may result from the difference in their granule structure.

## **B.5 References-Appendix B**

- Evans, A. (2005). Enzyme susceptibility of high-amylose starch precipitated from sodium hydroxide dispersions at different precipitation conditions. PhD thesis. The Pennsylvania State University, University Park, PA.
- Zeeman, S.C., Northrop, F., Smith, A.M., ap Rees, T. (1998). A starch-accumulating mutant of *Arabidopsis thaliana* deficient in a starch-hydrolysing enzyme. *Plant J.* 15, 357–365.
- Zeeman S.C, Smith S. M., Smith A.M. (2007). The diurnal metabolism of leaf starch. *Biochem. J.* 401(1), 13-28.

# HUAN XIA

---

---

## EDUCATION

THE PENNSYLVANIA STATE UNIVERSITY, University Park, PA

**Doctor of Philosophy in Food Science**, 12/2009

- *Dissertation*: Structure and function of endosperm starch from maize mutants deficient in one or more starch-branching enzyme isoform activities

**Master of Science in Food Science**, 8/2005

- *Thesis*: Branching pattern differences among amylopectins of several maize genotypes

SOUTHERN YANGTZE UNIVERSITY (Now Jiangnan University), Wuxi, P.R.China

**Bachelor of Engineering in Biotechnology**, 6/2002

- *Thesis*: Identification and cloning of a novel aldehyde dehydrogenase gene from *Thermoanaerobacter ethanolicus*

## AWARDS

- **Graduate Fellowships**: Institute of Food Technologists (IFT) Carbohydrate Division (2008-2009) ~ American Association of Cereal Chemistry (AACC) International: Anheuser-Busch/Campbell Taggart (2008-2009) & Charles Becker (2006-2007) ~ PSU (2002-2003)
- **Graduate Scholarships**: PSU William B. Roskam II Memorial Food Science (2007-2009) ~ PSU Ira W. Minter Food Science (2004-2007)
- **Product Development**: 1<sup>st</sup> Place, 5<sup>th</sup> Annual Almond Innovations Contest, Almond Board of California (2007) ~ 1<sup>st</sup> Place (Snack Category), 1<sup>st</sup> Annual Almond Innovations Contest, Almond Board of California (2003)
- **Research**: Outstanding Poster Award in Cereal Chemistry, the Corn Refiners Association (2004&2009)

## CERTIFICATES

- Seven Principles of Hazard Analysis Critical Control Point (HACCP), International Meat and Poultry HACCP Alliance, 5/2008
- The Graduate School Teaching, The Pennsylvania State University, 5/2008

## PUBLICATIONS

- **Xia, Huan** and Thompson, DB. 2006. Debranching of  $\beta$ -dextrins to explore branching patterns of amylopectins from three maize genotypes. *Cereal Chemistry* 83(6):668-676.
- **Xia, Huan**, et al. An evolutionary perspective on the function of maize endosperm starch-branching enzyme I isoform. (In preparation for *The Plant Cell*).
- **Xia, Huan**, et al. Functional and structural analysis of maize endosperm starch deficient in one or two starch-branching enzyme isoforms reveals specific function of each isoform in starch biosynthesis. (In preparation for *Plant Physiology*).
- Yandeau-Nelson MD, Laurens L, **Xia H**, et al. Starch Branching Enzyme IIa is required for proper diurnal cycling of starch in maize leaves. (In preparation for *Plant Physiology*).
- **Xia, Huan** et al. 2001. Bioconversion and anti-hyperlipemia effect of Cholest-4-en-3-one. *The Creative Forum of Chinese Medicine* Vol.2 (4):80-84.

## PRESENTATIONS

8 presentations at 2004-2009 AACC International meetings and PSU expositions